

1983

# The Aerodynamic Loads On A Flat Plate Between Parallel Walls Due To Rotational Flow Disturbances

Hani Abdel-razik Alnakeeb

Follow this and additional works at: <https://ir.lib.uwo.ca/digitizedtheses>

---

## Recommended Citation

Alnakeeb, Hani Abdel-razik, "The Aerodynamic Loads On A Flat Plate Between Parallel Walls Due To Rotational Flow Disturbances" (1983). *Digitized Theses*. 1232.  
<https://ir.lib.uwo.ca/digitizedtheses/1232>

This Dissertation is brought to you for free and open access by the Digitized Special Collections at Scholarship@Western. It has been accepted for inclusion in Digitized Theses by an authorized administrator of Scholarship@Western. For more information, please contact [tadam@uwo.ca](mailto:tadam@uwo.ca), [wlsadmin@uwo.ca](mailto:wlsadmin@uwo.ca).

The author of this thesis has granted The University of Western Ontario a non-exclusive license to reproduce and distribute copies of this thesis to users of Western Libraries. Copyright remains with the author.

Electronic theses and dissertations available in The University of Western Ontario's institutional repository (Scholarship@Western) are solely for the purpose of private study and research. They may not be copied or reproduced, except as permitted by copyright laws, without written authority of the copyright owner. Any commercial use or publication is strictly prohibited.

The original copyright license attesting to these terms and signed by the author of this thesis may be found in the original print version of the thesis, held by Western Libraries.

The thesis approval page signed by the examining committee may also be found in the original print version of the thesis held in Western Libraries.

Please contact Western Libraries for further information:

E-mail: [libadmin@uwo.ca](mailto:libadmin@uwo.ca)

Telephone: (519) 661-2111 Ext. 84796

Web site: <http://www.lib.uwo.ca/>

# CANADIAN THESES ON MICROFICHE

I.S.B.N.

# THESES CANADIENNES SUR MICROFICHE



National Library of Canada  
Collections Development Branch

Canadian Theses on  
Microfiche Service

Ottawa, Canada  
K1A 0N4

Bibliothèque nationale du Canada  
Direction du développement des collections

Service des thèses canadiennes  
sur microfiche

## NOTICE

The quality of this microfiche is heavily dependent upon the quality of the original thesis submitted for microfilming. Every effort has been made to ensure the highest quality of reproduction possible.

If pages are missing, contact the university which granted the degree.

Some pages may have indistinct print especially if the original pages were typed with a poor typewriter ribbon or if the university sent us a poor photocopy.

Previously copyrighted materials (journal articles, published tests, etc.) are not filmed.

Reproduction in full or in part of this film is governed by the Canadian Copyright Act, R.S.C. 1970, c. C-30. Please read the authorization forms which accompany this thesis.

THIS DISSERTATION  
HAS BEEN MICROFILMED  
EXACTLY AS RECEIVED.

## AVIS

La qualité de cette microfiche dépend grandement de la qualité de la thèse soumise au microfilmage. Nous avons tout fait pour assurer une qualité supérieure de reproduction.

S'il manque des pages, veuillez communiquer avec l'université qui a conféré le grade.

La qualité d'impression de certaines pages peut laisser à désirer, surtout si les pages originales ont été dactylographiées à l'aide d'un ruban usé ou si l'université nous a fait parvenir une photocopie de mauvaise qualité.

Les documents qui ont déjà l'objet d'un droit d'auteur (articles de revue, examens publiés, etc.) ne sont pas microfilmés.

La reproduction, même partielle, de ce microfilm est soumise à la Loi canadienne sur le droit d'auteur, SRC. 1970, c. C-30. Veuillez prendre connaissance des formules d'autorisation qui accompagnent cette thèse.

LA THÈSE A ÉTÉ  
MICROFILMÉE TELLE QUE  
NOUS L'AVONS REÇUE

THE AERODYNAMIC LOADS ON A  
FLAT PLATE BETWEEN PARALLEL  
WALLS DUE TO ROTATIONAL FLOW  
DISTURBANCES

by

Hani Abdel-Razik Alnakeeb

Faculty of Engineering Science

Submitted in partial fulfillment  
of the requirements for the degree of  
Doctor of Philosophy

Faculty of Graduate Studies  
The University of Western Ontario  
London, Ontario  
December, 1982

DEDICATION

To my mother  
and  
the memory of my father

h

## ABSTRACT

In the thesis the effects of rotational flow disturbances on a body placed in an inviscid, incompressible fluid stream, and in particular the case of a flat plate situated midway between two parallel planes were studied. A single vortex approaching the flat plate was first considered and then expanded to simulate the effects of pseudo-turbulence on the flat plate.

The finite-element and finite-difference numerical methods were evaluated in the thesis and arguments were made in support of using the finite-difference approach rather than the finite-element approach. The fact that the finite-difference technique was used for the particular flow problems studied in the thesis does not detract from the usefulness of finite-element methods for other flow problems particularly when further research has been made on variational methods applied to the non-linear fluid flow equations.

Theory for a "Rotational Channel Vortex" was developed and used to provide the upstream boundary conditions to the solution for the unsteady flow over a semi-infinite and then a finite flat plate. Also, new techniques were introduced in the thesis to predict the internal and external boundary conditions. It was found during the study that several methods were available to predict the boundary conditions on the flat plate but it was shown to be most important to select the appropriate method to formulate

the correct boundary conditions on a body immersed in an unsteady rotational flow. The use of pseudo-turbulence models to simulate the approaching flow was also considered and it was shown that the loading on the plate could be determined using this approach. For instance the results showed that it was possible to predict the instantaneous unsteady loads on the flat plate from a particular approaching pseudo-turbulence with a particular power spectral density of the velocity fluctuations.

## ACKNOWLEDGEMENTS

It is my pleasure to express my deepest and sincere gratitude to Professor T.E. Base for his guidance, valuable advice and continuous encouragement throughout the course of this work.

Thanks are extended to Professor J.D. Tarasuk and Professor H. Rasmussen for their constructive discussions and continuous support.

Appreciation is also expressed to other members of the Faculty of Engineering Science and the Department of Applied Mathematics. Thanks are due to Mrs. Debby Main for her meticulous typing of the thesis.

Financial support from the National Research Council and from The University of Western Ontario is also gratefully acknowledged.



## TABLE OF CONTENTS

	Page
CERTIFICATE OF EXAMINATION .....	ii
ABSTRACT .....	iii
ACKNOWLEDGEMENTS .....	v
TABLE OF CONTENTS .....	vi
LIST OF FIGURES .....	viii
NOMENCLATURE .....	xi
CHAPTER 1 - INTRODUCTION .....	1
1.1 General Introduction .....	1
1.2 Literature Survey .....	3
1.3 The Present Work .....	12
CHAPTER 2 - THE FINITE-ELEMENT APPROACH FOR SOLVING POTENTIAL FLOW PROBLEMS .....	15
2.1 Introduction .....	15
2.2 Test Problem - Potential Flow Around A Circular Cylinder .....	19
CHAPTER 3 - THE FINITE-DIFFERENCE ANALOGUE TO INVISCID, INCOMPRESSIBLE FLUID FLOW EQUATIONS .....	30
3.1 Introduction .....	30
3.2 The Governing Equations .....	30
3.3 Deducing the Finite-Difference Poisson's Equation with Variable Mesh Spacing .....	33
3.4 Finite-Difference Analogue for the Vorticity (Helmholtz) Equation .....	39
3.5 Computational Procedure for One Step in Time Level .....	42
3.6 Time Increment Control Facility .....	43
CHAPTER 4 - SIMPLE VORTEX MODELS AND VORTEX EXPRESSION .....	45
4.1 Vortex Flows .....	45
4.2 Simple Vortex Models .....	46
4.3 Vortex Expression .....	50
CHAPTER 5 - BOUNDARY CONDITIONS .....	66
5.1 Introduction .....	66
5.2 The Upstream Boundary .....	68
5.3 The Boundary Conditions at the Upper and Lower Planes .....	70
5.4 The Outflow Boundary Conditions .....	74
5.5 The Boundary Conditions on the Flat Plate .....	79

	Page
CHAPTER 6 - THE EFFECT OF A "REAL" VORTEX APPROACHING A FLAT PLATE PLACED BETWEEN TWO PARALLEL PLANES, IN AN INVISCID, INCOMPRESSIBLE FLUID FLOW .....	80
6.1 Introduction .....	80
6.2 Effect of the Rotational Disturbance on the Stream Function Contours and Stability Conditions .....	82
6.3 Calculation of Pressure on the Flat Plate .....	96
6.4 Lift and Pitching Moment Coefficients .....	99
6.5 Estimating the Flat Plate Stream Function Value .....	100
CHAPTER 7 - SIMULATION OF TURBULENCE AND ITS EFFECT ON A SEMI-INFINITE FLAT PLATE .....	117
7.1 Introduction .....	117
7.2 Description of the Considered Problem .....	118
7.3 The Pseudo-Turbulence Boundary Conditions .....	120
7.4 Statistical Analysis and Results .....	125
CHAPTER 8 - CONCLUSIONS .....	137
8.1 General Conclusions .....	137
8.2 Recommendations for Future Studies .....	141
* * *	
APPENDIX A. THE EQUATIONS OF MOTION FOR AN INCOMPRESSIBLE FLUID FLOW .....	143
APPENDIX B. DERIVATION OF THE STREAM FUNCTION EQUATION FOR A VORTEX BETWEEN TWO PARALLEL PLANES .....	146
APPENDIX C. AUTO-CORRELATION AND POWER SPECTRAL DENSITY FUNCTION .....	151
.. C.1 Auto-Correlation .....	151
.. C.2 Transformed Power Spectral Density Functions ..	152
APPENDIX D. COMPUTER PROGRAM FOR SINGLE VORTEX MODEL .....	155
APPENDIX E. COMPUTER PROGRAMS FOR THE PSEUDO- TURBULENCE MODEL .....	174
REFERENCES .....	211
VITA .....	218

## LIST OF FIGURES

Figure	Description	Page
2-1	Coarse finite-element mesh with straight boundaries	24
2-2	Stream lines for potential flow around a cylinder using the coarse finite-element mesh of Figure (2-1)	24
2-3	Finer finite-element mesh with straight boundaries	26
2-4	Stream lines using the finite-element mesh of Figure (2-3)	26
2-5	Finite-element mesh with circular boundary	28
2-6	Stream lines using the finite-element mesh of Figure (2-5)	28
3-1	Semi-infinite flat plate between two parallel planes	33
3-2	Change in mesh spacing	33
3-3	Schematic sketch of the mesh with variable size	36
3-4	Relative number of iterations from Roache [1976]	38
3-5	Flow chart illustrating computational procedure at a general time step	44
4-1	Periodic distribution of images	51
4-2	Potential vortex midway between two parallel planes	55
4-3	Potential vortex at one-third the distance between the two parallel planes	56
4-4	Rotational vortex midway between two parallel planes	57
4-5	Rotational vortex at one-third the distance between the two parallel planes	58
4-6	Array of five rotational vortices	59

Figure	Description	Page
4-7 to 4-14	Changes of the lateral velocity component (v) along the x axis and the longitudinal velocity component (u) along the y axis, for different $y_0/a$ ratios	61 to 64
6-1	Schematic sketch showing the flow field with the finite-difference mesh near the flat plate	81
6-2	Initial stream lines with no disturbances	84
6-3	Vortex relative positions in the flow field	85
6-4	Change of outflow stream function with time	86
6-5 and 6-6	Vorticity in channel flow	87
6-7 to 6-18	Vortex approaching semi-infinite flat plate with $R_S = 4.35$	89 to 91
6-19 to 6-24	Vortex approaching semi-infinite flat plate with $R_S = 0.62$	94 to 95
6-25	Lift coefficient versus time with the flat plate stream function independent of time	102
6-26	Lift coefficient versus time with the flat plate stream function dependent on the outflow boundary	102
6-27	Lift coefficient versus time with the flat plate stream function dependent on flow conditions at the leading edge	104
6-28	Change of pitching moment coefficient with time	104
6-29	Effect of increasing the convergence criterion " $\epsilon$ " on the lift coefficient	105
6-30	Lift coefficient versus time (run number (1))	107
6-31	Pitching moment coefficient versus time (run number (1))	108
6-32	Lift Coefficient versus time (run number (2))	109
6-33	Pitching moment coefficient versus time (run number (2))	110

Figure	Description	Page
6-34	Lift coefficient versus time (run number (3))	111
6-35	Pitching moment coefficient versus time (run number (3))	112
6-36	Maximum lift coefficient versus $Hr_c^*/C$	114
6-37	Maximum pitching moment coefficient versus $Hr_c^*/C$	115
6-38 to 6-40	Vortex approaching finite flat plate	116
7-1	Schematic diagram showing four boxes for real vortices with the flat plate in Box C (solution domain)	119
7-2	Initial distribution of the random vortices in Boxes A and B	121
7-3	Initial distribution of random vortices in Boxes C and D	122
7-4	Variation of the conditioned longitudinal velocity component with time	127
7-5	Auto-correlation for the conditioned longitudinal velocity component	129
7-6	Power spectral density for the conditioned longitudinal velocity component	130
7-7	Variation of the conditioned lateral velocity component with time	131
7-8	Auto-correlation for the conditioned lateral velocity component	132
7-9	Power spectral density for the conditioned lateral velocity component	133
7-10	Lift coefficient versus time	134
7-11	Pitching moment coefficient versus time	135

## NOMENCLATURE

a	distance between the two planes
A	constant
[A]	square matrix
{B}	column matrix
B	constant
c	constant
C	constant
C	chord of flat plate
$C_L$	lift coefficient
$C_m$	pitching moment coefficient
f	general function
f	frequency
$G_{ii}$	power spectral density function
h	space step
H	distance between the parallel planes
$I'(\psi)$	variational functional
I	imaginary part
K	constant
m	number of unknown parameters in the element
m	number of vortices
$N_j(x,y)$	element shape function, $j=1,m$
p	pressure
P	total pressure
Q	a function related to u and v defined following Equation (3.9).
r	radial coordinate

$r_c$	the vortex core radius
$r_e^*$	equivalent radial distance (dimensionless) defined by Equation (4.27)
$R_s$	Rossby's number $R_s = \frac{\Gamma}{U_\infty r_c^* H}$
$R_{ii}$	auto-correlation coefficient
$S$	space increment ratio in the x direction
$t$	time
$u$	longitudinal velocity component
$u'$	fluctuating component of the velocity in the x direction
$u'$ r.m.s.	root mean square of the fluctuations in the x direction
$U_c$	convective vortex velocity
$\underline{U}$	velocity vector
$v$	lateral velocity component
$v'$	fluctuating component of the velocity in the y direction
$v'$ r.m.s.	root mean square of the fluctuations in the y direction
$v_\theta$	tangential velocity
$x$	cartesian coordinate in the x direction
$x_0$	the vortex centre x coordinate, (Initial Position)
$y$	cartesian coordinate in the y direction
$y_0$	the vortex centre y coordinate, (Initial Position)
$Z$	space increment ratio in the y direction
$z$	complex number: $z = x + iy$
$w$	complex potential: $w = \phi + i\psi$

## GREEK LETTERS

$\nabla$	vector operator
$\nabla^2$	the Laplacian transformation
$\Gamma$	vortex strength
$\Delta$	area of finite element
$\Delta$	increment
$\Delta$	difference
$\delta$	increment
$\epsilon$	order of accuracy
$\theta$	angle
$\mu$	dynamic viscosity
$\nu$	kinematic viscosity
$\xi$	vortex centre position
$\rho$	fluid density
$\sigma$	standard deviation
$\tau$	time delay
$\phi$	the velocity potential
$\chi_1, \chi_2$	constants
$\psi$	the stream function
$\omega$	relaxation factor
$\underline{\Omega}$	vorticity vector: $\underline{\Omega} = \nabla \times \underline{U}$
$\langle \quad \rangle$	time mean square

## SUPERSCRIPTS

$l$	iteration number
$k$	time level
*	dimensionless



## SUBSCRIPTS

e	element
E	East
i,j,k	nodal points
N	North
S	South
v	due to vortex
$\Omega$	domain
w	wall
W	West
$\infty$	conditions of uniform flow

# CHAPTER 1

## INTRODUCTION

### 1.1 GENERAL INTRODUCTION

This thesis investigates first the effects of isolated stream disturbances, such as vortex flows, and then distributed unsteady rotational flow disturbances, such as pseudo-turbulent flow, over a flat plate situated between two parallel planes in an inviscid and incompressible fluid.

The Navier-Stokes equations are capable of describing analytically a large class of unsteady or time dependent flow problems of practical interest. However, the enormous mathematical difficulties encountered when solving these equations have so far prevented obtaining a single analytic solution in which the convective terms interact in a general way with the viscous friction terms. This is due mostly to the non-linear terms contained in the Navier-Stokes equations. Exact solutions of these equations, even without the complexities of unsteady disturbances in the flow stream, exist only in a few simple cases as, for example, the fully developed laminar flow in a pipe or channel, Hiemenz stagnation flow and Couette flow. Schlichting [1979] (discusses several of these 'exact' solutions.

The importance of the present study arises from the fact that most of the flows which occur in practical applications are turbulent. For instance, turbulence is experienced when a fluid flows along a circular pipe at a

Reynold's number higher than the Reynolds criterion or when a fluid is contained in the space between two concentric cylinders which rotate in opposite sense at high speed. Since the flows, just mentioned, are continuously affected by the containing walls, such turbulence is called "wall turbulence". Turbulent flows also occur when a fluid flow exhausts from an orifice at high speed or flows over a grid of bars placed normal to the stream direction. The turbulent flow which exists downstream of the jet or grid of bars is called "Free turbulence".

One essential feature of turbulent fluid flow is that the fluid appears as a conglomeration of rotating flows which intermingle and wander along separate paths in a random manner. In a model of such a flow, a mathematical expression that appears suitable, to express such a motion, is the vortex.

The possibility of studying the effect of stream turbulence on the flow characteristics by using a mathematical model to represent the approaching flow, was enhanced by the successful works of other researchers as, for example, the work by Lilly [1969], Base [1970] and Ahmadi and Goldschmidt [1971]. In the present work a single vortex and a turbulence model were used to simulate the upstream boundary conditions, while the Navier-Stokes equations were solved near the solid body to predict the variation of the flow characteristics with time. The pseudo-turbulence model used for determining the upstream boundary conditions, has

recently been described in the literature by the acronym "FAVR", which in full form is "Finite Area Vortex Regions".

A typical physical problem for example, that encompasses these difficulties, is the case of an aircraft flying through the trailing vortex wake of another aircraft. The introduction of large "jumbo" jets in the commercial sector has seen the waiting period between subsequent flights from airports, increased to avoid possible crashes due to large accelerations caused by aircraft trailing vortex interference. This phenomenon is of such importance that a complete Conference was devoted to the study of "Aircraft wake turbulence", edited by Olsen *et al* [1970]. In order to design safe aircraft, numerical solutions using, if necessary, techniques predicting aerodynamic wing loading must be available to the designer.

This study may also be of special interest in the case of studying the aerodynamic loading on a bridge subjected to a turbulent storm. The method may also be used to simulate the effect of a single vortex or a tornado on a particular high-rise building which would act as a thin flat plate subjected to a single vortex.

## 1.2. LITERATURE SURVEY

In this study, since the pseudo-turbulence was assumed to be between two parallel planes, then the "no flow through the solid wall" condition also had to apply to the vortex model. This meant that special functions had to be devel-

oped that not only were rotational but also satisfied the essential wall boundary conditions of the non-porous wall.

Previous studies on such rotational functions applied to inviscid and incompressible flow are scarce and only the potential functions are mentioned in the classical works of Lamb [1932] and Prandtl and Tietjens [1934].

Nevertheless a survey will be presented in this Section of relevant studies and including numerical methods for solving fluid flow problems.

On the subject of the effects of unsteady flows and disturbance on solid bodies and surfaces, Lighthill [1954] studied the response of laminar skin friction and heat transfer to harmonic fluctuations in the flow stream velocity around a cylindrical body. The study was limited to fluctuations of small magnitude relative to the main flow while constant in direction. Glauert [1956] investigated the problem of the two-dimensional laminar boundary layer on an infinite flat plate normal to the approaching stream for the case when the plate was making transverse oscillations in its own plane. In his work, the oscillations of the flat plate were limited to be harmonic. Ting [1960] studied the problem of the development of a boundary layer over a flat plate in the presence of approaching shear flow. A similarity solution was obtained for large approaching vorticity while for moderate free stream vorticity the governing equation was replaced by an approximate one for which a similarity solution existed. A similar problem

concerning the shear flow past a flat plate was also studied by Mark [1962], while an investigation for the pressure gradient induced by a shear flow past a flat plate was presented by Glauert [1962]. Camiletti and Zamir [1980/1981] examined the characteristics of laminar, steady, incompressible flow past a semi-infinite flat plate placed symmetrically in a two-dimensional channel. In their work the incident Poiseuille flow was perturbed in the core by boundary layers growing on the wall and on the plate. Expressions for the stream function and pressure gradient were determined by the method of matched asymptotic expansions.

In another study the evolution of an infinitely long straight vortex filament in the presence of an approaching rigid sphere was considered by Dhanak [1981]. Similar to the study in this thesis, the fluid was regarded as being inviscid and incompressible. The shape of the vortex filament when the sphere was sufficiently far away from the vortex was determined approximately using linear theory. The subsequent evolution was followed numerically by integrating the non-linear equation of motion.

Numerical methods have also been used with considerable success in the study of unsteady flows approaching solid bodies. In these studies the finite-difference method has extensively used. For example, Fromm and Harlow [1963] described a numerical method for the solution of a finite-difference approximation to the partial differential equations of an unsteady, incompressible and viscous fluid flow.

In their work they studied the development of a vortex street behind a plate and rectangular cylinder which was impulsively accelerated to a constant speed in a channel of finite width.

Thoman and Szewczyk [1969] studied the time-dependent viscous flow over a circular cylinder for a range of Reynold's number from 1 to  $3 \times 10^5$ . In this study, the authors gave more emphasis to the features of flow development when the flow started impulsively from rest. The method was of the explicit type of solution and included a directional difference scheme for the non-linear terms which enhanced the stability of the solution so that a high value of Reynold's number could be achieved.

The problem of calculating the initial flow past a cylinder in a viscous fluid was also investigated by Son and Hanratty [1969] who tried to solve numerically the time-dependent equations of motion in order to extend the range of available data on the steady flow around a cylinder to large values of Reynold's number. Dennis and Staniforth [1970] later suggested a method in which the cylinder was mapped to a straight line by using a conformal transformation. This method could be used to solve the equations for higher values of Reynold's number. Jain and Rao [1969] investigated the numerical solutions with particular emphasis on the existence of the limiting steady state of the Karman vortex street for different Reynold's number.

Phillips and Ackerberg [1973] considered the problem

7

of an unsteady flow over a semi-infinite flat plate which was parallel to the oncoming free stream. The fluid velocity outside the boundary layer, similarly to Lighthill's solution mentioned previously, was assumed to vary with time sinusoidally in magnitude but not in direction. An implicit finite-difference scheme of the second order accuracy was employed using a variable mesh size across the boundary layer.

Cebeci and Smith [1970] suggested an implicit finite-difference method for solving the steady laminar and turbulent boundary layer equations for compressible and incompressible flows about two-dimensional and axisymmetric bodies. In this method the momentum equation was linearized by replacing the Reynold's stress ( $\rho u \overline{v}$ ) by an eddy viscosity term using Prandtl's mixing theory. More applications of this method were later reported by Cebeci, Smith and Mosinski [1970].

A Crank-Nicolson finite-difference scheme with a variable grid was investigated by Blottner [1974] and it was shown that the scheme was more efficient and more accurate for solving turbulent boundary layer equations than the previous methods used. De Rivas [1972] studied the truncation error associated with the use of non-uniform grids in finite-difference equations. He showed that although the finite-difference schemes that used uniform grids were the simplest and most accurate, the use of a suitable transformation function for stretching the finite grid coordi-



nates could be useful in decreasing the truncation error with non-uniform grid schemes.

To decrease the truncation error associated with the finite-difference approximation, Hirsh [1975] applied a higher order finite-difference scheme for solving fluid mechanics problems. In a comparison between computed results obtained by using second order and also fourth order methods, it was shown that the accuracy achieved by the fourth order computations were significantly better as would be expected for the same mesh size. It may be mentioned that in general it is the author's opinion that accuracy is not the only criterion when seeking a solution by finite-difference methods. The stability of the solution is of equal, or even more, importance.

Dwyer and McCroskey [1972] summarized the many difficulties associated with the numerical solution of the three-dimensional and unsteady boundary layer problems as:

- 1) obtaining proper and consistent initial and boundary conditions for the equations.
- 2) developing a stable and unique numerical scheme to solve the equations.
- 3) calculating the flow up to the separation line.

In the same work, Dwyer and McCroskey developed an implicit finite-difference scheme which was used to integrate the three-dimensional time-dependent boundary layer equations. It was noted that it was best to use an implicit scheme when studying the case of a solid body in a fluid

flow because of the stability problems that can occur with explicit schemes particularly near the leading edge of the body.

Other work on the use of finite-difference approximation to solve boundary layer equations include the works by Singleton and Nash [1974], Cooper and Reshotko [1975] and Cebeci [1975].

Another numerical approach to solve the flow equations is the finite element method. In 1971, deVries and Norrie applied the finite element method to solve field problems governed by Laplace's equation, and in particular, to potential flow problems. The method of solution was then applied to the problem of a potential flow with a uniform velocity approaching irregularly shaped bodies between two parallel walls, and to the problem of the flow over an aerofoil set at an angle of attack to the incident stream. Vooren and Labrujere [1974] solved the case of an incompressible, inviscid flow over an aerofoil in a non-uniform stream using the finite element method. Another application of the finite element method to solve potential flow problems was given by Doctors [1970].

A numerical method for solving the Navier-Stokes equations using the variational approach was developed by Atkinson *et al.* [1969, 1970] for the class of creeping flows where the inertia forces were negligibly small compared to the viscous forces. Thompson and Haque [1973] developed a higher order finite element method for the analysis of the

creeping flow of an incompressible material.

Cheng [1972] suggested a finite element method for solving the Navier-Stokes equations for any arbitrary region of interest. The method for solving the development with time of an unsteady flow approaching steady state was suggested previously by Crocco [1965]. This method was applied to study the planar two-dimensional viscous flow inside a channel with a constriction. Olson [1974] applied the finite element method to solve steady two-dimensional and axisymmetric flow problems. This method of solution was verified by applying it to the solution of the circulatory flow in a square cavity and the flow over a circular cylinder. Bratanow and Ecer [1974] also used the finite element variational approach and apparently have developed a more general approach to the unsteady viscous flow over an oscillating aerofoil.

Smith and Brebbia [1975] described a finite element method for the solution of transient, incompressible viscous flow in two-dimensions. They applied this method to study the development of the vortex street behind a rectangular obstruction where the flow has been impulsively accelerated to a constant speed in a channel of finite width. The Reynold's number range investigated was between 20 and 100.

Recently, Badr [1977] and Badr and Base [1978/1979] used the finite element variational approach to study the response of the laminar layer on a flat plate to free stream disturbances. In this study the rotational disturbances

were simulated by randomly positioned modified Rankine vortices which were superimposed on the oncoming uniform stream.

More applications of the finite element method for solving fluid flow problems include the works of Guymon [1972], Baker [1973], Lieber and Attia [1974] and Taylor and Hood [1975].

Due to the difficulties, up till now, in obtaining a general numerical solution for the Navier-Stokes equations, considerable experimental testing has been performed in order to obtain important information on the effects of an approaching turbulent flow on the loads on a body placed in the flow. Kestin [1966] investigated the effect of turbulence intensity on the drag coefficient of an infinite cylinder in cross flow. It was found that there was a critical range of Reynold's number for which the drag coefficient depended strongly on the turbulence intensity as well as on the Reynold's number. Outside this range the effect of turbulence intensity on the drag coefficient was found to be negligible. Erens and Chasteau [1974] carried out measurements of the response of the laminar boundary layer to free stream disturbances. In this work they concentrated on the frequency analysis of the streamwise component of the laminar boundary layer velocity fluctuations at various points along the length of a flat plate. No measurements were reported for the variation of lift and drag due to the disturbed stream. Perry *et al.* [1981] used a smoke tunnel

to carry out a visual study of turbulent spots and showed that these spots consisted essentially of an array of vortices.

In the field of aeronautics, the response of aircraft to free stream disturbance has centred on the power spectral methods. These methods circumvent direct treatment of random time functions by relating the statistics of a linear system's response to those of the excitation through a non-statistical 'transfer function'. For more details about these methods see Liepmann [1952,1955], Sears [1956] and Filotas [1969].

### 1.3. THE PRESENT WORK

The intent of the present work is to study the effects of stream disturbances on a flat plate situated midway between two parallel planes in an unsteady, incompressible, inviscid, rotational fluid flow.

An initial solution for a potential flow test problem using the finite element variational approach, together with the discussion which led to the using of finite-difference methods in the final "solution" are presented in Chapter 2. The governing fluid flow equations and the finite-difference analogue together with the method of solution are presented in Chapter 3.

Chapter 4 presents simple vortex models as well as the derivation for the mathematical expression for the rotational vortex used to simulate the stream disturbances be-

tween two parallel planes. This new rotational vortex expression between two parallel planes will be called the "equivalent modified Rankine vortex"\* and will be used to simulate the flow stream disturbances in Chapters 6 and 7.

Due to the importance and the effect of boundary conditions on the final fluid flow solution, a complete chapter (Chapter 5) was devoted to address the methods used to evaluate the different boundary conditions. New techniques for evaluating the time-changing boundary conditions around the solution domain and on the flat plate were introduced and resulted in faster convergence towards a solution as well as having the downstream and the solid body boundary conditions dependent on the flow conditions upstream.

In Chapter 6 the new rotational vortex expression discussed in Chapter 4 as well as the new boundary condition techniques discussed in Chapter 5 are applied to study the problem of a single "real" vortex approaching a flat plate between two parallel planes in an inviscid, incompressible fluid flow. A complete discussion of results are also presented in the same Chapter.

The effect of flow stream pseudo-turbulence on the flat plate, together with the resulting time variations of the plate lift and pitching moment coefficients are presented in Chapter 7. The same Chapter also presents statistical analysis used to analyze the computed data together with the conclusions of this study, on pseudo-turbulent flow approaching a thin flat plate.

\*Alternatively it is called "Rotational Channel Vortex"

Finally in Chapter 8, the general ~~conclusions~~ conclusions concerning the approach including the finite-difference method and the results of the two particular flows are presented.

## CHAPTER 2

### THE FINITE ELEMENT APPROACH FOR SOLVING POTENTIAL FLOW PROBLEMS

#### 2.1. INTRODUCTION

Two major types of numerical methods for solving differential equations have been established. The first is the use of finite-difference methods, which are presented in Chapter 3, in which the direct substitution of the derivatives in the governing equations by their finite-difference approximation will result in the difference analogue of the equations. The application of this analogue to each of the mesh points in the flow field will result in a system of difference equations which can be solved to obtain the required numerical solution. The second method, which is discussed in this Chapter, is the use of the finite element approximation where the characteristic equations can be derived by using the variational formulation of the governing equations. The basic idea of using the finite element method, when used to solve field problems, is to divide the solution domain into a finite number of subdomains or elements. The shape of the element to be used may be triangular, rectangular, quadrilateral or curved. Once the type of element has been chosen and a finite element mesh has been constructed, the behaviour of the unknown field variable over each element can be approximated by



continuous functions expressed in terms of the nodal values of the field variable, or in terms of a subset of generalized variables, and sometimes the nodal values of its derivatives up to a certain order. The approximate representation of a two-dimensional field variable  $\phi(x,y)$  within an element 'e' can be written in terms of the element unknown parameters at the nodal points  $\phi_j$  as,

$$\phi^{(e)}(x,y) = \sum_{j=1}^m N_j(x,y)\phi_j \quad (2.1)$$

where  $m$  is the number of unknown parameters and  $N_j(x,y)$ ,  $j=1, m$  are the element shape functions.

The element shape function is usually chosen to satisfy certain continuity requirements of the field variable and its derivatives at the element interfaces joining the nodal points. More details concerning types of element shape functions are given in Zienkiewicz [1971] and Huebner [1975].

The main approaches to derive the finite element characteristic equations for the governing physical equations of the problem are:

1) The Variational Approach

In this approach, a physical problem governed by a set of differential equations, may be equivalently expressed as an extremum problem by the methods of calculus of variations. For example, if one considers the simple problem of potential flow governed by Laplace's equation

$$\frac{\partial^2 \psi}{\partial x^2} + \frac{\partial^2 \psi}{\partial y^2} = 0 \quad (2.2)$$

where  $\psi$  is the stream function, then this problem may be solved by extremizing the following integral or functional as it is usually called:

$$I(\psi) = \iint_{\Omega} \frac{1}{2} \left[ \left( \frac{\partial \psi}{\partial x} \right)^2 + \left( \frac{\partial \psi}{\partial y} \right)^2 \right] dx dy \quad (2.3)$$

with respect to the unknown function  $\psi$ .

In general, it can be shown by using variational methods, (in particular, Euler's theorem), that the extremization of the general functional  $I(\psi)$  where

$$I[\psi(x,y)] = \iint_{\Omega} f\left(x,y,\psi, \frac{\partial \psi}{\partial x}, \frac{\partial \psi}{\partial y}\right) dx dy \quad (2.4)$$

will result in the following differential equation

$$\frac{\partial f}{\partial \psi} - \frac{\partial}{\partial x} \left[ \frac{\partial f}{\partial \left( \frac{\partial \psi}{\partial x} \right)} \right] - \frac{\partial}{\partial y} \left[ \frac{\partial f}{\partial \left( \frac{\partial \psi}{\partial y} \right)} \right] = 0 \quad (2.5)$$

Using the same theorem, it follows that the extremization of the functional  $I(\psi)$  in Equation (2.3) is a necessary and sufficient condition for the satisfaction of Equation (2.2).

## 2) The Weighted Residual Approach

In this approach two steps have to be carried out. The first step is to assume a general behaviour of the dependent field variable in such a way that it can approximately satisfy the given differential equation and the associated boundary conditions. The substitu-

tion of this approximation into the differential equation results in some errors called residuals. These residuals are required to vanish in some average sense over the entire solution domain. The next operation is to solve the equations resulting from the first step to find the approximate solution.

3) The Direct Method

This method can be used only for relatively simple problems. The procedure is to apply the governing equations to each individual element which results in a number of algebraic equations. The set of equations arising from the different elements can be arranged in a matrix form and solved to obtain the required solution.

The details of the three different approaches, including many applications are given in Zienkiewicz [1971], Huebner [1975] and Dasai [1972].

In the following section a simple test problem is solved by the variational finite element approach, with a discussion of the problems encountered which were a deciding factor to use the finite-difference approximations in solving the unsteady, inviscid, incompressible fluid flow over a semi-infinite flat plate situated midway between two parallel planes.

## 2.2 TEST PROBLEM - POTENTIAL FLOW AROUND A CIRCULAR CYLINDER

The finite element technique was tested by applying it to the two-dimensional potential flow problem of a cylinder in a uniform stream. The velocity-stream function relationship was defined as follows:

$$u = \frac{\partial \psi}{\partial y}, \quad v = -\frac{\partial \psi}{\partial x} \quad (2.6)$$

Since the potential flow is irrotational then,

$$\nabla \times \underline{U} = 0 \quad (2.7)$$

Hence, for a two-dimensional potential flow,

$$\frac{\partial v}{\partial x} - \frac{\partial u}{\partial y} = 0 \quad (2.8)$$

Substituting Equations (2.6) into Equation (2.8) results in obtaining Laplace's equation which is,

$$\frac{\partial^2 \psi}{\partial x^2} + \frac{\partial^2 \psi}{\partial y^2} = 0 \quad (2.9)$$

Solving Equation (2.9) together with the associated boundary conditions would result in the stream function distribution in the potential flow, and substituting back into Equations (2.6) would result in obtaining the velocity field.

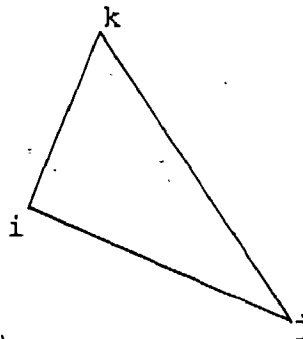
## 2.3 DERIVING THE FINITE ELEMENT EQUATIONS FOR THE TEST PROBLEM

The variational functional of Laplace's equation was

given in the previous section, which is

$$I(\psi) = \iint_{\Omega} \frac{1}{2} \left[ \left( \frac{\partial \psi}{\partial x} \right)^2 + \left( \frac{\partial \psi}{\partial y} \right)^2 \right] dx dy \quad (2.3)$$

A triangular shape element was chosen where the nodes are situated at the vertices of the triangle, as shown in the figure below.



In order to extremize the above variational functional, a linear shape function was assumed to represent the variation of the field variable over each element, such that

$$\psi = Ax + By + C \quad (2.10)$$

where  $\psi$  is the stream function at the point having coordinates  $x$  and  $y$ .  $A$ ,  $B$  and  $C$  are constants to be determined in terms of the nodal variables.

Substituting the nodal variables and their coordinates into Equation (2.10), the following equations can be obtained:

$$\psi_i = Ax_i + By_i + C \quad (2.11)$$

$$\psi_j = Ax_j + By_j + C \quad (2.12)$$

$$\psi_k = Ax_k + By_k + C \quad (2.13)$$

Solving for the constants A, B and C and substituting into Equation (2.10), the value of the stream function  $\psi$  at any point within the element can be written as dependent on the nodal values ( $\psi_i, \psi_j, \psi_k$ ), hence,

$$\psi = N_i \psi_i + N_j \psi_j + N_k \psi_k \quad (2.14)$$

where

$$N_i = [(x_j y_k - x_k y_j) + (y_j - y_k)x + (x_k - x_j)y] / 2\Delta \quad (2.15)$$

$$N_j = [(x_k y_i - x_i y_k) + (y_k - y_i)x + (x_i - x_k)y] / 2\Delta \quad (2.16)$$

$$N_k = [(x_i y_j - x_j y_i) + (y_i - y_j)x + (x_j - x_i)y] / 2\Delta \quad (2.17)$$

and

$$2\Delta = \begin{vmatrix} 1 & 1 & 1 \\ x_i & x_j & x_k \\ y_i & y_j & y_k \end{vmatrix} \quad (2.18)$$

= twice the area of the triangle  $ijk$

Substituting for the variable  $\psi$  from Equation (2.14) into the variational functional, Equation (2.3), yields

$$I_e = \iint_e \frac{1}{2} \left[ \left( \frac{\partial N_i}{\partial x} \psi_i + \frac{\partial N_j}{\partial x} \psi_j + \frac{\partial N_k}{\partial x} \psi_k \right)^2 + \left( \frac{\partial N_i}{\partial y} \psi_i + \frac{\partial N_j}{\partial y} \psi_j + \frac{\partial N_k}{\partial y} \psi_k \right)^2 \right] dx dy \quad (2.19)$$

where the subscript  $e$  denotes the element.

The variational functional for the whole domain  $\Omega$  can be written as,

$$I_{\Omega} = \sum_e I_e \quad (2.20)$$

Using the variational principle that a solution would exist if the functional is extremized, then

$$\begin{aligned} \left[ \frac{\partial I}{\partial \psi_i} \right]_{\Omega} &= \sum_e \frac{\partial I_e}{\partial \psi_i} \\ &= \sum_e \iint \left[ \left( \frac{\partial N_i}{\partial x} \psi_i + \frac{\partial N_j}{\partial x} \psi_j + \frac{\partial N_k}{\partial x} \psi_k \right) \frac{\partial N_i}{\partial x} \right. \\ &\quad \left. + \left( \frac{\partial N_i}{\partial y} \psi_i + \frac{\partial N_j}{\partial y} \psi_j + \frac{\partial N_k}{\partial y} \psi_k \right) \frac{\partial N_i}{\partial y} \right] dx dy \quad (2.21) \end{aligned}$$

where

$$\frac{\partial N_i}{\partial x} = \frac{y_j - y_k}{2\Delta} \quad (2.22)$$

$$\frac{\partial N_i}{\partial y} = \frac{x_k - x_j}{2\Delta} \quad (2.23)$$

$$\frac{\partial N_j}{\partial x} = \frac{y_k - y_i}{2\Delta} \quad (2.24)$$

and so on.

Equation (2.21) can be rewritten as follows:

$$\frac{\partial I_{\Omega}}{\partial \psi_i} = \sum_e (M_i \psi_i + M_j \psi_j + M_k \psi_k) = 0 \quad (2.25)$$

where

$$M_i = \frac{1}{4\Delta} \{ (y_j - y_k)^2 + (x_j - x_k)^2 \} \quad (2.26)$$

$$M_j = \frac{1}{4\Delta} \{ (y_i - y_k)(y_j - y_k) + (x_i - x_k)(x_j - x_k) \} \quad (2.27)$$

$$M_k = \frac{1}{4\Delta} \{ (y_i - y_j)(y_j - y_k) + (x_i - x_j)(x_j - x_k) \} \quad (2.28)$$

Applying Equation (2.25) to every nodal point inside the domain, would result in  $n$  linear algebraic equations with  $n$  unknowns ( $n$  is the number of nodal points). Solving these equations together with the boundary conditions would result in obtaining the stream function distribution inside the domain.

The velocities could be obtained using Equations (2.6) which are

$$u = \frac{\partial \psi}{\partial y} \quad \text{and} \quad v = - \frac{\partial \psi}{\partial x} \quad (2.6)$$

Substituting for  $\psi$  from Equation (2.14) results in,

$$\begin{aligned} u &= \frac{\partial N_i}{\partial y} \psi_i + \frac{\partial N_j}{\partial y} \psi_j + \frac{\partial N_k}{\partial y} \psi_k \\ &= \left[ (x_k - x_j) \psi_i + (x_i - x_k) \psi_j + (x_j - x_i) \psi_k \right] / 2\Delta \quad (2.29) \end{aligned}$$

and

$$v = - \left[ (y_j - y_k) \psi_i + (y_k - y_i) \psi_j + (y_i - y_j) \psi_k \right] / 2\Delta \quad (2.30)$$

From Equations (2.29) and (2.30) it can be seen that the velocities ( $u$  and  $v$ ) for each element are constant, which would represent the velocities at the centroid of each triangle.

Figure (2-1) shows a coarse finite element mesh with straight boundaries for a potential flow around a cylinder.



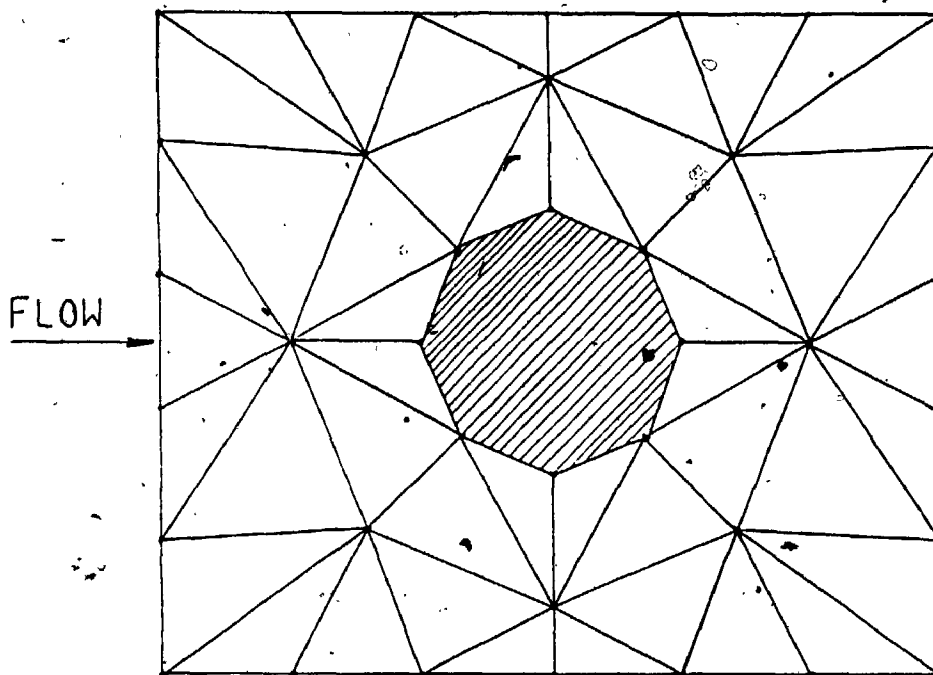


Figure (2-1) Coarse finite element mesh with straight boundaries.

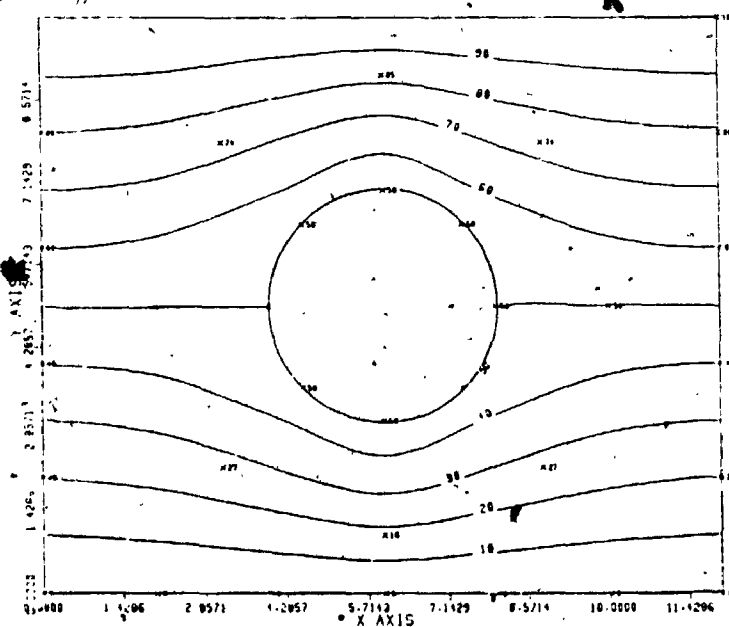


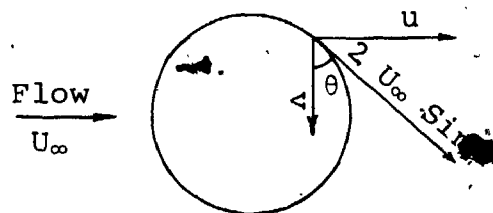
Figure (2-2) Stream lines for potential flow around a cylinder using the coarse finite element mesh of Figure (2-1).

The corresponding stream function contours (stream lines) obtained by the use of the finite element approach are shown in Figure (2-2).

A finite element mesh was then constructed such that the centroids of the triangles adjacent to the cylinder would lie on its surface, so that the constant velocities obtained for each one of those elements would represent the velocities of the centroid point on the cylinder surface. Figures (2-3) and (2-4) show the finite element mesh used and the corresponding stream lines. The velocities were then compared to the values obtained from the theoretical solution for potential flow around a cylinder, as shown in the diagram, (see Glauert [1959]), which are,

$$u = 2 U_{\infty} \sin\theta \cos\theta$$

$$v = - 2 U_{\infty} \sin\theta \sin\theta$$



Such a finite element mesh gave a percentage error of 35% in the values of the velocities on the cylinder surface. Investigating the source of error, it was found that for the elements adjacent to the cylinder, the aspect ratio used (height of triangle/base of triangle) was about 1:8. Upon modifying the aspect ratio of the same elements to be close to unity, while the centroid would no longer lie on the cylinder surface, the percentage error was reduced considerably to about 2%.

Another numerical solution was carried out by increas-

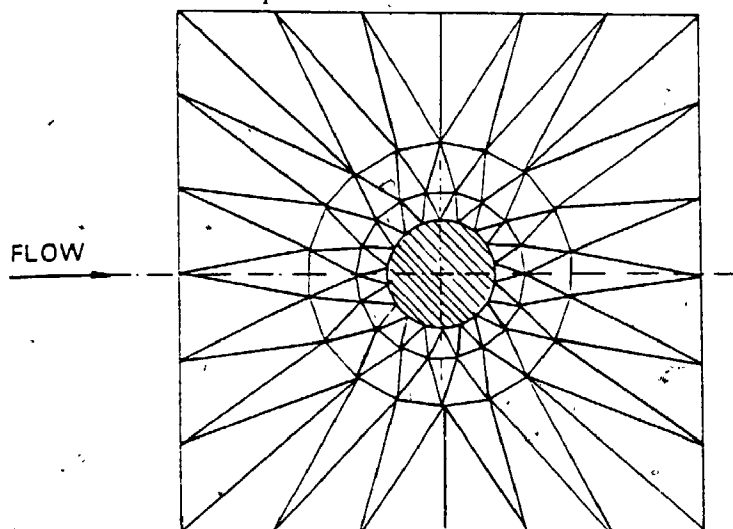


Figure (2-3) Finer finite element mesh with straight boundaries.

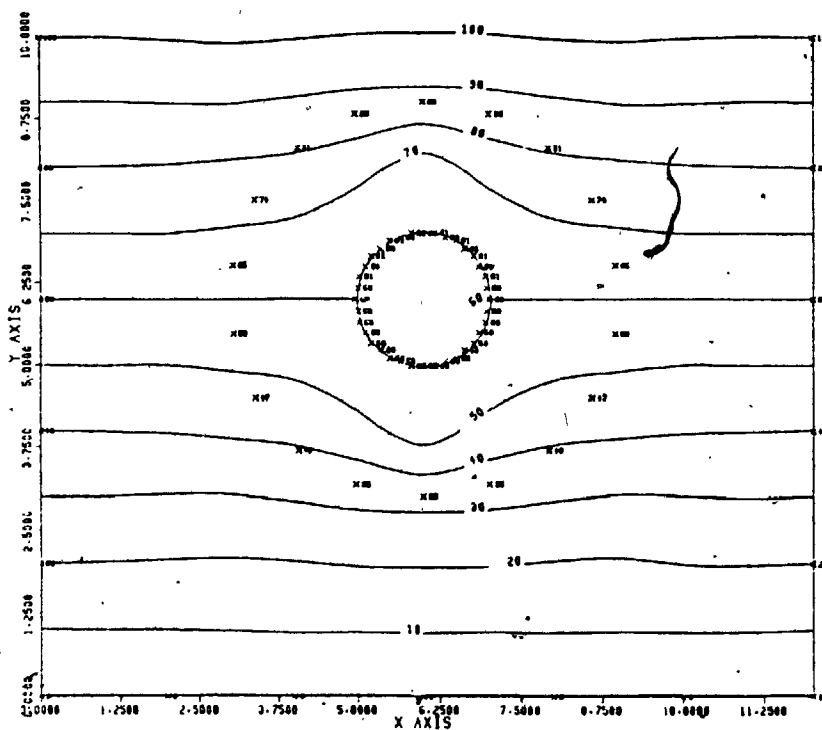


Figure (2-4) Stream lines using the finite element mesh of Figure (2-3).

ing the total number of elements in the flow domain, while keeping the number of nodal points on the cylinder constant. In this case, also a larger circular outer boundary was used, as shown in Figure (2-5). Ironically, although the total number of elements was increased, it was found that the accuracy decreased and was worse than for the case using straight outer boundaries to the solution domain (see Figure (2-3)). The stream function contours for this finite element mesh stencil are shown in Figure (2-6).

From the attempts reported above, it was shown that the accuracy of the solution was very much dependent on the finite element mesh stencil shape. Also, these studies illustrated the importance of the aspect ratio of the element over the number of elements used in terms of obtaining a more reliable solution.

The above mentioned problems may be attributed to the type of element as well as the shape function used. In order to overcome these problems intuitively, a higher order or isoparametric element should be used.

It was noticed while using the finite element approach in solving this test problem, that the mesh symmetry did affect the solution. For example, an asymmetrical mesh around the cylinder produced an asymmetrical velocity distribution. This result was also confirmed by Rasmussen [1980], Mahmoud [1981] and Gadallah [1982].

In order to obtain a more reliable solution using the finite element method, the finite element mesh stencil has to be

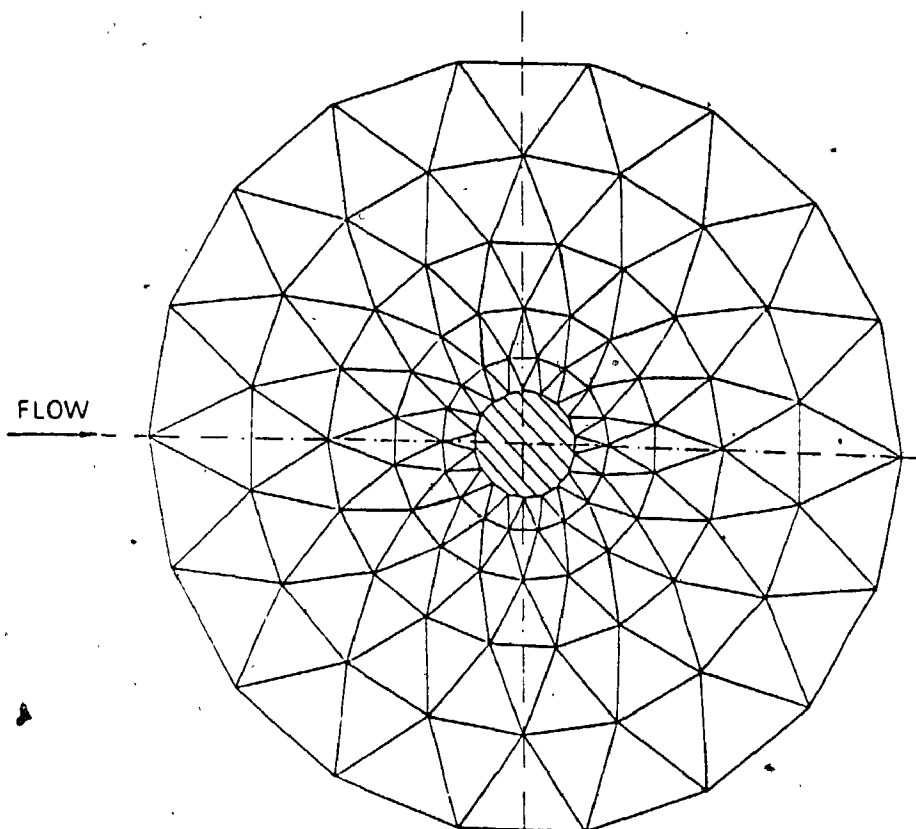


Figure (2-5) Finite element mesh with circular boundary.

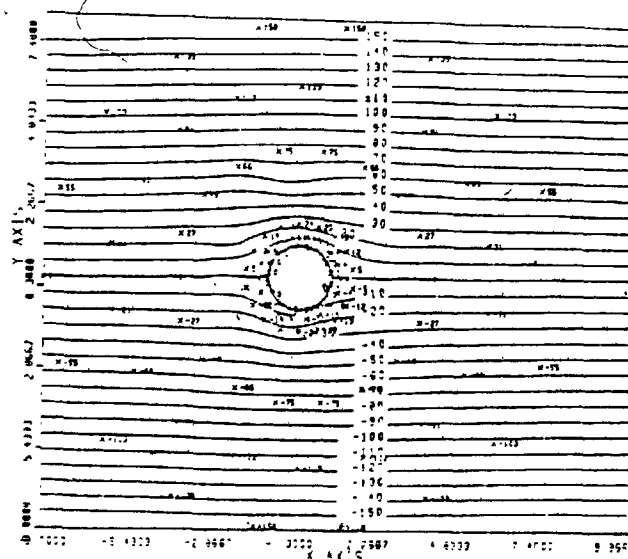


Figure (2-6) Stream lines using the finite element mesh of Figure (2-5).

symmetrical. This symmetry problem makes the finite element method not so attractive a method in solving fluid flow problems over solid bodies with complex geometries and approaching asymmetrical unsteady flow. In the next Chapter the alternative approach to solving the fluid flow problems, the finite-difference method, is discussed.

## CHAPTER 3

### THE FINITE-DIFFERENCE ANALOGUE TO INVISCID, INCOMPRESSIBLE FLUID FLOW EQUATIONS

#### 3.1 INTRODUCTION

In spite of the fact that the numerical methods will never lead to an exact solution, the success which has been achieved in solving different problems with a relatively high degree of accuracy, has greatly enhanced the importance and effectiveness of these methods as an efficient approach for solving general field problems. Developments in numerical procedures were encouraged by the invention and fast development of the electronic digital computer.

In this Chapter, the equations used in solving two-dimensional incompressible flow problems are first presented, followed by their finite difference analogue used in the present work.

#### 3.2 THE GOVERNING EQUATIONS

The fundamental equations for the incompressible flow of a Newtonian fluid with no body forces and constant properties are the momentum equations (Navier-Stokes) and the continuity equation (see, e.g., Lamb [1932], or Schlichting [1979]). These equations can be written as follows:

$$\left(\frac{\partial}{\partial t} + \underline{U} \cdot \underline{\nabla}\right) \underline{U} = -\frac{1}{\rho} \underline{\nabla} p + \nu \nabla^2 \underline{U} \quad (3.1)$$

$$\text{and } \underline{\nabla} \cdot \underline{U} = 0 \quad (3.2)$$

where

$\underline{U}$  is the velocity vector

$p$  is the pressure

$t$  is the time

$\rho$  is the mass density of the fluid

and  $\nu$  is the kinematic viscosity of the fluid.

In the case of two-dimensional flow in the  $(x,y)$  plane, the equation of continuity can be satisfied by introducing the stream function  $\psi$  such that,

$$u = \frac{\partial \psi}{\partial y} \quad \text{and} \quad v = - \frac{\partial \psi}{\partial x} \quad (3.3)$$

where  $u$  and  $v$  are the velocity components in the  $x$  and  $y$  directions respectively.

Eliminating the pressure term from Equation (3.1), (see Appendix (A)), and introducing the vorticity vector  $\underline{\Omega}$  defined by the expression

$$\underline{\Omega} \equiv \nabla \times \underline{U} \quad (3.4)$$

the resulting equations can be written in two-dimensional form as follows:

$$\frac{\partial \Omega}{\partial t} + u \frac{\partial \Omega}{\partial x} + v \frac{\partial \Omega}{\partial y} = \nu \nabla^2 \Omega \quad (3.5)$$

where

$$-\Omega = \nabla^2 \psi \quad (3.6)$$

$$\nabla^2 = \frac{\partial^2}{\partial x^2} + \frac{\partial^2}{\partial y^2}$$



and  $\Omega$  is written as the component  $\Omega_z$  in the vorticity vector  $\underline{\Omega}$ .

Equation (3.5) is called the Helmholtz vorticity transport equation and Equation (3.6) is called the stream function equation.

For the case under study of an incompressible inviscid fluid flow where the kinematic viscosity coefficient is considered to be zero ( $\nu = 0$ ), then the right-hand side of the Helmholtz equation would vanish, while the continuity equation remains the same, so the equations to solve would be:

$$\nabla^2 \psi = - \Omega \quad (3.6)$$

$$\text{and } \frac{\partial \Omega}{\partial t} + u \frac{\partial \Omega}{\partial x} + v \frac{\partial \Omega}{\partial y} = 0 \quad (3.7)$$

It may be of interest to mention that Equation (3.7) is first order in space and time, and the solution for all  $x, y > 0$  and  $t > 0$  is completely specified by an initial condition function,  $\Omega(x, y, 0)$ , and boundary condition values,  $\Omega(0, y, t)$  and  $\Omega(x, 0, t)$ .

A relationship between the pressure field and velocity field can be obtained from Equation (3.1), (see Appendix (A)), and can be written in the two-dimensional form as,

$$\nabla^2 p = - \rho Q \quad (3.8)$$

where

$$Q = 2 \left( \frac{\partial u}{\partial y} \frac{\partial v}{\partial x} - \frac{\partial u}{\partial x} \frac{\partial v}{\partial y} \right) \quad (3.9)$$

Equation (3.8) can be used to obtain the pressure distribution from the known velocity distribution if the boundary conditions of the pressure are known.

### 3.3 DEDUCING THE FINITE-DIFFERENCE POISSON'S EQUATION WITH VARIABLE MESH SPACING

The equations derived in the previous section may now be approximated by finite-differences for a rectangular mesh stencil. A particular case of a semi-infinite thin flat plate set between two parallel planes was initially considered. In the regions close to the boundaries and near the flat plate, as shown in Figure (3-1), where the flow velocity gradients were expected to change rapidly, smaller mesh sizes were used for the purpose of obtaining both higher resolution and accuracy.

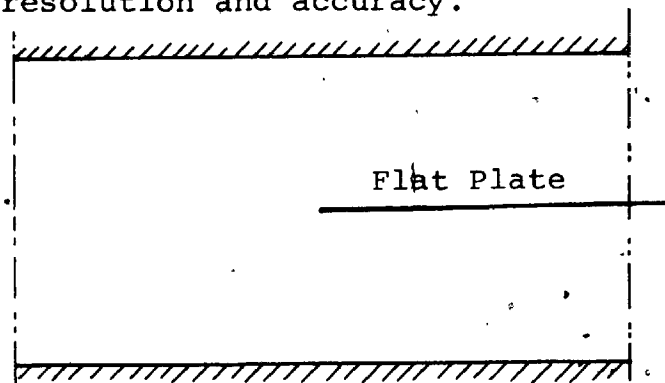


Figure (3-1) Semi-infinite flat plate between two parallel planes



Figure (3-2) Change in mesh spacing

Expanding a function  $f$  in a Taylor series, forward and backward from a point within the domain with different mesh sizes  $\Delta X_1$  and  $\Delta X_2$  as shown in Figure (3-2), gives

$$\begin{aligned} f_{i+1} &= f_i + \left. \frac{\partial f}{\partial x} \right|_i \Delta X_2 + \frac{1}{2} \left. \frac{\partial^2 f}{\partial X^2} \right|_i \Delta X_2^2 \\ &+ \frac{1}{6} \left. \frac{\partial^3 f}{\partial X^3} \right|_i \Delta X_2^3 + O(\Delta X_2^4) \end{aligned} \quad (3.10)$$

$$\begin{aligned} f_{i-1} &= f_i - \left. \frac{\partial f}{\partial x} \right|_i \Delta X_1 + \frac{1}{2} \left. \frac{\partial^2 f}{\partial X^2} \right|_i \Delta X_1^2 \\ &- \frac{1}{6} \left. \frac{\partial^3 f}{\partial X^3} \right|_i \Delta X_1^3 + O(\Delta X_1^4) \end{aligned} \quad (3.11)$$

The expression for the derivative  $\left. \frac{\partial f}{\partial x} \right|_i$  can be obtained by subtracting Equation (3.11) from Equation (3.10) so that,

$$\begin{aligned} f_{i+1} - f_{i-1} &= \left. \frac{\partial f}{\partial x} \right|_i (\Delta X_2 + \Delta X_1) \\ &+ \frac{1}{2} \left. \frac{\partial^2 f}{\partial X^2} \right|_i (\Delta X_2^2 - \Delta X_1^2) + O(\Delta X^3) \end{aligned} \quad (3.12)$$

where  $O(\Delta X^3)$  means the largest of  $O(\Delta X_1^3)$  or  $O(\Delta X_2^3)$ , and dividing by the total space increment so that,

$$\begin{aligned} \left. \frac{\partial f}{\partial x} \right|_i &= \frac{f_{i+1} - f_{i-1}}{\Delta X_2 + \Delta X_1} - \frac{1}{2} \left. \frac{\partial^2 f}{\partial X^2} \right|_i \frac{\Delta X_2^2 - \Delta X_1^2}{\Delta X_2 + \Delta X_1} \\ &+ O(\Delta X^2) \end{aligned} \quad (3.13)$$

This means that the form

$$\left. \frac{\partial f}{\partial x} \right|_i = \frac{f_{i+1} - f_{i-1}}{\Delta X_2 + \Delta X_1} \quad (3.14)$$

is of second order accuracy if:

$$\left. \begin{aligned} &0 \left( \frac{\Delta X_2^2 - \Delta X_1^2}{\Delta X_2 + \Delta X_1} \right) \leq 0 (\Delta X_1^2) \\ \text{or } &0 (\Delta X_2 - \Delta X_1) \leq 0 (\Delta X_1^2) \end{aligned} \right\} \quad (3.15)$$

and for  $\Delta X_2$  very small, the accuracy at a field point  $i$  deteriorates to first order in  $\Delta X_1$ . When  $\Delta X_1$  equals  $\Delta X_2$ , Equation (3.14) becomes second order accuracy since the second term in Equation (3.13) would cancel.

The expression for the second derivative is obtained by multiplying Equation (3.11) by  $S^2 = (\Delta X_2/\Delta X_1)^2$  and adding the result to Equation (3.10) so that:

$$\begin{aligned} f_{i+1} - (1+S^2)f_i + S^2f_{i-1} &= \frac{\partial f}{\partial x} \Big|_i \Delta X_2 (1-S) \\ &+ \frac{\partial^2 f}{\partial X^2} \Big|_i \Delta X_2^2 + \frac{1}{6} \frac{\partial^3 f}{\partial X^3} \Big|_i \Delta X_2^2 (\Delta X_2 - \Delta X_1) \\ &+ 0 (\Delta X^4) \end{aligned} \quad (3.16)$$

Solving for  $\frac{\partial^2 f}{\partial X^2} \Big|_i$  gives

$$\begin{aligned} \frac{\partial^2 f}{\partial X^2} \Big|_i &= \frac{f_{i+1} - (1+S^2)f_i + S^2f_{i-1}}{\Delta X_2^2} - \frac{\partial f}{\partial x} \Big|_i \left( \frac{1-S}{\Delta X_2} \right) \\ &- \frac{1}{6} \frac{\partial^3 f}{\partial X^3} \Big|_i (\Delta X_2 - \Delta X_1) + 0 (\Delta X^2) \end{aligned} \quad (3.17)$$

Substituting for the first derivative  $\frac{\partial f}{\partial x} \Big|_i$  from Equation (3.14) into Equation (3.17) gives,

$$\frac{\partial^2 f}{\partial X^2} \Big|_i = \frac{(1+S^2)f_{i+1} - (1+S)(1+S^2)f_i + S(S^2+1)f_{i-1}}{(1+S)\Delta X_2^2} + O(\Delta X_2 - \Delta X_1, \Delta X^2) \tag{3.18}$$

which is of second order accuracy for equal spacing ( $\Delta X_1 = \Delta X_2$ ) and first order for unequal spacing ( $\Delta X_1 \neq \Delta X_2$ ). This fact is illustrated by the last term in Equation (3.18).

Modifying Equation (3.18) for the two-dimensional partial derivatives and substituting into Poisson's Equation (3.6) which is,

$$\frac{\partial^2 \psi}{\partial x^2} + \frac{\partial^2 \psi}{\partial y^2} = -\Omega$$

then:

$$\begin{aligned} & \frac{(1+S^2)\psi_{i+1,j} - (1+S)(1+S^2)\psi_{i,j} + S(S^2+1)\psi_{i-1,j}}{(1+S)\Delta X_2^2} \\ & + \frac{(1+Z^2)\psi_{i,j+1} - (1+Z)(1+Z^2)\psi_{i,j} + Z(Z^2+1)\psi_{i,j-1}}{(1+Z)\Delta Y_2^2} \\ & = -\Omega_{i,j} \end{aligned} \tag{3.19}$$

where

$Z = \frac{\Delta Y_2}{\Delta Y_1}$  as shown in Figure (3-3).

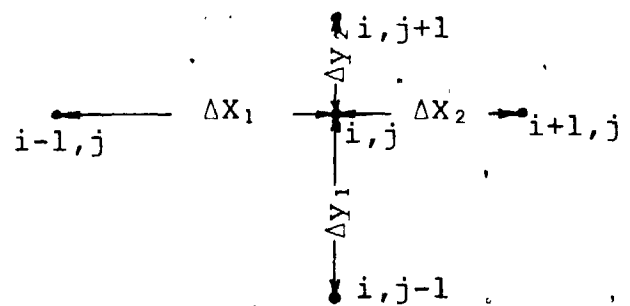


Figure (3-3) Schematic sketch of the mesh with variable size

Solving for  $\psi_{i,j}$  gives

$$\begin{aligned} \psi_{i,j} = & [B\{(1+S^2) \psi_{i+1,j} + S(S^2+1) \psi_{i-1,j}\} \\ & + A\{(1+Z^2) \psi_{i,j+1} + Z(Z^2+1) \psi_{i,j-1}\} \\ & + A \times B \Omega_{i,j}] / E \end{aligned} \quad (3.20)$$

where

$$A = (1+S) \Delta X_2^2 \quad (3.21)$$

$$B = (1+Z) \Delta Y_2^2 \quad (3.22)$$

$$\text{and } E = B(1+S)(1+S^2) + A(1+Z)(1+Z^2) \quad (3.23)$$

Equation (3.20) was solved by using the Gauss-Siedel iteration technique with an over-relaxation factor of 1.6. This factor was chosen by trial and error and was employed to accelerate the iterative process. The variation of the number of iterations for various over-relaxation factors for a typical computer program is shown in Figure (3-4), (ref. Roache [1976]).

The over-relaxation factor ( $\omega$ ) was used in determining the stream function value by the following equation, (see Hornbeck, R.W. [1975]),

$$\psi_{i,j}^{(\ell+1)} = \omega \psi_{i,j}^{(\ell+1)*} + (1-\omega) \psi_{i,j} \quad (3.24)$$

where  $(\ell+1)$  is the current iteration and  $(\ell)$  is the preceding iteration. The quantity  $\psi_{i,j}^{(\ell+1)*}$  was the value of the

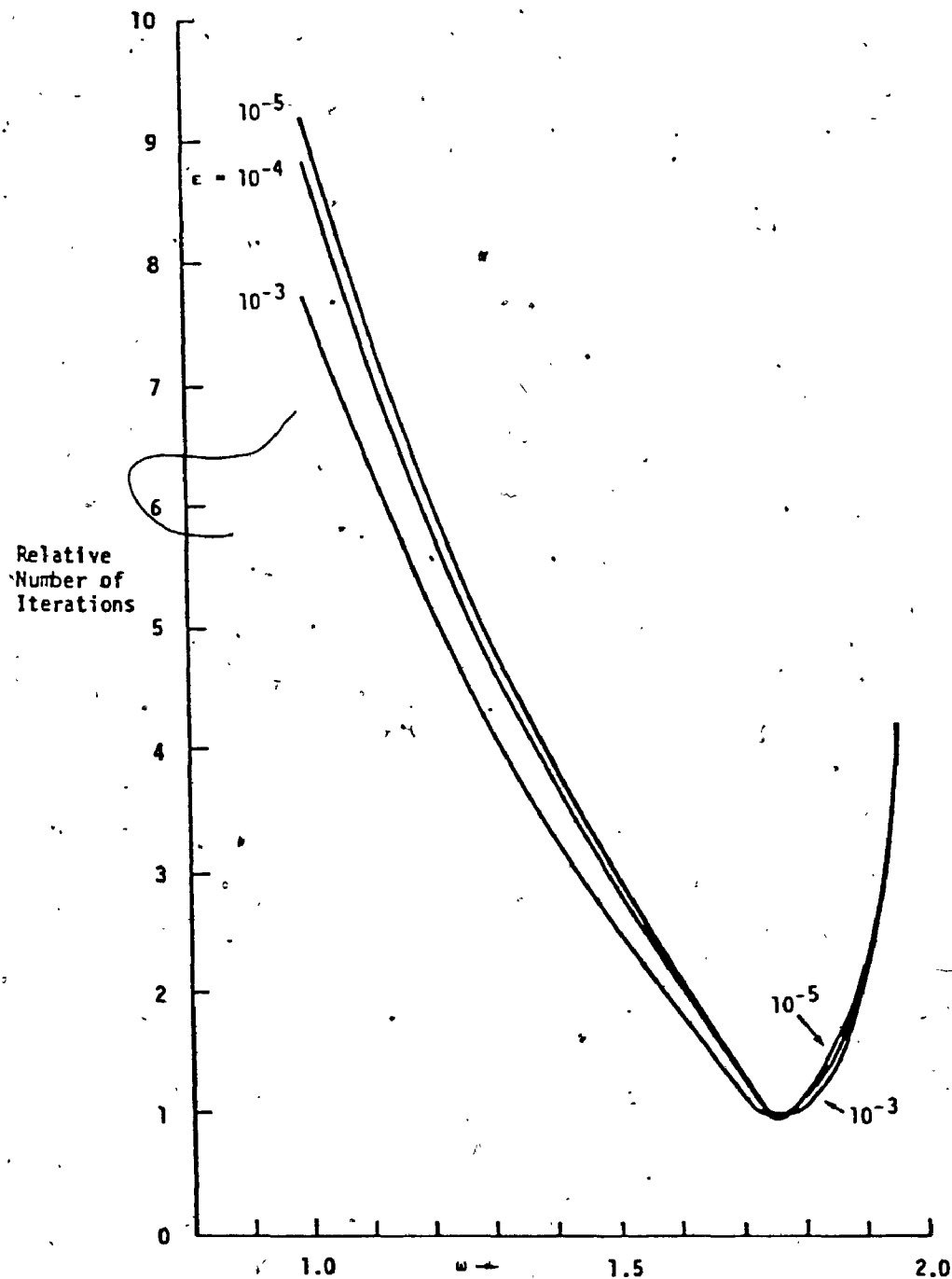


Figure (3-4) Relative number of iterations based on  
 $\psi_{\max}^{(k+1)} - \psi_{\max}^{(k)} = \epsilon$  from Roache [1976].

stream function obtained from the current iteration using Equation (3.20).

The iteration was terminated when a convergence criterion of the form:

$$\left| \psi_{i,j}^{(\ell+1)} - \psi_{i,j}^{(\ell)} \right| \leq \epsilon$$

was satisfied.

In this analysis an order of accuracy value was chosen to be  $\epsilon = 10^{-3}$ , since it was uneconomical and impractical to consider a higher accuracy since the equations were first order accurate in  $\Delta X$ .

#### 3.4 FINITE DIFFERENCE ANALOGUE FOR THE VORTICITY (HELMHOLTZ) EQUATION

An implicit method was employed in order to eliminate the stability problems when using larger time steps. It was recommended by Dwyer and McCroskey [1972] to use implicit schemes because of the stability problems that can occur with explicit methods when solving the flow field near the leading edge of a solid body. The following finite-difference approximations were used to replace the individual terms of Equation (3.7) when applied to a typical field point  $(i, j)$ :

$$\left[ \frac{\partial \Omega}{\partial t} \right]_{i,j} \approx \frac{\Omega_{i,j}^{(k+1)} - \Omega_{i,j}^{(k)}}{\Delta t} \quad (3.25)$$



$$\left[ \frac{\partial \Omega}{\partial x} \right]_{i,j} \approx \frac{\Omega_{i+1,j} - \Omega_{i-1,j}}{\Delta X_i + \Delta X_{i-1}} \quad (3.26)$$

$$\left[ \frac{\partial \Omega}{\partial y} \right]_{i,j} \approx \frac{\Omega_{i,j+1} - \Omega_{i,j-1}}{\Delta Y_j + \Delta Y_{j-1}} \quad (3.27)$$

Writing the spatial derivatives at the new time level (k+1) and substituting into Equation (3.7) gives,

$$\begin{aligned} \frac{\Omega_{i,j}^{(k+1)} - \Omega_{i,j}^{(k)}}{\Delta t} + \left[ u_{i,j} \frac{\Omega_{i+1,j} - \Omega_{i-1,j}}{\Delta X_i + \Delta X_{i-1}} \right]^{(k+1)} \\ + \left[ v_{i,j} \frac{\Omega_{i,j+1} - \Omega_{i,j-1}}{\Delta Y_j + \Delta Y_{j-1}} \right]^{(k+1)} = 0 \end{aligned} \quad (3.28)$$

Rearranging Equation (3.28), the following equation was then obtained:

$$\begin{aligned} \Omega_{i,j}^{(k+1)} + u_{i,j} \chi_1 (\Omega_{i+1,j} - \Omega_{i-1,j})^{(k+1)} \\ + v_{i,j} \chi_2 (\Omega_{i,j+1} - \Omega_{i,j-1})^{(k+1)} = \Omega_{i,j}^{(k)} \end{aligned} \quad (3.29)$$

where

$$\chi_1 = \Delta t / (\Delta X_i + \Delta X_{i-1}) \quad (3.30)$$

$$\text{and } \chi_2 = \Delta t / (\Delta Y_j + \Delta Y_{j-1}) \quad (3.31)$$

The velocities  $u_{i,j}$  and  $v_{i,j}$  were obtained by solving the stream function equation (Poisson's equation), Equation (3.20), at the new time step and substituting into the following equations:

$$u_{i,j} \approx \frac{\psi_{i,j+1} - \psi_{i,j-1}}{\Delta Y_{j-1} + \Delta Y_j} \quad (3.32)$$

$$v_{i,j} = - \frac{\psi_{i+1,j} - \psi_{i-1,j}}{\Delta X_{i-1} + \Delta X_i} \quad (3.33)$$

For the points adjacent to the outflow boundary or the leading edge of the flat plate, the spacial derivative with respect to x was obtained by taking the backward differences, hence, Equation (3.29) had the following form:

$$\begin{aligned} \Omega_{i,j}^{(k+1)} \left[ 1 + u_{i,j} \frac{\Delta t}{\Delta X_{i-1}} \right] - u_{i,j} \frac{\Delta t}{\Delta X_{i-1}} \Omega_{i-1,j}^{(k+1)} \\ + v_{i,j} \chi_2 (\Omega_{i,j+1} - \Omega_{i,j-1})^{(k+1)} = \Omega_{i,j}^{(k)} \end{aligned} \quad (3.34)$$

Similarly, for the points adjacent to the upper boundary, or near to the underside of the flat plate, backward differences were also employed to obtain the spacial derivative with respect to y. In this case Equation (3.29) took the form:

$$\begin{aligned} \Omega_{i,j}^{(k+1)} \left[ 1 + v_{i,j} \frac{\Delta t}{\Delta y_{j-1}} \right] + u_{i,j} \chi_1 (\Omega_{i+1,j} - \Omega_{i-1,j})^{(k+1)} \\ - v_{i,j} \frac{\Delta t}{\Delta y_{j-1}} \Omega_{i,j-1}^{(k+1)} = \Omega_{i,j}^{(k)} \end{aligned} \quad (3.35)$$

The application of Equations (3.29), (3.34) or (3.35) to the mesh points results in a system of linear algebraic equations which can be written in a matrix form as:

$$[A] \{\Omega\}^{(k+1)} = \{B\} \quad (3.36)$$

where [A] is a square matrix of coefficients, and {Ω} and {B} are column matrices. Solving these linear algebraic equations would result in obtaining the vorticity distribu-

tion at the new time step.

### 3.5 COMPUTATIONAL PROCEDURE FOR ONE STEP IN TIME LEVEL

The computational procedure for solving the finite-difference analogue, presented in Sections 3.2 and 3.3, for one step in time increment was as follows:

- 1) The stream function  $\psi$  and vorticity  $\Omega$  were assumed to be known at the  $k$  time level.
- 2) Knowing the values of  $\psi^{(k+1)}$  on the boundaries and  $\Omega^{(k+1)}$  on the upstream boundary, the relaxation method given in Section 3.2 was then used to get a better approximation for  $\psi^{(k+1)}$ .
- 3) A new velocity distribution  $u_{i,j}$  and  $v_{i,j}$  was obtained using Equations (3.32) and (3.33).
- 4) The corresponding lower wall and upper flat plate vorticity were then obtained from the stream function distribution using the relation  $\Omega_w = -\frac{\partial^2 \psi}{\partial y^2}$ .
- 5) The values of the velocities  $u_{i,j}$  and  $v_{i,j}$  were then substituted into the vorticity transport numerical analogue (Equations (3.29), (3.34) or (3.35)) to give a better approximate to the vorticity distribution at the new time level  $(k+1)$ .
- 6) Comparing  $\Omega^{(k+1)}$  with the previous approximation and on the condition that the convergence criteria had been achieved, go to step 7), otherwise return to step 2) and repeat.

- 7) Save the values of  $\psi_{i,j}^{(k+1)}$ ,  $u_{i,j}^{(k+1)}$ ,  $v_{i,j}^{(k+1)}$  and  $\Omega_{i,j}^{(k+1)}$  at the new time step.

Figure (3-5) shows the flow chart for the computational procedure at a general time step.

### 3.6 TIME INCREMENT CONTROL FACILITY

The solution routine was provided with a time increment control facility which made it possible to obtain a complete solution with less computer time.

Smaller time increments were used when the number of iterations between the Helmholtz equation and Poisson's equation had increased. This indicated rapid changes in the flow characteristics as the disturbances were close or in the solution domain. When the disturbances were far from the solution domain, flow characteristics had slower changes as well as less iterations were needed to obtain a solution. Hence, a larger time step was chosen such that the maximum time step used was equal to or less than that dictated by the stability conditions as will be discussed in Chapter 6.

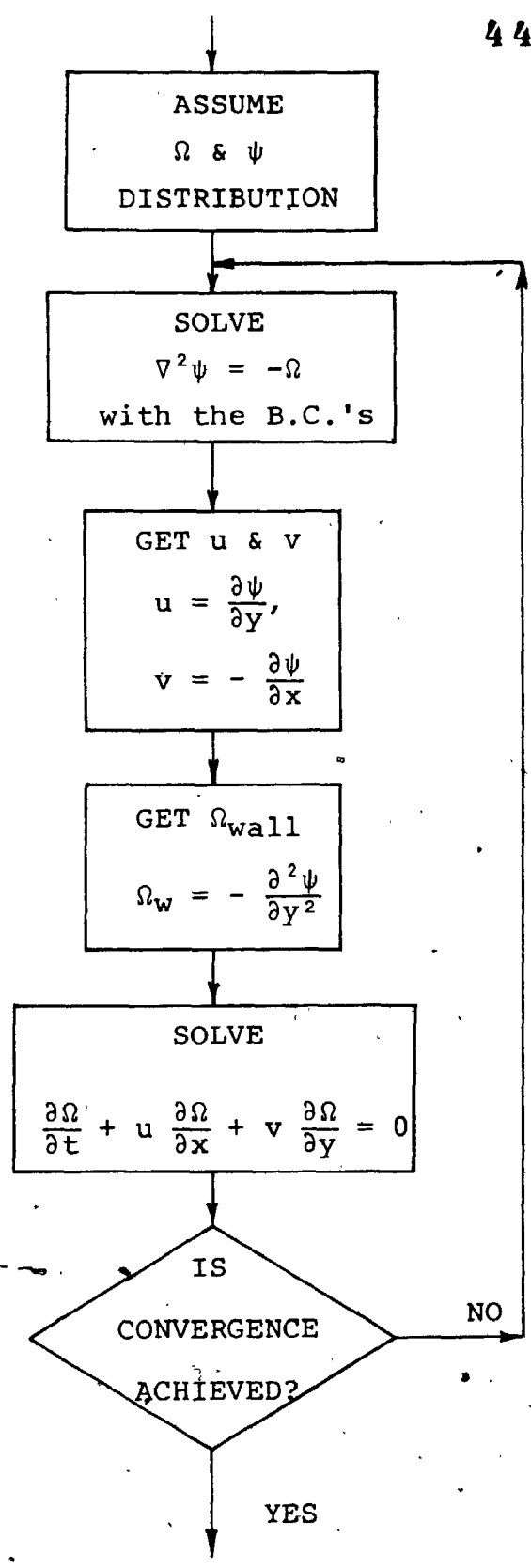


Figure (3-5)

Flow chart illustrating computational procedure at a general time step.

CHAPTER 4  
SIMPLE VORTEX MODELS  
AND THE VORTEX EXPRESSION

4.1 VORTEX FLOWS

In the numerical solution of the fluid flow equations the unsteady boundary conditions were provided by vortex models. One way of studying an unsteady rotational flow is by considering arrays of vortices moving in the fluid flow. The vortex, which is the basis of any vortex model, may be considered to be a circulatory motion around a stationary or a moving point in space. A potential vortex is the special case where the velocity, due to the vortex, at every point is perpendicular to the radius vector from the vortex centre. The value of the velocity is inversely proportional to the distance from the vortex centre. Clearly when the radius tends to zero, then for the potential vortex a singular point exists. A flow composed of such vortices would have many singularities at the vortex centres, but for the remainder of the region a potential would exist. The equation in terms of the potential, to solve for an incompressible, irrotational flow of such vortices is a linear equation. The complete solution may be obtained by summing several solutions in order that the initial and boundary conditions may be satisfied.

Onsager [1949] made a study of the interference effects of arrays of potential vortices of random sign. Using

statistical arguments, he showed that the vortices separate into positive and negative groups. Crow [1967] has shown how groups of potential vortices of the same sign tend to cluster.

The unsteady flow over bluff bodies was studied by Sarpkaya [1963]. By developing potential flow equations for the flow over a cylinder of arbitrary shape, with the addition of specified numbers of moving and growing vortices, he calculated the fluctuating lift and drag on the cylinder. The work illustrates how the structure of the free flow downstream of the cylinder can be related to the fluctuating loads on the cylinder.

These works on configurations of potential vortices are interesting as a means to model flows, but the essential requirement is for a potential to exist. In real turbulent flows, in general, this is not the case and a potential may not be defined since the flow is rotational. Prandtl and Tietjens [1934] and Lamb [1932] contain much of the earlier work on the theorems concerning vortex flows.

#### 4.2 SIMPLE VORTEX MODELS

Mathematical studies of vortex models are computed models of real unsteady rotational flows and the vortex is the essential fundamental element of these models.

Neither the "free vortex", where the tangential velocity varies inversely as the radius from the centre of the vortex, nor the "forced vortex", where in this case the

tangential velocity is proportional to the radius, are suitable vortex expressions for an actual real flow model. The potential vortex has a region of infinite velocity and it is an accepted fact that mathematical singularities do not occur in nature. The velocity of the forced vortex becomes too large at large distance.

Rankine (see Lamb [1932]) replaced the singularity at the centre of the vortex by a solid moving core of radius ' $r_c$ '. The tangential velocity within this core was given by,

$$V_{\theta} = \text{constant} \cdot r \quad (4.1)$$

Outside the vortex core, the tangential velocity was given by,

$$V_{\theta} = \text{constant} \cdot \frac{r_c^2}{r} \quad (4.2)$$

However, the Rankine Vortex, as defined above, is not a continuous function and therefore would not be suitable as a vortex expression for use as a vortex model.

The vortex generating function representing the velocity field of a vortex could be of the form,

$$V_{\theta} = f(\underline{x}, \underline{\xi}, \Gamma_1, r_c) \quad (4.3)$$

where  $V_{\theta}$  is the tangential velocity,  $\underline{x}$  is the field or observer point and  $\underline{\xi}$  is the vortex centre position. The terms  $\Gamma_1$  and  $r_c$  are called the variable constraints of the vortex generating function and are in this case the circu-



lation constant ( $\Gamma_1$ ) and the vortex core radius ( $r_c$ ) respectively. The variable constraints are either constant or functions of time.

Now the stream function of a modified Rankine Vortex can be defined as,

$$\psi = -\frac{\Gamma_1}{2\pi} \log_e \left[ (r_c^2 + (x - \xi)^2 + (y - \eta)^2) \right] + \text{constant} \quad (4.4)$$

and then, using Equations (3.3) and (4.4), the velocity components are,

$$u = -\frac{\Gamma_1}{\pi} (y - \eta)/D \text{ and } v = \frac{\Gamma_1}{\pi} (x - \xi)/D \quad (4.5)$$

The tangential velocity about the centre of the vortex ( $\xi, \eta$ ) from these two components is then,

$$V_\theta = \Gamma_1 r / \pi D \quad (4.6)$$

In these expressions  $D = r_c^2 + (x - \xi)^2 + (y - \eta)^2$  and  $\Gamma_1$  is the circulation constant and is the line integral of the tangential velocity  $(V_\theta)_{\max}$  around the vortex core.

Therefore

$$\Gamma_1 = 2 \pi r_c V_{\theta \max} \quad (4.7)$$

where the vortex core radius by definition, is the radius where the vortex tangential velocity is maximum.

The velocity distribution near the vortex centre varies approximately linearly with radius similarly to a forced

vortex and,

$$V_{\theta} \approx \left( \frac{\Gamma_1}{\pi r_c^2} \right) r \quad \text{when } r \ll r_c \quad (4.8)$$

At a much greater radius from the vortex centre compared with the vortex core radius, the modified Rankine Vortex behaves as a free vortex and,

$$V_{\theta} \approx \left( \frac{\Gamma_1}{\pi} \right) \frac{1}{r} \quad \text{when } r \gg r_c \quad (4.9)$$

The circulation, which is the line integral of the velocity around the vortex given by,

$$\Gamma = \oint_C \underline{V} \cdot \underline{ds} \quad (4.10)$$

increases steadily with increase of radius. When the radius is infinite then the circulation is twice the value of the "vortex circulation constant".

The vorticity distribution for the modified Rankine Vortex is derived from the equation,

$$\Omega = \frac{\partial v}{\partial x} - \frac{\partial u}{\partial y} \quad (4.11)$$

which gives,

$$\Omega = 2 \Gamma_1 r_c^2 / \pi D^2 \quad (4.12)$$

From Equation (4.12) it can be seen that the vorticity is a maximum at the vortex centre and at a radius equal to the vortex core radius, it reduces to a quarter of this value. At a long distance from the vortex centre, the vorticity tends to zero, showing the tendency to approach irro-

tational flow in this region.

The above mathematical vortex model could be used to simulate the two-dimensional rotational disturbance in a free stream. However, in the present work, where the vortex is between two parallel planes, a new mathematical model of a rotational vortex was derived, such that the lateral velocity component at the walls was zero.

#### 4.3 VORTEX EXPRESSION (EQUIVALENT TO MODIFIED RANKINE VORTEX)

In this Section an equivalent to the modified Rankine Vortex equation between two parallel planes was obtained. This equation was then used to represent the mathematical model of the rotational disturbance in the flow.

Writing the complex potential for a two-dimensional potential vortex,

$$w = -\frac{i\Gamma}{2\pi} \ln z \quad (4.13)$$

where

$$w = \phi + i\psi \quad (4.14)$$

$$\text{and } z = x + iy \quad (4.15)$$

When a potential vortex lies between two parallel planes, the image of the vortex in one plane produces an image in the other plane, and so on, until, to satisfy completely the pair of boundary conditions, an infinite

sequence of symmetrically placed images must be used.

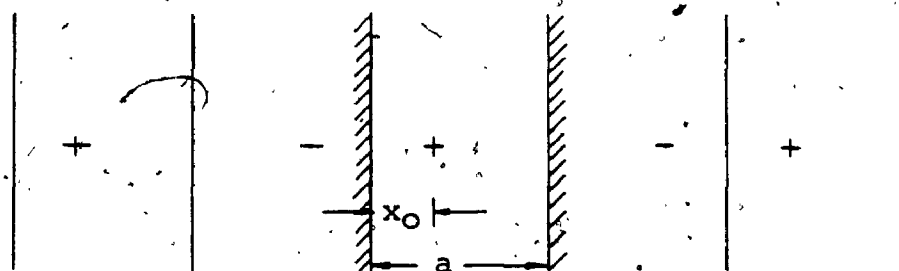


Figure (4-1) Periodic distribution of images

For instance, if the two planes are perpendicular to the  $x$  axis, one cutting through the origin and the other at  $x = a$ , and if the vortex is at  $x = x_0$  ( $x_0 < a$ ), then there must be a set of images at the points  $x = x_0 + 2ma$  ( $m = \pm 1, \pm 2, \dots$ ), all of the same sign as the original, plus another set of opposite signs at the points  $x = -x_0 + 2na$  ( $n = 0, \pm 1, \pm 2, \dots$ ) as in Figure (4-1).

The stream function due to this arrangement of the vortex plus its images is the imaginary part of the logarithm of a function which has poles at  $x = x_0 + 2ma$ , and zeros at  $x = -x_0 + 2na$ , (see Morse and Feshbach [1953]). Hence, the complex potential would be:

$$w = -\frac{i\Gamma}{2\pi} \ln \left\{ \frac{\sin[(\pi/2a)(x_0 + z)]}{\sin[(\pi/2a)(x_0 - z)]} \right\} \quad (4.16)$$

which is adjusted so that the function in parentheses is unity at  $x = 0$  and, by periodicity, it will be  $\pm 1$  at  $x = na$ . Therefore the complex potential of both parallel planes is zero.

In order to obtain the stream function value, the

imaginary part of Equation (4.16) was determined (see Appendix (B) for proof). The stream function value may be written as:

$$\psi = I(w) \quad (4.17)$$

$$\text{and } \psi = -\frac{\Gamma_0}{4\pi} \ln \left[ \frac{A+B}{C} \right] \quad (4.18)$$

where

$$A = [1 - K^2 \tan^2 cx - K^2 \tanh^2 cy + \tan^2 cx \tanh^2 cy]^2 \quad (4.19)$$

$$B = [2 K \tanh cy + 2 K \tan^2 cx \tanh cy]^2 \quad (4.20)$$

$$C = [(1 - K \tan cx)^2 + (K \tanh cy + \tan cx \tanh cy)^2]^2 \quad (4.21)$$

$$K = \cot \frac{\pi}{2a} x_0 \quad (4.22)$$

$$c = \frac{\pi}{2a} \quad (4.23)$$

Comparing Equation (4.18) to the stream function equation of a potential vortex which is of the form

$$\psi = -\frac{\Gamma_0}{2\pi} \ln r \quad (4.24)$$

this suggests that the value of  $\frac{A+B}{C}$  would act as an equivalent radial distance from the vortex centre to a field point.

It is shown in Appendix (B) that as A, B and C tend to a value of zero at the vortex centre, then the quotient  $\frac{A+B}{C}$  tends to a value of infinity. Therefore, in this

analysis the stream function expression used for a vortex positioned between two parallel planes was written in an equivalent form as follows:

$$\psi = \frac{\Gamma_0}{4\pi} \ln \left( \frac{C}{A+B} \right) \quad (4.25)$$

The quotient  $\frac{C}{A+B}$  now tends to zero as A, B and C tend to zero value.

Equation (4.25) can be written as

$$\psi = \frac{\Gamma_0}{2\pi} \ln r_e^* \quad (4.26)$$

where

$$r_e^* = \sqrt{\frac{C}{A+B}} \quad (4.27)$$

$r_e^*$  will be called the dimensionless equivalent radial distance from the vortex centre to a field point for a potential vortex between two parallel planes.

Equation (4.26) was used to test the finite-difference analogue and the method of solution presented in Chapter 3 when a potential vortex situated between two parallel planes approached the solution domain with no solid body within. The stream function values on the boundaries surrounding the solution domain were evaluated numerically using Equation (4.26), while the interior stream function distribution was obtained by numerically solving the Helmholtz and Poisson's equations. The exact and computed stream function values were in good agreement with a percentage deviation of about 0.01%.

In order to remove the singularity at the vortex centre, Equation (4.26) can be modified similarly to the classical modified Rankine Vortex.

The vortex expression (4.26) would now take the form:

$$\psi = -\frac{\Gamma_0}{2\pi} \ln(r_e^{*2} + r_c^{*2}) \quad (4.28)$$

where  $r_c^*$  is the dimensionless vortex core radius similar to  $r_e^*$  defined above.

The minus sign on the right-hand side of the above equation was so that the circulation was positive in the counter-clockwise sense  $\left[ \text{since } V_\theta = -\frac{\partial\psi}{\partial r} \right]$ .

To have zero stream function value on the walls, Equation (4.28) was rewritten again after subtracting a constant value from it which compensates for the addition of the dimensionless vortex core radius term, and

$$\begin{aligned} \psi &= -\frac{\Gamma_0}{2\pi} [\ln(r_e^{*2} + r_c^{*2}) - \ln(1 + r_c^{*2})] \\ &= -\frac{\Gamma_0}{2\pi} \ln \frac{r_e^{*2} + r_c^{*2}}{1 + r_c^{*2}} \end{aligned} \quad (4.29)$$

Equation (4.29) is the final form of the "real" vortex equation between two parallel planes, which was used in the computer program.

Figure (4-2) shows the contour plot of Equation (4.26) for a potential vortex positioned mid-way between the planes and Figure (4-3) shows the vortex offset from the centre line. Similarly, streamline contour plots for a rotational vortex are shown in Figures (4-4) and (4-5). Figure (4-6) shows

### PLOTTING DERIVED EQUATION OF STREAM FUNCTION

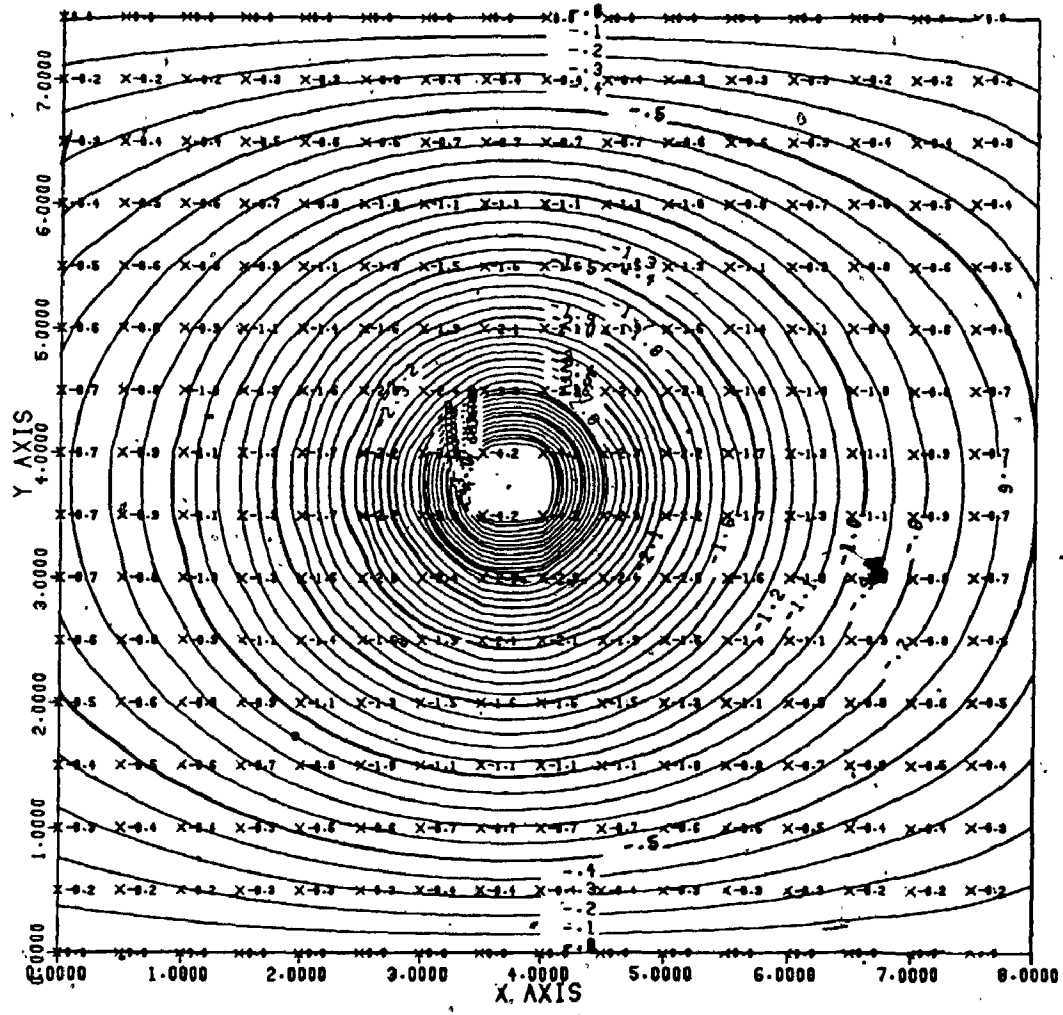


Figure (4-2) Potential vortex midway between two parallel planes.



## PLOTTING DERIVED EQUATION OF STREAM FUNCTION

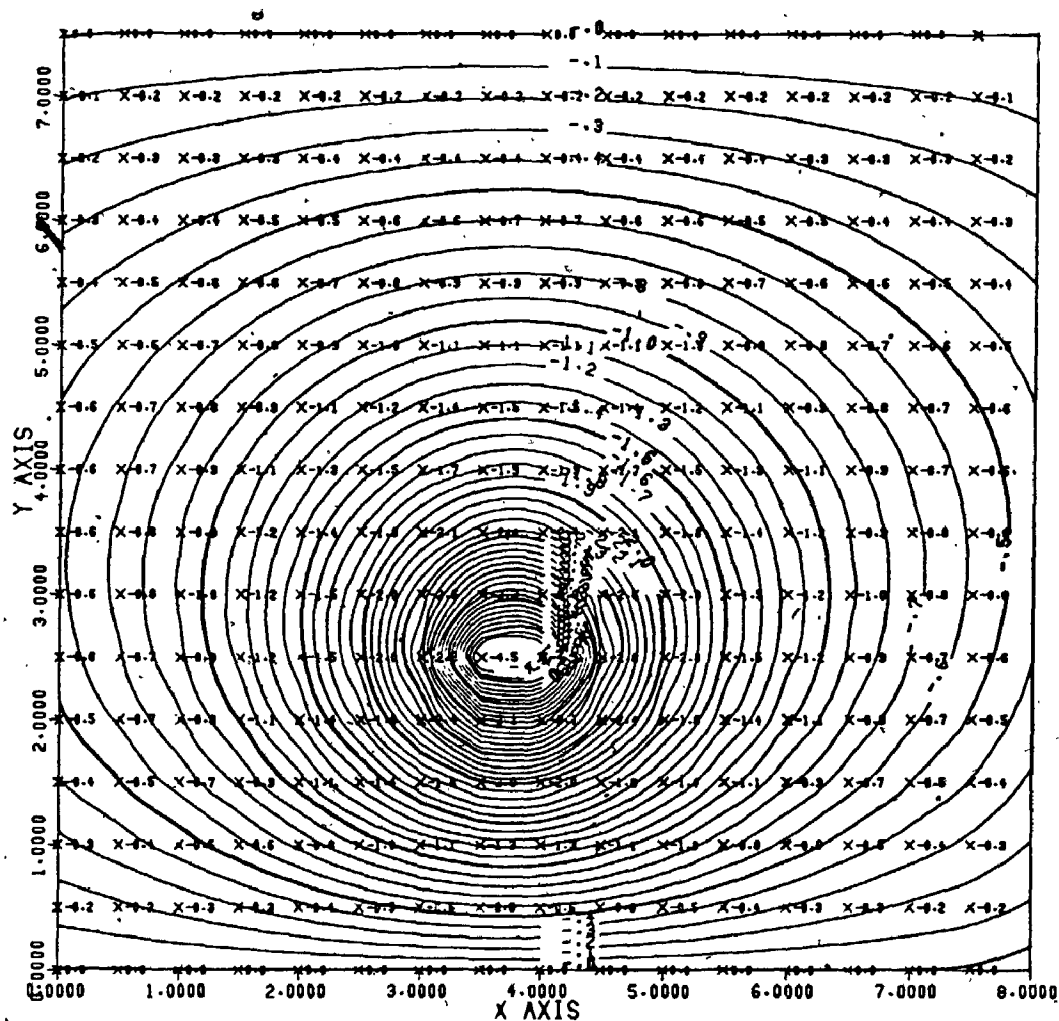


Figure (4-3) Potential vortex at one-third the distance between the two parallel planes.

PLOTTING DERIVED EQUATION OF STREAM FUNCTION

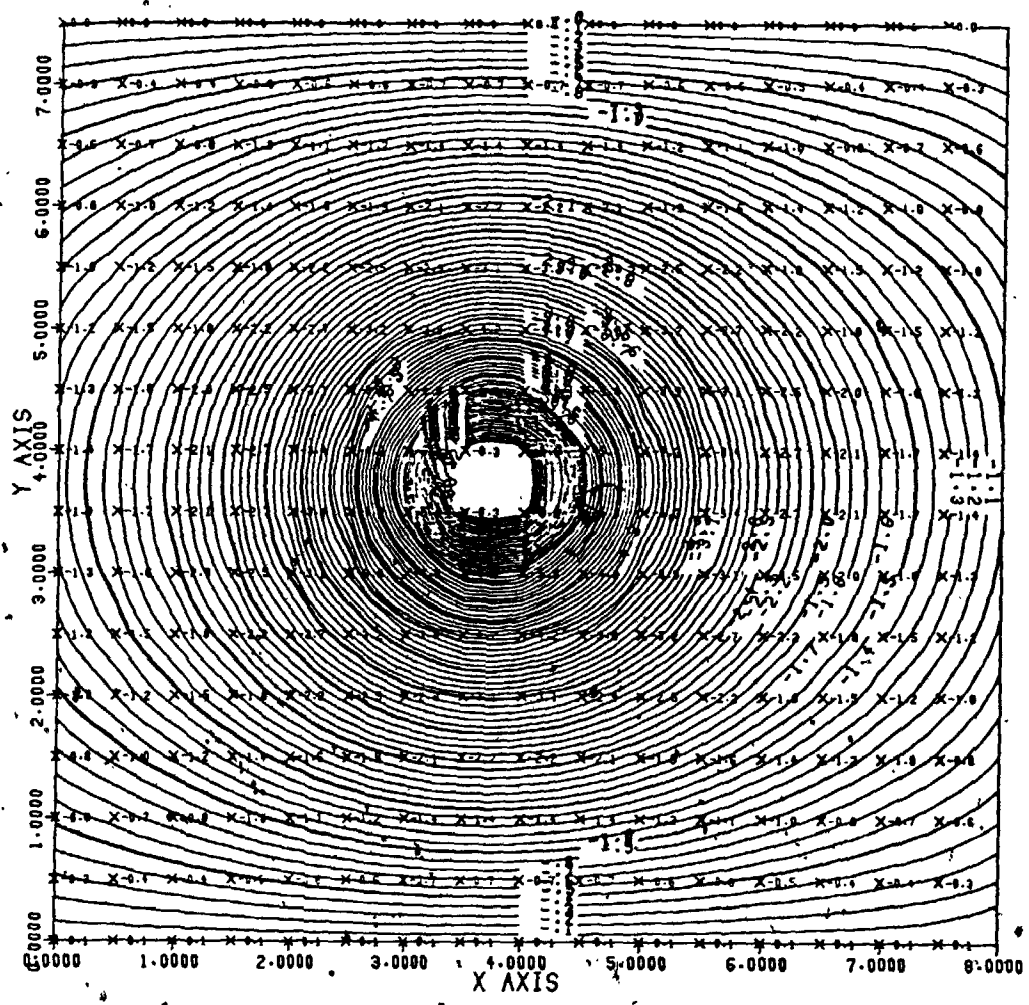


Figure (4-4) Rotational vortex midway between two parallel planes:

PLOTTING DERIVED EQUATION OF STREAM FUNCTION

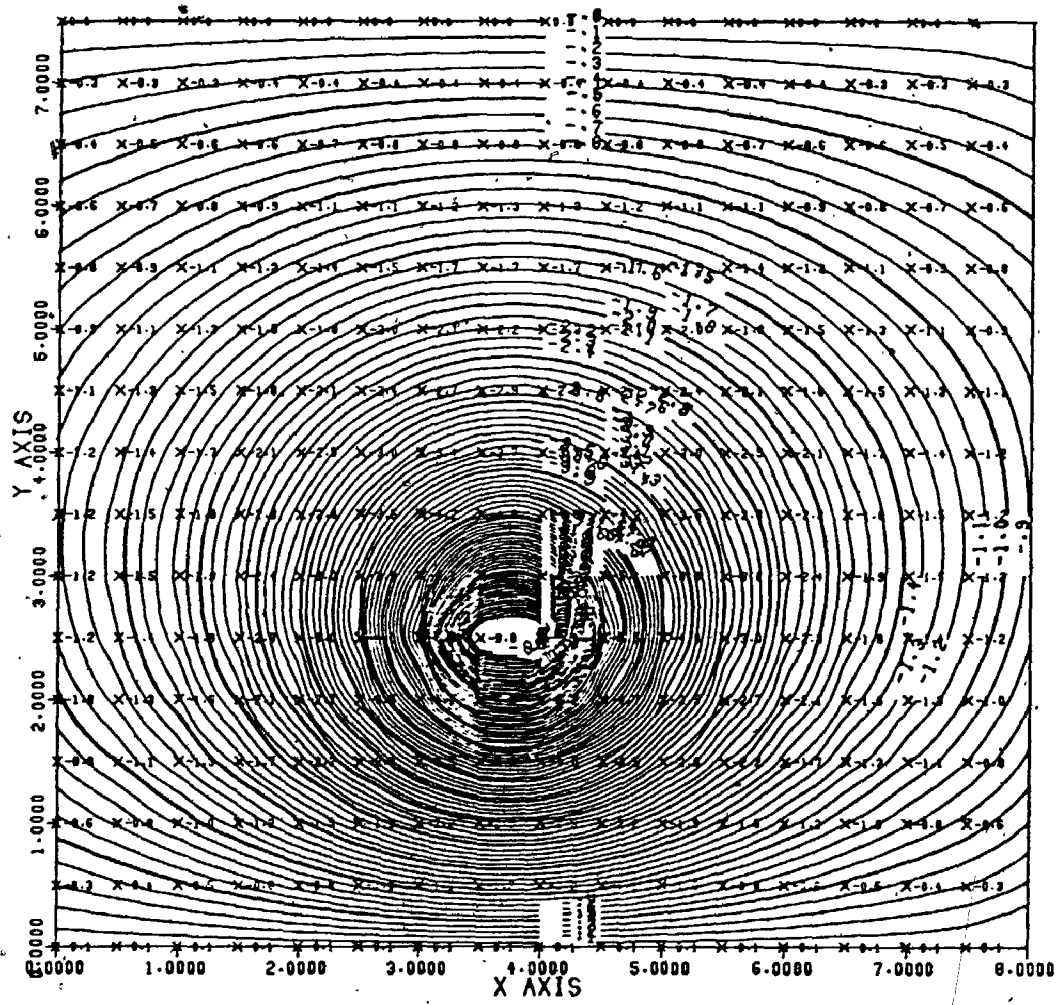


Figure (4-5) Rotational vortex at one-third the distance between the two parallel planes.

## ARRAY OF FIVE VORTICES (ROTATIONAL FLOW)

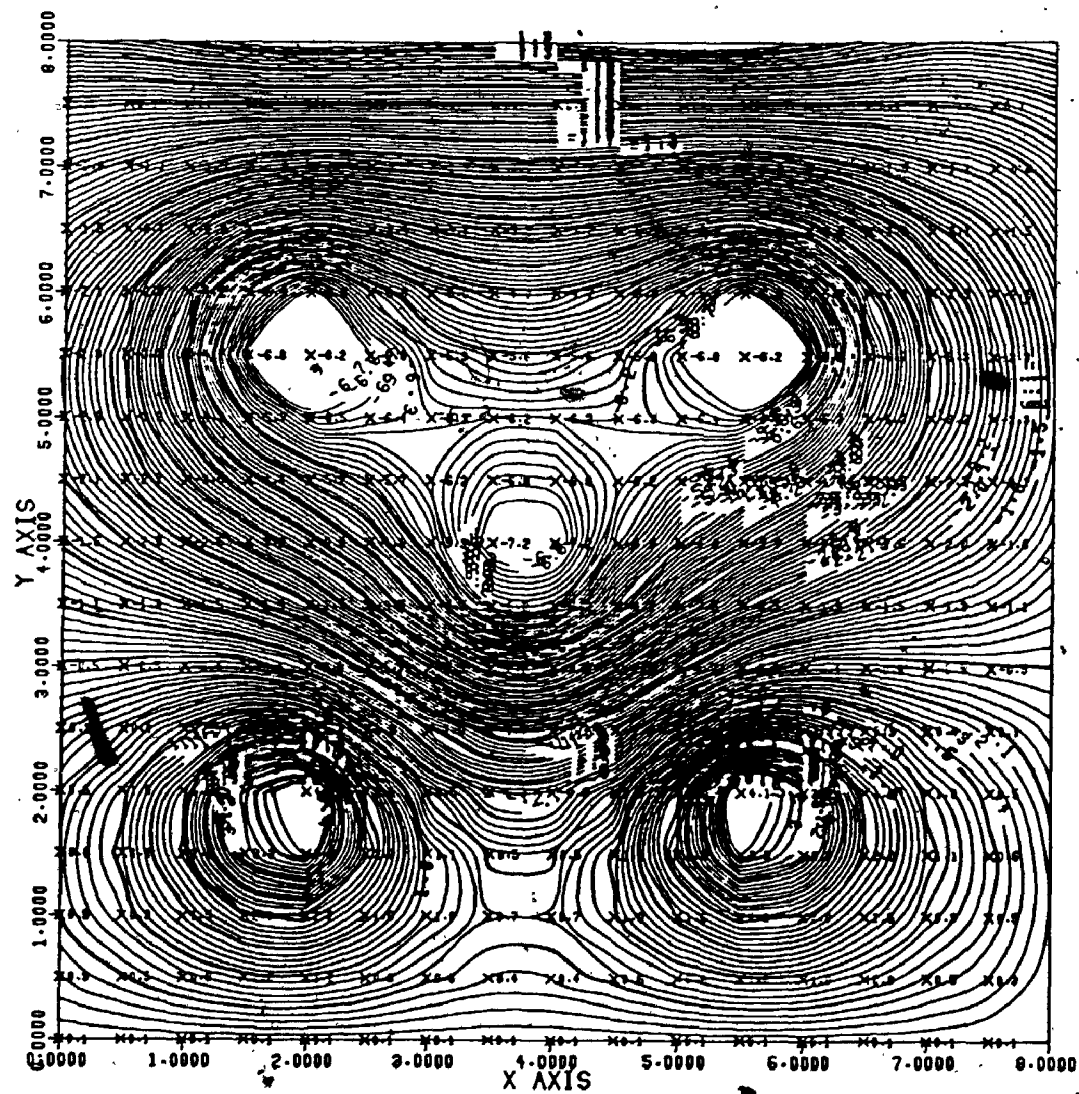


Figure (4-6) Array of five rotational vortices.

the combined effect of five vortices expressed by Equation (4.29) in the flow domain.

In the case of the flow in the x direction, simply x and y are interchanged in the equation of  $r_e^*$ , while x would be expressed as:

$$x = x_0 - U_c t \quad (4.30)$$

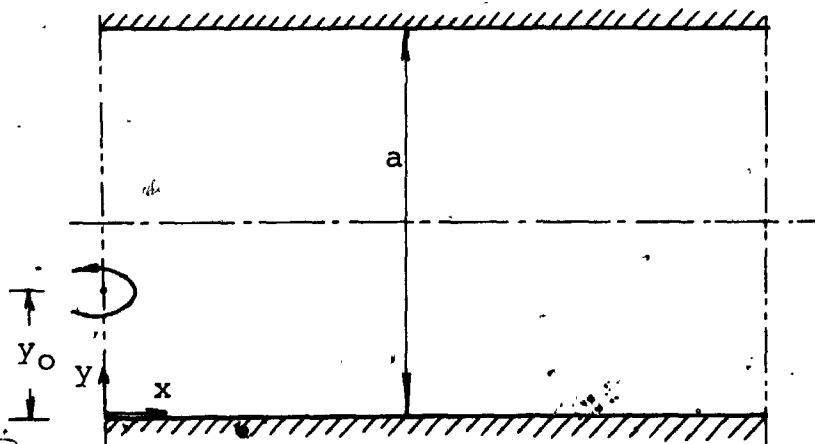
where  $x_0$  is the initial x coordinate for the vortex centre,  $U_c$  is the convective vortex velocity, and t is the time.

In this case K would take the form:

$$K = \cot \frac{\pi}{2a} y_0 \quad (4.31)$$

where  $y_0$  is the y coordinate for the vortex centre.

Figures (4-7) to (4-14) show the changes of the lateral velocity component (v) along the x axis and the longitudinal velocity component (u) along the y axis respectively, for different  $y_0/a$  ratios, where  $y_0$  is the distance from one of the planes to the vortex centre and 'a' is the distance between the planes as illustrated in the following diagram.



Vortex at the entrance of the domain

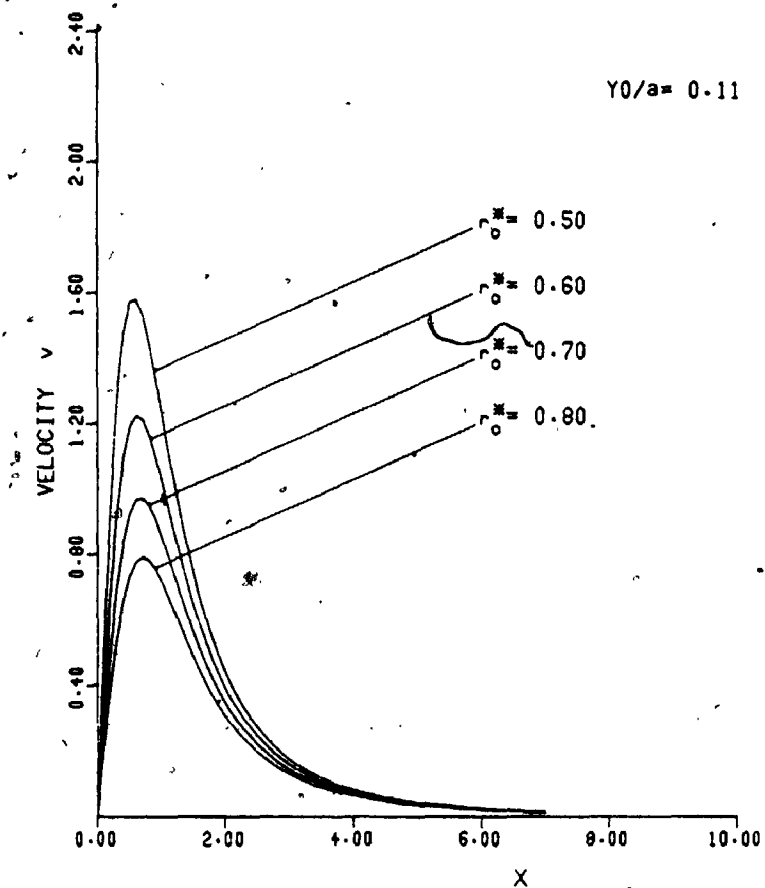


Figure (4-7)

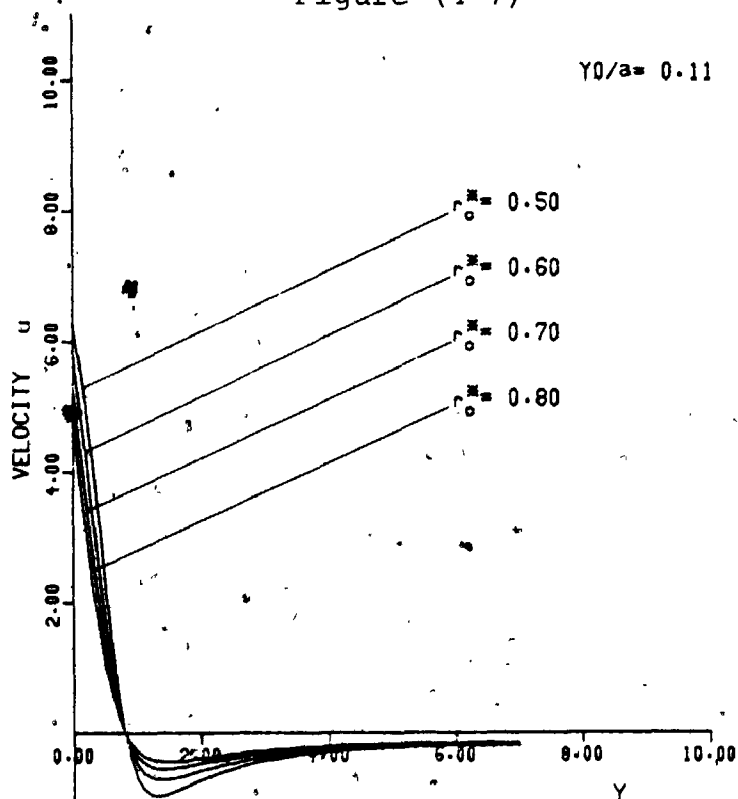


Figure (4-8)

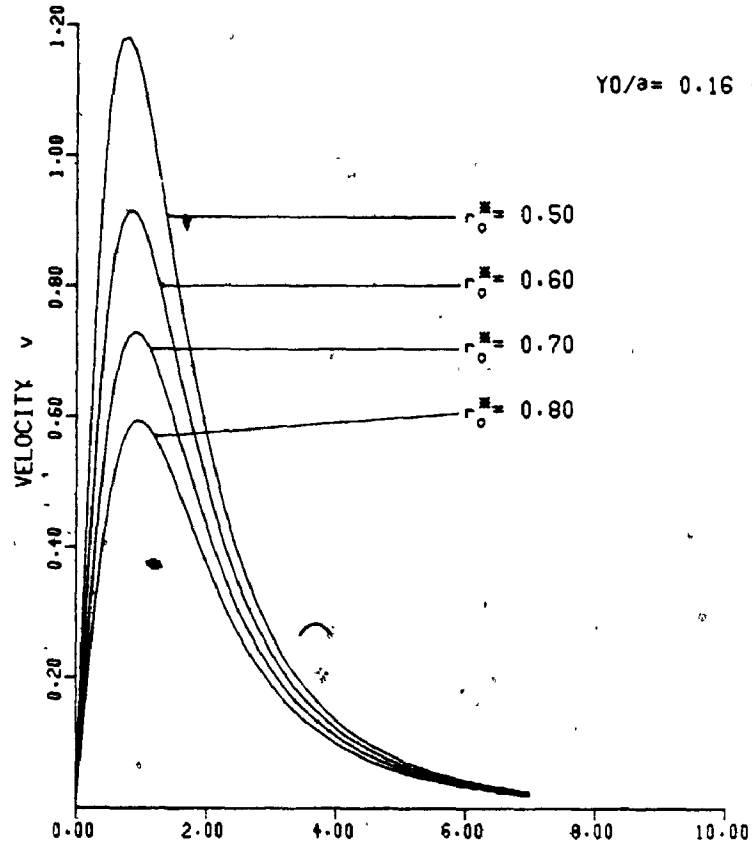


Figure (4-9)

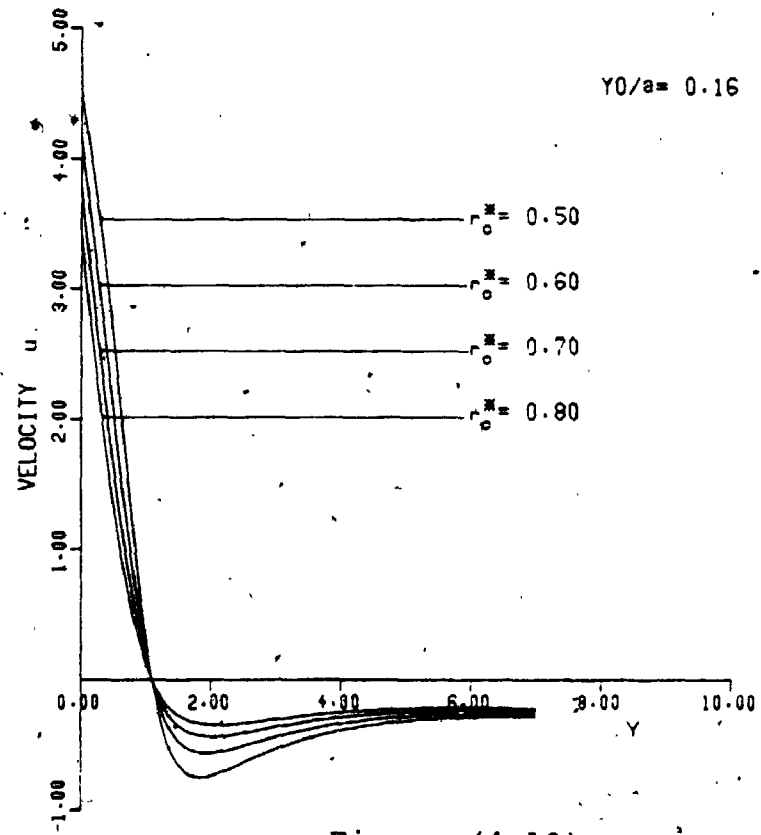


Figure (4-10)

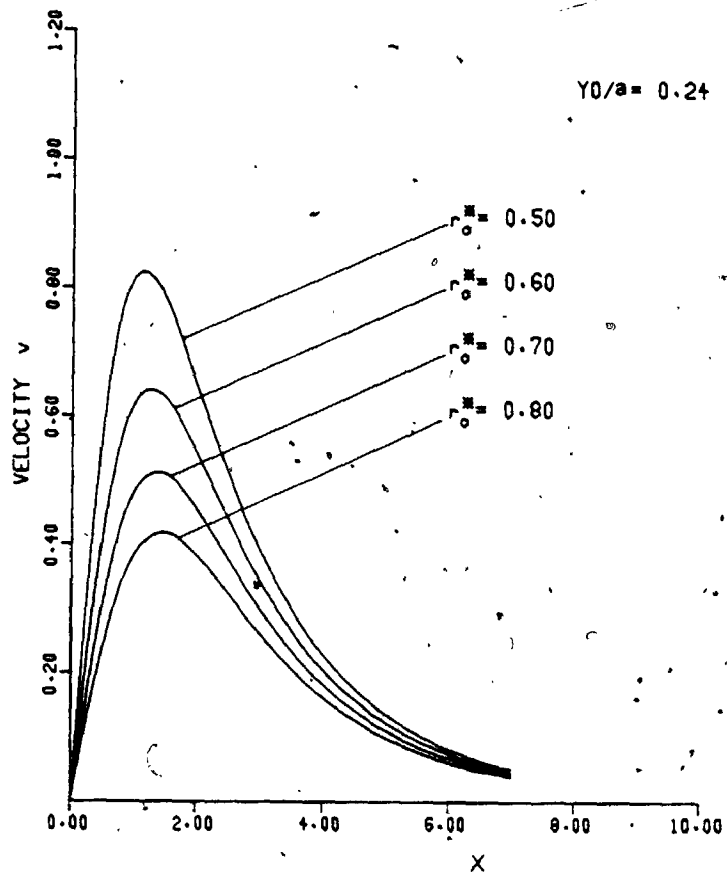


Figure (4-11)

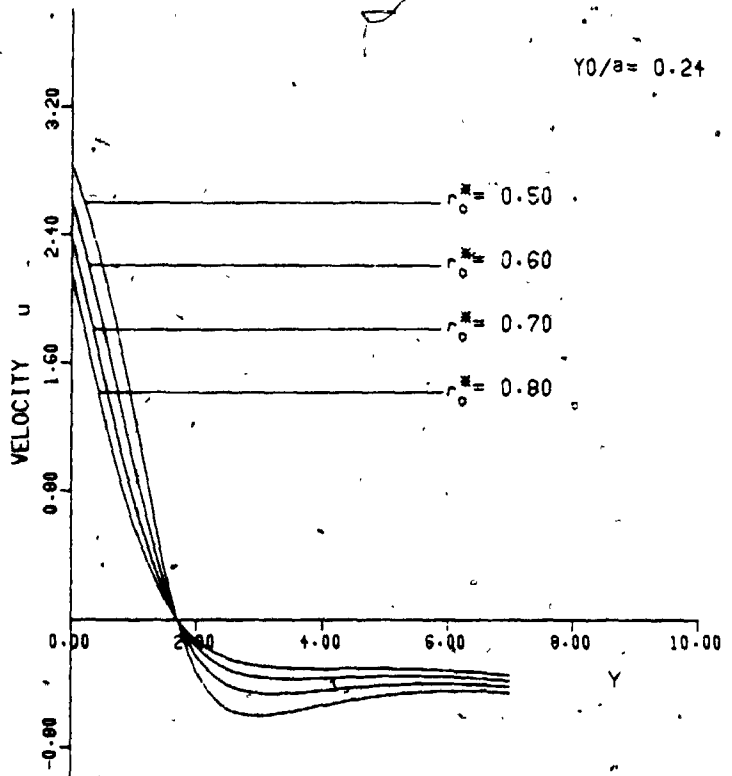


Figure (4-12)



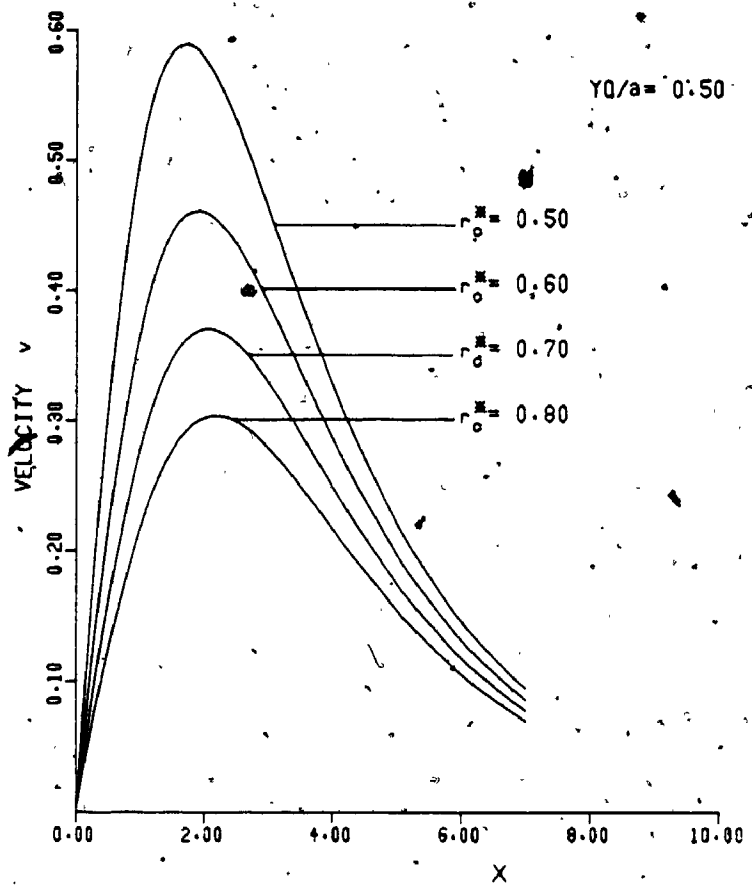


Figure (4-13)

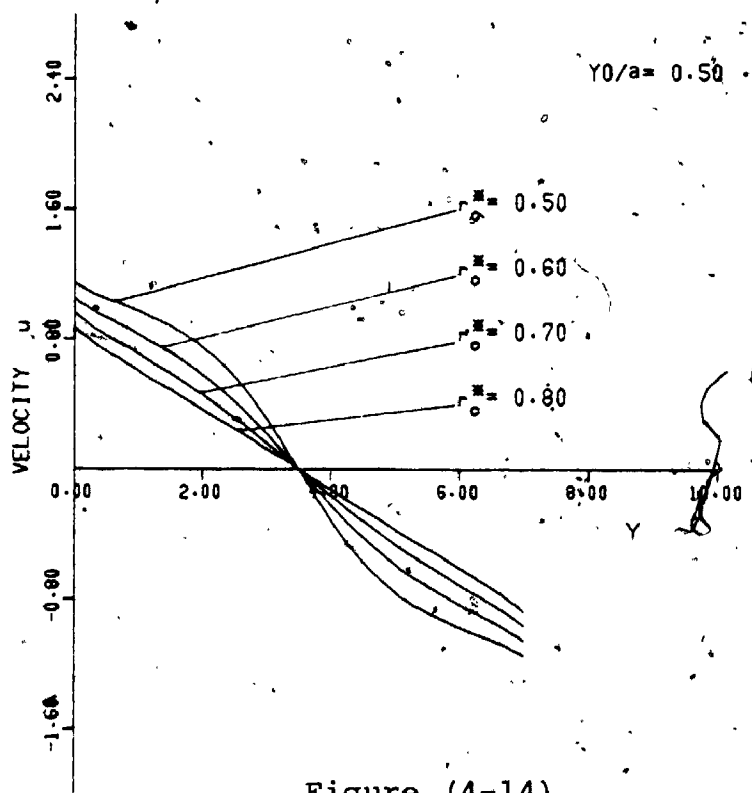


Figure (4-14)

An equation for a vortex situated between two parallel planes was also developed and reported by Thomson [1958] using a conformal mapping technique. However, the function developed by Thomson is limited only to a position on the centre-line between the two parallel planes, while as shown in Figures (4-2) to (4-6) the function, developed by the author, is flexible in both positions between the two plates, and also, is either potential or rotational.



## CHAPTER 5

### BOUNDARY CONDITIONS

#### 5.1 INTRODUCTION

This Chapter concerns the methods devised to determine the boundary conditions around the domain and on the flat plate. Meaningful solutions of physical problems involving field variables require adequate knowledge of the boundary conditions. The Navier-Stokes equations and the continuity equation, whose solutions are being sought, are the governing differential equations common to a variety of many flow patterns. These flow patterns can be drastically different from one another, not only quantitatively, but also in character, merely because of some differences in the imposed conditions at the flow boundaries. Improper or imprecise numerical treatment of the boundary conditions invariably leads to unreliable or unacceptable solutions. In recent years, considerable effort by many researchers has been in progress, to analyze the errors in numerical solutions caused by inconsistencies generated at the flow boundaries. Several authors treating different types of flow problems (see Wu [1976], Moretti [1969] and Roache [1976]) are all in agreement that the proper handling of boundary conditions is of dominant importance in the numerical solution of flow problems.

In most of the numerical studies carried out previously to solve flow problems, the boundary conditions were made

to satisfy certain assumptions which were approximations to the real physical problem. For example, in the work by Cheng [1972], Poiseuille flow was assumed at the upstream and downstream boundaries, while Smith and Brebbia [1975] assumed both the normal derivatives of the vorticity and stream function to have a value of zero at the exit enforcing the flow to be parallel even though within the domain flow disturbances occurred. The question arises how far must a downstream boundary be placed in a rotational flow over an obstacle before perturbations due to the obstacle in the flow are negligible and can be ignored.

The traditional boundary conditions used in numerical problems were either Dirichlet conditions where the function values were specified, Neumann conditions where the normal gradients were specified, or mixed conditions, sometimes called Robin's, where a weighted combination of function value and normal gradients are specified.

In the present work, Dirichlet type boundary conditions were used with modifications. The boundary conditions that can be used in a numerical scheme to simulate the real boundary conditions depend on the physical problem under consideration. In this work the emphasis was to study the time-dependent flow problem over a semi-infinite flat plate which was assumed to be situated midway between two parallel walls as shown in Figure (6-1) of Chapter 6.

The determination of the boundary conditions on the four sides of the flow field and on the flat plate were as

follows.

## 5.2 THE UPSTREAM BOUNDARY

Several methods have been recorded in the literature to specify the upstream boundary when dealing with the problem of flow over a solid body. In most of these studies the upstream boundary conditions were completely independent of the conditions inside the flow field. Examples of these approximations are the works by Pao and Daugherty [1969] who specified  $\Omega = 0$  and  $\frac{\partial \psi}{\partial y} = U_0$  thus fixing  $\psi$  on the upstream boundary and Kawaguti [1965] who used a solution for fully developed Poiseuille flow to fix both  $\psi$  and  $\Omega$ . In some other cases, the work by Thoman and Szewczyk [1969] for example, the upstream boundary conditions depended on the conditions inside the flow domain by assuming that  $v = -\frac{\partial \psi}{\partial x} = 0$  and hence  $\psi_{1,j} = \psi_{2,j}$  at that boundary, where suffices 1 and 2 imply the boundary and one mesh step within the domain respectively.

In the present work concerning a rotational disturbance approaching a thin flat plate, the upstream boundary conditions were assumed to be explicitly specified according to a special generating function and completely independent of the flow conditions within the domain.

The distribution of the stream function on the upstream boundary was obtained from the following expression:

$$\psi = \psi_U + \psi_V \quad (5.1)$$

$$= U_{\infty} * Y + \left( \frac{-\Gamma}{2\pi} \right) * \ln \frac{r_e^{*2} + r_c^{*2}}{1 + r_c^{*2}} \quad (5.2)$$

where

$\psi_U$  is the stream function due to the uniform flow,

$\psi_V$  is the stream function due to the vortex,

$U_{\infty}$  is the undisturbed velocity of approach,

$Y$  is the distance from the lower wall,

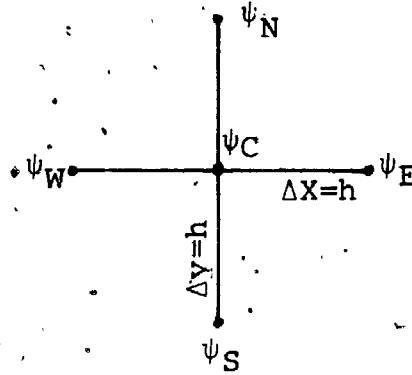
$\Gamma$  is the vortex strength,

$r_c^*$  is the vortex dimensionless core radius,

and  $r_e^*$  is the equivalent dimensionless radial distance from the vortex centre to a field point.

The derivation of the stream function and the equivalent dimensionless radial distance of a vortex between two parallel walls was shown in the previous Chapter. Equation (4.27) for evaluating the equivalent dimensionless radial distance ( $r_e^*$ ) takes into account the location of the vortex centre.

In the computer program it was found that it is more efficient to obtain the vortex stream function derivatives numerically (with respect to spatial coordinates) rather than using the full mathematical expression for them. The stream function values, due to the vortex, were calculated at the 'north', 'east', 'south', 'west', and at the centre of each upstream grid point as shown in the diagram on the following page.



*Obtaining vorticity at a point from stream function values*

The vorticity and the velocity components were obtained at each upstream grid point as follows:

$$\Omega_C = -\nabla^2\psi \approx -\frac{\psi_E + \psi_W + \psi_N + \psi_S - 4\psi_C}{h^2} \quad (5.3)$$

$$u_C = \frac{\partial\psi}{\partial y} \approx \frac{\psi_N - \psi_S}{2h} \quad (5.4)$$

$$v_C = -\frac{\partial\psi}{\partial x} \approx -\frac{\psi_E - \psi_W}{2h} \quad (5.5)$$

The subscripts E, W, N, S and C would denote east, west, north, south, and centre of each grid point respectively. The step  $h$  was taken with very small size ( $h = 0.0001$ ) but not too small a value to invoke large round-off errors. Subroutine 'VORT', in Appendix (D), was used to evaluate the vorticity and velocity components at each grid point.

### 5.3. THE BOUNDARY CONDITIONS AT THE UPPER AND LOWER PLANES

Since  $v = -\frac{\partial\psi}{\partial x} = 0$  on the upper and lower walls, then the stream function value  $\psi$  will be constant with respect to  $x$  along these boundaries. The constant stream function values were determined from the known upstream conditions.

The lower wall stream function value was taken to be zero, while the upper value was calculated from the integral,

$$\psi = \int u \, dy \quad (5.6)$$

Since the volume flow rate of fluid along the channel due to the vortex is zero then:

$$\psi_{\text{upper plane}} = U_{\infty} * H \quad (5.7)$$

where H is the distance between the two walls.

The vorticity values were only required on the lower wall, since for inviscid, incompressible fluid flow, the vorticity equation is a first order, non-linear partial differential equation with respect to space and time, (See Equation (3.7)).

The vorticity on the lower plane was estimated from the stream function-vorticity relationship as follows:

$$\begin{aligned} \bar{\Omega} &= - \nabla^2 \psi \\ &= - \left( \frac{\partial^2 \psi}{\partial x^2} + \frac{\partial^2 \psi}{\partial y^2} \right) \end{aligned}$$

Since  $\frac{\partial^2 \psi}{\partial x^2} = 0$  along the planes, then:

$$\begin{aligned} \Omega_{\text{plane}} &= - \frac{\partial^2 \psi}{\partial y^2} \\ &\approx - \frac{\psi_{\text{plane}} - 2\psi_1 + \psi_2}{\Delta Y^2} + 0(\Delta Y) \end{aligned} \quad (5.8)$$

It is of interest that for the case of a viscous fluid flow, the method used to determine plane vorticity from the



stream function would remain the same.

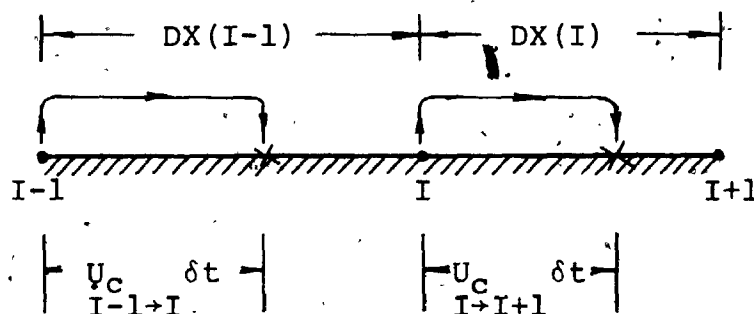
Because the computer program was written for variable mesh size, then this enabled the first four rows of grid points near the parallel planes to be of equal smaller spacings than within the domain in order to increase the first order accuracy of their vorticity values (see Equation (5.8)).

Recently, Cooke [1981] developed independently a similar approach which extrapolated the stream function near the wall to obtain the wall vorticity and numerically satisfy the no-slip condition in a viscous fluid flow.

Before the general method of solution was applied, a preliminary method was introduced to predict initial plane vorticity values. These vorticity values could then be used as the first estimate of the plane vorticity values in the iterative process for obtaining a complete solution at the new time step.

The approach was based on the fact that for inviscid, incompressible unsteady fluid flow between two parallel planes, the planes are always streamlines for all time. Also, from the Helmholtz vorticity equation for an inviscid fluid flow which is  $\frac{D\Omega}{Dt} = 0$ , then this implies that the vorticity is convected along each streamline with the same constant value.

The diagram on the following page shows the value of the vorticity at a general plane point I and at a general time level k which is written  $(\Omega^k(I))$ .



Estimating plane vorticity at a general time step

This value would move to a new position at the new time step, the coordinate of which is given by the expression  $U_C \delta t$ . The same analysis can also be applied to the vorticity at the point (I-1). By interpolating between these two new positions for the vorticity value then:

$$\Omega^{k+1}(I) \approx \Omega^k(I-1) + \left( \frac{Dx(I-1) - U_C \delta t}{U_C \delta t + Dx(I-1) - U_C \delta t} \right) * (\Omega^k(I) - \Omega^k(I-1)) \quad (5.9)$$

where the superscripts  $k$  and  $k+1$  denote the present and new time level respectively.

The convective velocities are calculated as the average velocities between the two neighbouring points at the present time level.

$$U_C_{I-1 \rightarrow I} = \frac{U^k(I-1) + U^k(I)}{2} \quad (5.10)$$

$$U_C_{I \rightarrow I+1} = \frac{U^k(I) + U^k(I+1)}{2} \quad (5.11)$$

By using this method in the solution routine; it was

possible to save approximately 15% of the computer time in order to obtain a complete solution.

#### 5.4 THE OUTFLOW BOUNDARY CONDITIONS

In a typical numerical solution, the evaluation of the stream function and vorticity at the outflow boundary is one of the most interesting computational boundary problems. In order to avoid large computational time in the case of studying the unsteady flow over an obstacle, a method to predict the downstream boundary conditions close to the obstacle is developed. This technique avoids the long integrations necessary to a downstream boundary where perturbations are of small order of magnitude.

Plotkin *et al* [1968] and Yoshizawa [1970], approached the downstream boundary problem by using an asymptotic solution applicable at large, but finite, distances from the region of interest. In the work by Allen and Southwell [1955], Michael [1966], and Son and Hanratty [1969], a potential flow solution was used to simulate the downstream conditions. Katsanis [1967] used uniform flow with  $u =$  constant and  $v = 0$  at the upstream and downstream boundaries, whereas Paris and Whitaker [1965] used a less restrictive type of downstream boundary where  $v = 0$  and established flow existed such that  $\frac{\partial \Omega}{\partial x} = 0$ , were assumed at the outflow of a two-dimensional channel. Roache [1976] stated that from previous experience when solving flow problems numerically, that catastrophic instabilities may be propagated

upstream from the outflow boundary, and cause the solution to go numerically unstable. The same author presented a well documented survey of the boundary conditions used previously with fluid flow problems.

In the present work, the problem concerns a real vortex with distributed vorticity approaching a thin flat plate. The fluid is assumed to be incompressible and inviscid, and the approaching flow is two-dimensional, unsteady and rotational. Rewriting the governing equations introduced in Chapter 3, which are:

$$\nabla^2 \psi = - \Omega \quad (3.6)$$

$$\frac{\partial \Omega}{\partial t} + u \frac{\partial \Omega}{\partial x} + v \frac{\partial \Omega}{\partial y} = 0 \quad (3.7)$$

It can be seen that both the stream function  $\psi$  and the vorticity  $\Omega$  are functions of the independent variables, the spatial variables "x, y" and the time "t", although the independent variable "t" is not explicitly present in Equation (3.6).

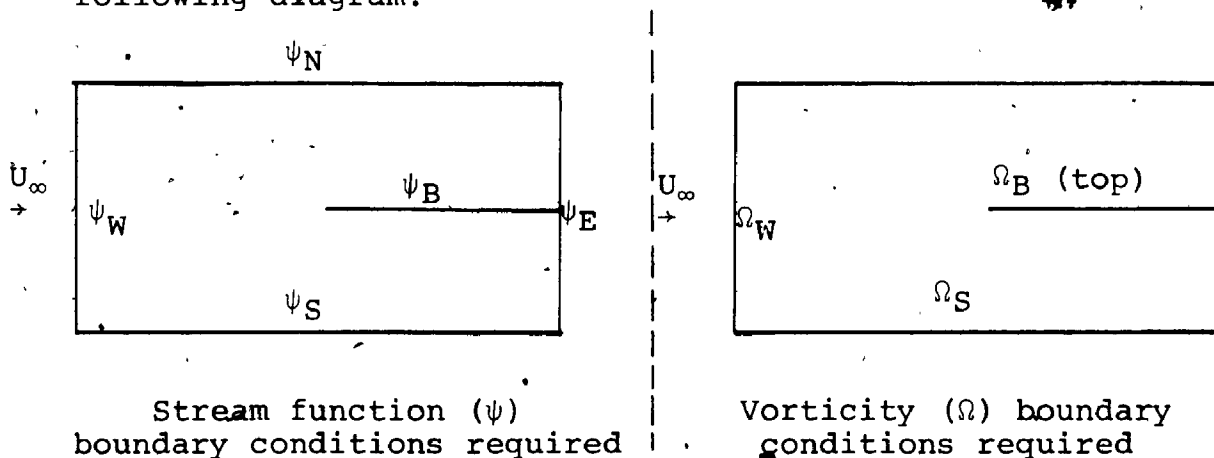
That is:

$$\psi \equiv \psi (x, y, t) \quad (5.12)$$

$$\text{and } \Omega \equiv \Omega (x, y, t) \quad (5.13)$$

Equation (3-6) is a second order linear partial differential equation, and therefore, in two-dimensional space, requires the values of the stream function to be known on all exterior and interior boundaries.

Equation (3.7) however, is a first order non-linear differential equation in vorticity " $\Omega$ ", and therefore requires boundary conditions only at parts of the boundary, preferably where "inflow" occurs. This is shown in the following diagram.



Where the subscripts N, S, E, W and B denote North, South, East, West and body (flat plate) respectively.

Therefore, in order to obtain a solution for Equation (3.7), it is not necessary to specify the vorticity at the outflow boundary.

For the stream function and the special case of uniform flow in the x-direction, changes in the x-direction are therefore an order of magnitude greater than the flow in the y-direction, and near the boundaries it can be written that:

$$\psi \doteq \psi(x, t) \quad (5.14)$$

Writing the Taylor series for this function in terms of the two variables, then:

$$\psi(t_0 + \delta t_2, x_0 + \delta x_2) = \psi(t_0, x_0) + \frac{(x-x_0)}{1!} \left[ \frac{\partial \psi}{\partial x} \right]_{x_0, t_0}$$

$$+ \frac{(t-t_0)}{1!} \left( \frac{\partial \psi}{\partial t} \right)_{x_0, t_0} + \dots + O(\delta t_2 \delta x_2) \quad (5.15)$$

Using centered differences to evaluate the stream function derivative with respect to  $x$ , with variable mesh size, gives the following approximate expression:

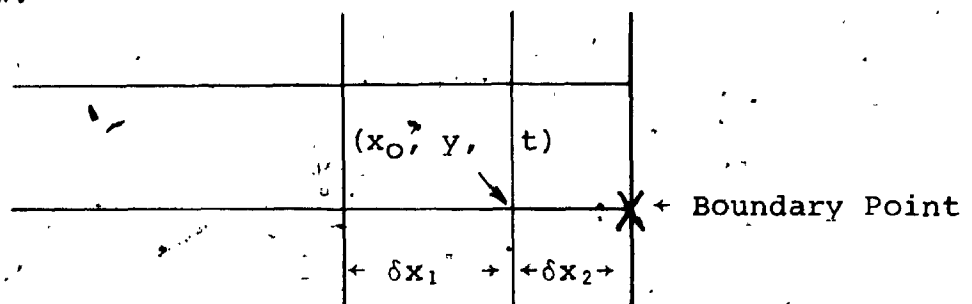
$$\left( \frac{\partial \psi}{\partial x} \right)_{x_0, t_0} \approx \frac{\psi(x_0 + \delta x_2) - \psi(x_0 - \delta x_1)}{\delta x_1 + \delta x_2} + \dots + O(\delta x) \quad (5.16)$$

It is of interest to note that if  $\delta x_1 = \delta x_2$ , Equation (5.16) would be of second order accurate (see Roache [1976]).

Using backward difference technique, a similar expression for the partial derivative of the stream function with respect to time, also gives:

$$\left( \frac{\partial \psi}{\partial t} \right)_{x_0, t_0} \approx \frac{\psi(x_0, t_0) - \psi(x_0, t_0 - \delta t_1)}{\delta t_1} + \dots + O(\delta t_1) \quad (5.17)$$

where  $\delta t_1$  is the previous time step,  $\delta t_2$  is the new time step and  $\delta x_1$  and  $\delta x_2$  are the mesh sizes which may be either constant in value or may vary. This is shown in the diagram below.



Boundary Point in a variable mesh size

Substituting Equations (5.16) and (5.17) into (5.15), would result in

$$\begin{aligned} \psi(t_0 + \delta t_2, x_0 + \delta x_2) &= \psi(t_0, x_0) \\ &+ [\psi(t_0, x_0 + \delta x_2) - \psi(t_0, x_0 - \delta x_1)] \\ &* \frac{\delta x_2}{(\delta x_1 + \delta x_2)} + [\psi(t_0, x_0) \\ &- \psi(t_0 - \delta t_1, x_0)] * \frac{\delta t_2}{\delta t_1} \end{aligned} \quad (5.18)$$

For constant space and time steps, Equation (5.18) reduces to the following expression:

$$\begin{aligned} \psi^{k+1}(x_0 + \delta x) &= 2\psi^k(x_0) + [\psi^k(x_0 + \delta x) \\ &- \psi^k(x_0 - \delta x)]/2 - \psi^{k-1}(x_0) \end{aligned} \quad (5.19)$$

where the superscript  $k$ , denotes the time level. In the solution, the interior point values near the outflow boundary,  $\psi^{k-1}(x_0)$ , can be stored as a vector and eventually save computer storage space.

A similar expression can be obtained for the vorticity by replacing  $\psi$  by  $\Omega$  when the outflow boundary vorticity values are required, as in the case of viscous fluid flow.

In this case the vorticity equation becomes a second order equation and the outflow boundary vorticity would be required, so that,

$$\begin{aligned} \Omega(t_0 + \delta t_2, x_0 + \delta x_2) &= \Omega(t_0, x_0) + [\Omega(t_0, x_0 + \delta x_2) \\ &- \Omega(t_0, x_0 - \delta x_1)] * \frac{\delta x_2}{\delta x_1 + \delta x_2} + [\Omega(t_0, x_0) \end{aligned}$$

$$- \Omega(t_0 - \delta t_1, x_0) \left[ \frac{\delta t_2}{\delta t_1} \right] \quad (5.20)$$

### 5.5 THE BOUNDARY CONDITIONS ON THE FLAT PLATE

On the flat plate, the lateral velocity component was always zero, so that

$$v = - \frac{\partial \psi}{\partial x} = 0$$

This meant that the stream function value  $\psi$  would be constant along the length of the flat plate.

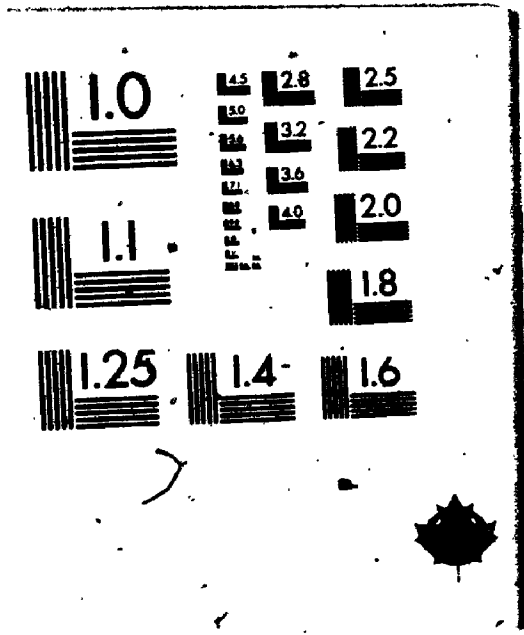
A similar technique with minor modifications to the prediction of the outflow boundary was adopted to estimate the new stream function value for the flat plate at the new time step.

Equation (5.8) was used to obtain the vorticity values on the upper side of the plate, since the lower side vorticity was not required to obtain a solution for the first order inviscid vorticity equation.

This Chapter has shown how in general the important boundary conditions are determined. The following Chapters utilize this theory together with the flow equations to obtain solutions of physical flow problems.



2



## CHAPTER 6

### THE EFFECT OF A "REAL" VORTEX APPROACHING A FLAT PLATE PLACED BETWEEN TWO PARALLEL PLANES IN AN INVISCID, INCOMPRESSIBLE FLUID FLOW

#### 6.1 INTRODUCTION

This Chapter investigates the effect of a two-dimensional rotational vortex approaching a flat plate, set at zero incidence, between two parallel planes in an inviscid, incompressible fluid flow. The vorticity stream function method, described fully in Chapter 3, was used to obtain the solution. The vortex expression obtained in Chapter 4, Equation (4.28), was used to simulate a rotational disturbance in the flow stream which affected the flow in the solution domain through its effect on the upstream boundary.

Figure (6-1) shows a schematic sketch of the fluid flow problem under consideration.

The flat plate was situated midway between the two parallel planes with its leading and trailing edges situated between the mesh points as shown. The main flow approached the flat plate from left to right with an undisturbed velocity of  $U_\infty$ , and the vortex was released at a distance  $x_0$  upstream of the solution domain and  $y_0$  from the lower plane. The introduction of the new outflow technique, discussed in Chapter 5, and also applying it to the flat plate, made it possible to expand the study to include variable chord lengths of the flat plate as will be seen during the course

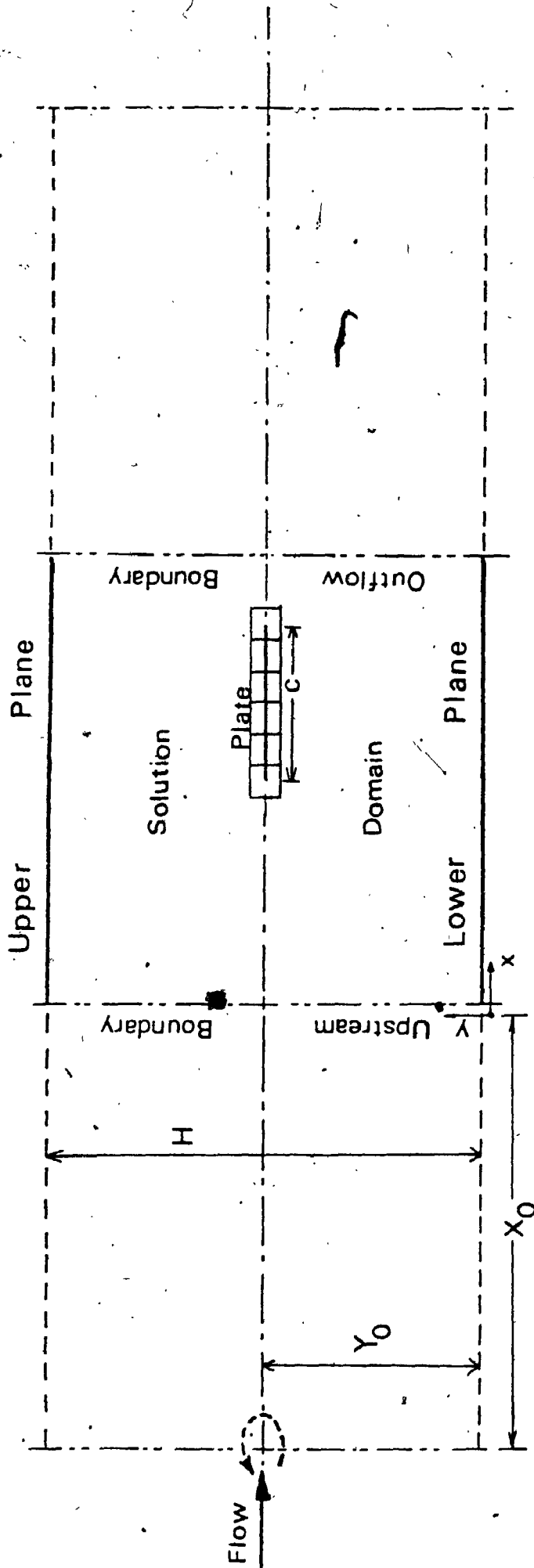


Figure (6-1) Schematic sketch showing the flow field with the finite-difference mesh near the flat plate.

of discussions. The limitation to the case of one approaching vortex simplified the analysis of the results and in this case was used to demonstrate the method. However, this does not imply a limitation to the method of solution as will be shown in Chapter 7 where a vortex array is studied. The effect of the vortex on the time variation of the stream function contours, and the lift and pitching moment coefficients on the flat plate were investigated as described in the following sections.

#### 6.2 EFFECT OF THE ROTATIONAL DISTURBANCE ON THE STREAM FUNCTION CONTOURS AND STABILITY CONDITIONS

This section investigates the effect of a rotational disturbance on the shape of the stream function contours and also the subsequent motion of the disturbance with time when originally positioned on the centreline between two parallel planes. Stream function contours were plotted at different time levels while the rotational disturbance was being convected by the main stream towards the plate, subsequently passing through the solution domain and finally exiting from the outflow boundary. Initially, a steady state solution, with zero vorticity, was assumed to exist in the flow field. The mathematical model presented in Chapter 4, where the flow disturbance was considered to be in the form of a "real" vortex, was used to simulate the flow stream disturbance. The centre of the equivalent modified Rankine vortex was assumed to be initially located far up-

stream of the solution domain such that its influence on the flow pattern at the upstream boundary of the solution domain was negligible. Figure (6-2) shows the initial stream function contours at time  $t = 0$ . The solution procedure for solving the time dependent governing equations, presented previously in Chapter 3, section 3.4 was used in this analysis. The boundary conditions were developed by using the methods mentioned earlier in Chapter 5. The introduction of the new technique to estimate the outflow boundary conditions based on previous flow within the solution domain at a previous time made it possible to solve this problem with minimal size of solution domain. The solution was continued until the vortex reached the upstream boundary of the solution domain. At this point in time, when the vortex entered the solution domain, it became a rotational disturbance. The resulting disturbance impinged on the flat plate and was then convected downstream allowing the flow region to return again to its original steady state. Figure (6-3) shows the vortex relative positions in the flow field, while Figure (6-4) shows the corresponding changes of the stream function values that took place at the outflow boundary. From Figure (6-5), for a channel flow without the flat plate, it can be seen that although the vortex was released midway between the two parallel planes, its centre was convected in the direction of rotation towards one of the planes upon reaching the solution domain. A possible explanation of this phenomenon is that this shift can be attributed

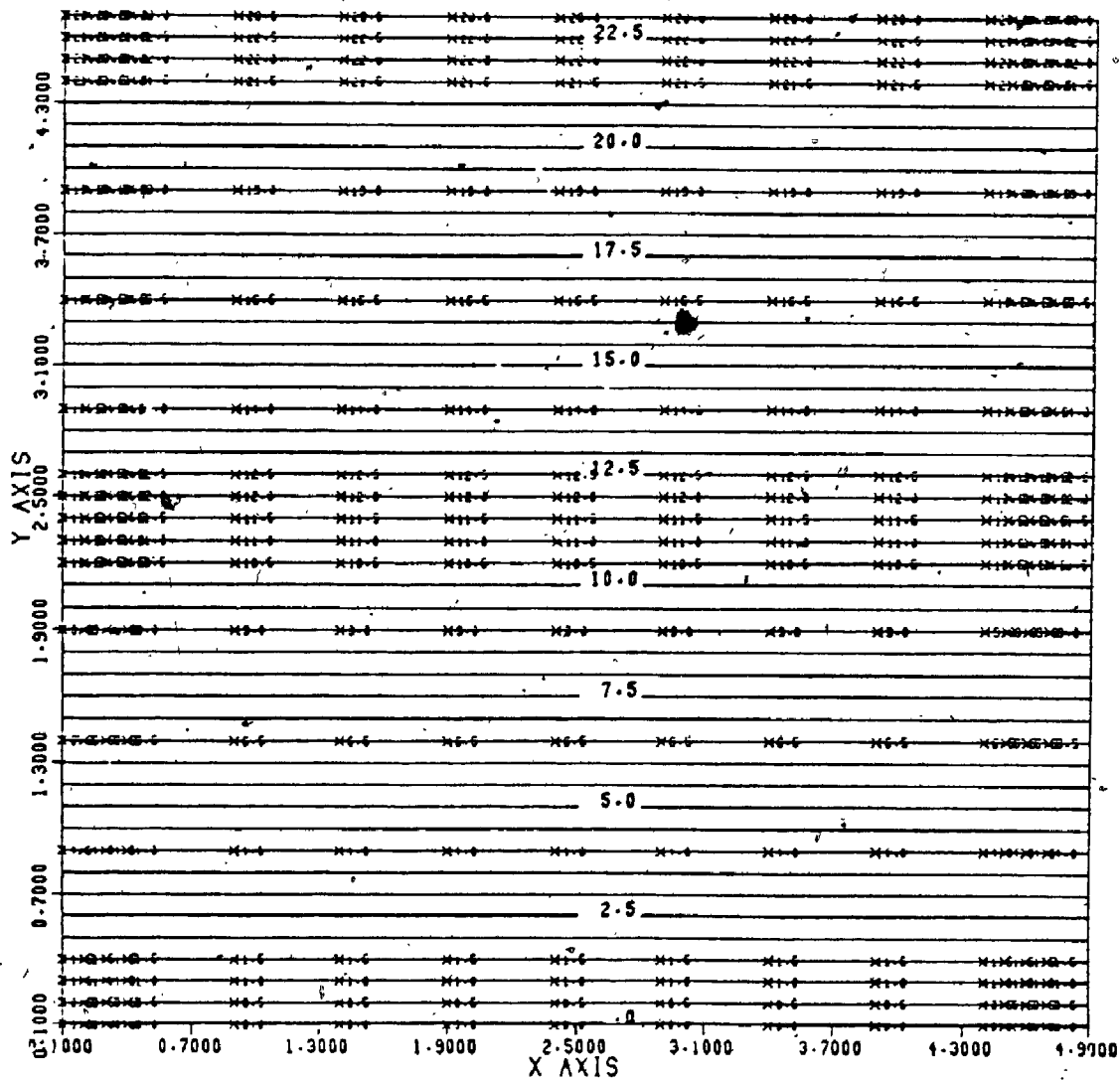


Figure (6-2) Initial streamlines with no disturbance.

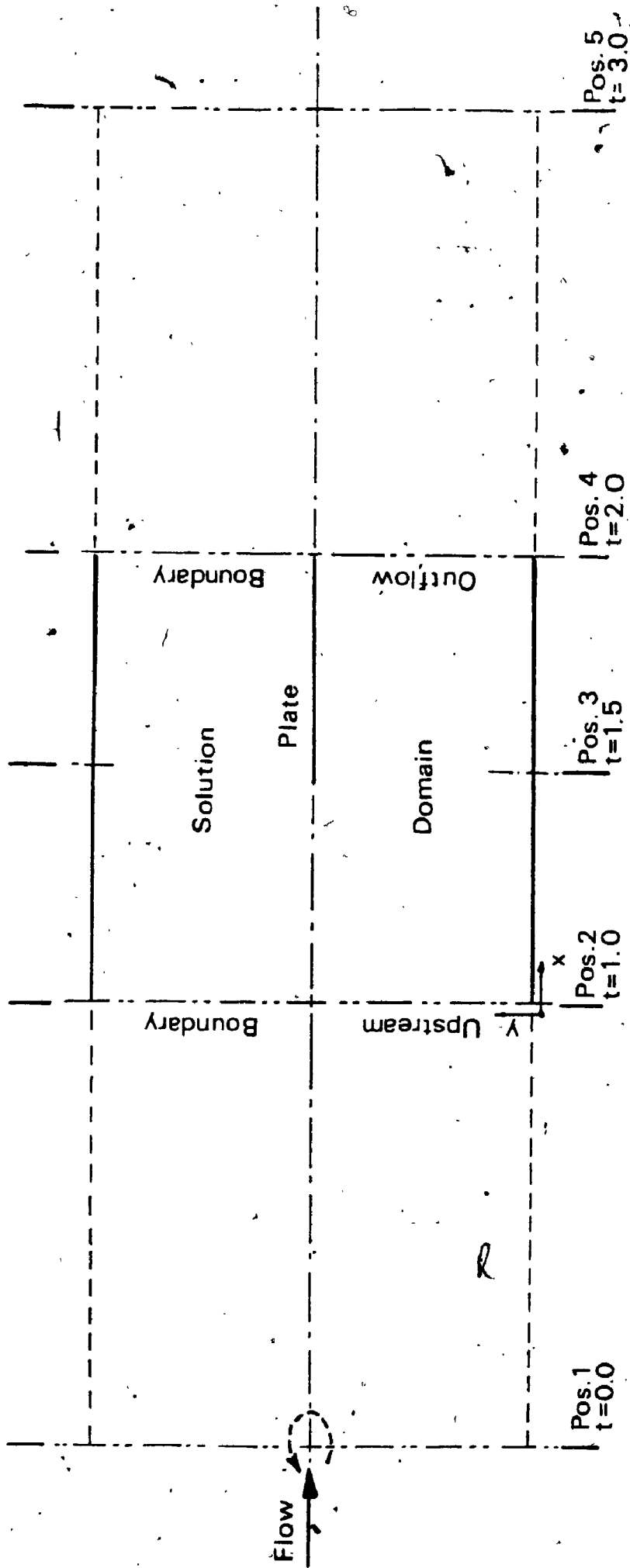


Figure (6-3) vortex relative positions in the flow field.

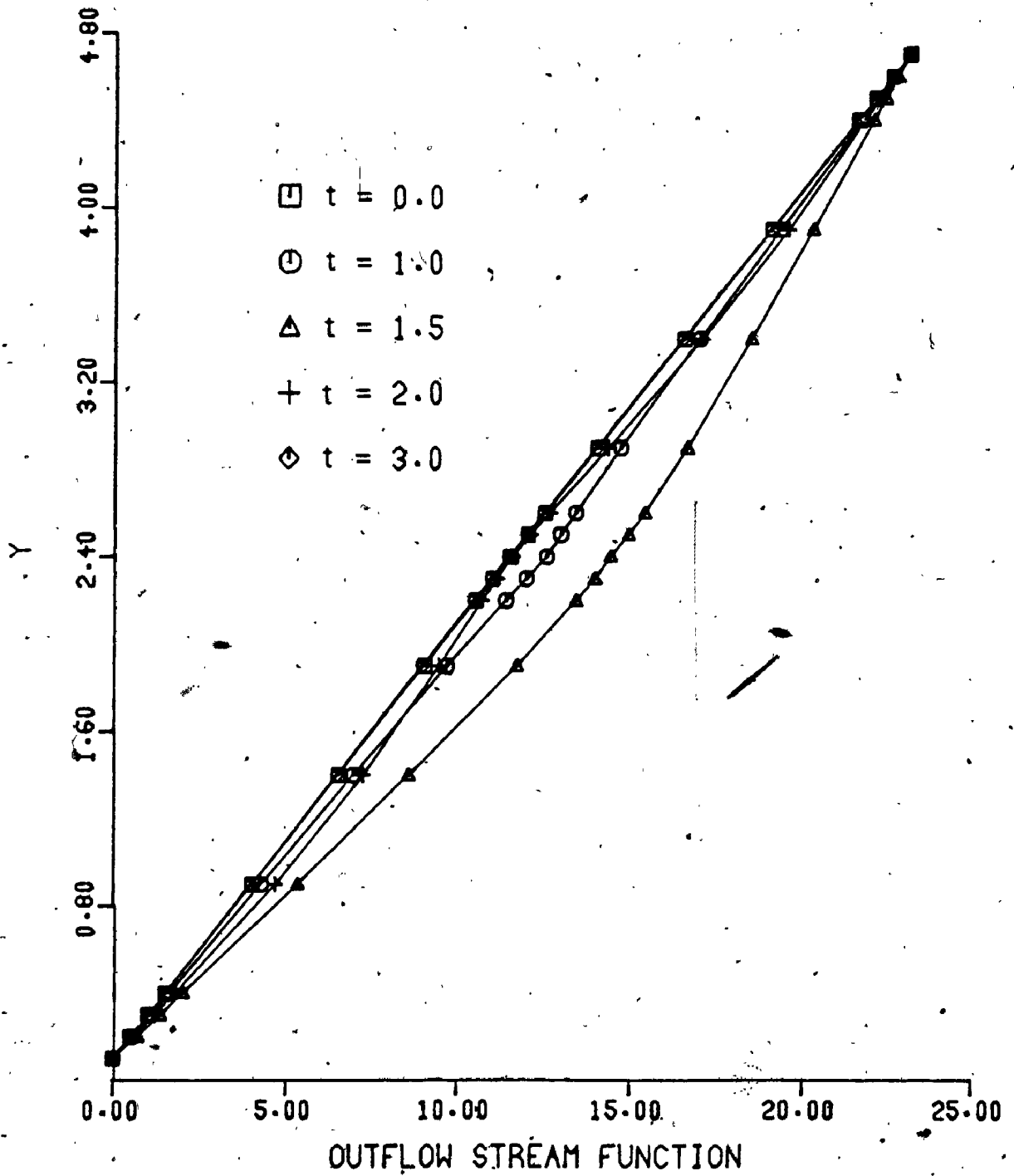


Figure (6-4) Change  $\delta f$  of outflow stream function with time



VORTICITY IN CHANNEL FLOW.  $T=4.7$ .  $X_0=-3$ .  $U=1.0$ .

$\Gamma = -10$

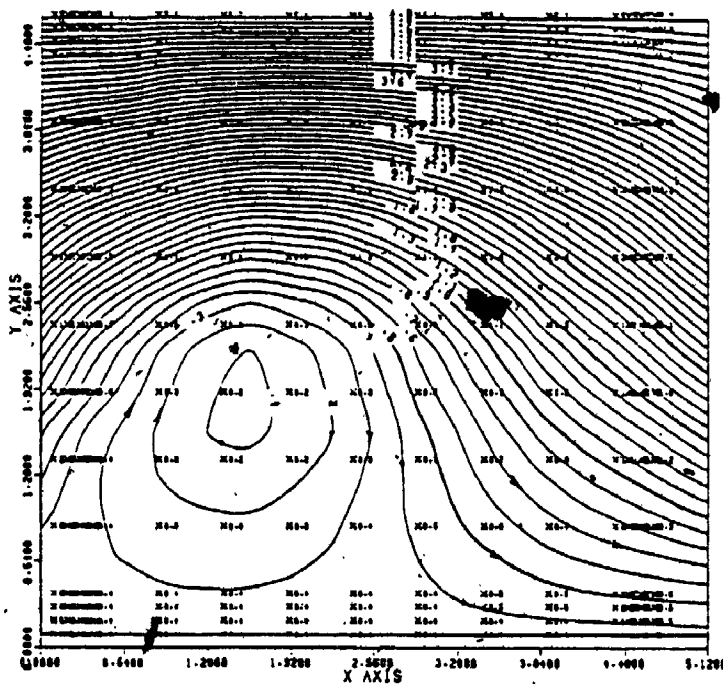


Figure (6-5)

VORTICITY IN CHANNEL FLOW.  $T=0.47$ .  $X_0=-3$ .  $U=10$ .

$\Gamma = -10$

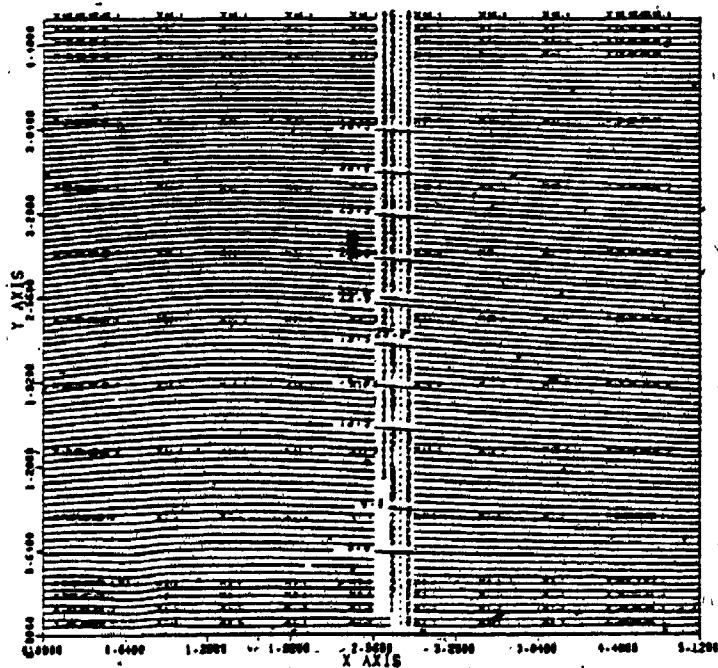


Figure (6-6)

to the wall effects on the rotational disturbance and pressure field as well as the relative velocity between the disturbance centre and the main flow. When the vortex, with clockwise circulation as shown in Figure (6-5), entered the upstream region of the solution domain, the flow for this configuration had a predominant downward motion. This downward motion persisted for the time while the complete finite rotational disturbance entered the domain and resulted in the original vortex, now a rotational disturbance, acquiring a motion towards the lower boundary.

Figure (6-6) shows the effect of increasing the velocity of approach  $U_\infty$  while keeping the vortex circulation  $\Gamma$  constant. The effect of this change increases the value of linear momentum over the value of the angular momentum. This resulted in a less distinguished vortex in the stream function contours.

Introducing the Rossby number as:

$$R_s = \frac{\Gamma}{U_\infty r_C^* H} \quad (6.1)$$

where

$\Gamma$  is the original vortex circulation constant

$U_\infty$  is the undisturbed velocity of the flow

$r_C^*$  is the dimensionless core radius

and  $H$  is the distance between the two parallel planes

then the previous result can be re-stated that as the Rossby number ( $R_s$ ) increases, the angular momentum effect increases.

Figures (6-7) to (6-18) show the change of stream func-

VORTEX APPROACHING SEMI-INFINITE PLATE,  $U=1.0$ ,  
 $\text{GAMA} = 10, T=0.8$

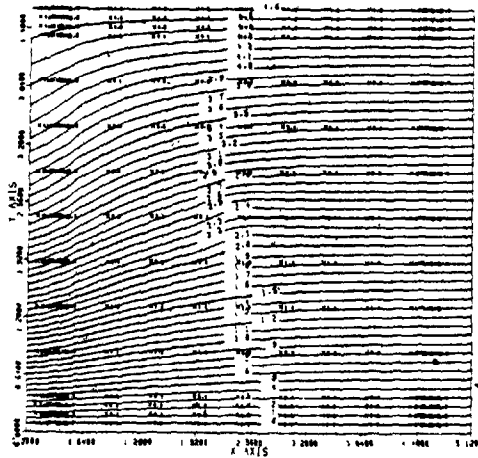


Figure (6-7)

VORTEX APPROACHING SEMI-INFINITE PLATE,  $U=1.0$ ,  
 $\text{GAMA} = 10, T=3.1$

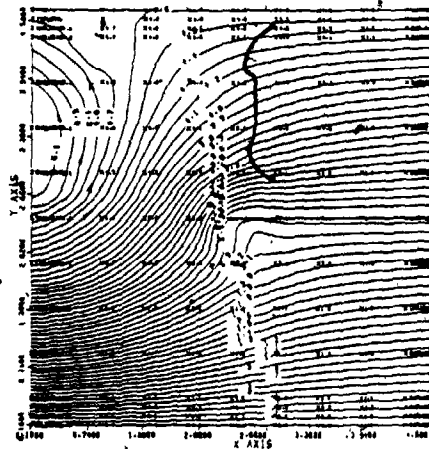


Figure (6-8)

VORTEX APPROACHING SEMI-INFINITE PLATE,  $U=1.0$ ,  
 $\text{GAMA} = 10, T=4.9$

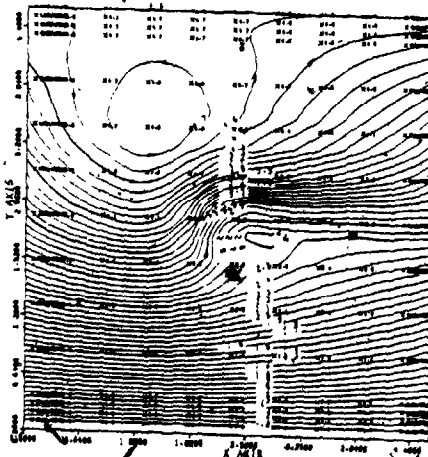


Figure (6-9)

VORTEX APPROACHING SEMI-INFINITE PLATE,  $U=1.0$ ,  
 $\text{GAMA} = 10, T=6.0$

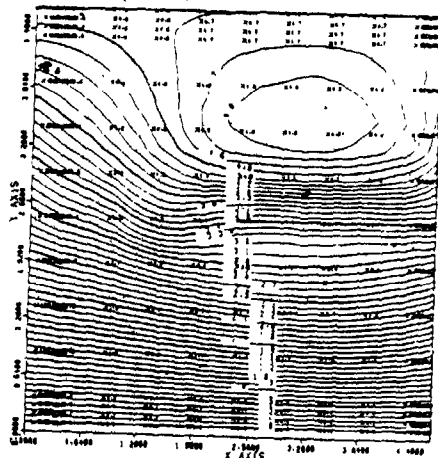


Figure (6-10)

VORTEX APPROACHING SEMI-INFINITE PLATE.  $U=1.0$ .  
 $\text{GAMA} = 10, T=7.0$

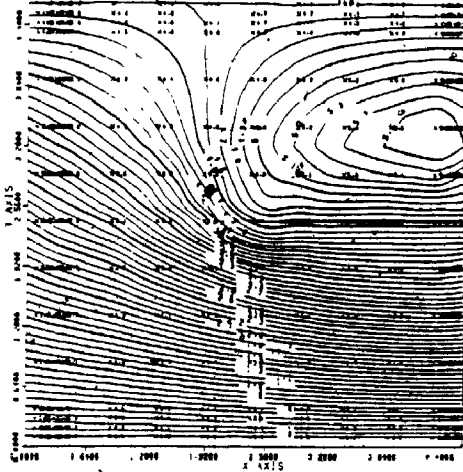


Figure (6-11)

VORTEX APPROACHING SEMI-INFINITE PLATE.  $U=1.0$ .  
 $\text{GAMA} = 10, T=7.5$

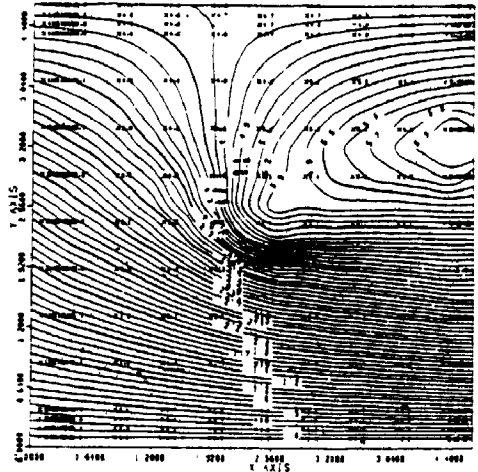


Figure (6-12)

VORTEX APPROACHING SEMI-INFINITE PLATE.  $U=1.0$ .  
 $\text{GAMA} = 10, T=8.0$

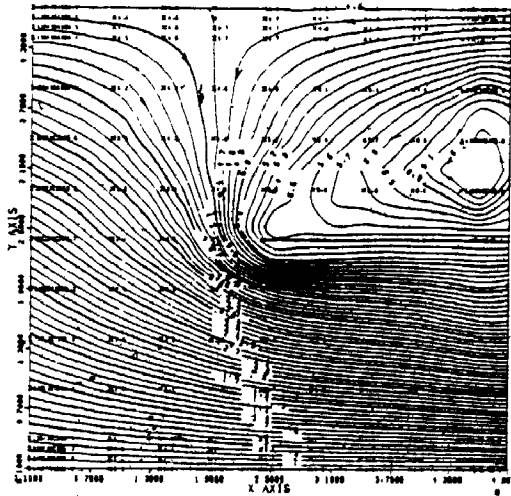


Figure (6-13)

VORTEX APPROACHING SEMI-INFINITE PLATE.  $U=1.0$ .  
 $\text{GAMA} = 10, T=8.5$

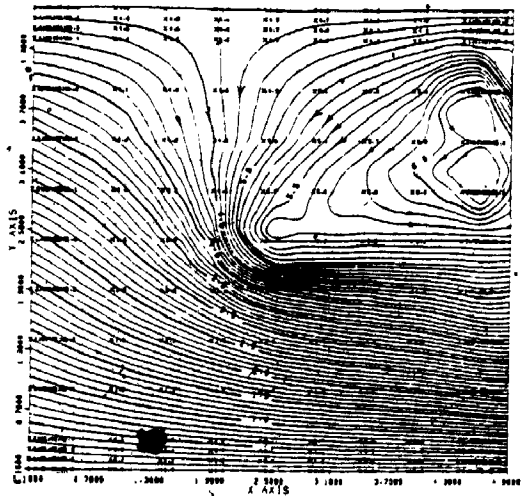


Figure (6-14)

VORTEX APPROACHING SEMI-INFINITE PLATE.  $U=1.0$ .  
 $\text{GAMA}=10, T=8.6$

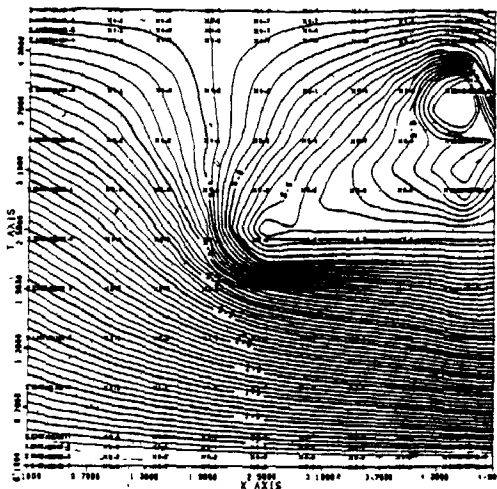


Figure (6-15)

VORTEX APPROACHING SEMI-INFINITE PLATE.  $U=1.0$ .  
 $\text{GAMA}=10, T=8.7$

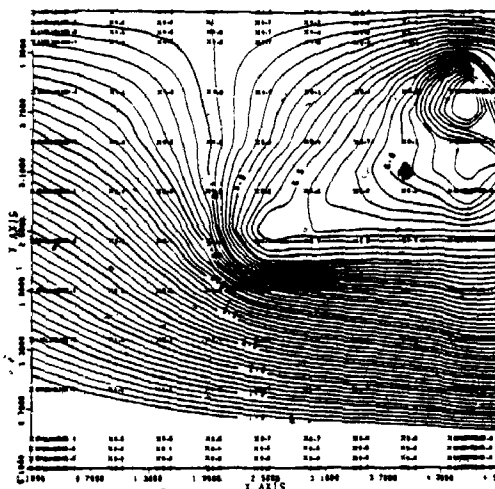


Figure (6-16)

VORTEX APPROACHING SEMI-INFINITE PLATE.  $U=1.0$ .  
 $\text{GAMA}=10, T=8.8$

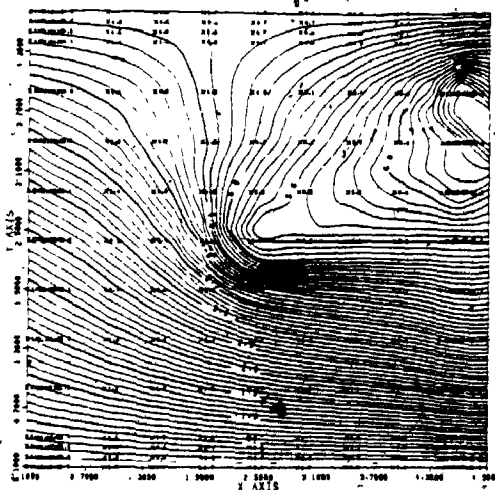


Figure (6-17)

VORTEX APPROACHING SEMI-INFINITE PLATE.  $U=1.0$ .  
 $\text{GAMA}=10, T=8.9$

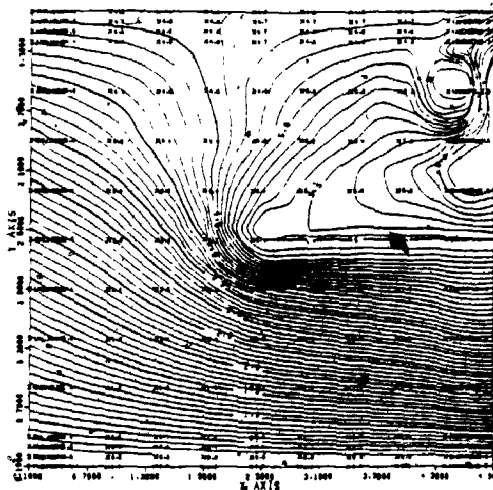


Figure (6-18)

tion contour plots with time for a vortex with counter-clockwise circulation and a value  $\Gamma = 10 \text{ m}^2/\text{s}$ , dimensionless radius  $r_c^* = 0.5$  and approaching the solution domain with a velocity  $U_\infty = 1.0 \text{ m/s}$  and impinging on a semi-infinite flat plate situated midway between the parallel planes. The Rossby number for this flow was  $R_s = 4.35$ .

These Figures show that the vortex centre was convected in the direction of rotation upon entering the solution domain as was explained earlier. The Figures also show that a stagnation point which was formed on the lower side of the flat plate, as the disturbance was approaching the plate, moved on to the upper side of the flat plate while the disturbance was being convected over it. The same Figures also show that the rotational disturbance at this Rossby number was bounded by a contour line joining a leading and trailing stagnation point on the upper plane. Outside this boundary contour line there was no reversed flow. As the time progressed further, the leading stagnation point on the upper wall left the domain, subjecting the outflow boundary to reversed flow conditions which resulted in an instability of the numerical solution.

Several numerical experiments were carried out using different values of  $\Gamma$ ,  $U_\infty$  and  $r_c^*$ , and hence, different Rossby numbers. From these computations it was realized that the numerical techniques introduced were more stable for Rossby numbers less than a value of one, that is:

$$R_s < 1$$

(6.2)

Figures (6-19) to (6-24) show the change of stream function contour plots with time for a flow with  $R_s = 0.62$  ( $\Gamma = 10 \text{ m}^2/\text{s}$ ,  $U_\infty = 5 \text{ m/s}$  and  $r_c^* = 0.7$ ). It can be seen from these figures that the disturbance was less distinguishable and that the solution was stable while the disturbance passed all the way through and away from the solution domain.

The stability was not only affected by the Rossby number, but there was another inherent stability condition due to the finite-difference formulation in order to limit error growth with time. In the stability analysis presented by Roache [1976], a necessary condition for stability for an inviscid and incompressible fluid flow using the forward time centred space method was given as;

$$\delta t \leq \frac{2\Delta X}{U} \quad (6.3)$$

where

$\Delta X$  is the mesh size

and  $U$  is the vortex convective velocity.

However, Base [1969] who presented stability and error analysis for the case of a modified Rankine vortex in an inviscid and incompressible fluid flow, derived the condition for a stable solution, with a percentage error of less than 0.3% in the values of vorticity, which was:

$$\delta t \leq \frac{0.2 r_c}{U} \quad (6.4)$$

where

$r_c$  is the modified Rankine vortex core radius

VORTEX APPROACHING SEMI-INFINITE PLATE, U=5.  
GAMA=10, T=0.6

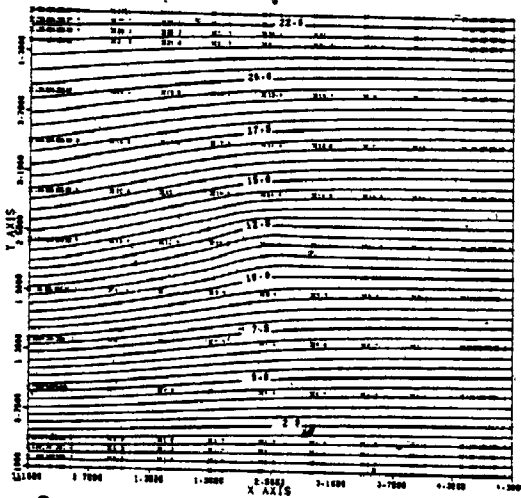


Figure (6-19)

VORTEX APPROACHING SEMI-INFINITE PLATE, U=5.  
GAMA=10, T=1.00

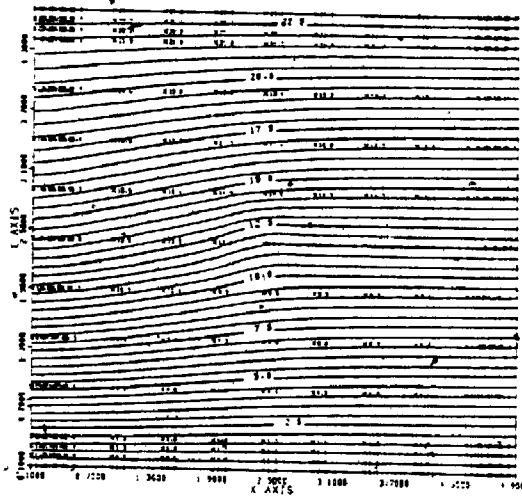


Figure (6-20)

VORTEX APPROACHING SEMI-INFINITE PLATE, U=5.  
GAMA=10, T=0.80

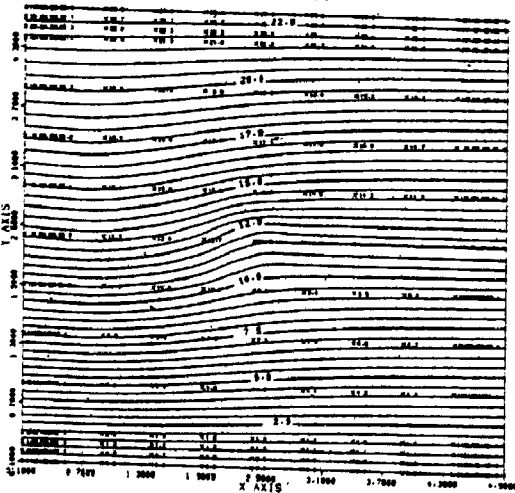


Figure (6-21)

VORTEX APPROACHING SEMI-INFINITE PLATE, U=5.  
GAMA=10, T=1.10

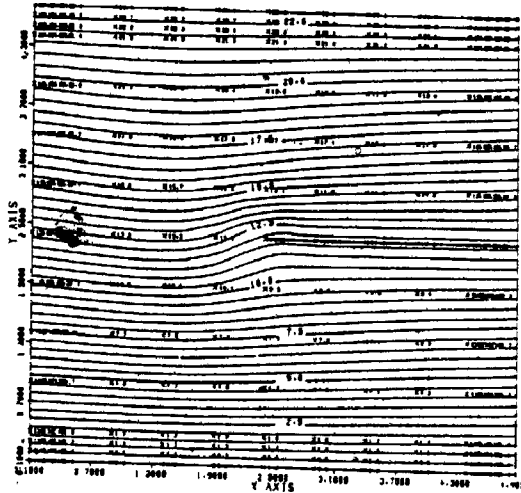


Figure (6-22)



VORTEX APPROACHING SEMI-INFINITE PLATE, U=5.  
GAMA=10, T=1.5

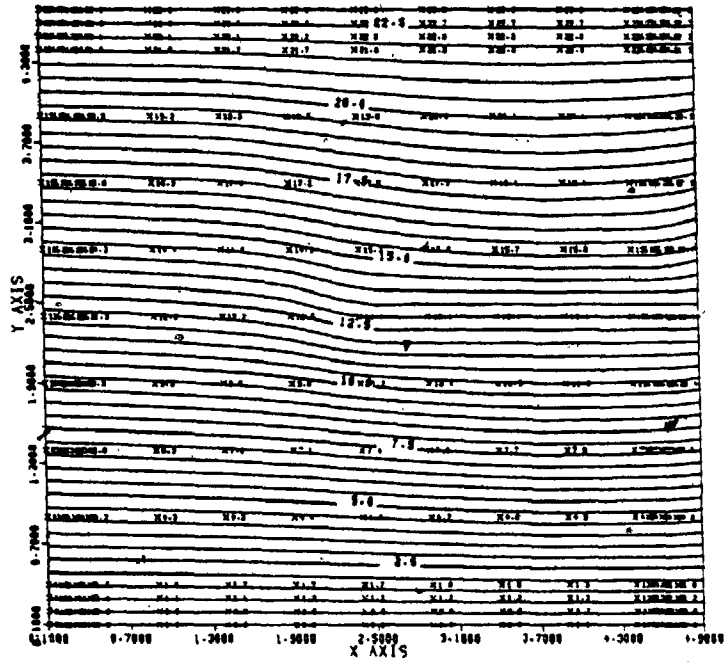


Figure (6-23)

VORTEX APPROACHING SEMI-INFINITE PLATE, U=5.  
GAMA=10, T=2.46

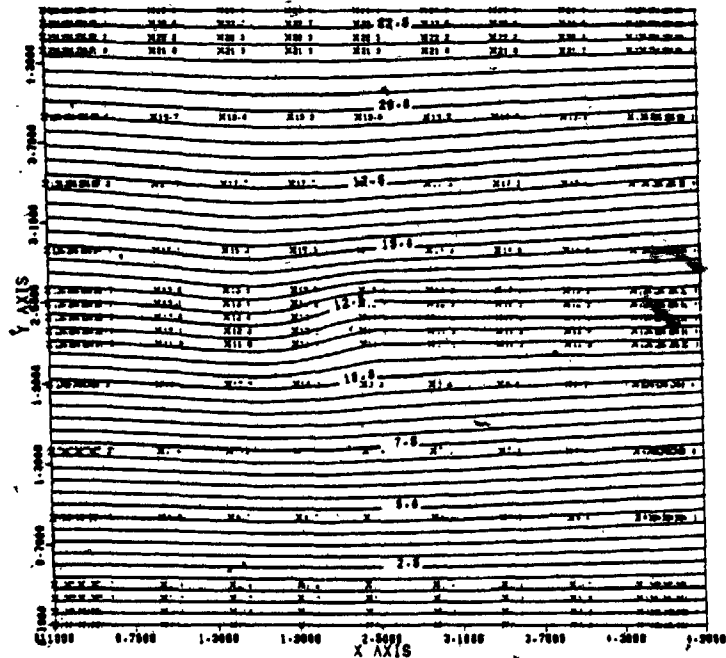


Figure (6-24)

and  $U$  is the vortex convective velocity.

Comparing Equations (6.3) and (6.4) when  $\Delta X$  and  $r_c$  are of the same order of magnitude, it can be seen that Equation (6.3) is less restrictive and therefore is superseded by Equation (6.4).

In the case of the equivalent modified Rankine vortex used in this study, Equation (6.4) was modified to take the form.

$$\delta t \leq \frac{0.04 H r_c^*}{U} \quad (6.5)$$

So, in order to achieve a stable solution with percentage error equal to or less than 0.3% for an equivalent modified Rankine vortex in an inviscid, rotational and incompressible fluid flow, Equations (6.2) and (6.5) had to be satisfied.

### 6.3 CALCULATION OF PRESSURE ON THE FLAT PLATE

In general, the lift force on a flat plate or an aerofoil at incidence to an approaching free stream is manifested as a pressure difference between the top and bottom surfaces. The lift force can be obtained by either considering the change of momentum of the incident flow stream or by vortex theory. In the vortex theory a bound vortex is assumed to exist within the aerofoil or flat plate with a circulation strength related to the lift on the plate. When the lift changes (in order to satisfy Kelvin theorem) a vortex of opposite sign to the bound vortex is shed from the plate

trailing edge and then is convected downstream. In the present study, however, the fluid is assumed inviscid, hence there is no mechanism to generate this vortex.

In the classical potential flow solution for lifting aerofoils, in three-dimensional studies, Lanchester's theory is applied. In the two-dimensional theory, the bound vortex strength is determined by the Kutta-Joukowski condition. The following example illustrates the importance of the assumption of whether the fluid is viscous or inviscid. The lift force on a thin flat plate at incidence to a uniform free stream is determined by integration of the pressures on the plate. From the normal force to the thin plate, a 'drag' force will appear due to the incidence of the thin plate. However, since the flow is inviscid then this drag force should be zero. This dilemma may be resolved by considering an infinite pressure acting on the infinitesimal area at the leading and trailing edges of the thin flat plate. For a semi-infinite flat plate the Kutta-Joukowski condition is not required since in this case a trailing edge will not exist. Consequently, in this study, the lift force on the finite flat plate would be due to the "external" pressure field alone. This is an idealized model and in practice, for a real fluid, both components of lift force will result.

In order to determine the lift on the plate due to the approaching flow it was necessary to determine the pressure difference between the top and bottom surfaces of the flat

plate as a function of time and position.

Writing the x component of Navier-Stokes equation as,

$$\frac{\partial u}{\partial t} + u \frac{\partial u}{\partial x} + v \frac{\partial u}{\partial y} = -\frac{1}{\rho} \frac{\partial p}{\partial x} + \nu \left( \frac{\partial^2 u}{\partial x^2} + \frac{\partial^2 u}{\partial y^2} \right) \quad (6.6)$$

For an inviscid flow ( $\nu = 0$ ) and at the plate surface the transverse velocity component "v" is equal to zero so that Equation (6.6) reduces to,

$$\frac{\partial u}{\partial t} + u \frac{\partial u}{\partial x} = -\frac{1}{\rho} \frac{\partial p}{\partial x} \quad (6.7)$$

Integrating Equation (6.7) with respect to x from the leading edge to a point x on the flat plate then,

$$\int_0^x \frac{\partial u}{\partial t} dx + \int_0^x u \frac{\partial u}{\partial x} dx = \int_0^x -\frac{1}{\rho} \frac{\partial p}{\partial x} dx \quad (6.8)$$

Since x is not a function of the time t, then Equation (6.8) can be written as,

$$\begin{aligned} \frac{\partial}{\partial t} \int_0^x u dx + \int_0^x u \frac{\partial u}{\partial x} dx &= \int_0^x -\frac{1}{\rho} \frac{\partial p}{\partial x} dx \\ \frac{\partial}{\partial t} \int_0^x u dx + \frac{u_x^2 - u_0^2}{2} &= -\frac{1}{\rho} (p_x - p_0) \end{aligned} \quad (6.9)$$

where the subscripts x and o denote the points x and the leading edge respectively.

The static and dynamic pressures at the leading edge can be grouped together so that Equation (6.9) can be rewritten as,

$$\frac{\partial}{\partial t} \int_0^x u dx + \frac{u_x^2}{2} = -\frac{1}{\rho} p_x + \frac{1}{\rho} p_0 \quad (6.10)$$

where  $P_0$  denotes the total pressure at the leading edge.

It may be noted that the stagnation point, where the measured pressure is equal to the total pressure ( $P_0$ ), is not necessarily at the leading edge as shown in Figures (6-7) to (6-24).

Furthermore, by assuming that the total pressure at the top and bottom surfaces is unique at the leading edge, the difference in pressure between the bottom and top surfaces at a point on the plate can be obtained from the following equation:

$$\begin{aligned} \Delta p &= -\rho \left[ \left( \frac{\partial}{\partial t} \int_0^x u \, dx + \frac{u_x^2}{2} \right)_B - \left( \frac{\partial}{\partial t} \int_0^x u \, dx + \frac{u_x^2}{2} \right)_T \right] \\ &= -\rho \left[ \frac{\partial}{\partial t} \int_0^x (u_B - u_T) \, dx + \frac{u_{xB}^2 - u_{xT}^2}{2} \right] \end{aligned} \quad (6.11)$$

where the subscripts B and T denote the bottom and top surfaces of the flat plate respectively.

#### 6.4 LIFT AND PITCHING MOMENT COEFFICIENTS

Knowing the variation of the pressure difference  $\Delta p$  between the top and bottom surfaces on the flat plate as a function of distance  $x$  and time  $t$ , then the lift coefficient  $C_L$  and the pitching moment coefficient about the leading edge  $C_m$  were obtained from the following relationships,

$$C_L = \frac{\int_0^c \Delta p \, dx}{\frac{1}{2} \rho U_\infty^2 c} \quad (6.12)$$

$$C_m = \frac{\int_0^C \Delta p \times dx}{\frac{1}{2} \rho U_\infty^2 C^2} \quad (6.13)$$

where  $C$  is the length of the flat plate:

The velocities on the top and bottom surfaces of the flat plate were obtained numerically from the velocity stream function relation  $\left[ u = \frac{\partial \psi}{\partial y} \right]$  using forward and backward differences, respectively, thus satisfying the Kutta-Joukowski condition of having finite velocity at the trailing edge.

The integration terms in Equations (6.11), (6.12) and (6.13) were carried out by a modified trapezoidal rule, since the spatial steps were not equal.

It may be noted that the equation for the pressure (on the flat plate) for unsteady, rotational and inviscid flow is more complicated than that for viscous flow since in the viscous case the no-slip condition on the flat plate simplifies the pressure equation (where  $u = v = 0$  and  $\frac{\partial u}{\partial t} = 0$ ).

Subroutine (LIFTC) was used to calculate the lift and pitching moment coefficients in the main program presented in Appendix (D).

## 6.5 ESTIMATING THE FLAT PLATE STREAM FUNCTION VALUE

This section presents three different methods which were employed to estimate the flat plate stream function together with the resulting lift coefficient versus time plots. A discussion of these plots is helpful in deciding upon the

most appropriate method to be used to obtain the fluid flow solution around the flat plate. These methods are:

- 1) A simple straightforward method in which the flat plate stream function value was set to be constant for all time and was determined from the potential flow solution assuming the initial uniform approaching flow.
- 2) In order to allow the flat plate stream function to change with time, it was suggested to use a semi-infinite flat plate whose stream function value was determined at each time step as the average value of the two neighbouring points lying on the outflow boundary.
- 3) A technique similar to the one presented in Chapter 5 was used again with modifications to predict the stream function value on the flat plate at the new time steps. This technique was developed on the basis of a Taylor series expansion of the stream function values, which contained the entire kinematics of the problem, with respect to time and space near the leading edge of the plate. The stream function value for the flat plate at each time step in this case would be dependent on the leading edge conditions.

Figures (6-25) and (6-26) show the variation of the lift coefficient versus time for the stream function values on the flat plate determined using methods 1) and 2) respectively. Figure (6-25) shows that the lift force does not change sign as the vortex passes through the domain, however,

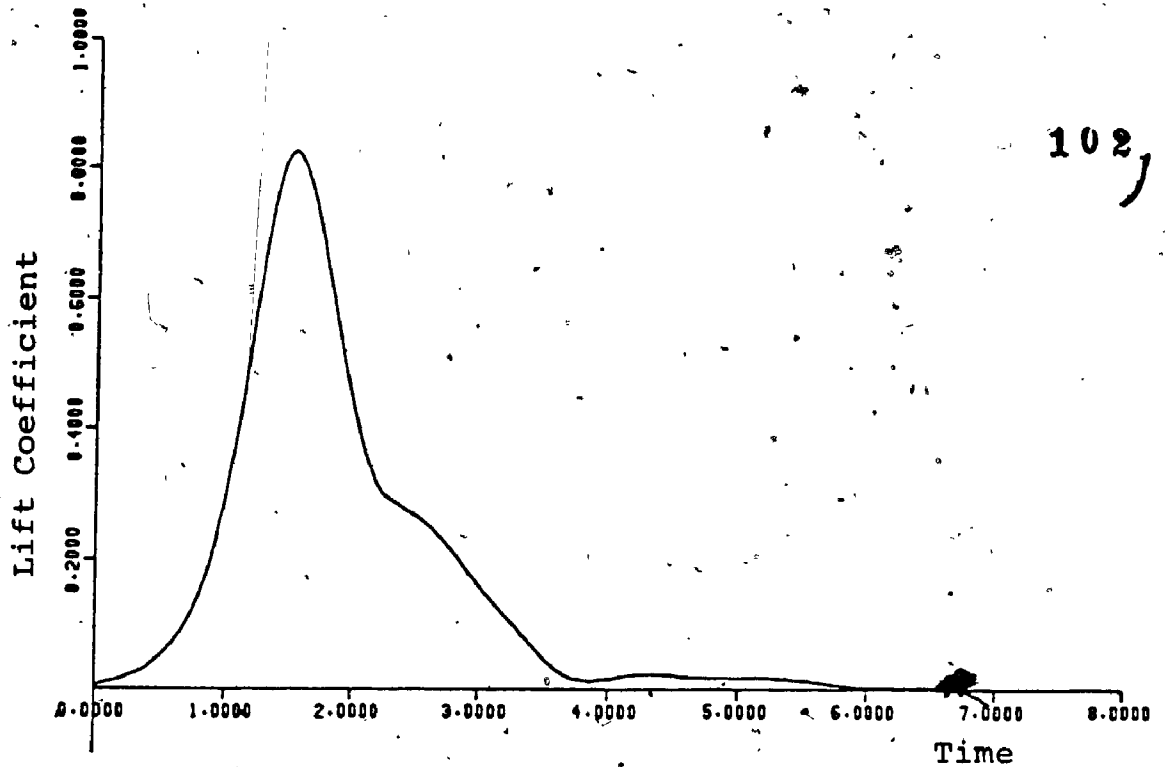


Figure (6-25) Flat plate stream function independent of time.

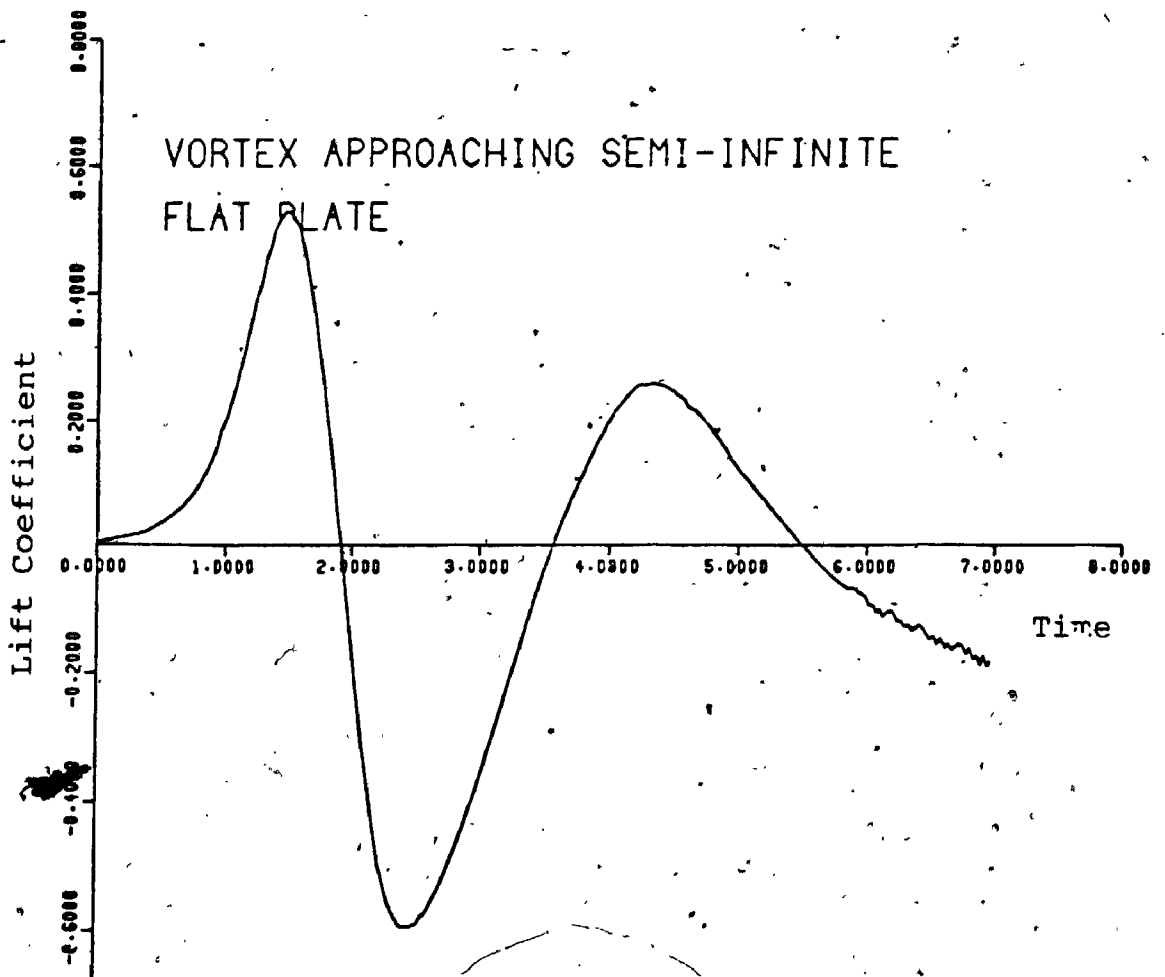


Figure (6-26) Flat plate stream function dependent on outflow boundary.



Figure (6-26) shows a reversal of the sign when the flat plate stream function value depended on the outflow boundary conditions. It can be seen that both figures disagree qualitatively with the effect of the approaching vortex on the flat plate. In this case, prior to the vortex entering the domain, more fluid flows underneath the plate than above it with a resultant downward lift force due to the pressure difference around the plate.

Figures (6-27) and (6-28) show the changes of the lift and pitching moment coefficients about the leading edge with time using method 3). In the case of semi-infinite flat plate the chord length was based on the length within the solution domain. Similarly to method 2), method 3) also has shown a reversal in sign of the lift force, but is more realistic in direction to the nature of the flow and pressure.

As the time proceeded forward and the disturbance was further downstream and away from the solution domain, the lift and pitching moment coefficients reduced down to a value of zero. The sudden release of the vortex at a distance  $x_0$  upstream of the solution domain resulted in the small disturbance at the early time steps as shown in Figures (6-27) and (6-28). The same figures also show a small oscillation in the lift and pitching moment coefficients before decaying to zero value. These oscillations may be attributed to the computer round-off error and the value of the convergence criterion ( $\epsilon$ ) used. Figure (6-29) shows the effect of the convergence criterion  $\epsilon$  when it was taken to be ten

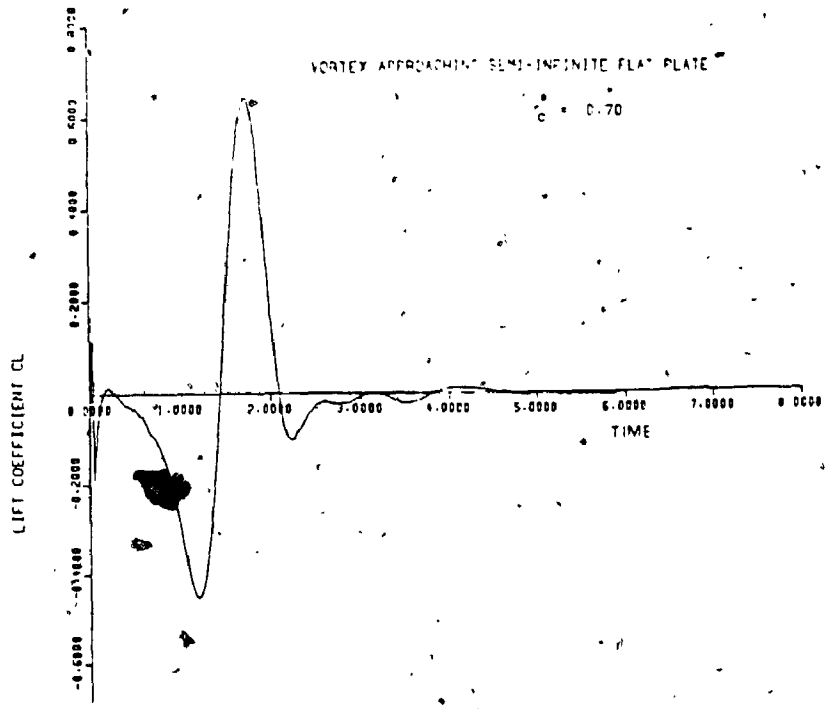


Figure (6-27) Flat plate stream function dependent on flow conditions at the leading edge.

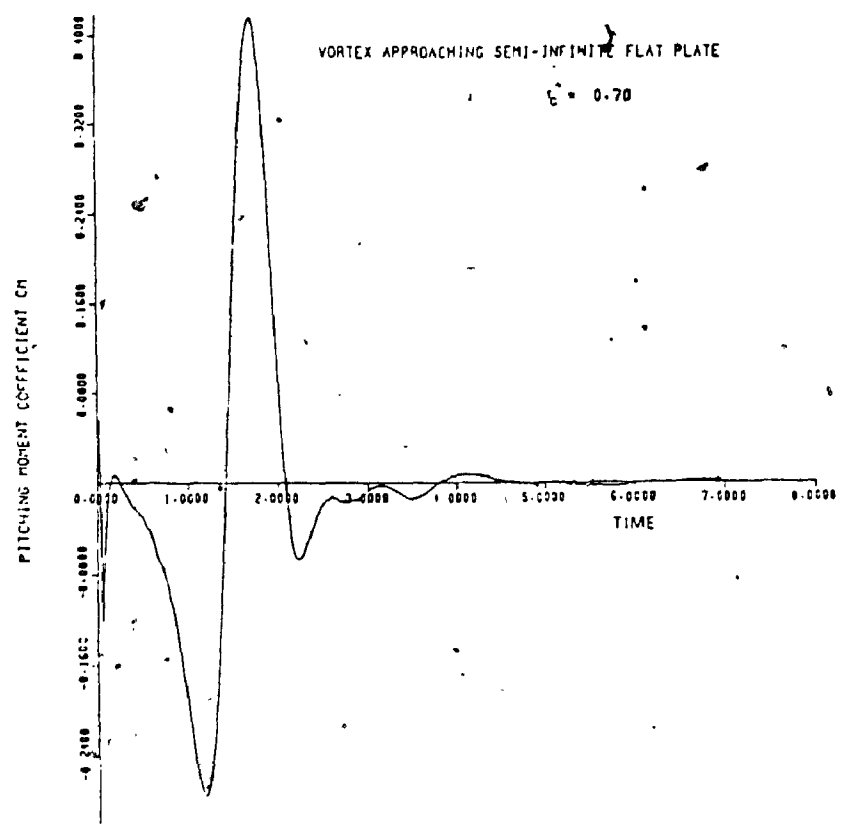


Figure (6-28) Change of pitching moment coefficient with time.

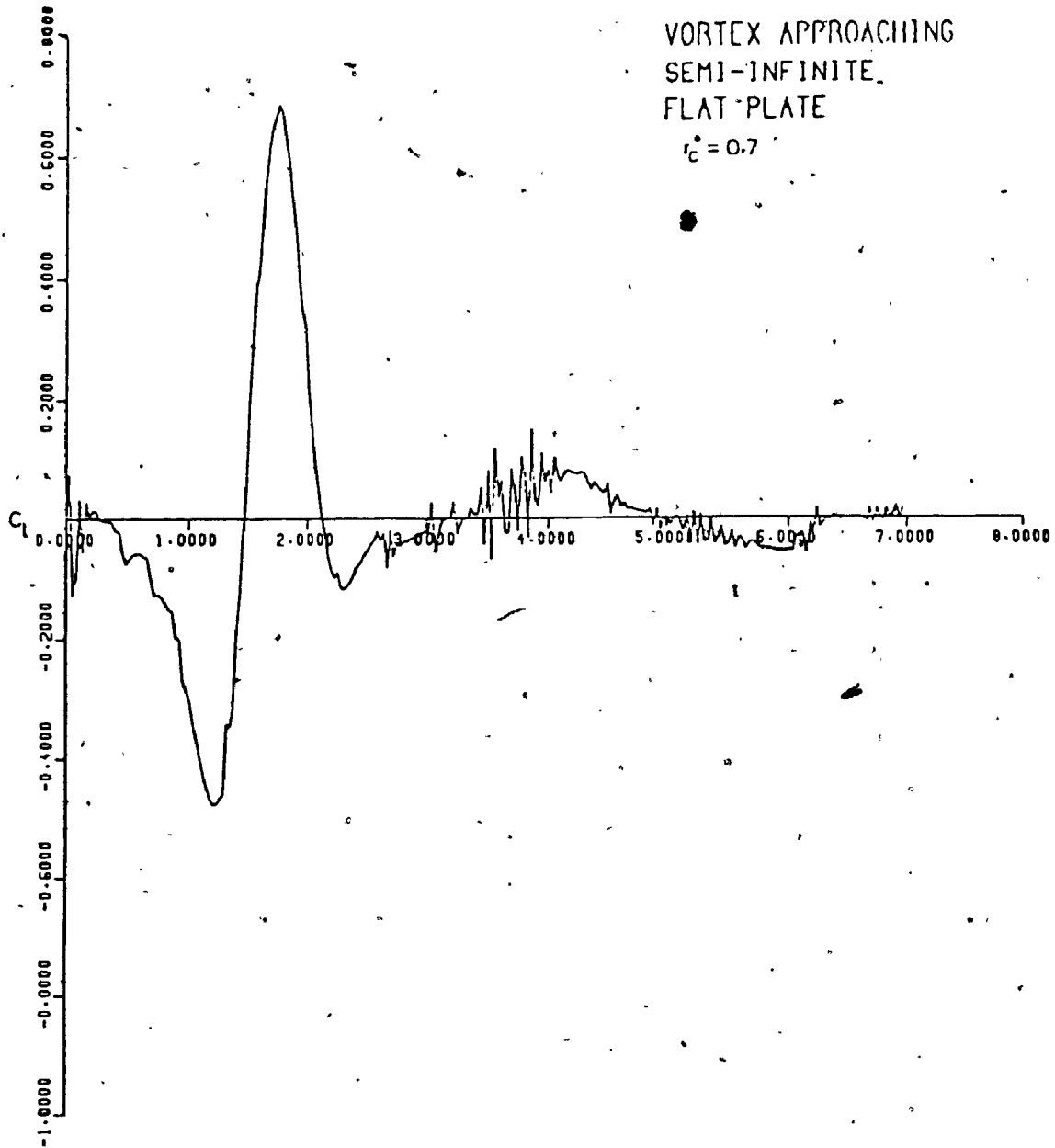


Figure (6-29) Effect of increasing the convergence criterion " $\epsilon$ ".

times the value used to obtain Figure (6-27). It can be seen from this plot that the amplitude and the frequency of these oscillations increased with the increase of the value of the convergence criterion  $\epsilon$ . In the study, the computer cpu time was almost doubled by changing the convergence criterion an order of magnitude from 0.01 to 0.001.

With the flat plate stream function values dependent on the flow conditions at the leading edge, it became possible to extend the studies to include finite flat plates with different chord lengths and not only semi-infinite plates. Figures (6-30) and (6-31) show the plate lift and pitching moment coefficients versus time for a vortex flow with a dimensionless core radius  $r_c^* = 0.7$  and for different flat plate chord lengths. It can be seen from these figures that, for a constant vortex size, the greater the flat plate chord length the greater the maximum lift and pitching moment coefficients. The effect of changing the chord of the plate also changed the flow pattern and so the shorter chord plate did not experience exactly the same pressure field as the longer chord length plate. Figures (6-32) to (6-35) show the same relations while fixing the chord length  $C$  and changing the vortex dimensionless core radius  $r_c^*$ . It can be seen from these figures that, for a constant chord length, the smaller the vortex dimensionless core radius the greater the maximum plate lift and pitching moment coefficients.

The above results can be summarized in Figures (6-36)

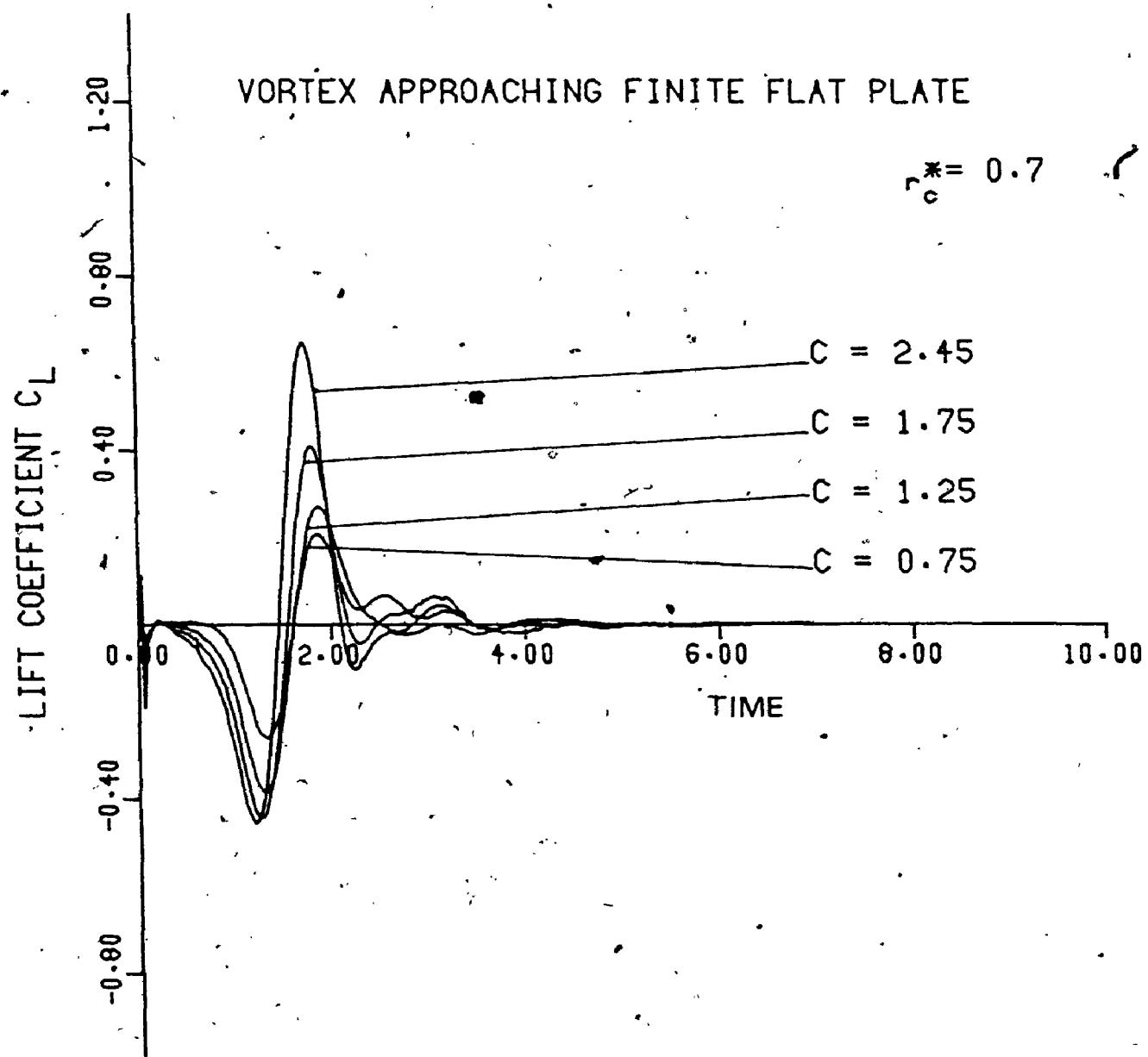


Figure (6-30) Lift coefficient versus time (run number (1)).

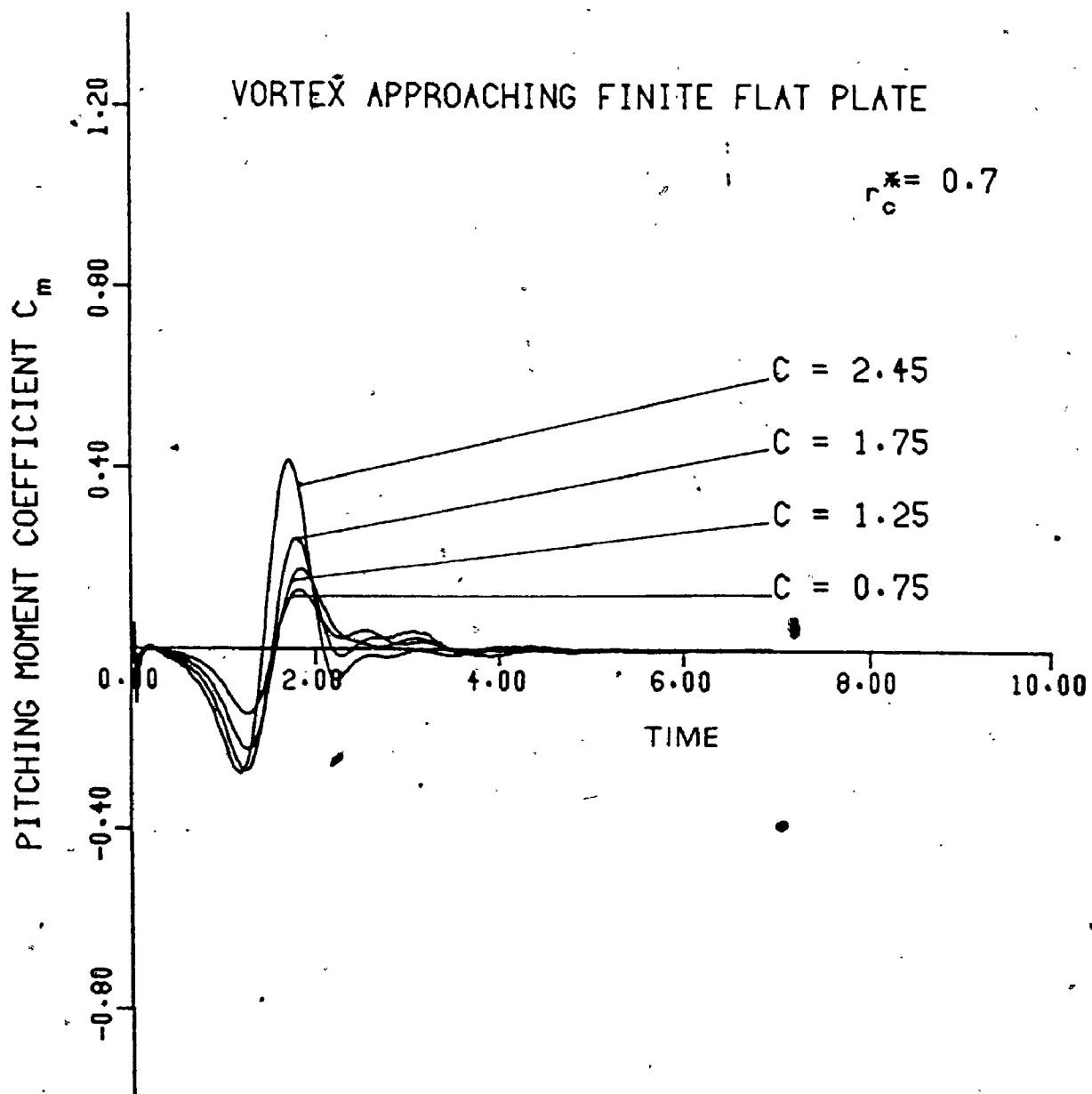


Figure (6-31) Pitching moment coefficient versus time (run number (1)).

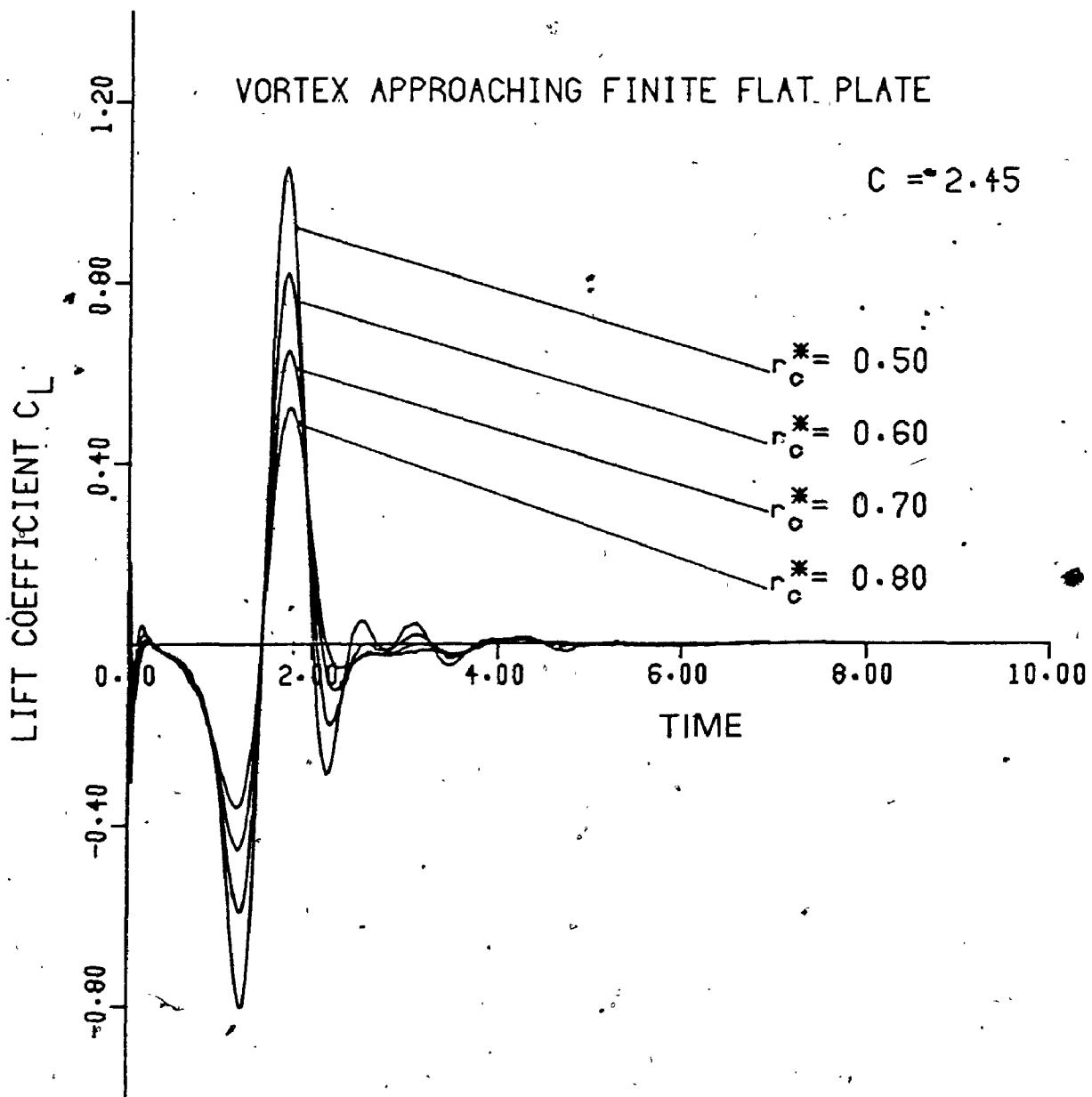


Figure (6-32) Lift coefficient versus time (run number (2)).

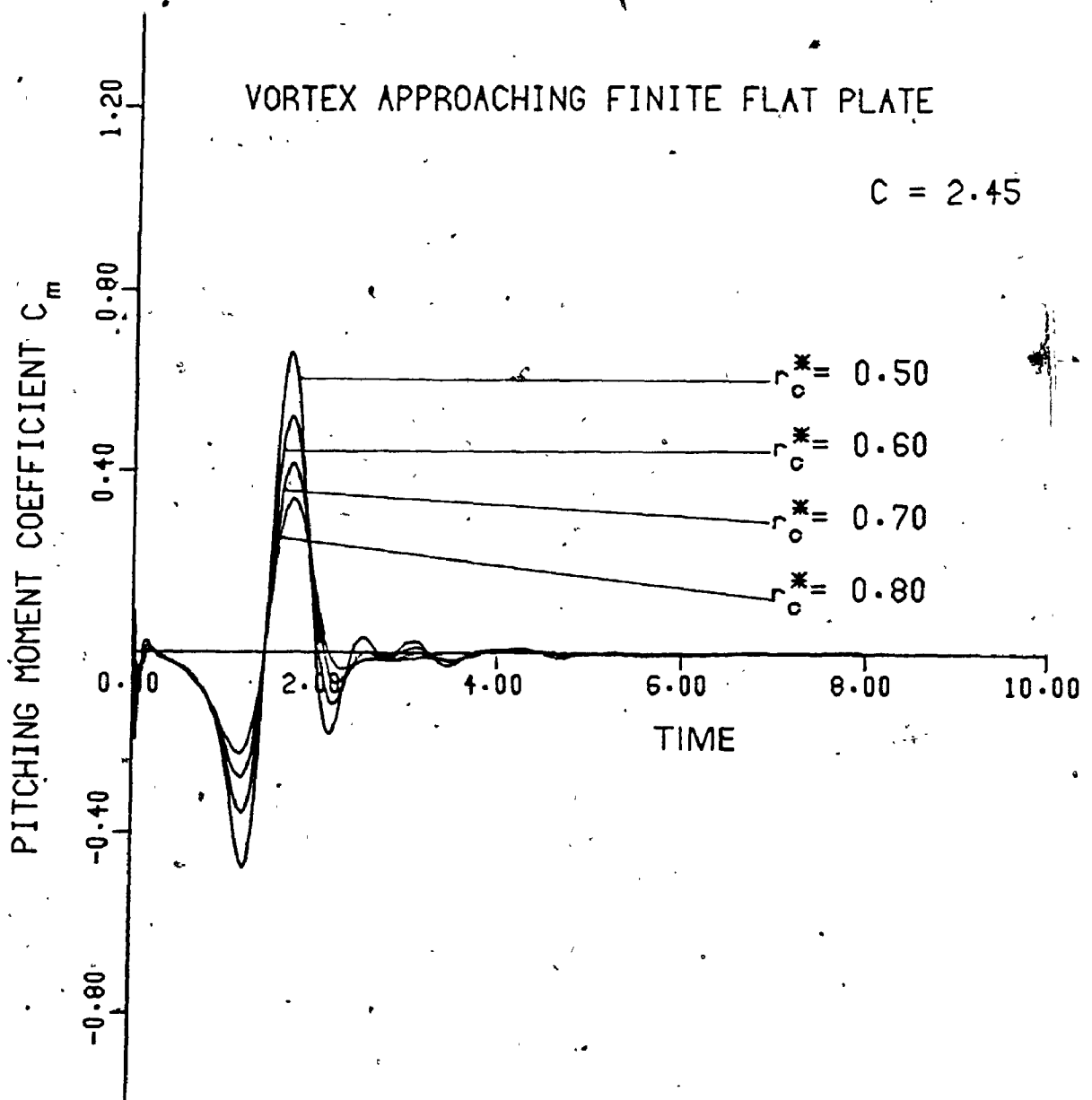


Figure (6-33) Pitching moment coefficient versus time (run number (2)).



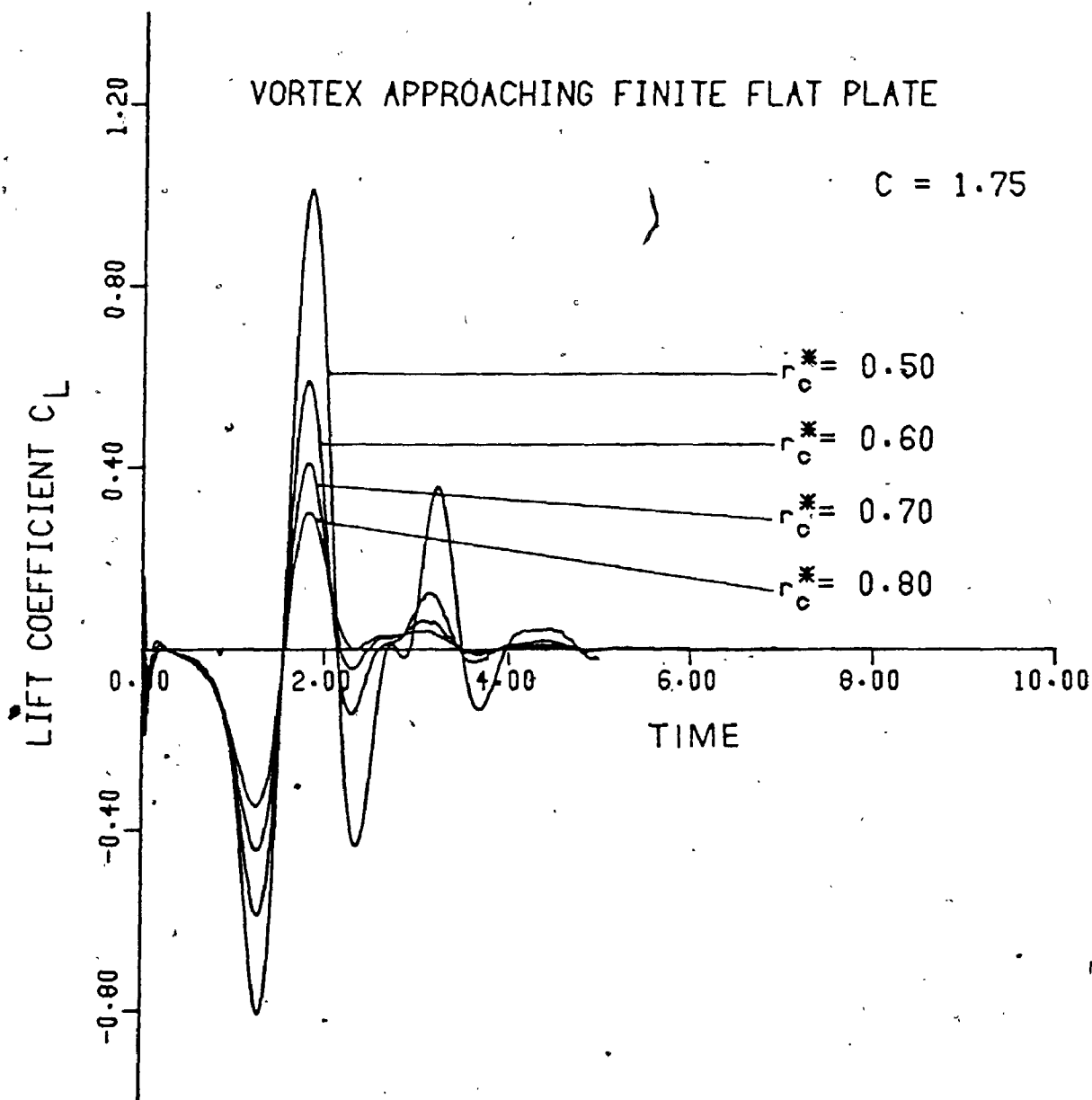


Figure (6-34) Lift coefficient versus time (run number (3)).

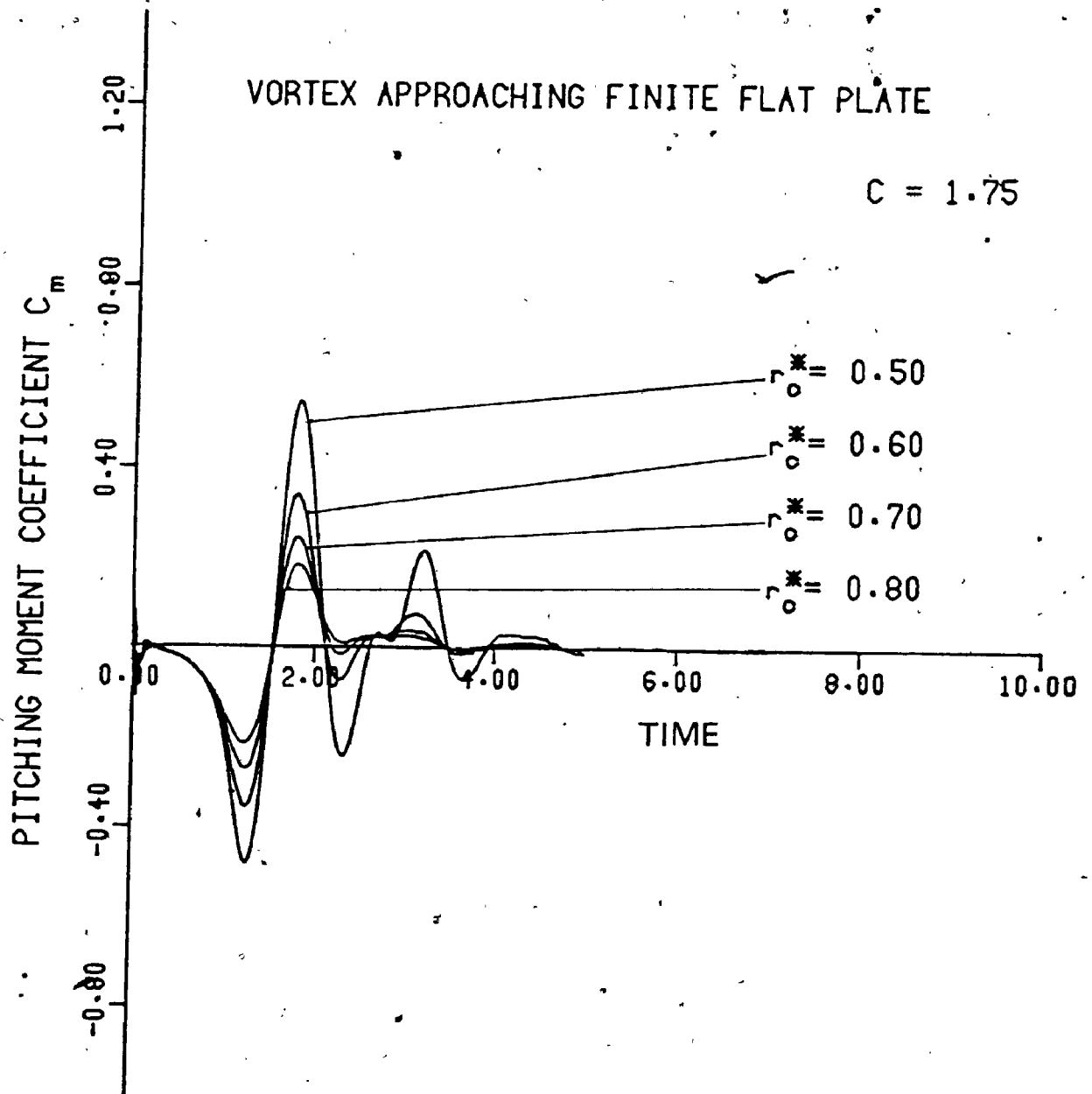


Figure (6-35) Pitching moment coefficient versus time (run number (3)).

and (6-37). where the maximum lift and pitching moment coefficients are plotted versus the dimensionless quantity  $Hr_C^*/C$ . It can be seen from these figures that the maximum plate lift and pitching moment coefficients are directly proportional to the chord length and indirectly proportional to the vortex size. Figures (6-38) to (6-40) show the change of stream function contours with time for a finite flat plate in a flow having a Rossby number of 0.62.

The study in this Chapter besides illustrating the numerical technique also indicated the importance of determining the correct stream function value on the plate. The computer programs were very stable for Rossby number value less than unity, provided that other criteria were satisfied as mentioned previously in this Chapter.

In the next Chapter a model of pseudo-turbulence, based on a convected random array of real vortices or eddies, will be introduced and similarly as with the single vortex discussed in this Chapter the effects of this pseudo-turbulent flow on the lift and pitching moment on a flat plate will be studied.

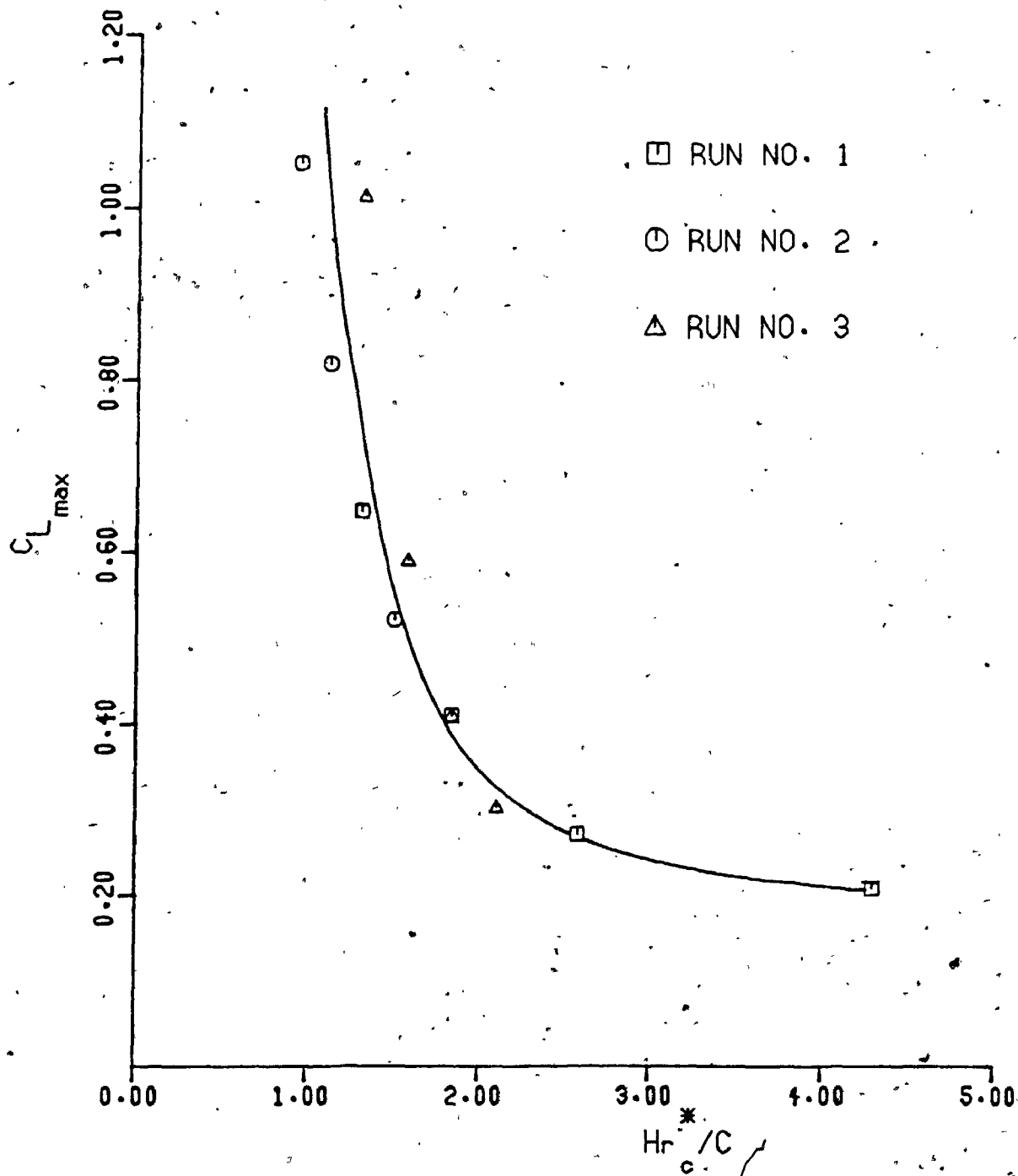


Figure (6-36) Maximum lift coefficient versus  $(Hr_c^*/C)$ .

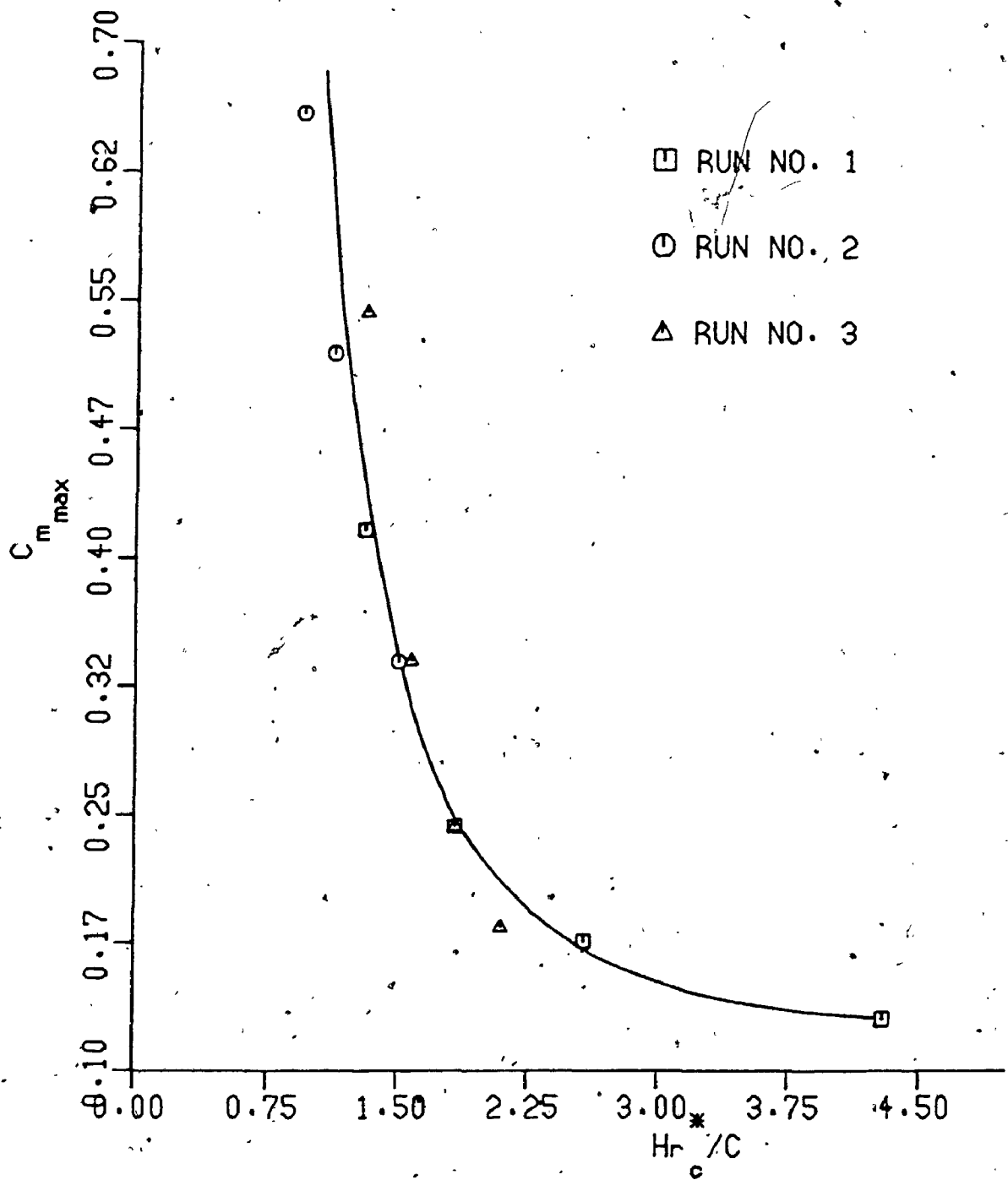


Figure (6-37) Maximum pitching moment coefficient versus  $Hr_c^*/C$ .

VORTEX APPROACHING FINITE PLATE.  $U=5$ .  $\text{GAMA}=10$ .  
 $RC=0.7$ .  $T=1.652$

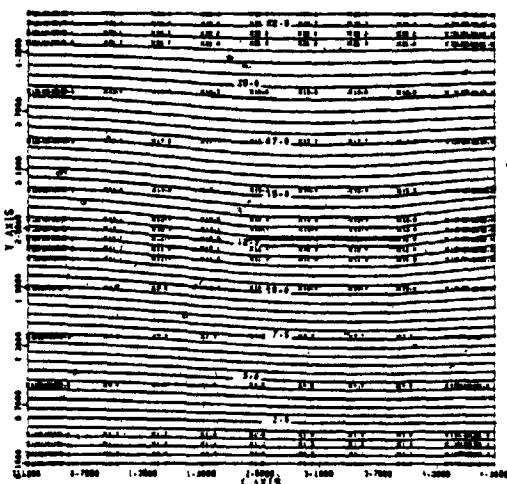


Figure (6-38)

VORTEX APPROACHING FINITE PLATE.  $U=5$ .  $\text{GAMA}=10$ .  
 $RC=0.7$ .  $T=1.344$

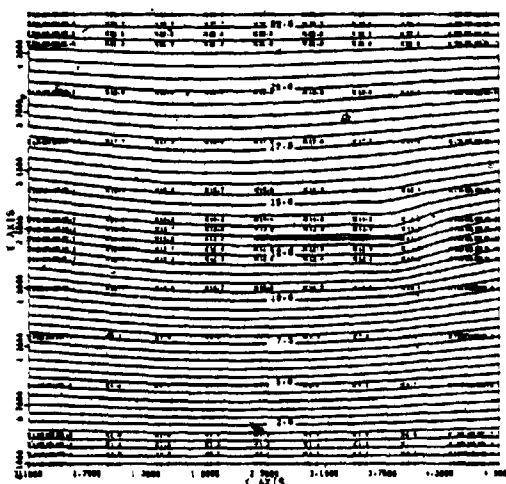


Figure (6-39)

VORTEX APPROACHING FINITE PLATE.  $U=5$ .  $\text{GAMA}=10$ .  
 $RC=0.7$ .  $T=1.36$

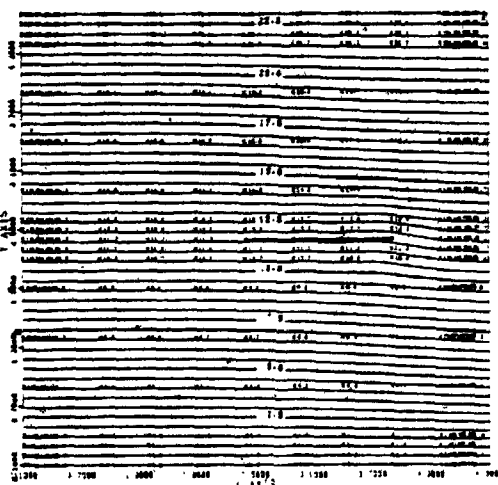


Figure (6-40)

## CHAPTER 7.

### SIMULATION OF TURBULENCE

#### AND ITS EFFECT ON A SEMI-INFINITE FLAT PLATE

##### 7.1 INTRODUCTION

Recently there has been particular interest given to simulating unsteady flows, such as turbulence, using computer simulation experiments. The success that has been achieved in these studies has made it possible to investigate the effects of pseudo-turbulence on a body using a mathematical model to simulate the approaching turbulent flow.

Lilly [1969] developed a numerical simulation technique for two-dimensional turbulence. In this approach, Lilly considered an incompressible turbulent velocity field to be idealized as a random vector field governed in time and two-dimensional space by the Navier-Stokes equations.

Base [1970] developed a method that can be used for simulating pseudo-turbulence of different statistical characteristics and to obtain a continuous velocity time history at each point in the flow field. In this approach the eddy structure of the turbulence was represented by groups of randomly positioned moving "real" vortices. It was found that by changing the rotational core size of the individual "real" vortices and also by changing the mean distance between them, the statistical characteristics of the pseudo-turbulence were changed. Another contribution in the numerical solution of two-dimensional turbulence is found in the

work of Ahmadi and Goldschmidt [1971] where a numerically simulated turbulent field was forced to satisfy the Navier-Stokes equation and stationarity.

The method to model turbulence used in this Chapter follows the approach described by Base [1970]: The computer simulated model of pseudo-turbulence was used to generate the upstream boundary conditions for an incompressible and inviscid fluid flow over a semi-infinite flat plate between two parallel planes. The continuity and momentum conservation equations were solved near the plate by using the finite difference methods presented in Chapter 3. The resulting random longitudinal and lateral velocities were sampled and the corresponding auto-correlation and power spectra were plotted. The effects of this pseudo-turbulent flow on the lift and pitching moment coefficients on the flat plate were also plotted.

## 7.2 DESCRIPTION OF THE CONSIDERED PROBLEM

The problem considered was that of a semi-infinite thin flat plate set at zero incidence to an initially uniform flow. The turbulent fluid flow was modelled by groups of randomly positioned moving vortices to represent the eddy structure of the turbulence. Figure (7-1) shows four boxes A, B, C and D for the vortices, with box C representing the solution domain where the flat plate is situated midway between the upper and lower planes. Initially the vortices were randomly positioned in boxes A, B, C and D as shown in



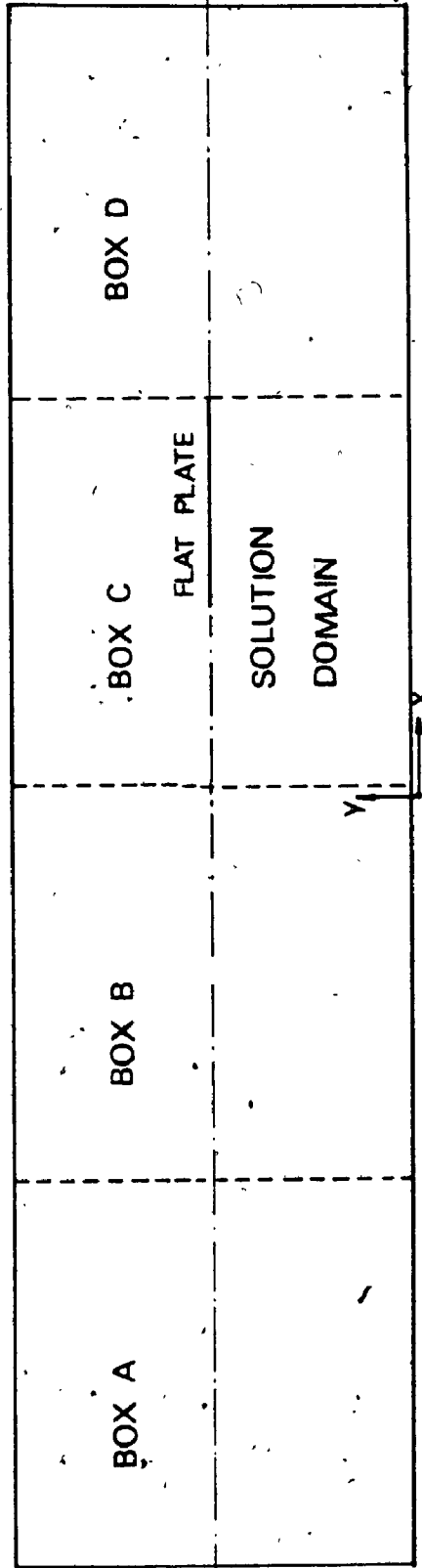


Figure (7-1) Schematic diagram showing four boxes for real vortices with the flat plate in BOX C (solution domain).

Figures (7-2) and (7-3). With the increase of time, the vortices were convected by the flow until a total time of one "vortex model cycle" ( $t_{\text{cycle}}$ ) had elapsed. With further increase of time and with no further increase in the number of vortices being added to the model, the program was so scaled that within this time period the vortices had moved approximately one box length downstream. At this particular time period approximately one-quarter of the total number of vortices farthest downstream, that by now had little influence at the upstream boundary of the solution domain, were removed and replaced by the same number of similar vortices with new random positions and new signs upstream of the flat plate. These added vortices had little influence on the conditions at the upstream boundary of the solution domain.

The vortex model then continued and the process repeated again so that a continuous pseudo-turbulence vortex model was achieved. By this means, the vortex model provided a continuous velocity field at the upstream boundary of the solution domain. Hence, the pseudo-turbulence entered the solution domain through its effect on the upstream boundary while the corresponding effect on the flat plate was investigated by solving numerically the Navier-Stokes equations in the solution domain surrounding it.

### 7.3 THE PSEUDO-TURBULENCE BOUNDARY CONDITIONS

In general, for a rotational fluid flow, the effects from all the disturbances cannot be summed, as is possible

# RANDOM VORTICES IN BOXES A AND B

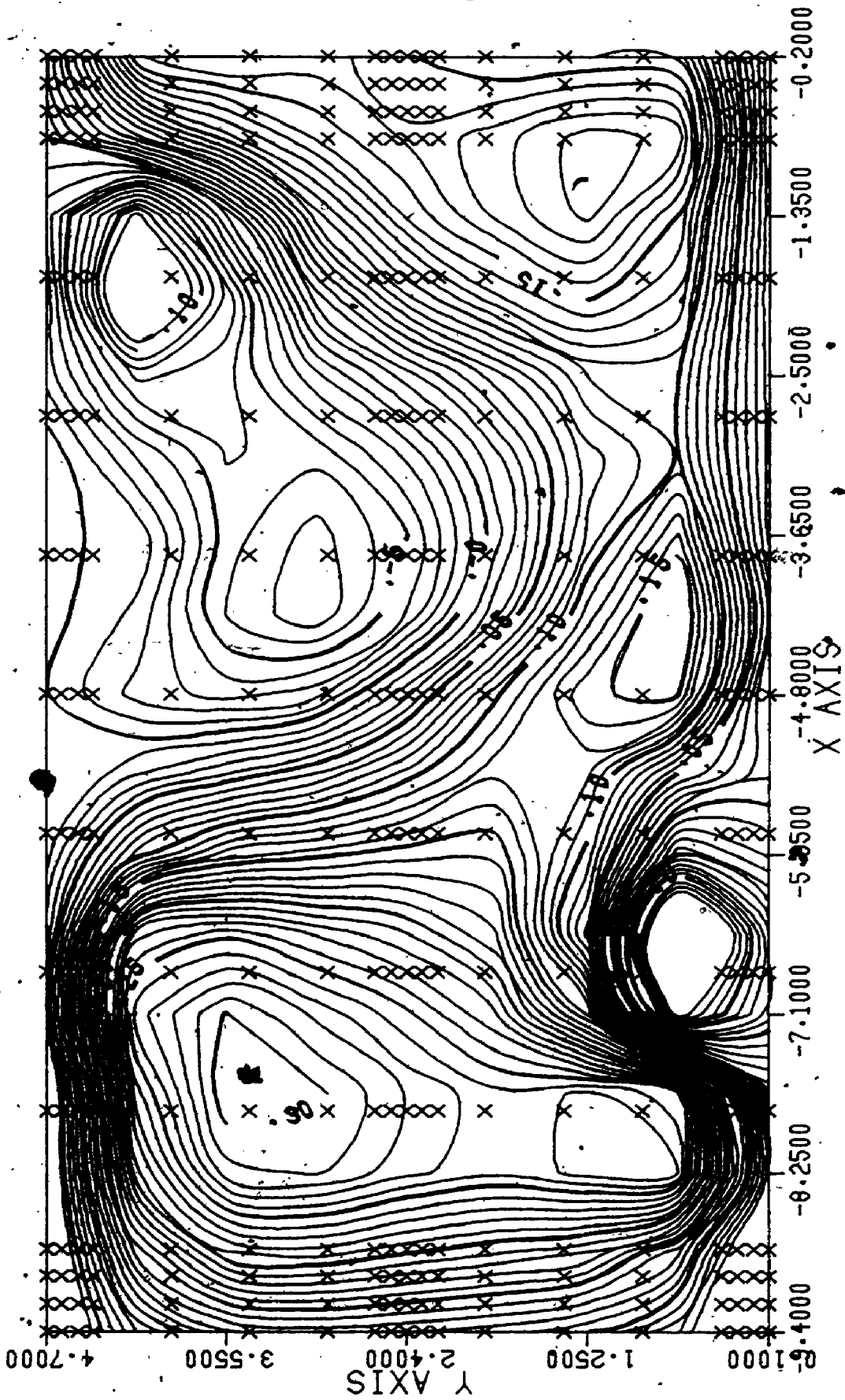


Figure (7-2) Initial distribution of the random vortices in BOXES A and B.

RANDOM VORTICES IN BOXES C AND D

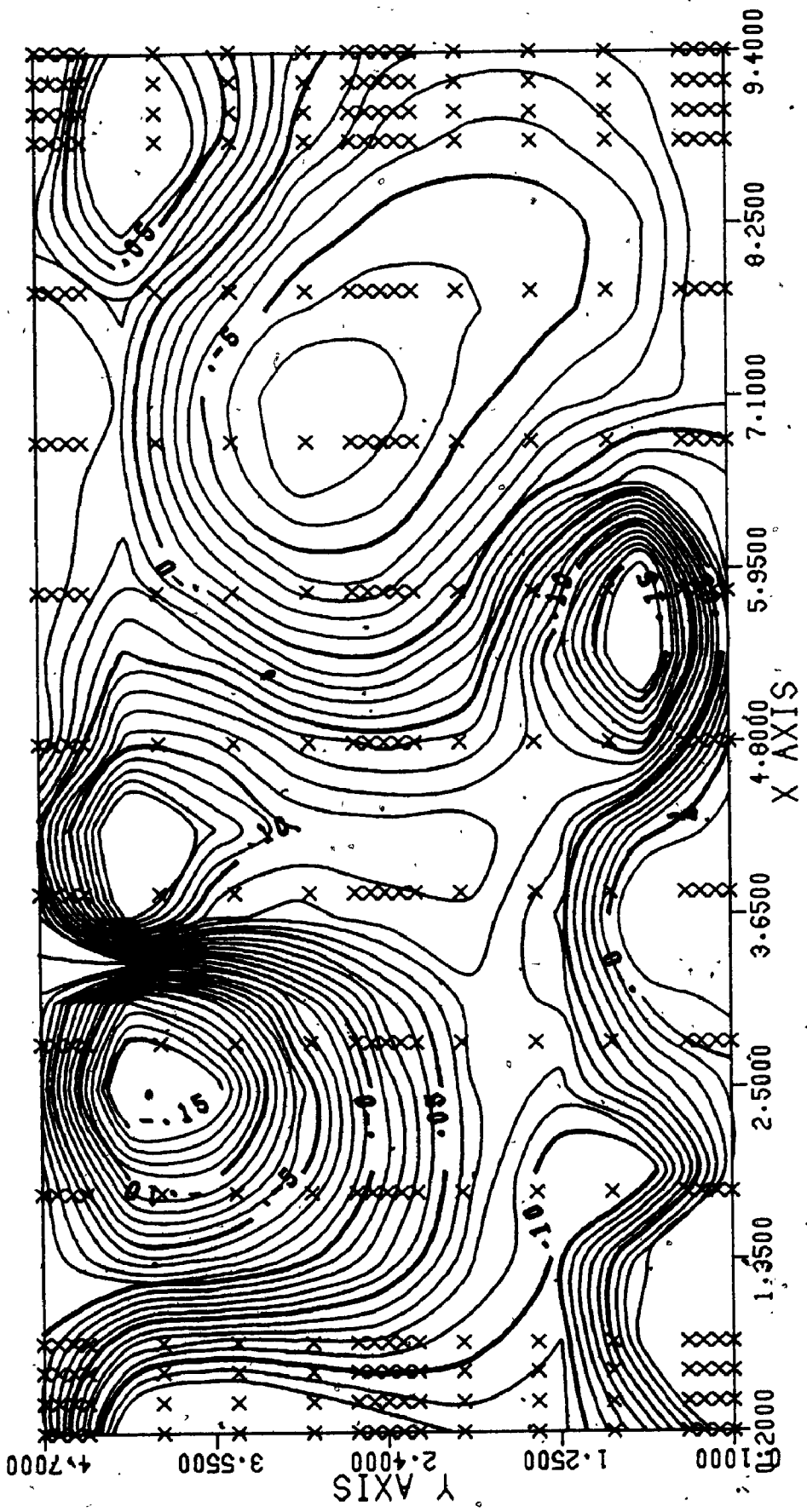


Figure (7-3) Initial distribution of random vortices in BOXES C and D.

for a potential flow, since the angular momentum equation is non-linear. However, for an incompressible fluid flow the continuity equation is linear and so, in principle, the velocity at a point can still be written as the sum,

$$\underline{V} = \underline{V}_1 + \underline{V}_2 + \underline{V}_3 + \dots + \underline{V}_N \quad (7.1)$$

provided each velocity contribution ( $V_1, V_2, \dots, V_N$ ) is known. In the complete mathematical solution of most problems this is not possible, since the velocity field is not known and is the required solution. In the present Chapter, the stream function on the upstream boundary is assumed to be equal to the summation of the contributions of each individual random "real" vortex whose expression was given in Chapter 4, Equation (4.29), so that,

$$\psi = \psi_1 + \psi_2 + \psi_3 + \dots + \psi_N \quad (7.2)$$

Differentiating Equation (7.2) with respect to  $y$  and  $x$  respectively would give,

$$\frac{\partial \psi}{\partial y} = \frac{\partial \psi_1}{\partial y} + \frac{\partial \psi_2}{\partial y} + \frac{\partial \psi_3}{\partial y} + \dots + \frac{\partial \psi_N}{\partial y} \quad (7.3)$$

$$\text{and } \frac{\partial \psi}{\partial x} = \frac{\partial \psi_1}{\partial x} + \frac{\partial \psi_2}{\partial x} + \frac{\partial \psi_3}{\partial x} + \dots + \frac{\partial \psi_N}{\partial x} \quad (7.4)$$

Using the stream function definition which is,

$$u = \frac{\partial \psi}{\partial y} \quad \text{and} \quad v = - \frac{\partial \psi}{\partial x}$$

then,

$$u = u_1 + u_2 + u_3 + \dots + u_N \quad (7.5)$$

$$V = V_1 + V_2 + V_3 + \dots + V_N \quad (7.6)$$

The tacit assumption then was that the velocity at any field point ( $\underline{x}$ ) was given by the sum of the contributions from the real vortices.

The velocity ( $u_i$ ) therefore at an upstream boundary point ( $\underline{x}_i$ ) was given by:

$$u_i = \sum_{m=1}^N (u_i)_m \quad (7.7)$$

where  $\underline{x}_i$  was the position vector of the upstream boundary point,  $u_i$ ,  $i=1,2$  were the velocity components in the x and y directions, and  $(u_i)_m$  was the contribution to the velocity at the point ( $\underline{x}_i$ ) due to the  $m^{\text{th}}$  vortex and N was the total number of vortices representing the model. It could also be shown, from Equation (7.7) that the spatial derivative at the point ( $\underline{x}_i$ ) was also equal to the sum of the derivative contributions from the complete array of vortices so that,

$$\frac{\partial u_i}{\partial x_i} = \sum_{m=1}^N \left( \frac{\partial u_i}{\partial x_i} \right)_m, \quad i=1,2 \quad (7.8)$$

Since a condition for the vortex generating function was that the continuity equation be satisfied so that,

$$\left( \frac{\partial u_i}{\partial x_i} \right)_m = 0 \quad (7.9)$$

then by substituting Equation (7.9) into (7.8) the result was,

$$\frac{\partial u_i}{\partial x_i} = 0 \quad (7.10)$$

The continuity equation was therefore satisfied implicitly throughout the whole vortex model which ensured that it was kinematically possible. Further details concerning the vortex model from which this present study was developed are presented by Base [1970]. The computational procedures and the methods used to evaluate the other boundary conditions required to obtain a solution of the fluid flow equations were similar to those for a single vortex presented in the previous Chapters.

#### 7.4 STATISTICAL ANALYSIS AND RESULTS

In order to describe a turbulent flow in mathematical terms it is convenient to separate the flow into a mean motion and into a fluctuation, or eddying motion. Denoting the time-average of the  $u$ -component of velocity by  $\bar{u}$  and its velocity of fluctuation by  $u'$ , the relations for the velocity components can be written as,

$$u = \bar{u} + u' \quad ; \quad v = \bar{v} + v' \quad (7.11)$$

(a) (b)

The time-averages are defined at a fixed point in space and are given, for example, by

$$\bar{u} = \lim_{T \rightarrow \infty} \frac{1}{T} \int_0^T u(t) dt \quad (7.12)$$

When writing a computer program to estimate the mean value, if the time increment between each digitized value  $(u)_m$  is the same, then Equation (7.12) may be approximated by:

$$\bar{u} \approx \frac{1}{N} \sum_{m=1}^N (u)_m \quad (7.13)$$

where  $N$  is the total number of numbers representing the total sample length.

It is understood that the mean values are taken over a sufficiently long interval of time, for them to be completely independent of time. Thus, by definition, the time-averages of all quantities describing the fluctuations are equal to zero and,

$$\bar{u}' = 0 \quad \bar{v}' = 0 \quad (7.14)$$

The mean square value is given by the expression

$$\sigma^2 = \lim_{T \rightarrow \infty} \frac{1}{T} \int_0^T (u - \bar{u})^2 dt \quad (7.15)$$

Equation (7.15) may be rearranged, using the above definition of the mean value to give,

$$\sigma^2 = \lim_{T \rightarrow \infty} \frac{1}{T} \int_0^T u^2 dt - \bar{u}^2 \quad (7.16)$$

and this may similarly be approximated in a computer program by,

$$\sigma^2 \approx \frac{1}{N} \sum_{m=1}^N (u)_m^2 - \bar{u}^2 \quad (7.17)$$

The standard deviation ( $\sigma$ ), or the root mean square of the fluctuations ( $u'_{r.m.s.}$ ), is given by the positive square root of Equation (7.17).

Figure (7-4) shows the variations of the conditioned longitudinal velocity component  $\left[ \frac{u'}{u'_{r.m.s.}} \right]$ , at an upstream



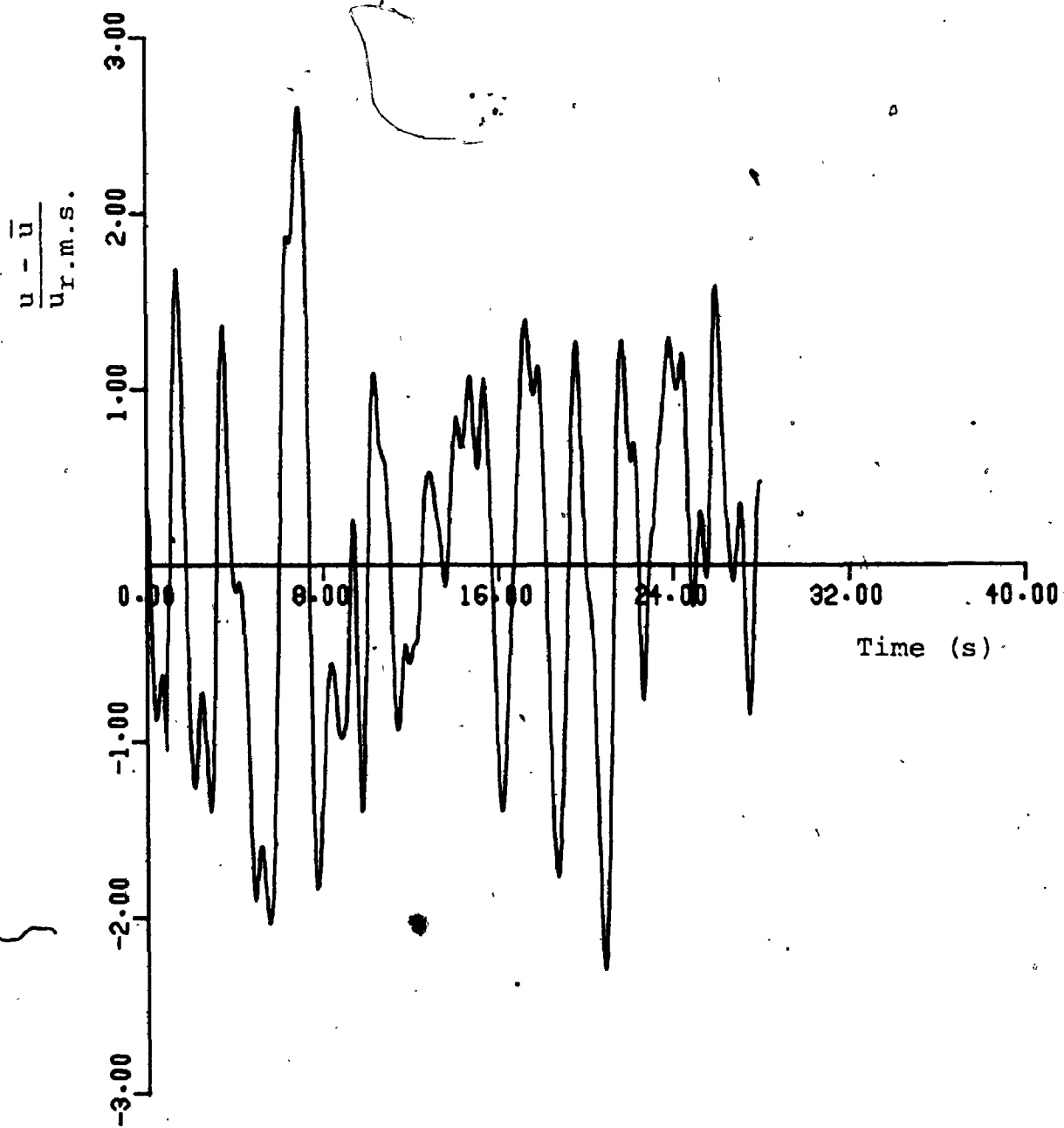


Figure (7-4) Variation of the conditioned longitudinal velocity component with time.

boundary point, with respect to time for a pseudo-turbulence vortex model with mean dimensionless radius  $r_c^* = 0.7$ , mean approaching velocity of 5.0 m/s, and mean circulation constant of 1.0 m<sup>2</sup>/s ( $R_{S_{\text{mean}}} = 0.062$ ). Figures (7-5) and (7-6) show the corresponding auto-correlation and power spectral density for such a conditioned signal. For further details concerning this analysis see Appendix (C).

Similarly Figures (7-7), (7-8) and (7-9) show the time variations, auto-correlation, and power spectral density for the conditioned lateral velocity component.

Figures (7-4) to (7-9) show that the randomness and disorderliness is maintained as in true turbulence by using this pseudo-turbulence vortex model which ensured a continuous random signal.

The resulting time-variations of lift and pitching moment coefficients, obtained by solving the stream function equation and Helmholtz equation in the solution domain, are shown in Figures (7-10) and (7-11).

The numerical methods presented and the computer programs developed, see Appendix (E), to solve these equations with the associated boundary conditions were extremely stable to the unsteady, continuous and stochastic changes that took place on the upstream boundary. To obtain a solution for the approaching pseudo-turbulence required more iterations than for a single approaching vortex studied in the previous Chapters.

In this pseudo-turbulence study the stability criterion

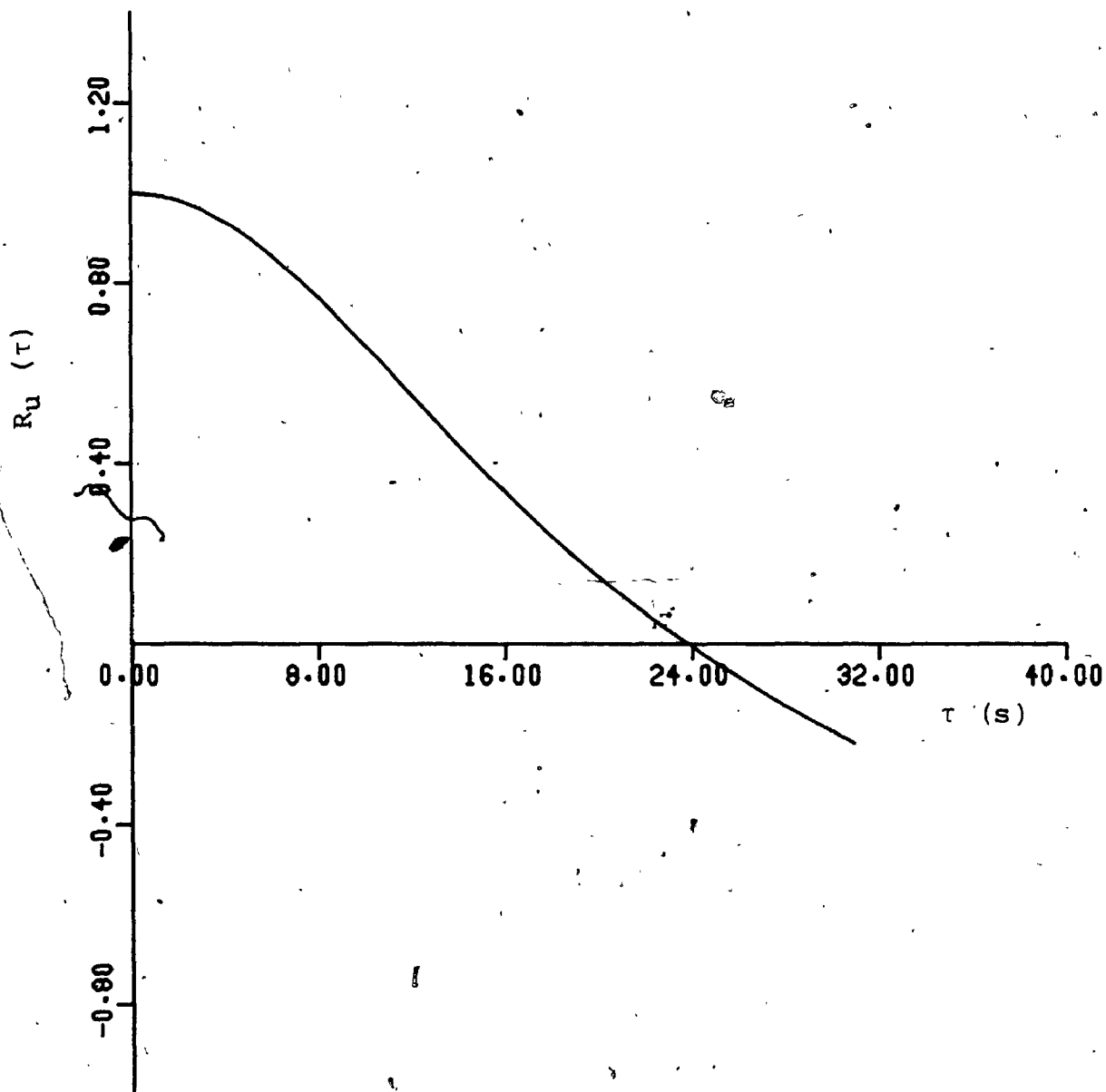


Figure (7-5) Auto-correlation for the conditioned longitudinal velocity component

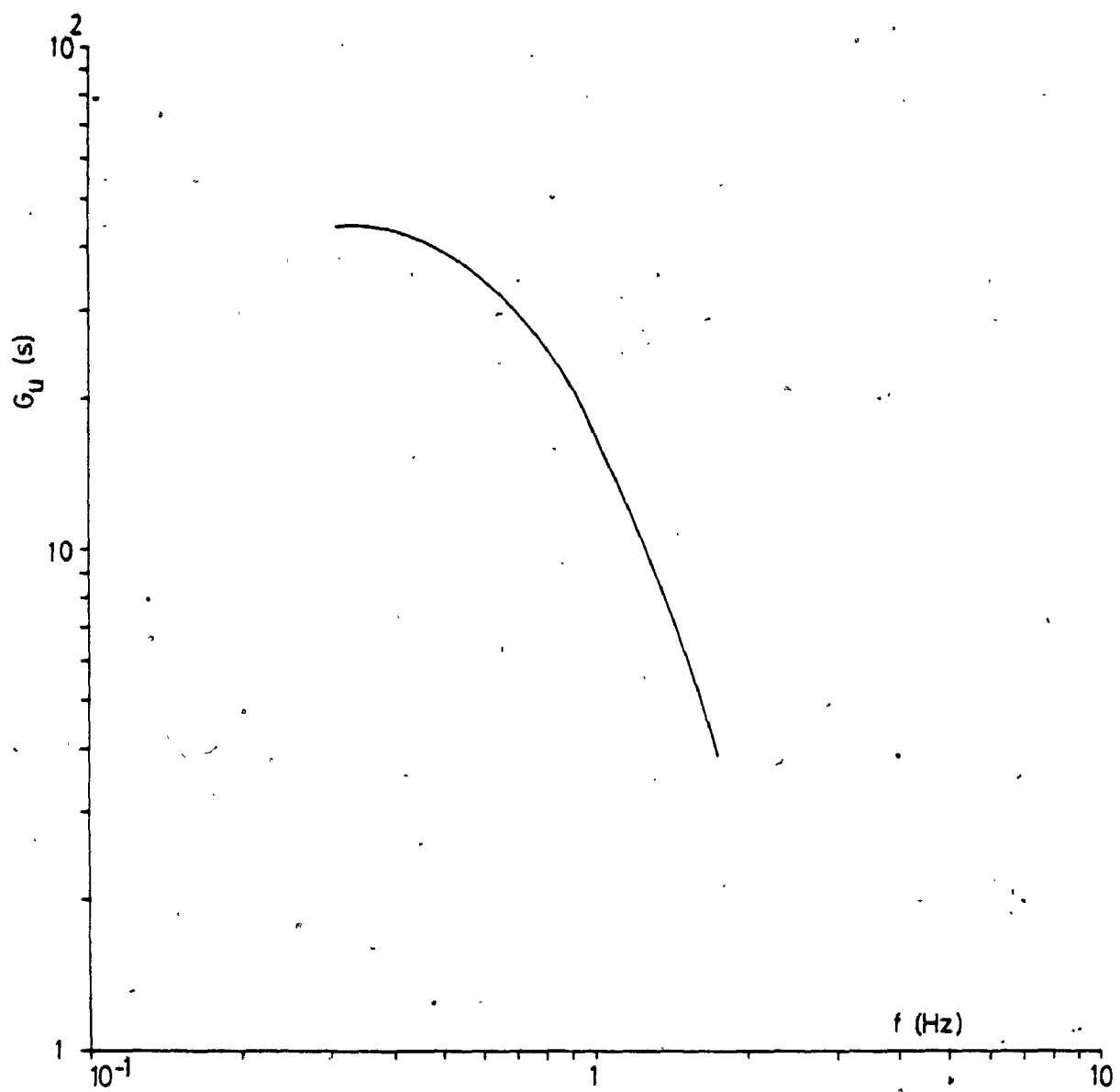


Figure (7-6) Power spectral density for the conditioned longitudinal velocity component.

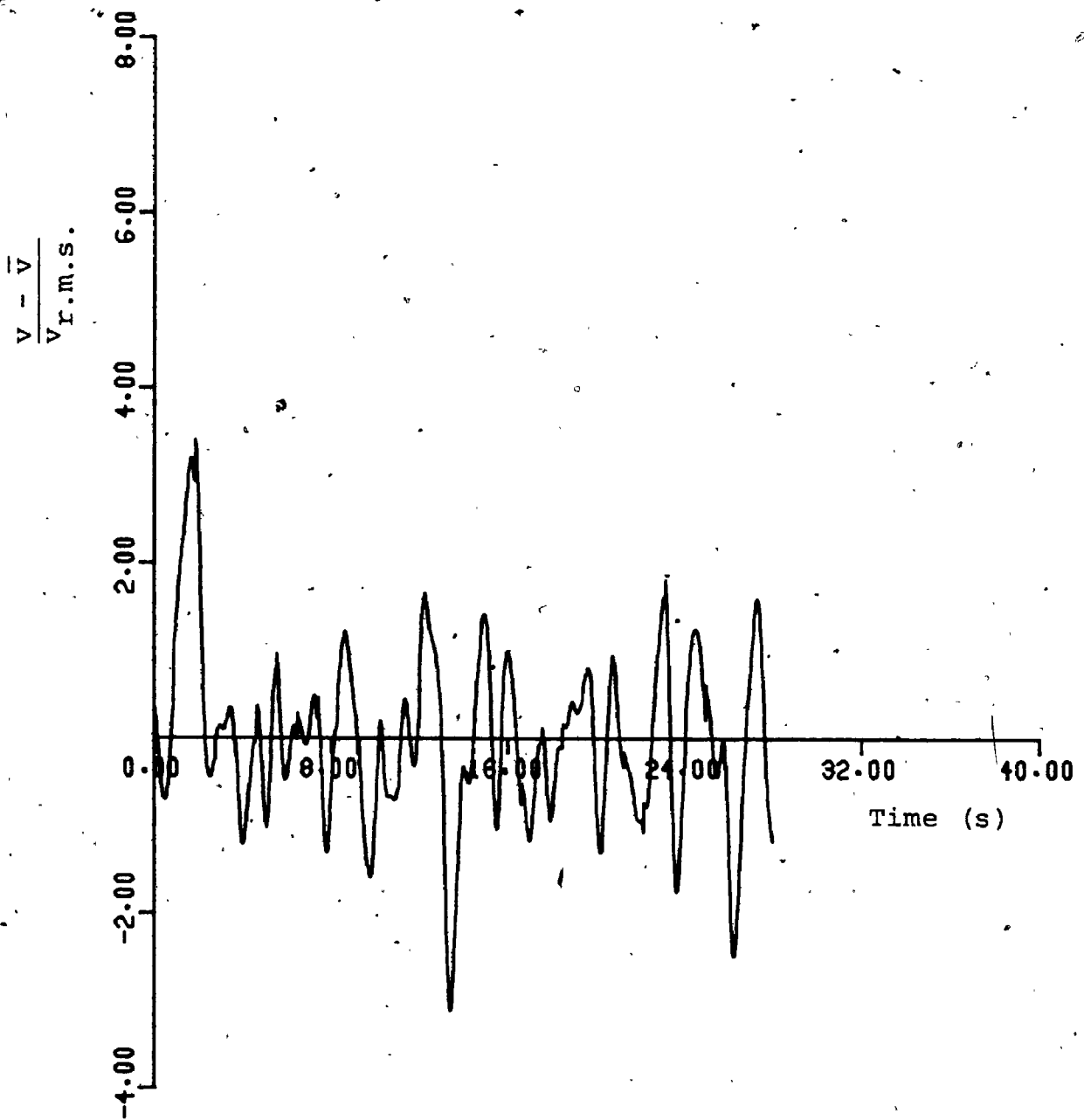


Figure (7-7) Variation of the conditioned lateral velocity component with time.

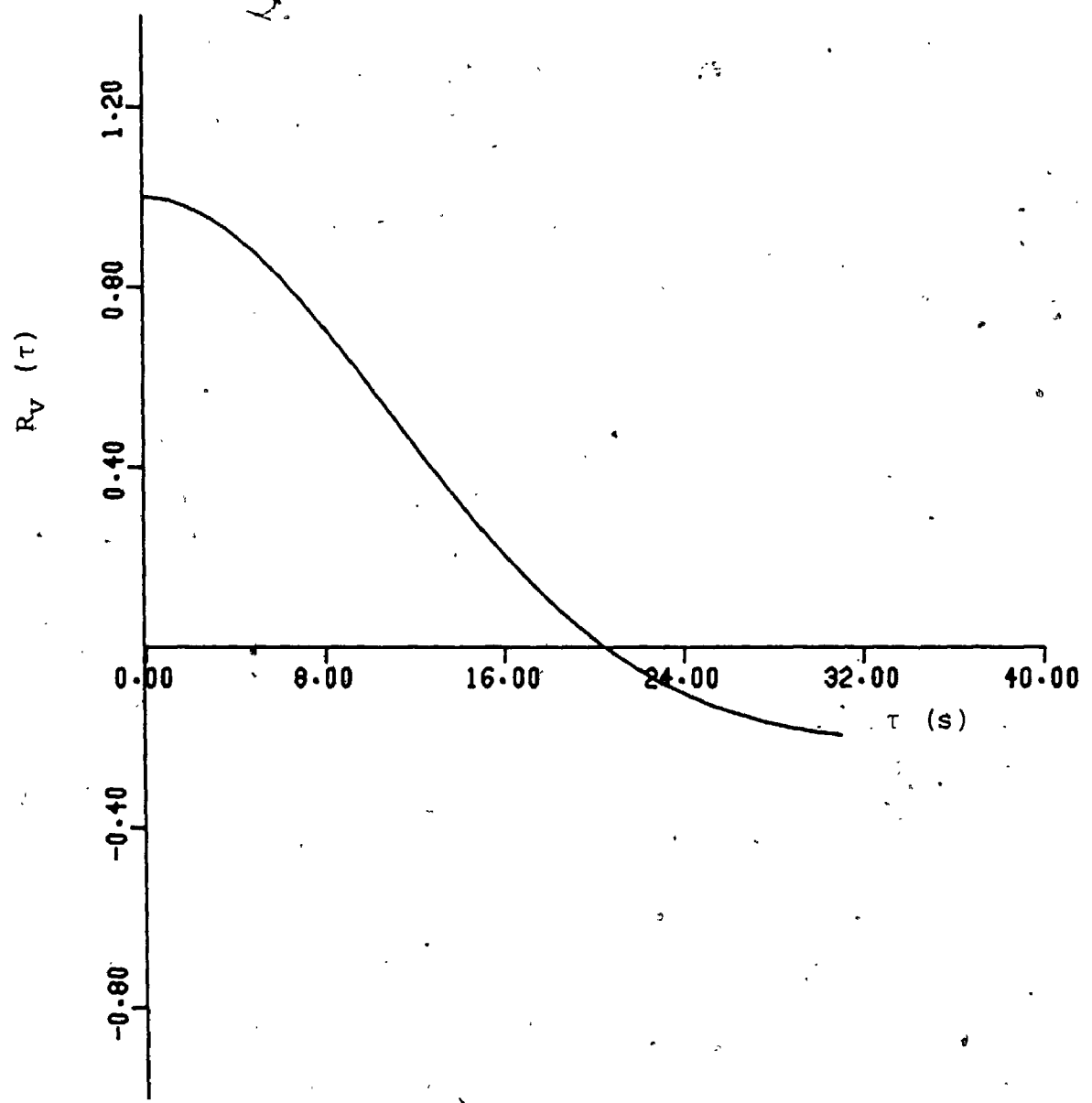


Figure (7-8) Auto-correlation for the conditioned lateral velocity component.

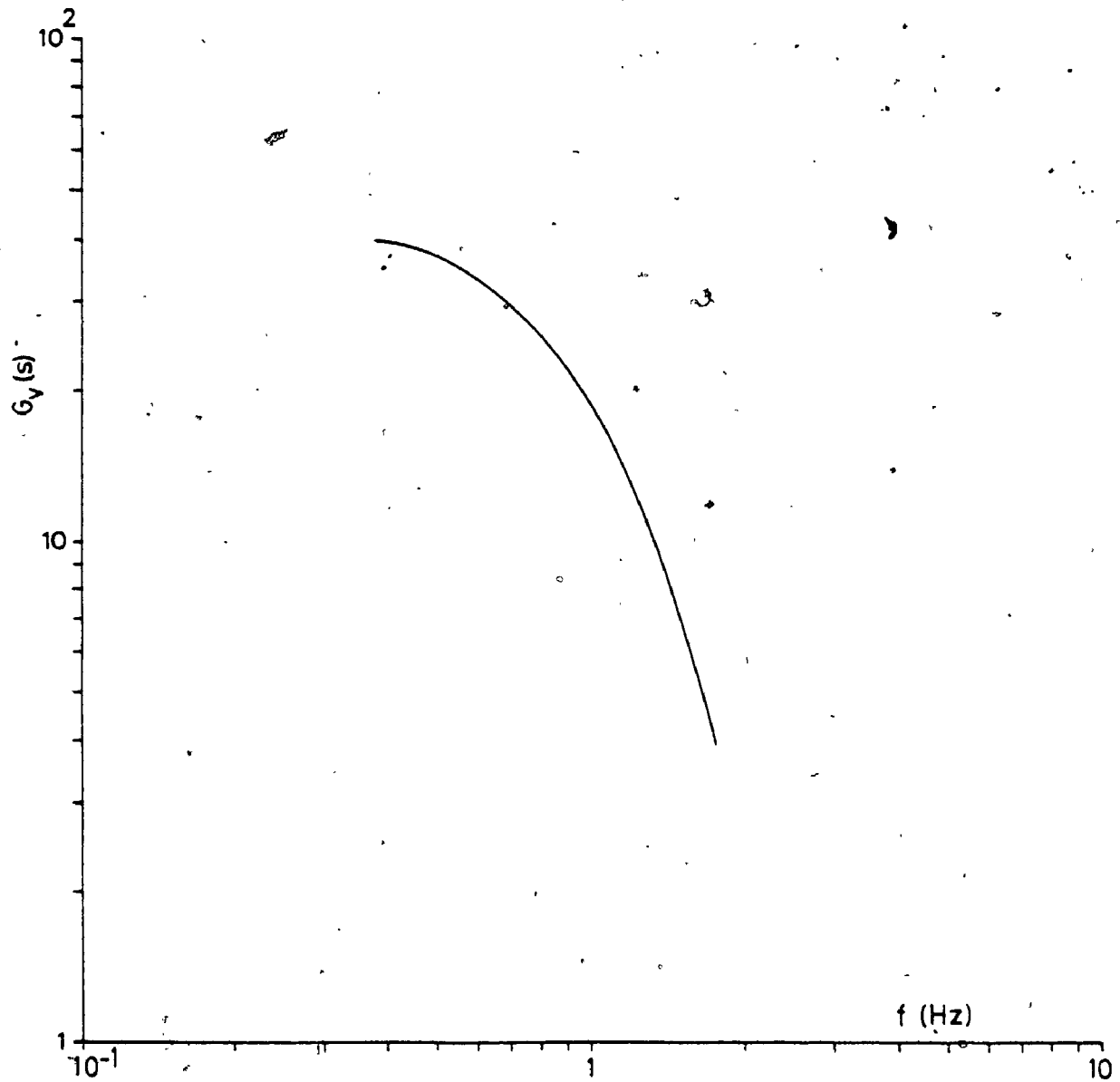


Figure (7-9) Power spectral density for the conditioned lateral velocity component.

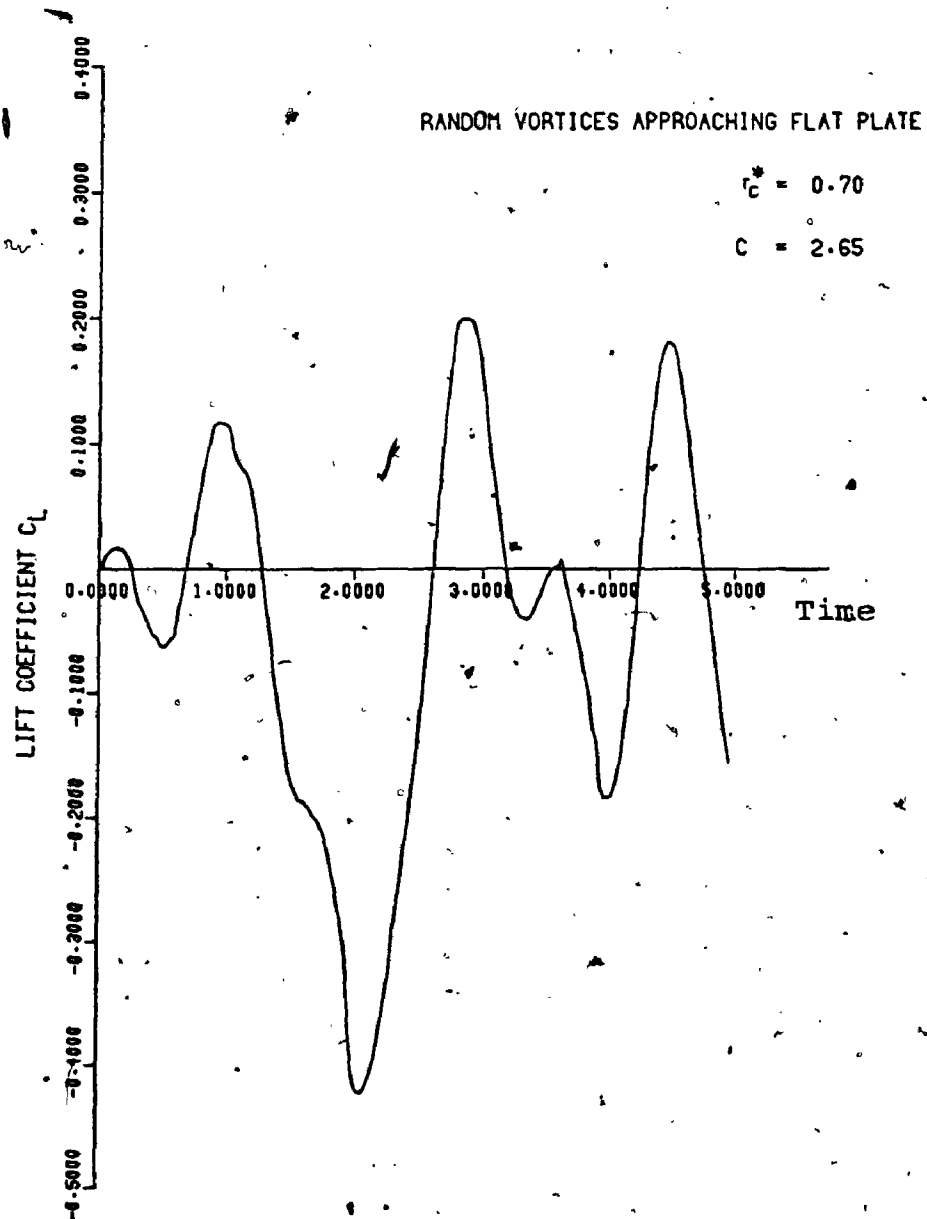


Figure (7-10) Lift coefficient versus time.



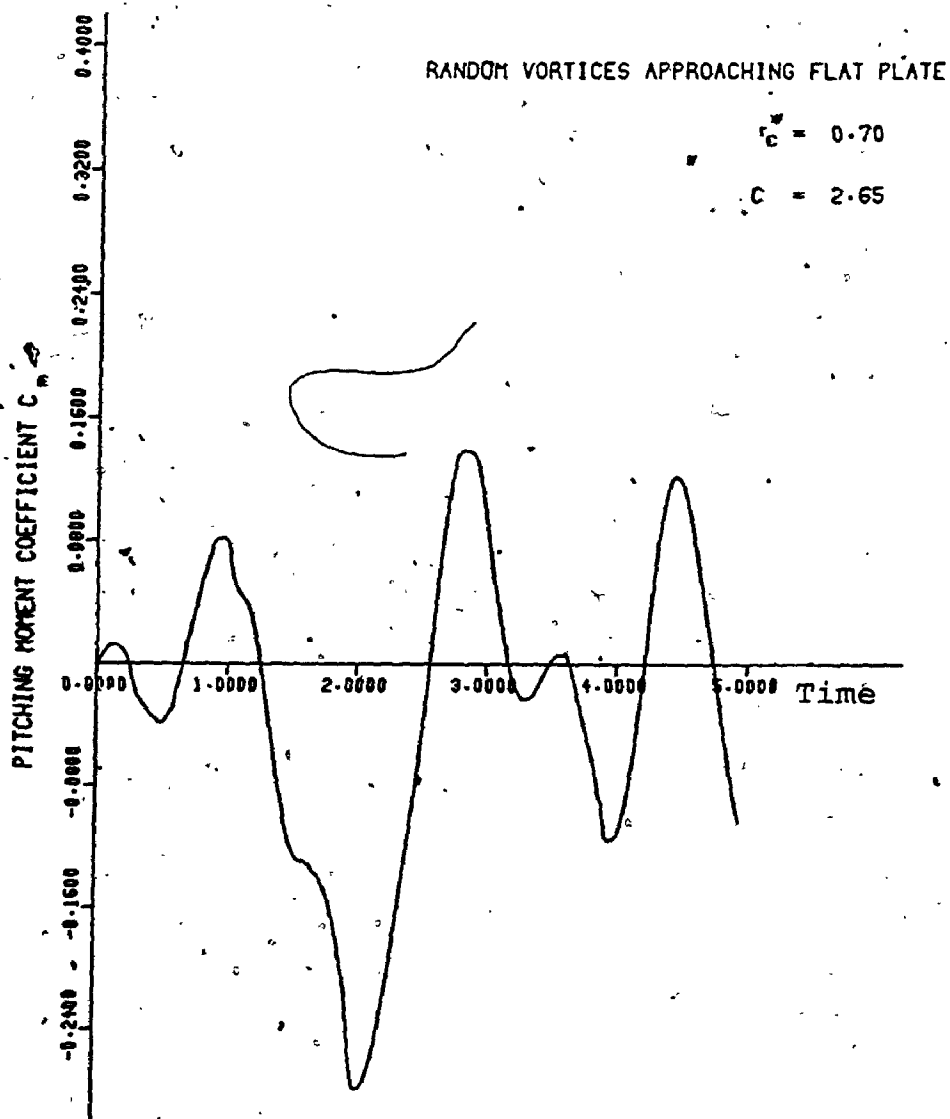


Figure (7-11) Pitching moment coefficient versus time.

and accuracy were the same as for a single vortex discussed in Chapter 6.

It is of interest to mention that in order to compute the one pseudo-turbulence model just discussed, of 5 seconds real time duration, a total of 8690 CPU computer seconds were required. At the present charge rate at the University Computer Centre, this was equivalent to a financial charge of \$933 for an overnight run ( $Q_2$ ).

It has been shown that the pseudo-turbulence model could be run with different model parameters to produce the effect of different pseudo-turbulence on the flat plate. Therefore, only one model was studied to illustrate the technique. For further models, provided the stability criteria were satisfied, different pseudo-turbulent structures could be studied by changing the input data to the computer program.

## CHAPTER 8

### CONCLUSIONS

#### 8.1 GENERAL CONCLUSIONS

The main objective of this study was to investigate the influence of a two-dimensional, unsteady, incompressible inviscid fluid flow stream with rotational disturbances approaching a body situated between two parallel planes.

The governing equations were written in the form of the Helmholtz vorticity transport equation and the stream function equation. An implicit finite-difference method with variable mesh size and also facility for variable time step control was developed for solving these equations. This method consisted of an iterative solution between the stream function equation and the Helmholtz vorticity equation in order to achieve a convergence. A new modified vortex mathematical expression was developed to represent a real vortex positioned between two parallel planes. This expression satisfied the "no flow through the solid wall" boundary condition and also was rotational. New techniques were also developed to estimate the time-changing boundary conditions around the solution domain and also on the body. The introduction of these techniques assured that the solution converged faster than traditional methods as well as having the downstream and body boundary conditions dependent on the flow conditions upstream.

The method of solution and the numerical techniques

were tested by comparing the computed stream function values to those obtained analytically when a potential vortex situated between two parallel planes (Equation (4.26)) approached the solution domain with no solid body within. The comparison between the exact and the computed solution was in good agreement with a percentage deviation of approximately 0.01%. The variable time step control made it possible to obtain solutions which would have needed more iterative attempts with a fixed time step to obtain. When the disturbances were close or within the solution domain where rapid changes took place in the flow characteristics, smaller time steps were used. Larger time steps were used when the disturbances were far from the solution domain. The maximum time step used was less or equal to that obtained from stability criteria discussed in Chapter 6.

The finite-difference techniques introduced in this thesis were developed in order to study the effect of a two-dimensional rotational disturbance in the approaching stream impinging on a flat plate situated midway between two parallel planes. In this problem the rotational disturbance was simulated by an "equivalent modified Rankine vortex" which was set initially far from the plate such that its influence on the flow pattern on the upstream boundary was almost negligible. The stream lines in this initial case were lines parallel to the x axis. The vortex was then convected, with no viscous diffusion, along with the free stream until it entered the solution domain, impinged on the plate and

was convected out of the downstream boundary. At this point in time the fluid flow within the domain returned to its original steady state. The new technique for determining the magnitude of the outflow boundary and the body stream function values which were dependent on the flow conditions upstream, made it possible to study the lift and pitching moment coefficients on both semi-infinite and finite flat plates, for the inviscid fluid case. Stream function contours as well as the time variation of lift and pitching moment coefficients for the flat plate were plotted. The method of solution was extremely stable provided that the Rossby number value was less than unity. A complete discussion and full analysis of the results were presented in Chapter 6, and showed that the results were consistent with the physical situation of the considered problem.

This study was then extended to investigate the effect of flow stream pseudo-turbulence on a thin flat plate set at zero incidence to an initially uniform flow. A computer simulation technique to generate pseudo-turbulence, based on the work by Base [1970,1974], was used to generate the upstream boundary conditions to the solution domain around the flat plate. The stream function equation and the vorticity transport equation were solved around the plate using the same numerical techniques and methods developed previously in this thesis. The time-varying lift and pitching moment coefficients on the flat plate were plotted. The auto-correlation and the power spectrum were also plotted.

for long samples of the longitudinal and lateral velocity components. This study showed that using this pseudo-turbulence model ensured the randomness and disorderliness, as in the true turbulence, while satisfying the conservation of mass and angular momentum equations within the domain. In the pseudo-turbulence study the stability criterion and accuracy were the same as for the single vortex case discussed in Chapter 6.

It has been shown that even with the assumption of inviscid fluid flow, the fluctuating loads due to the unsteady approaching rotational flow may be determined and eventually could be used for practical engineering design studies, for example, the important problem of the case of an aircraft crossing the wake flow of another aircraft. In particular, by studying the response of an aircraft wing to a discrete vortex or even pseudo-turbulence it could provide information that eventually could be used to reduce the hazard of wake turbulence, not only by indicating modifications to the aerodynamics of the aircraft that generates the wake, but also predicting the response of the following aircraft.

In the case of a bridge response to unsteady flow, the three-dimensional nature of turbulence would reduce the effect of aerodynamic loading predicted by the two-dimensional pseudo-turbulence model used in this thesis. The behaviour of the three-dimensional structure can deviate from that of the two-dimensional models, however the two-dimensional

study would indicate the important parameters with respect to relating the spectrum of the load or lift force on the bridge to the approaching flow structure. In future studies three-dimensional pseudo-turbulence models would be more suited to predict the aerodynamic loads on bridges.

## 8.2 RECOMMENDATIONS FOR FUTURE STUDIES

The following are some recommendations that may be considered for future studies to pursue in this research area:

- 1) The plate studied in this analysis was assumed to be infinitesimally thin. In future studies an aerofoil shape with thickness could be introduced into the computer program for analysis. This analysis would be applicable to the practical case of an engine turbine blade subjected to turbulent flow where estimates of the fluctuating lift may be required.
- 2) In other studies, the case where there are more than one solid body in the solution domain could be considered, for example, a cascade of blades in a turbine.
- 3) This present study considered an inviscid fluid. In future study the viscous terms in the Helmholtz vorticity equation could be included. Studies on the effect of Reynold's number variations on the lift and drag coefficients, of a body such as an aerofoil, could then be determined.
- 4) Finally, studies on the effects of changing the turbu-

lence statistical characteristics on the lift and drag forces on a flat plate or aerofoil in a viscous fluid flow could be attempted.



APPENDIX (A)

THE EQUATIONS OF MOTION

FOR AN INCOMPRESSIBLE FLUID FLOW

The equations of motion in the case of a three-dimensional, unsteady, incompressible fluid flow (Navier-Stokes equation) can be written in vector form as:

$$\left( \frac{\partial}{\partial t} + \underline{U} \cdot \underline{\nabla} \right) \underline{U} = - \frac{1}{\rho} \underline{\nabla} P + \nu \nabla^2 \underline{U} \quad (\text{A-1})$$

and the continuity equation as:

$$\underline{\nabla} \cdot \underline{U} = 0 \quad (\text{A-2})$$

Taking the vector curl of Equation (A-1) and noting that:

$$(\underline{U} \cdot \underline{\nabla}) \underline{U} = \frac{1}{2} \underline{\nabla} U^2 - \underline{U} \times (\underline{\nabla} \times \underline{U})$$

the following equation can then be obtained:

$$\left( \frac{\partial}{\partial t} + (\underline{U} \cdot \underline{\nabla}) \right) \underline{\Omega} = (\underline{\Omega} \cdot \underline{\nabla}) \underline{U} + \nu \nabla^2 \underline{\Omega} \quad (\text{A-3})$$

where  $\underline{\Omega}$  is the vorticity vector defined by:

$$\underline{\Omega} = \underline{\nabla} \times \underline{U} \quad (\text{A-4})$$

In the case of two-dimensional flow where there is no change with respect to the z direction  $\left( \frac{\partial}{\partial z} = 0 \right)$ , only one component of the vorticity ( $\Omega_3$ ) exists which is perpendicular to the plane of motion such that,

$$\Omega_3 = \frac{\partial v}{\partial x} - \frac{\partial u}{\partial y} \quad (\text{A-5})$$

Also the first term on the right hand side of Equation (A-3), (vorticity stretching or amplification term), would vanish.

In this case the stream function  $\psi$  may be introduced such that,

$$u = \frac{\partial \psi}{\partial y}, \quad v = -\frac{\partial \psi}{\partial x}$$

and Equations (A-3) and (A-4) can be written as,

$$\frac{\partial \Omega}{\partial t} + u \frac{\partial \Omega}{\partial x} + v \frac{\partial \Omega}{\partial y} = \nu \nabla^2 \Omega \quad (\text{A-6})$$

$$\text{and } -\Omega = \nabla^2 \psi \quad (\text{A-7})$$

where

$$\nabla^2 = \frac{\partial^2}{\partial x^2} + \frac{\partial^2}{\partial y^2} \quad \text{and } \Omega = \Omega_3$$

Equations (A-6) and (A-7) are known as the vorticity transport (Helmholtz) and stream function equations respectively.

An expression for the pressure can be obtained by taking the divergence of the two sides of Equation (A-1) and by using the continuity Equation (A-2). The following equation was obtained,

$$\nabla \cdot (\underline{U} \cdot \nabla) \underline{U} = -\frac{1}{\rho} \nabla^2 p \quad (\text{A-8})$$

which can be written in two-dimensional, cartesian coordi-

nates as,

$$\frac{\partial^2 P}{\partial x^2} + \frac{\partial^2 P}{\partial y^2} = -\rho Q \quad (\text{A-9})$$

where

$$Q = 2 \left( \frac{\partial u}{\partial y} \frac{\partial v}{\partial x} - \frac{\partial u}{\partial x} \frac{\partial v}{\partial y} \right) \quad (\text{A-10})$$

## APPENDIX (B)

### DERIVATION OF THE STREAM FUNCTION

### EQUATION FOR A VORTEX BETWEEN TWO

### PARALLEL PLANES

In this Appendix the analysis necessary to obtain the stream function Equation (4.18) for a vortex positioned between two parallel planes is presented.

Rewriting the complex potential discussed in Chapter 4 for this flow regime using the method of images, Equation (4.16), which is:

$$w = - \frac{i\Gamma_0}{2\pi} \ln \left\{ \frac{\text{Sin}[(\pi/2a)(x_0 + z)]}{\text{Sin}[(\pi/2a)(x_0 - z)]} \right\} \quad (4.16)$$

where

$$w = \phi + i \psi \quad (4.14)$$

$$z = x + i y \quad (4.15)$$

$$i = \sqrt{-1}$$

$\Gamma_0$  = circulation constant

$a$  = ~~distance between~~ the two parallel planes

and  $x_0$  = the x coordinate of the vortex centre, (see Figure (4-1), measured from one of the planes.

Using trigonometric relations to analyze the term between the parentheses in Equation (4.16), which will be denoted by  $F$ , and putting  $c = \pi/2a$ , results in

$$F = \frac{\text{Sin}[c(x_0 + z)]}{\text{Sin}[c(x_0 - z)]}$$

$$= \frac{\sin cx_0 \cos cz + \cos cx_0 \sin cz}{\sin cx_0 \cos cz - \cos cx_0 \sin cz}$$

$$= \frac{1 + \cot cx_0 \tan cz}{1 - \cot cx_0 \tan cz}$$

Putting  $K = \cot cx_0$  and substituting for  $z$  from Equation (4.15), then

$$F = \frac{1 + K \tan[c(x + iy)]}{1 - K \tan[c(x + iy)]}$$

$$= \frac{1 + K \frac{\tan cx + \tan icy}{1 - \tan cx \tan icy}}{1 - K \frac{\tan cx + \tan icy}{1 - \tan cx \tan icy}}$$

Noting that from the relations between trigonometric and hyperbolic functions we have,

$$\tan icy = i \tanh cy$$

then,

$$F = \frac{(1 + K \tan cx) + i(K \tanh cy - \tan cx \tanh cy)}{(1 - K \tan cx) - i(K \tanh cy + \tan cx \tanh cy)}$$

Substituting  $X = \tan cx$  and  $Y = \tanh cy$  in the above equation, and rewriting it as a function of the new variables  $X$  and  $Y$ , results in,

$$F = \frac{(1 + KX) + i(KY - XY)}{(1 - KX) - i(KY + XY)}$$

Multiplying both the numerator and the denominator by the conjugate of the denominator yields,

$$\begin{aligned}
 F &= \frac{[(1 + KX) + i(KY - XY)][(1 - KX) + i(KY + XY)]}{(1 - KX)^2 + (KY + XY)^2} \\
 &= \frac{(1 - K^2X^2 - K^2Y^2 + X^2Y^2) + i(2KY + 2KX^2Y)}{(1 - KX)^2 + (KY + XY)^2} \\
 &= R e^{i\theta}
 \end{aligned} \tag{B-1}$$

where

$$R = \sqrt{\frac{(1 - K^2X^2 - K^2Y^2 + X^2Y^2)^2 + (2KY + 2KX^2Y)^2}{[(1 - KX)^2 + (KY + XY)^2]^2}} \tag{B-2}$$

$$\text{and } \theta = \tan^{-1} \frac{2KY + 2KX^2Y}{1 - K^2X^2 - K^2Y^2 + X^2Y^2} \tag{B-3}$$

Equation (4.16) can now be written as

$$\begin{aligned}
 w &= -\frac{i\Gamma_0}{2\pi} \ln(\text{Re}^{i\theta}) \\
 &= -\frac{i}{2\pi} \Gamma_0 [\ln R + i\theta]
 \end{aligned} \tag{B-4}$$

Since the stream function  $\psi$  is the imaginary part of Equation (B-4), then

$$\psi = I(w) = -\frac{\Gamma_0}{2\pi} \ln R \tag{B-5}$$

$$= -\frac{\Gamma_0}{4\pi} \ln \left[ \frac{A + B}{C} \right] \tag{B-6}$$

where

$$A = (1 - K^2X^2 - K^2Y^2 + X^2Y^2)^2 \tag{B-7}$$

$$B = (2KY + 2KX^2Y)^2 \tag{B-8}$$

$$C = [(1 - KX)^2 + (KY + XY)^2]^2 \tag{B-9}$$

$$X = \tan \frac{\pi}{2a} x \quad (B-10)$$

$$Y = \tanh \frac{\pi}{2a} Y \quad (B-11)$$

$$K = \cot \frac{\pi}{2a} x_0 \quad (B-12)$$

As it was mentioned in Chapter 4 the value of  $\frac{A+B}{C}$  would act as a non-dimensional equivalent radial distance from the vortex centre to a field point.

Direct substitution of the vortex coordinates ( $x = x_0$  and  $y = 0$ ) into the term  $\frac{A+B}{C}$  would result in an undetermined value. Taking the limits of this term as  $Y \rightarrow 0$  and  $KX \rightarrow 1$  would result in the following:

$$\begin{aligned} \lim_{\substack{Y \rightarrow 0 \\ KX \rightarrow 1}} \frac{A+B}{C} &= \lim_{KX \rightarrow 1} \frac{[(1 - K^2 X^2)]^2}{[(1 - KX)^2]^2} \\ &= \lim_{KX \rightarrow 1} \frac{[(1 - KX)(1 + KX)]^2}{[(1 - KX)^2]^2} \\ &= \lim_{KX \rightarrow 1} \frac{(1 + KX)^2}{(1 - KX)^2} = \infty \end{aligned}$$

In order to have a non-dimensional equivalent radial distance that would tend to zero at the vortex centre, similarly as for the modified Rankine vortex discussed in Chapter 4, Equation (B-6) can be written in another equivalent form as,

$$\psi = \frac{\Gamma_0}{4\pi} \ln \frac{C}{A+B} \quad (B-13)$$

$$\psi = \frac{\Gamma}{2\pi} \ln r_e$$

where

$$r_e^* = \sqrt{\frac{C}{A + B}} \tag{B-14}$$

Similarly if the coordinates of the parallel planes ( $x = 0$  or  $x = a$ ) were substituted into Equation (B-14), the variable of  $r_e^*$  would tend to a value of unity.

The dimensionless variable  $r_e^*$  would be called the dimensionless equivalent radial distance from the vortex centre to the field point, which varies from a value of zero at the vortex centre to one on the two parallel planes. These limits:

$$r_e^* = 0 \quad \text{at the vortex centre}$$

$$\text{and } r_e^* = 1 \quad \text{at the planes}$$

are independent of the actual vortex position between the parallel planes.





## APPENDIX (C)

### AUTO-CORRELATION AND POWER SPECTRAL DENSITY FUNCTION

#### C.1 AUTO-CORRELATION

The auto-correlation function of random data describes the general dependence of the values of the data at one time step on the values of another time. For a continuous record  $u(t)$  at a single measuring point, if the record is stationary then the auto-correlation function  $R_{ii}(\tau)$  may be estimated from a sample of length  $\tau$  as follows.

The auto-correlation covariance is given by the expression:

$$\begin{aligned} & \langle u_i(t) u_i(t + \tau) \rangle \\ &= \lim_{T \rightarrow \infty} \frac{1}{T} \int_0^T u_i(t) u_i(t + \tau) dt \end{aligned} \quad (C.1)$$

and the auto-correlation coefficient by:

$$\begin{aligned} R_{ii}(\tau) &= \langle u_i(t) u_i(t + \tau) \rangle / \\ & \left( \langle u_i^2(t) \rangle \right)^{1/2} \left( \langle u_i(t + \tau) \rangle \right)^{1/2} \end{aligned} \quad (C.2)$$

assuming the integral above to exist. When estimating on a digital computer the auto-correlation covariance from a given array, Equation (C.1) is approximated by,

$$\langle u_i(t) u_i(t + \tau) \rangle = \frac{1}{N-r} \sum_{n=1}^{N-r} (u_i)_n (u_i)_{n+r}$$

$$r = 0, 1, 2 \dots m \quad (C.3)$$

where  $r$  is the lag number,  $m$  the maximum lag, and  $N_0$  is the total sample length.

In the analysis the total sample length  $N$  and the maximum lag have to be such as to provide reasonable accuracy. The equivalent error "E" is defined as:

$$E = \left( \frac{\text{maximum lag}}{\text{total sample length}} \right)^{\frac{1}{2}} = \left( \frac{m}{N} \right)^{\frac{1}{2}} \quad (C.4)$$

When analyzing, if possible, the maximum lag is made such a value so as to make the maximum equivalent error equal to or less than the estimated error of the experimental tests.

The quantity  $R_{ii}(\tau)$  is always a real-valued even function with a maximum value of unity at  $\tau = 0$ . In equation form,

$$R_{ii}(\tau) = R_{ii}(-\tau) \quad (C.5)$$

$$\text{and } R_{ii}(\tau) \leq 1 \quad (C.6)$$

## C.2 TRANSFORMED POWER SPECTRAL DENSITY FUNCTIONS

The power spectral density function of random data describes the general frequency composition of the data in terms of the spectral density of its mean square value. It is obtained by taking the Fourier transform of the auto-correlation coefficient. The relationship between the two functions

is given by,

$$G_{ii}(f) = 4 \int_0^{\infty} R_{ii}(\tau) \cos 2\pi f \tau \, d\tau \quad (C.7)$$

Since the power spectral density is obtained from the auto-correlation coefficients, then both these quantities contain the same amount of information concerning the signal, only the presentation is different. The shape of the correlation curve determines the form of the transformed power spectral curve and vice versa. For instance, if a signal is uncorrelated for a very small time lag, as shown in Figure (C-1), then the signal will have a large frequency range.

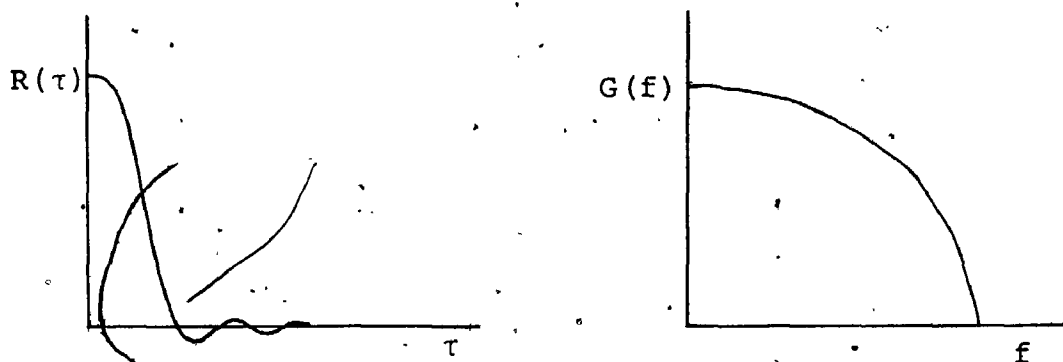


Figure (C-1)

As the time scale of the signal increases, however, then the frequency band containing most of the energy becomes narrower. This is shown in Figure (C-2).

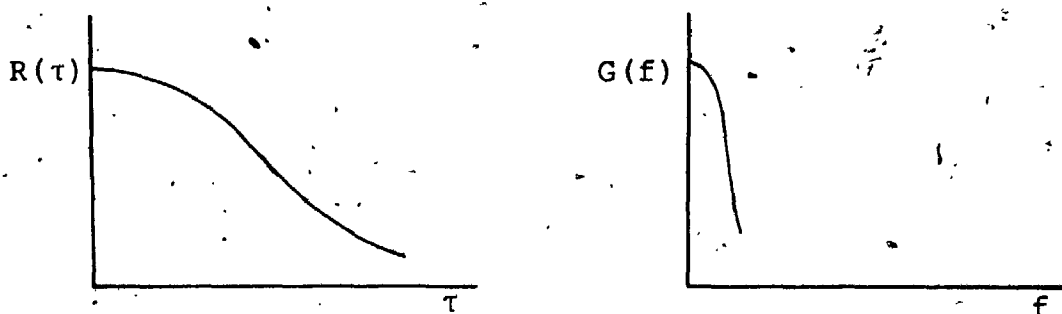


Figure (C-2)

For further details regarding the theory relating the power spectral density function to the auto-correlation, see Bendat and Piersol [1971].

APPENDIX (D)  
COMPUTER PROGRAM  
FOR SINGLE VORTEX MODEL

```

PROGRAM FLOW11 (INPUT,OUTPUT,TAPE7,DEBUG=OUTPUT)
C CCCCCCCCCCCCCCCCCCCCCCCCCCCCCCCCCCCCCCCCCCCCCCCCCCCCCCCCCCCCC
C PROGRAM FLOW TO SOLVE FOR A SINGLE VORTEX APPROACHING C
C C C C
C A FLAT PLATE BETWEEN TWO PARALLEL PLANES C
C C C
C CCCCCCCCCCCCCCCCCCCCCCCCCCCCCCCCCCCCCCCCCCCCCCCCCCCCCCCCCCCCC
COMMON F(25,25),OMEG(25,25),BOMEG(25,25)
COMMON X(25),Y(25),DX(25),DY(25),U(25,25),V(25,25),CP(25,25)
COMMON FI(25),IPVT(250),M,N,M1,M2,N1,MM2,NM2,UI,ITN,IC,DT,T
COMMON FP(25,25)
DIMENSION TI(250),CL(250),CM(250),XDUM(1000),YDUM(1000)
, YDUMM(1000)
C OMEGA=RELAXATION FACTOR
C F(I,J)=STREAM FUNCTION VALUE AT THE POINT (I,J)
C OMEG(I,J)=VORTICITY
C MAXIT=MAX. NO OF ITERATIONS PERMITTED
C UI=VELOCITY OF STREAM
OMEGA=1.60
READ *,M,M1,M2,N,N1
PRINT 102,M,M1,M2,N,N1
102 FORMAT(5I5)
UI=5.0
NM2=N-1
MM2=M-1
NU1=N1+1
NL1=N1-1
READ *,(DY(J),J=1,N)
PRINT 105,(DY(J),J=1,N)
READ 105,(DX(I),I=1,M)
PRINT 105,(DX(I),I=1,M)
105 FORMAT(22F5.2)
M3=M+1
N3=N+1
M2=M
X(1)=0.0
Y(1)=0.0
DO 13 J=2,N3
Y(J)=Y(J-1)+DY(J-1)
13 CONTINUE
DO 15 I=2,M3
X(I)=X(I-1)+DX(I-1)
15 CONTINUE
RC=0.7
PI=ABS(ACOS(-1.0))
X0=-4.7
Y0=(Y(N)-Y(1))/2.0
GAMA=10.0

```

```

IA=1
C THE NEXT FIVE LINES ARE ADDED TO HAVE FOUR RUNS WITH
C VARIABLE VORTEX RADII OR VARIABLE CHORD LENGTHS
C DO 78 IK=1,4
C M2=M
C RC=0.4+0.1*IK
C M2=M1+IK
C IF(IK.EQ.4)M2=MM2
AL=X(M2)-X(M1)+.25
CALL BNDCN(F,M,M1,M2,N,N1,DY,UI)
DTM=0.2*RC/UI
DT=DTM
T=0.0
DO 12 I=1,M3
DO 12 J=1,N3
OMEG(I,J)=0.0
BOMEG(I,J)=OMEG(I,J)
12 CONTINUE
KT=1
DO 75 KK=1,250
IC=0
CALL POIS
IF(KK.EQ.1)GO TO 77
CALL HELM,
XRETURNS(10)
77 CONTINUE
CALL LIFTC(CL,CM,KT)
TI(KT)=T
XDUM(IA)=TI(KT)
YDUM(IA)=CL(KT)
YDUMM(IA)=CM(KT)
IA=IA+1
C *****
C PRINTING OUTPUT
C *****
PRINT 115, TI(KT), CL(KT)
115 FORMAT(2X, 'TIME =', F10.4, 1X, 'LIFT COEFF. =', F10.5)
PRINT 110, T
110 FORMAT(1X, 'VALUES OF VORTICITY AT T=', F8.4)
PRINT 103, ((OMEG(I,J), I=2, M), J=2, N)
PRINT 25, OMEGA, ITN, T
25 FORMAT(/, 1X, 'RELAX =', F10.4, 3X, 'ITN =', I10, 3X, 'TIME=', F10.4,
$/, 1X, 'STREAM FUNCTION F(I,J)')
PRINT 103, ((F(I,J), I=2, M), J=2, N)
103 FORMAT(15F8.3)
PRINT 111
111 FORMAT(5X, 'VALUES OF U(I,J)', /)
PRINT 103, ((U(I,J), I=2, M), J=2, N)

```

```

PRINT 112
112 FORMAT(5X, 'VALUES OF V(I,J)',/)
PRINT 103, ((V(I,J), I=2, M), J=2, N)
PRINT 113
113 FORMAT(5X, 'COEFF. OF PRESSURE',/)
PRINT 103, ((CP(I,J), I=2, M), J=2, N)
WRITE(7, *) T
DO 20 I=2, M
DO 20 J=2, N
20 WRITE(7, 108) X(I), Y(J), F(I, J)
108 FORMAT(3F10.4)
PRINT 114, TI(KT), CL(KT), CM(KT), RC, KT
114 FORMAT(1X, 'TIME=', F10.4, 1X, 'CL(KT)=', F10.4, 1X, 'CM(KT)=',
X, F10.4, 1X, 'RC=', F10.4, 1X, 'KT=', I4)
WRITE(7, 116) TF(KT), CL(KT), CM(KT), RC, KT
*116 FORMAT(4F10.4, I4)
KT=KT+1
DTC=DT
DO 14 I=2, M
DO 14 J=2, N
FP(I, J)=F(I, J)
14 CONTINUE
10 CONTINUE
C *****
C CHANGING BOUNDARY WITH TIME *
C *****
IF(IC.LT.5) DT=DT*2.
IF(DT.GT.DTM) DT=DTM
IF(DT.LT.DTM/8.0) STOP
T=T+DT
U(M3, 2)=U(M, 2)
DO 21 I=3, M
U1=(U(I, 2)+U(I-1, 2))/2.
U2=(U(I, 2)+U(I+1, 2))/2.
OMEG(I, 2)=OMEG(I-1, 2)+(DX(I-1)-U1*DT)*(OMEG(I, 2)-OMEG(I-1, 2))
$/ (U2*DT+DX(I-1)-U1*DT)
21 CONTINUE
I=2
DO 16 J=1, N3
CALL UPSTF(F, X, Y, X0, Y0, UI, DX, DY, GAMA, RC, N, T, I, J)
16 CONTINUE
17 CONTINUE
Z=(F(M1, N1)-F(M1-2, N1))*(X(M1)-X(M1-1))/(DX(M1-2)+DX(M1-1))
IF(KK-1) 24, 26, 24
26 DO 23 J=2, N
F(M, J)=F(MM2, J)+(F(M, J)-F(MM2-1, J))/2.0
23 CONTINUE
F(M1, N1)=F(M1-1, N1)+Z

```



```

      GO TO 27
24   DO 29 J=2,N
      F(M,J)=F(MM2,J)+(F(M,J)-F(MM2-1,J))/2.0+(F(MM2,J)-FI(J))*DT/DTO
29   CONTINUE
      F(M1,N1)=F(M1-1,N1)+Z+(F(M1-1,N1)-FI(N+1))*DT/DTO
27   DO 22 J=2,N
22   FI(J)=F(MM2,J)
      FI(N+1)=F(M1-1,N1)
      DO 36 I=M1,M2
36   F(I,N1)=F(M1,N1)
C    F(M,N1)=(F(M,N1+1)+F(M,N1-1))/2.0
C    DO 32 I=M1,M3
C    F(I,N1)=F(M,N1)
C32  CONTINUE
      I=2
      DO 31 J=2,N
      CALL VORT(F,OMEG,X,Y,XO,YO,UI,DX,DY,GAMA,RC,N,T,I,J)
31   CONTINUE
75   CONTINUE
      KTT=KTT-1
      DO 40 I=1,KTT
      L=I
      IF(TI(I).GT.4.8)GO TO 41
40   CONTINUE
41   CONTINUE
      LL=L-1
      SUM1=0.0
      DO 42 I=2,LL
      SUM1=SUM1+CL(I)*
42   CONTINUE
      CLAV=(DT*(CL(1)+CL(L)+2.*SUM1)/2.)/(TI(L)-TI(1))
      PRINT 43,RC,CLAV
43   FORMAT(1X,'RC=',F10.5,1X,'CLAV=',F14.7,/)
      PRINT 120,(TI(I),I=1,KTT)
120  FORMAT(/,1X,'TIME CHANGE',/,16F8.5)
      PRINT 130,(CL(I),I=1,KTT)
130  FORMAT(1X,'LIFT COEF.',/,16F8.5)
      CALL PLTCLT(TI,CL,KTT,AL,RC,1)
      CALL PLTCLT(TI,CM,KTT,AL,RC,2)
78   CONTINUE
      CALL PLTALL(XDUM,YDUM,4*KTT,KTT,1)
      CALL PLTALL(XDUM,YDUM,4*KTT,KTT,2)
90   CONTINUE
      CALL EXIT
      END

```

```
      SUBROUTINE BNDCN(F,M,M1,M2,N,N1,DY,UI)
C CCCCCCCCCCCCCCCCCCCCCCCCCCCCCCCCCCCCCCCCCCCCCCCCCCCCCCCCCCCCC
C   SUBROUTINE BNDCN TO EVALUATE STEADY STATE BOUNDARY CONDITIONS C
C CCCCCCCCCCCCCCCCCCCCCCCCCCCCCCCCCCCCCCCCCCCCCCCCCCCCCCCCCCCCC
  DIMENSION F(25,25),DY(25)
  N3=N+1
  M3=M+1
  DO 1 J=1,N3
  DO 1 I=1,M3
1   F(I,J)=0.0
  DO 11 I=1,M3
11  F(I,1)=-UI*DY(1)
  DO 2 J=2,N3
  F(1,J)=F(1,J-1)+UI*DY(J-1)
  F(2,J)=F(1,J)
  F(M+1,J)=F(1,J)
2   F(M,J)=F(1,J)
  DO 3 I=2,M
  DO 3 J=1,N3
  F(I,J)=F(1,J)
3   CONTINUE
40  PRINT 102
102 FORMAT(5X,'F(I,J) VALUES')
  PRINT 103,((F(I,J),I=2,M),J=2,N)
103 FORMAT(15F8.3)
  RETURN
  END
```

```

SUBROUTINE UPSTF(EPS,X,Y,XO,YO,UI,DX,DY,GAMA,RC,N,T,I,J)
C CCCCCCCCCCCCCCCCCCCCCCCCCCCCCCCCCCCCCCCCCCCCCCCCCCCCCCCCCCCCCCCCC
C
C SUBROUTINE UPSTF TO EVALUATE THE EQUIVALENT RANKINE VORTEX C
C EQUATION C
C CCCCCCCCCCCCCCCCCCCCCCCCCCCCCCCCCCCCCCCCCCCCCCCCCCCCCCCCCCCCCCCCC
C DIMENSION X(25),Y(25),EPS(25,25),DX(25),DY(25)
C YY=DY(1)
C PI=ABS(ACOS(-1.))
C C=PI/(2.*(Y(N)-YY))
C X(I)=X(I)-XO-UI*T
C Y(J)=Y(J)-YY
C IF(J-N)5,6,5
5 CONTINUE
C AK=1./(TAN(C*YO))
C AA=(1-AK**2*(TAN(C*Y(J)))**2-AK**2*(TANH(C*X(I)))**2+
C *(TAN(C*Y(J)))**2*(TANH(C*X(I)))**2)**2
C AB=(2.*AK*TANH(C*X(I))+2.*AK*(TAN(C*Y(J)))**2*TANH(C*X(I)))**2
C AC=((1.-AK*TAN(C*Y(J)))**2+(AK*TANH(C*X(I))+TAN(C*Y(J))
C **TANH(C*X(I)))**2)**2
C REQS=ABS(AC/(AA+AB))
C GO TO 7
6 CONTINUE
C REQS=1.0
7 CONTINUE
C EPS(I,J)=(-GAMA/(2.*PI))*(ALOG(REQS+RC**2)-ALOG(1.+RC**2))
C X(I)=X(I)+XO+UI*T
C Y(J)=Y(J)+YY
C EPS(I,J)=UI*Y(J)-UI*YY+EPS(I,J)
C RETURN
C END

```

```

SUBROUTINE VORT(F, OMEG, X, Y, XO, YO, UI, DX, DY, GAMA, RC, N, T, I, J)
C CCCCCCCCCCCCCCCCCCCCCCCCCCCCCCCCCCCCCCCCCCCCCCCCCCCCCCCCCCCCCCCCC
C SUBROUTINE VORT TO EVALUATE THE VORTICITY AND VELOCITY C
C COMPONENTS AT THE POINT X, Y DUE TO A VORTEX AT A POINT C
C XO, YO. C
C CCCCCCCCCCCCCCCCCCCCCCCCCCCCCCCCCCCCCCCCCCCCCCCCCCCCCCCCCCCCCCCCC
DIMENSION F(25,25), OMEG(25,25), DX(25), DY(25), X(25), Y(25)
, U(25,25), V(25,25)
H=0.0001
FC=F(I, J)
X(I)=X(I)+H
CALL UPSTF(F, X, Y, XO, YO, UI, DX, DY, GAMA, RC, N, T, I, J)
X(I)=X(I)-H
FE=F(I, J)
X(I)=X(I)-H
CALL UPSTF(F, X, Y, XO, YO, UI, DX, DY, GAMA, RC, N, T, I, J)
X(I)=X(I)+H
FW=F(I, J)
Y(J)=Y(J)+H
CALL UPSTF(F, X, Y, XO, YO, UI, DX, DY, GAMA, RC, N, T, I, J)
Y(J)=Y(J)-H
FN=F(I, J)
Y(J)=Y(J)-H
CALL UPSTF(F, X, Y, XO, YO, UI, DX, DY, GAMA, RC, N, T, I, J)
Y(J)=Y(J)+H
FS=F(I, J)
OMEG(I, J)=- (FW+FE+FN+FS-4.*FC)/H**2
V(I, J)=- (FE-FW)/(2.*H)
U(I, J)= (FN-FS)/(2.*H)
F(I, J)=FC
RETURN
END

```

## SUBROUTINE POIS

```

C CCCCCCCCCCCCCCCCCCCCCCCCCCCCCCCCCCCCCCCCCCCCCCCCCCCCCCCCCCCCC
C
C SUBROUTINE POIS TO SOLVE POISSONS EQUATION BY ITERATIONS ° C
C
C CCCCCCCCCCCCCCCCCCCCCCCCCCCCCCCCCCCCCCCCCCCCCCCCCCCCCCCCCCCCC
COMMON F(25,25), OMEG(25,25), BOMEG(25,25)
COMMON X(25), Y(25), DX(25), DY(25), U(25,25), V(25,25), CP(25,25)
COMMON FI(25), IPVT(250), M, N, M1, M2, N1, MM2, NM2, UI, ITN, IC, DT, T
COMMON FP(25,25)
ITN=0
MAXIT=500
ERR=0.001
OMEGA=1.6
A=OMEGA
B=1.-OMEGA
10 R=0.0
DO 28 I=3,MM2
DO 28 J=3,NM2
IF(J.EQ.N1.AND.I.GE.M1.AND.I.LE.M2)GO TO 28
50 S=DX(I)/DX(I-1)
Z=DY(J)/DY(J-1)
AA=(1+S)*DX(I)**2.
BB=(1+Z)*DY(J)**2.
E=BB*(1+S)*(1+S**2.)+AA*(1+Z)*(1+Z**2.)
FNEW=A*((BB*(F(I+1,J)*(1+S**2)+F(I-1,J)*(S**3+S))+AA*(F(I,J
$+1)*(1+Z**2)+F(I,J-1)*(Z**3+Z))+AA*BB*OMEG(I,J))/E)+B*F(I,J)
RESID=ABS(FNEW-F(I,J))
IF(RESID-R)35,35,36
36 R=RESID
35 F(I,J)=FNEW
28 CONTINUE
IF(R-ERR)60,61,61
61 ITN=ITN+1
IF(ITN-MAXIT)10,10,62
62 CONTINUE
PRINT 101,MAXIT
101 FORMAT(22HF FAILS TO CONVERGE IN, I5, 10HITERATIONS)
STOP
60 CONTINUE
DO 30 I=2,M
DO 30 J=2,N
U(I,J)=(F(I,J+1)-F(I,J-1))/(DY(J)+DY(J-1))
V(I,J)=(F(I-1,J)-F(I+1,J))/(DX(I)+DX(I-1))
CP(I,J)=1.-((U(I,J)**2+V(I,J)**2)/UI**2)
30 CONTINUE
DO 18 I=2,M
OMEG(I,2)=-((F(I,2)-2.*F(I,3)+F(I,4))/DY(2)**2.

```

```
OMEG(I,N)=-((F(I,N)-2.*F(I,N-1)+F(I,N-2))/DY(N-1))**2
18 CONTINUE
   J=N1
   DO 19 I=M1,M2
      OMEG(I,J)=-((F(I,J)-2.*F(I,J+1)+F(I,J+2))/DY(J))**2
19 CONTINUE
   RETURN
   END
```

```

SUBROUTINE HELM,
C CCCCCCCCCCCCCCCCCCCCCCCCCCCCCCCCCCCCCCCCCCCCCCCCCCCCCCCCCCCCC
C   SUBROUTINE HELM TO SOLVE HELMHOLTZ VORTICITY EQUATION USING C
C   BANDED MATRICES C
C CCCCCCCCCCCCCCCCCCCCCCCCCCCCCCCCCCCCCCCCCCCCCCCCCCCCCCCCCCCCC
XRETURNS(L)
COMMON F(25,25), OMEG(25,25), BOMEG(25,25)
COMMON X(25), Y(25), DX(25), DY(25), U(25,25), V(25,25), CP(25,25)
COMMON FI(25), IPVT(250), M, N, M1, M2, N1, MM2, NM2, UI, ITN, IC, DT, T
COMMON FP(25,25)
DIMENSION A1(250,39), B1(250)
C *****
C PORTION SOLVING HELMHOLTZ EQUATION *
C *****
C *****
C NN=NO. OF EQUATIONS OF VORTICITY
5 CONTINUE
ERR=0.001
NN=(MM2-2)*(NM2-2)-(M2-M1+1)
NI=MM2-2
NII=NI-(M2-M1+1)
NU1=N1+1
NL1=N1-1
NB=M-2
ND=2*NB-1
DO 55 I=1, NN
DO 55 J=1, ND
55 A1(I, J)=0.0
IJ=1
DO 74 J=3, NM2
DO 74 I=3, MM2
ID=IJ
IF(IJ.GT.NB) ID=NB
IF(J.EQ.N1.AND.I.GE.M1.AND.I.LE.M2) GO TO 74
ALM1=DT/(DX(I)+DX(I-1))
ALM2=DT/(DY(J)+DY(J-1))
AB=0.0
BC=0.0
A1(IJ, ID+1)=ALM1*U(I, J)
A1(IJ, ID+NI)=ALM2*V(I, J)
IF(J.EQ.N1.AND.I.EQ.M2+1) GO TO 65
IF(I-3) 66, 65, 66
65 AB=A1(IJ, ID+1)*OMEG(I-1, J)
GO TO 63
66 A1(IJ, ID-1)=-A1(IJ, ID+1)
63 CONTINUE
IF(I.GE.M1.AND.I.LE.M2.AND.J.EQ.NU1) 69, 85
85 CONTINUE

```

```

IF(J-3)71,69,71
69 BC=A1(IJ, ID+NI)*OMEG(I, J-1)
GO TO 64
71 A1(IJ, ID-NI)=-A1(IJ, ID+NI)
64 A1(IJ, ID)=1.00
IF(J.EQ.N1.AND.I.EQ.M1-1)67,87
87 CONTINUE
IF(I-MM2)68,67,68
67 A1(IJ, ID)=A1(IJ, ID)+U(I, J)*DT/DX(I-1)
A1(IJ, ID-1)=-U(I, J)*DT/DX(I-1)
A1(IJ, ID+1)=0.0
68 CONTINUE
IF(I.GE.M1.AND.I.LE.M2.AND.J.EQ.NL1)72,86
86 CONTINUE
IF(J-NM2)73,72,73
72 A1(IJ, ID)=A1(IJ, ID)+V(I, J)*DT/DY(J-1)
A1(IJ, ID-NI)=-V(I, J)*DT/DY(J-1)
A1(IJ, ID+NI)=0.0
73 B1(IJ)=BOMEG(I, J)+AB+BC
IF(J.EQ.N1.AND.I.LT.M1)20,21
20 CONTINUE
A1(IJ, ID+NII)=A1(IJ, ID+NI)
A1(IJ, ID+NI)=0.0
21 CONTINUE
IF((J.EQ.NU1.AND.I.LT.M1).OR.(J.EQ.N1.AND.I.GT.M2))76,70
76 CONTINUE
A1(IJ, ID-NII)=A1(IJ, ID-NI)
A1(IJ, ID-NI)=0.0
70 CONTINUE
IJ=IJ+1
74 CONTINUE
CALL CROUT(A1, NN, NB)
CALL SOLVE(A1, B1, B1, NN, NB)
IC=IC+1
IF(IC.GT.15)6,7
6 CONTINUE
T=T-DT
DT=DT/2.0
DO 8 J=2, N
DO 8 I=2, M
F(I, J)=FP(I, J)
OMEG(I, J)=BOMEG(I, J)
8 CONTINUE
RETURN L
7 CONTINUE
IL=1
R=0.0
DO 78 J=3, NM2

```



```
DO 78 I=3,MM2
IF(J.EQ.N1.AND.I.GE.M1.AND.I.LE.M2)GO TO 82
RES=ABS((B1(IL)-OMEG(I,J))/B1(IL))
RES=ABS((B1(IL)-OMEG(I,J)))
IF(RES.GT.R)R=RES
IL=IL+1
82 CONTINUE
78 CONTINUE
IF (R.LT.ERR) GO TO 79
80 IB=1
DO 81 J=3,NM2
DO 81 I=3,MM2
IF(J.EQ.N1.AND.I.GE.M1.AND.I.LE.M2)GO TO 83
OMEG(I,J)=B1(IB)
IB=IB+1
83 CONTINUE
81 CONTINUE
CALL POIS
GO TO 5
79 CONTINUE
IJ=1
DO 200 J=3,NM2
DO 200 I=3,MM2
IF(J.EQ.N1.AND.I.GE.M1.AND.I.LE.M2)GO TO 84
OMEG(I,J)=B1(IJ)
IJ=IJ+1
84 CONTINUE
200 CONTINUE
DO 15 J=2,N
DO 15 I=1,M
BOMEG(I,J)=OMEG(I,J)
15 CONTINUE
RETURN
END
```

```
SUBROUTINE CROUT (A,NEQ,NBAND)
DIMENSION A(250,39)
NA=NBAND-1
NTT=2*NBAND-1
DO 5 J=2,NBAND
5 A(1,J)=A(1,J)/A(1,1)
KY=NEQ-NA
KX=2
10 K1=KX+1
K2=KX-1
KA=KX+NA
KB=KA-1
KBND=KX-NBAND
IF (KX-KY) 15,15,12
12 KB=NEQ
KA=NEQ
15 DO 30 I=KX,KB
IF (I-NBAND) 16,16,17
16 KC=1
GO TO 18
17 KC=I-NA
18 SZ=0.
DO 20 J=KC,K2
IF (I-NBAND) 105,105,110
105 J1=J
GO TO 115
110 J1=J-I+NBAND
115 IF (J-NBAND) 120,120,125
120 J2=KX
GO TO 130
125 J2=KX-J+NBAND
130 SZ=SZ+A(I,J1)*A(J,J2)
20 CONTINUE
IF (I-NBAND) 140,140,150
140 J1=KX
GO TO 160
150 J1=KX-I+NBAND
160 A(I,J1)=A(I,J1)-SZ
30 CONTINUE
IF (KX-NEQ) 31,51,51
31 DO 50 J=K1,KA
IF (KX-NBAND) 32,32,34
32 KC=1
GO TO 36
34 KC=J-NA-1
36 SZ=0.
DO 40 I=KC,K2
IF (KX-NBAND) 165,165,170
```

```
165 I1=I
    GO TO 175
170 I1=I-KX+NBAND
175 IF (I-NBAND) 180,180,185
180 J1=J
    *GO TO 190
185 J1=J-I+NBAND
190 IF (J1-NTT) 195,195,40
195 SZ=SZ+A(KX,I1)*A(I,J1)
    40 CONTINUE
    IF (KBND) 200,200,210
200 J1=J
    J2=KX
    GO TO 220
210 J1=J-KX+NBAND
    J2=NBAND
220 A(KX,J1)=(A(KX,J1)-SZ)/A(KX,J2)
    50 CONTINUE
    51 KX=KX+1
    IF (KX-NEQ) 10,10,70
    70 CONTINUE
    RETURN
    END
```

```
SUBROUTINE SOLVE (A,F,SOL,NEQ,NBAND)
DIMENSION A(250,39),F(250),SOL(250)
NA=NBAND-1
KY=NEQ-NA
NTT=2*NBAND-1
F(1)=F(1)/A(1,1)
DO 110 KX=2,NEQ
K2=KX-1
IF (KX-NBAND) 10,10,20
10 KC=1
GO TO 30
20 KC=KX-NA
30 SZ=0.
DO 70 J=KC,K2
IF (KX-NBAND) 40,40,50
40 J1=J
GO TO 60
50 J1=J-KX+NBAND
60 SZ=SZ+A(KX,J1)*F(J)
70 CONTINUE
IF (KX-NBAND) 80,80,90
80 J1=KX
GO TO 100
90 J1=NBAND
100 F(KX)=(F(KX)-SZ)/A(KX,J1)
110 CONTINUE
SOL(NEQ)=F(NEQ)
KX=NEQ
120 L=KX-1
IF (KX-KY) 140,130,130
130 KA=NEQ
GO TO 150
140 KA=KX+NA-1
150 SZ=0.
DO 200 J=KX,KA
IF (L-NBAND) 160,160,170
160 J1=J
GO TO 180
170 J1=J-L+NBAND
180 IF (J1-NTT) 190,190,200
190 SZ=SZ+A(L,J1)*SOL(J)
200 CONTINUE
SOL(L)=F(L)-SZ
KX=KX-1
IF (L-1) 210,210,120
210 CONTINUE
RETURN
END
```

```
SUBROUTINE PLTCLT(T,CL,KT,AL,RG,NC)
DIMENSION T(250),CL(250)
CALL PLOTS(30,24.,10.75,2)
CALL PLTCOM(26HPLEASE USE .4 MM BLACK INC,26)
CALL PLOT(1.0,1.25,-3)
CALL SCALE4(T,8.0,KT,1,0,TMIN,TDA)
CALL SCALE4(CL,9.0,KT,1,0,CLMIN,CLDA)
CALL CRAXES(8.,9.,TMIN,CLMIN,TDA,CLDA,4)
CALL PLOT((T(1)-TMIN)/TDA,(CL(1)-CLMIN)/CLDA,3)
CALL LINE4(T,CL,KT,1,TMIN,TDA,CLMIN,CLDA,0,0,0)
CALL SYMBOL(2.5,8.5,.125,
X36HVORTEX APPROACHING FINITE FLAT PLATE,0.0,36)
CALL SYMBOL(5.,8.,.125,5HRC = ,0.0,5)
CALL NUMBER(5.6,8.,.125,RC,0.0,2)
CALL SYMBOL(5.,7.5,.125,5HL = ,0.0,5)
CALL NUMBER(5.6,7.5,.125,AL,0.0,2)
IF(NC.GT.1)GO TO 5
CALL SYMBOL(-.5,3.5,.125,19HLIFT COEFFICIENT CL,90.,19)
GO TO 10
5 CALL SYMBOL(-.5,2.9,.125,30HPITCHING MOMENT COEFFICIENT CM,
90.,30)
10 CONTINUE
CALL PLTERR(1)
C PAUSE
CALL ENDPLT
RETURN
END
```

```

SUBROUTINE PLTALL(XDUM,YDUM,N,NN,NC)
DIMENSION X1(250),X2(250),X3(250),X4(250),Y1(250),Y2(250)
1,Y3(250),Y4(250),XDUM(1000),YDUM(1000)
CALL PLOTS(30,10.0,10.75,2)
CALL PLTCOM(26HPLEASE USE .4 MM BLACK INC,26)
CALL PLOT(1.0,1.25,-3)
DO 5 I=1,NN
X1(I)=XDUM(I)
Y1(I)=YDUM(I)
X2(I)=XDUM(NN+I)
Y2(I)=YDUM(NN+I)
X3(I)=XDUM(2*NN+I)
Y3(I)=YDUM(2*NN+I)
X4(I)=XDUM(3*NN+I)
Y4(I)=YDUM(3*NN+I)
5 CONTINUE
CALL SCALE4(XDUM,8.0,N,1,0,XMIN,XDA)
CALL SCALE4(YDUM,9.0,N,1,0,YMIN,YDA)
CALL CRAXES(8.,9.,XMIN,YMIN,XDA,YDA,2)
CALL SYMBOL(2.5,8.5,.125,
X36HVORTEX APPROACHING FINITE FLAT PLATE,0.0,36)
IF(NC.GT.1)GO TO 8
CALL SYMBOL(-.5,3.5,.125,19HLIFT COEFFICIENT CL,90.,19)
GO TO 10
8 CALL SYMBOL(-.5,2.9,.125,30HPITCHING MOMENT COEFFICIENT CM,
$90.,30)
10 CONTINUE
CALL PLOT((X1(1)-XMIN)/XDA,(Y1(1)-YMIN)/YDA,3)
CALL LINE4(X1,Y1,NN,1,XMIN,XDA,YMIN,YDA,0,0,0)
CALL PLOT((X2(1)-XMIN)/XDA,(Y2(1)-YMIN)/YDA,3)
CALL LINE4(X2,Y2,NN,1,XMIN,XDA,YMIN,YDA,0,0,0)
CALL PLOT((X3(1)-XMIN)/XDA,(Y3(1)-YMIN)/YDA,3)
CALL LINE4(X3,Y3,NN,1,XMIN,XDA,YMIN,YDA,0,0,0)
CALL PLOT((X4(1)-XMIN)/XDA,(Y4(1)-YMIN)/YDA,3)
CALL LINE4(X4,Y4,NN,1,XMIN,XDA,YMIN,YDA,0,0,0)
CALL PLTERR(1)
CALL ENDPLT
RETURN
END

```

```

SUBROUTINE LIFTC(CL,CM,KT)
C CCCCCCCCCCCCCCCCCCCCCCCCCCCCCCCCCCCCCCCCCCCCCCCCCCCCCCCCCCCCC
C
C           SUBROUTINE LIFTC TO CALCULATE THE           C
C
C           LIFT AND PITCHING MOMENT COEFFICIENTS       C
C
C CCCCCCCCCCCCCCCCCCCCCCCCCCCCCCCCCCCCCCCCCCCCCCCCCCCCCCCCCCCCC
COMMON E(25,25), OMEG(25,25), BOMEG(25,25)
COMMON X(25), Y(25), DX(25), DY(25), U(25,25), V(25,25), CP(25,25)
COMMON FI(25), IPVT(250), M, N, M1, M2, N1, MM2, NM2, UI, ITN, IC, DT, T
COMMON FP(25,25)
DIMENSION CL(250), CM(250), G1(25), G2(25), G3(25), DU(25), DP(25)
AL=X(M2)-X(M1)+0.25
SUM1=0.0
SUM2=0.0
DO 35 I=M1, M2
  UB=(F(I, N1)-F(I, N1-1))/DY(N1-1)
  UT=(F(I, N1+1)-F(I, N1))/DY(N1)
  DU(I)=UB-UT
  G3(I)=(UB**2-UT**2)/2.0
  G2(I)=0.0
  DO 30 J=M1, I
    IF(J.EQ.M1)GO TO 30
    G2(I)=G2(I)+(DU(J-1)+DU(J))*DX(J-1)/2.0
30  CONTINUE
    G2(I)=G2(I)+0.5*DU(M1)*0.25
    IF(KT.EQ.1)G1(I)=G2(I)
    DP(I)=-((G2(I)-G1(I))/DT+G3(I))
    G1(I)=G2(I)
    IF(I.EQ.M1)GO TO 35
    SUM1=SUM1+DX(I-1)*(DP(I-1)+DP(I))/2.0
    SUM2=SUM2+DX(I-1)*(DP(I-1)*(X(I-1)-X(M1))+DP(I)*(X(I)-X(M1)))/2.
35  CONTINUE
    CL(KT)=SUM1/(0.5*UI**2*AL)
    CM(KT)=SUM2/(0.5*UI**2*AL**2)
RETURN
END

```

```

16 9 12 20 11
.1 .1 .1 .1 .5 .5 .5 .3 .1 .1 .1 .1 .3 .5 .5 .5 .1 .1 .1 .1
.10 .10 .10 .10 .50 .50 .50 .50 .50 .50 .50 .50 .10 .10
10 .10

```

APPENDIX (E)  
COMPUTER PROGRAMS  
FOR THE PSEUDO-TURBULENCE MODEL



```

PROGRAM MOD1 (INPUT,OUTPUT,TAPE7,DEBUG=OUTPUT)
C CCCCCCCCCCCCCCCCCCCCCCCCCCCCCCCCCCCCCCCCCCCCCCCCCCCCCCCCC
C
C PROGRAM MOD1.TO SOLVE FOR RANDOMELY POSITIONED VORTICES C
C
C APPROACHING A FLAT PLATE BETWEEN TWO PARALLEL PLANES C
C
C CCCCCCCCCCCCCCCCCCCCCCCCCCCCCCCCCCCCCCCCCCCCCCCCCCCCCCCCC
COMMON F(25,25),OMEG(25,25),BOMEG(25,25)
COMMON X(25),Y(25),DX(25),DY(25),U(25,25),V(25,25),CP(25,25)
COMMON FI(25),IPVT(250),M,N,M1,M2,N1,MM2,NM2,UI,ITN,IC,IT,T
COMMON FP(25,25)
DIMENSION TI(250),CL(250),CM(250),XDUM(1000),YDUM(1000)
, ,YDUMM(1000)
DIMENSION XV(100),YV(100),VCR(100),GAMMA(100),US(250),VS(250)
C OMEGA=RELAXATION FACTOR
C F(I,J)=STREAM FUNCTION VALUE AT THE POINT (I,J)
C OMEG(I,J)=VORTICITY
C MAXIT=MAX. NO OF ITERATIONS PERMITTED
C UI=VELOCITY OF STREAM
OMEGA=1.60
READ *,M,M1,M2,N,N1
PRINT 102,M,M1,M2,N,N1
102 FORMAT(5I5)
UI=5.0
NM2=N-1
MM2=M-1
NU1=N1+1
NL1=N1-1
READ *,(DY(J),J=1,N)
PRINT 105,(DY(J),J=1,N)
READ 105,(DX(I),I=1,M)
PRINT 105,(DX(I),I=1,M)
105 FORMAT(22F5.2)
M3=M+1
N3=N+1
M2=M3
X(1)=0.0
Y(1)=0.0
DO 13 J=2,N3
Y(J)=Y(J-1)+DY(J-1)
13 CONTINUE
DO 15 I=2,M3
X(I)=X(I-1)+DX(I-1)
15 CONTINUE
STGLN=X(M)-X(2)
AMW=Y(N)-Y(2)
RC=0.7

```

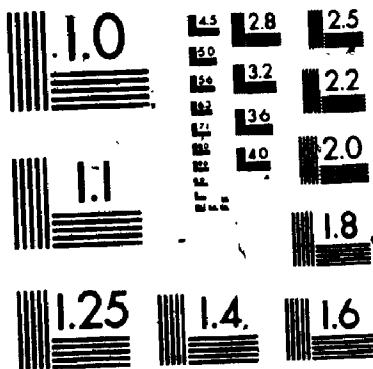
```

PI=ABS(ACOS*-1.0))
CIRC=1.0
WRITE(7,106)M,M1,M2,M3,MM2,N,N1,NM2,N3,STGLN,AMW,RC,CIRC
106 FORMAT(9I5,4F8.3)
WRITE(7,103)(X(I),I=1,M3)
WRITE(7,103)(Y(I),I=1,N3)
IA=1
C DO 78 IK=1,4
C RC=0.4+0.1*IK
C M2=M1+IK
C IF(IK.EQ.4)M2=MM2
AL=X(M2)-X(M1)+.25
CALL BND CN(F,M,M1,M2,N,N1,DY,DX,UI,U,V,CP)
DTM=0.2*RC/UI
DT=DTM
T=0.0
TT=0.0
DO 12 I=1,M3
DO 12 J=1,N3
OMEG(I,J)=0.0
BOMEG(I,J)=OMEG(I,J)
12 CONTINUE
KT=1
DO 75 KK=1,250
IC=0
CALL POIS
IF(KK.EQ.1)GO TO 77
CALL HELM,
XRETURNS(10)
77 CONTINUE
C XQC=X CO-ORDINATE FOR QUARTER CHORD POINT
C QCL=QUARTER CHORD LENGTH
QCL=0.25*(AL-.25)
XQC=X(M1)+QCL
CALL LIFTC(CL,CM,KT)
TI(KT)=T
US(KT)=U(2,N1)
VS(KT)=V(2,N1)
XDUM(IA)=TI(KT)
YDUM(IA)=CL(KT)
YDUMM(IA)=CM(KT)
IA=IA+1
C *****
C PRINTING OUTPUT
C *****
PRINT 115, TI(KT), CL(KT)
115 FORMAT(2X, 'TIME =', F10.4, 1X, 'LIFT COEFF. =', F10.5)
PRINT 110, T

```

# 3 3

OF / DE



```

110  FORMAT(1X,'VALUES OF VORTICITY AT T=',F8.4)
      PRINT 103,((OMEG(I,J),I=2,M),J=2,N)
      PRINT25,OMEGA,ITN,T
25.  FORMAT(/,1X,'RELAX = ',F10.4,3X,'ITN = ',I10,3X,'TIME=',F10.4,
      $/,1X,'STREAM FUNCTION F(I,J)')
      PRINT 103,((F(I,J),I=2,M),J=2,N)
103  FORMAT(15F8.3)
      PRINT 111
111  FORMAT(5X,'VALUES OF U(I,J)',/)
      PRINT 103,((U(I,J),I=2,M),J=2,N)
      PRINT 112
112  FORMAT(5X,'VALUES OF V(I,J)',/)
      PRINT 103,((V(I,J),I=2,M),J=2,N)
      PRINT 113
113  FQRMAT(5X,'COEFF. OF PRESSURE',/)
      PRINT 103,((CP(I,J),I=2,M),J=2,N)
      WRITE(7,103)((F(I,J),I=2,M),J=2,N)
      WRITE(7,103)((OMEG(I,J),I=2,M),J=2,N)
      WRITE(7,103)((U(I,J),I=2,M),J=2,N)
      WRITE(7,103)((V(I,J),I=2,M),J=2,N)
      WRITE(7,103)((CP(I,J),I=2,M),J=2,N)
      WRITE(7,104)US(KT),VS(KT),CL(KT),TI(KT),CM(KT),KT
104  FORMAT(5F8.3,I10)
      KT=KT+1
      DTO=DT
      DO 14 I=2,M
      DO 14 J=2,N
      FP(I,J)=F(I,J)
14  CONTINUE
10  CONTINUE
C *****
C  CHANGING BOUNDARY WITH TIME *
C *****
      IF(IC.LT.5)DT=DT*2.
      IF(DT.GT.DTM)DT=DTM
      IF(DT.LT.DTM/8.0)STOP
      T=T+DT
      TT=TT+DT
      U(M3,2)=U(M,2)
      DO 21 I=3,M
      U1=(U(I,2)+U(I-1,2))/2.
      U2=(U(I,2)+U(I+1,2))/2.
      OMEG(I,2)=OMEG(I-1,2)+(DX(I-1)-U1*DT)*(OMEG(I,2)-OMEG(I-1,2))
      $/(U2*DT+DX(I-1)-U1*DT)
21  CONTINUE
C *****
C  CALLING RANDOM VORTICES
C *****

```

```

IF(KK.GT.1)GO TO 16
CALL TURBFLO(AMW,STGLN,CIRC,RC,XV,YV,VCR,GAMMA,XERO)
16 CONTINUE
CALL WKSHT(TT,DT,XV,YV,VCR,GAMMA,X,Y,UI,OMEG,
&F,U,V,N,AMW,STGLN,CIRC,RC,XERO)
C *****
C *****
DO 17 I=3,M3
F(I,1)=F(2,1)
F(I,N3)=F(2,N3)
17 CONTINUE
Z=(F(M1,N1)-F(M1-2,N1))*(X(M1)-X(M1-1))/(DX(M1-2)+DX(M1-1))
IF(KK-1)24,26,24
26 DO 23 J=2,N
F(M,J)=F(MM2,J)+(F(M,J)-F(MM2-1,J))/2.0
23 CONTINUE
F(M1,N1)=F(M1-1,N1)+Z
GO TO 27
24 DO 29 J=2,N
F(M,J)=F(MM2,J)+(F(M,J)-F(MM2-1,J))/2.0+(F(MM2,J)-FI(J))*DT/DTO
E(M3,J)=F(M,J)
29 CONTINUE
F(M1,N1)=F(M1-1,N1)+Z+(F(M1-1,N1)-FI(N+1))*DT/DTO
27 DO 22 J=2,N
22 FI(J)=F(MM2,J)
FI(N+1)=F(M1-1,N1)
DO 36 I=M1,M2
36 F(I,N1)=F(M1,N1)
75 CONTINUE
KTT=KTT-1
DO 40 I=1,KTT
L=I
IF(TI(I).GT.4.8)GO TO 41
40 CONTINUE
41 CONTINUE
LL=L-1
SUM1=0.0
DO 42 I=2,LL
SUM1=SUM1+CL(I)
42 CONTINUE
CLAV=(DT*(CL(1)+CL(LL)+2.*SUM1)/2.)/(TI(LL)-TI(1))
PRINT 43,RC,CLAV
43 FORMAT(1X,'RC=',F10.5,1X,'CLAV=',F14.7,/)
PRINT 132
132 FORMAT(/,1X,'TIME CHANGE',/)
PRINT 120,(TI(I),I=1,KTT)
120 FORMAT(1X,16F8.4)
PRINT 134

```


```
134 FORMAT(/,1X,'LIFT COFF.',/)  
    PRINT 120,(CL(I),I=1,KTT)  
    CALL PLTCLT(TI,CL,KTT,AL,RC,1)  
    CALL PLTCLT(TI,CM,KTT,AL,RC,2)  
78  CONTINUE  
C   CALL PLTALL(XDUM,YDUM,4*KTT,KTT)  
90  CONTINUE  
    CALL EXIT  
    END
```

```

SUBROUTINE BNDN(F,M,M1,M2,N,N1,DY,DX,UI,U,V,CP)
C CCCCCCCCCCCCCCCCCCCCCCCCCCCCCCCCCCCCCCCCCCCCCCCCCCCCCCCCCCCCC
C   SUBROUTINE BNDN TO EVALUATE STEADY STATE BOUNDARY CONDITIONS C
C CCCCCCCCCCCCCCCCCCCCCCCCCCCCCCCCCCCCCCCCCCCCCCCCCCCCCCCCCCCCC

  DIMENSION F(25,25),DY(25),DX(25),U(25,25),V(25,25),CP(25,25)
  N3=N+1
  M3=M+1
  DO 1 J=1,N3
  DO 1 I=1,M3
1   F(I,J)=0.0
  DO 11 I=1,M3
11  F(I,1)=-UI*DY(1)
  DO 2 J=2,N3
    F(1,J)=F(1,J-1)+UI*DY(J-1)
    F(2,J)=F(1,J)
    F(M+1,J)=F(1,J)
  2   F(M,J)=F(1,J)
  DO 3 I=2,M
  DO 3 J=1,N3
    F(I,J)=F(1,J)
  3   CONTINUE
  DO 30 I=2,M
  DO 30 J=2,N
    U(I,J)=(F(I,J+1)-F(I,J-1))/(DY(J)+DY(J-1))
    V(I,J)=(F(I-1,J)-F(I+1,J))/(DX(I)+DX(I-1))
    CP(I,J)=1.-(U(I,J)**2+V(I,J)**2)/UI**2
  30  CONTINUE
  RETURN
  END

```



```

SUBROUTINE POIS
C CCCCCCCCCCCCCCCCCCCCCCCCCCCCCCCCCCCCCCCCCCCCCCCCCCCCCCCCCCCCC
C
C          SUBROUTINE POIS TO SOLVE POISSONS EQUATION BY ITERATIONS
C
C CCCCCCCCCCCCCCCCCCCCCCCCCCCCCCCCCCCCCCCCCCCCCCCCCCCCCCCCCCCCC
COMMON F(25,25), OMEG(25,25), BOMEG(25,25)
COMMON X(25), Y(25), DX(25), DY(25), U(25,25), V(25,25), CP(25,25)
COMMON FI(25), IPVT(250), M, N, M1, M2, N1, MM2, NM2, UI, ITN, IC, DT, T
COMMON FP(25,25)
ITN=0
MAXIT=500
ERR=0.001
OMEGA=1.6
A=OMEGA
B=1.-OMEGA
10  R=0.0
DO 28 I=3,MM2
DO 28 J=3,NM2
IF(J.EQ.N1.AND.I.GE.M1.AND.I.LE.M2)GO TO 28
50  S=DX(I)/DX(I-1)
Z=DY(J)/DY(J-1)
AA=(1+S)*DX(I)**2.
BB=(1+Z)*DY(J)**2.
E=BB*(1+S)*(1+S**2.)+AA*(1+Z)*(1+Z**2.)
FNEW=A*((BB*(F(I+1,J)*(1+S**2)+F(I-1,J)*(S**3+S))+AA*(F(I,J
$+1)*(1+Z**2)+F(I,J-1)*(Z**3+Z))+AA*BB*OMEG(I,J))/E)+B*F(I,J)
RESID=ABS(FNEW-F(I,J))
IF(RESID-R)35,35,36
36  R=RESID
35  F(I,J)=FNEW
28  CONTINUE
IF(R-ERR)60,61,61
61  ITN=ITN+1
IF(ITN-MAXIT)10,10,62
62  CONTINUE
PRINT 101,MAXIT
101  FORMAT(22HF FAILS TO CONVERGE IN,I5,10HITERATIONS)
STOP
60  CONTINUE
DO 30 I=3,M
DO 30 J=2,N
U(I,J)=(F(I,J+1)-F(I,J-1))/(DY(J)+DY(J-1))
V(I,J)=(F(I-1,J)-F(I+1,J))/(DX(I)+DX(I-1))
30  CONTINUE
DO 31 I=2,M
DO 31 J=2,N
CP(I,J)=1.-(U(I,J)**2+V(I,J)**2)/UI**2

```



```
31 CONTINUE
   DO 18 I=2,M
      OMEG(I,2)=-((F(I,2)-2.*F(I,3)+F(I,4))/DY(2))**2.
      OMEG(I,N)=-((F(I,N)-2.*F(I,N-1)+F(I,N-2))/DY(N-1))**2
18 CONTINUE
   J=N1
   DO 19 I=M1,M2
      OMEG(I,J)=-((F(I,J)-2.*F(I,J+1)+F(I,J+2))/DY(J))**2
19 CONTINUE
   RETURN
   END
```

```

SUBROUTINE HELM,
C CCCCCCCCCCCCCCCCCCCCCCCCCCCCCCCCCCCCCCCCCCCCCCCCCCCCCCCCCCCCC
C   SUBROUTINE HELM TO SOLVE HELMHOLTZ VORTICITY EQUATION USING C
C   BANDED MATRICES C
C CCCCCCCCCCCCCCCCCCCCCCCCCCCCCCCCCCCCCCCCCCCCCCCCCCCCCCCCCCCCC
XRETURNS(L)
COMMON F(25,25), OMEG(25,25), BOMEG(25,25)
COMMON X(25), Y(25), DX(25), DY(25), U(25,25), V(25,25), CP(25,25)
COMMON FI(25), IPVT(250), M, N, M1, M2, N1, MM2, NM2, UI, ITN, IC, DT, T
COMMON FP(25,25)
DIMENSION A1(250,39), B1(250)
C *****
C PORTION SOLVING HELMHOLTZ EQUATION *
C *****
C *****
C NN=NO. OF EQUATIONS OF VORTICITY
5 CONTINUE
ERR=0.001
NN=(MM2-2)*(NM2-2)-(M2-M1+1)
NI=MM2-2
NII=NI-(M2-M1+1)
NU1=N1+1
NL1=N1-1
NB=M-2
ND=2*NB-1
DO 55 I=1,NN
DO 55 J=1,ND
55 A1(I,J)=0.0
IJ=1
DO 74 J=3,NM2
DO 74 I=3,MM2
ID=IJ
IF(IJ.GT.NB)ID=NB
IF(J.EQ.N1.AND.I.GE.M1.AND.I.LE.M2)GO TO 74
ALM1=DT/(DX(I)+DX(I-1))
ALM2=DT/(DY(J)+DY(J-1))
AB=0.0
BC=0.0
A1(IJ, ID+1)=ALM1*U(I, J)
A1(IJ, ID+NI)=ALM2*V(I, J)
IF(J.EQ.N1.AND.I.EQ.M2+1)GO TO 65
IF(I-3)66,65,66
65 AB=A1(IJ, ID+1)*OMEG(I-1, J)
GO TO 63
66 A1(IJ, ID-1)=-A1(IJ, ID+1)
63 CONTINUE
IF(I.GE.M1.AND.I.LE.M2.AND.J.EQ.NU1)69,85
85 CONTINUE

```

```

IF(J-3)71,69,71
69 BC=A1(IJ, ID+NI)*OMEG(I, J-1)
GO TO 64
71 A1(IJ, ID-NI)=-A1(IJ, ID+NI)
64 A1(IJ, ID)=1.00
IF(J.EQ.N1.AND.I.EQ.M1-1)67,87
87 CONTINUE
IF(I-MM2)68,67,68
67 A1(IJ, ID)=A1(IJ, ID)+U(I, J)*DT/DX(I-1)
A1(IJ, ID-1)=-U(I, J)*DT/DX(I-1)
A1(IJ, ID+1)=0.0
68 CONTINUE
IF(I.GE.M1.AND.I.LE.M2.AND.J.EQ.NL1)72,86
86 CONTINUE
IF(J-NM2)73,72,73
72 A1(IJ, ID)=A1(IJ, ID)+V(I, J)*DT/DY(J-1)
A1(IJ, ID-NI)=-V(I, J)*DT/DY(J-1)
A1(IJ, ID+NI)=0.0
73 B1(IJ)=BOMEG(I, J)+AB+BC
IF(J.EQ.N1.AND.I.LT.M1)20,21
20 CONTINUE
A1(IJ, ID+NII)=A1(IJ, ID+NI)
A1(IJ, ID+NI)=0.0
21 CONTINUE
IF((J.EQ.NU1.AND.I.LT.M1).OR.(J.EQ.N1.AND.I.GT.M2))76,70
76 CONTINUE
A1(IJ, ID-NII)=A1(IJ, ID-NI)
A1(IJ, ID-NI)=0.0
70 CONTINUE
IJ=IJ+1
74 CONTINUE
CALL CROUT(A1, NN, NB)
CALL SOLVE(A1, B1, B1, NN, NB)
IC=IC+1
IF(IC.GT.15)6,7
6 CONTINUE
T=T-DT
DT=DT/2.0
DO 8 J=2, N
DO 8 I=2, M
F(I, J)=FP(I, J)
OMEG(I, J)=BOMEG(I, J)
8 CONTINUE
RETURN L
7 CONTINUE
IL=1
R=0.0
DO 78 J=3, NM2

```

```
DO 78 I=3,MM2
IF(J.EQ.N1.AND.I.GE.M1.AND.I.LE.M2)GO TO 82
RES=ABS((B1(IL)-OMEG(I,J))/B1(IL))
RES=ABS((B1(IL)-OMEG(I,J)))
IF(RES.GT.R)R=RES
IL=IL+1
82 CONTINUE
78 CONTINUE
IF (R.LT.ERR) GO TO 79
80 IB=1
DO 81 J=3,NM2
DO 81 I=3,MM2
IF(J.EQ.N1.AND.I.GE.M1.AND.I.LE.M2)GO TO 83
OMEG(I,J)=B1(IB)
IB=IB+1
83 CONTINUE
81 CONTINUE
CALL POIS
GO TO 5
79 CONTINUE
IJ=1
DO 200 J=3,NM2
DO 200 I=3,MM2
IF(J.EQ.N1.AND.I.GE.M1.AND.I.LE.M2)GO TO 84
OMEG(I,J)=B1(IJ)
IJ=IJ+1
84 CONTINUE
200 CONTINUE
DO 15 J=2,N
DO 15 I=1,M
BOMEG(I,J)=OMEG(I,J)
15 CONTINUE
RETURN
END
```

```
SUBROUTINE CROUT (A,NEQ,NBAND)
DIMENSION A(250,39)
NA=NBAND-1
NTT=2*NBAND-1
DO 5 J=2,NBAND
5 A(1,J)=A(1,J)/A(1,1)
KY=NEQ-NA
KX=2
10 K1=KX+1
K2=KX-1
KA=KX+NA
KB=KA-1
KBND=KX-NBAND
IF (KX-KY) 15,15,12
12 KB=NEQ
KA=NEQ
15 DO 30 I=KX,KB
IF (I-NBAND) 16,16,17
16 KC=1
GO TO 18
17 KC=I-NA
18 SZ=0.
DO 20 J=KC,K2
IF (I-NBAND) 105,105,110
105 J1=J
GO TO 115
110 J1=J-I+NBAND
115 IF (J-NBAND) 120,120,125
120 J2=KX
GO TO 130
125 J2=KX-J+NBAND
130 SZ=SZ+A(I,J1)*A(J,J2)
20 CONTINUE
IF (I-NBAND) 140,140,150
140 J1=KX
GO TO 160
150 J1=KX-I+NBAND
160 A(I,J1)=A(I,J1)-SZ
30 CONTINUE
IF (KX-NEQ) 31,51,51
31 DO 50 J=K1,KA
IF (KX-NBAND) 32,32,34
32 KC=1.
GO TO 36
34 KC=J-NA-1
36 SZ=0.
DO 40 I=KC,K2
IF (KX-NBAND) 165,165,170
```

```
165 I1=I
    GO TO 175
170 I1=I-KX+NBAND
175 IF (I-NBAND) 180,180,185
180 J1=J
    GO TO 190
185 J1=J-I+NBAND
190 IF (J1-NTT) 195,195,40
195 SZ=SZ+A(KX,I1)*A(I,J1)
    40 CONTINUE
    IF (KBND) 200,200,210
200 J1=J
    J2=KX
    GO TO 220
210 J1=J-KX+NBAND
    J2=NBAND
220 A(KX,J1)=(A(KX,J1)-SZ)/A(KX,J2)
    50 CONTINUE
    51 KX=KX+1
    IF (KX-NEQ) 10,10,70
    70 CONTINUE
    RETURN
    END
```

```
SUBROUTINE SOLVE (A,F,SOL,NEQ,NBAND)
DIMENSION A(250,39),F(250),SOL(250)
NA=NBAND-1
KY=NEQ-NA
NTT=2*NBAND-1
F(1)=F(1)/A(1,1)
DO 110 KX=2,NEQ
  K2=KX-1
  IF (KX-NBAND) 10,10,20
10 KC=1
  GO TO 30
20 KC=KX-NA
30 SZ=0.
  DO 70 J=KC,K2
  IF (KX-NBAND) 40,40,50
40 J1=J
  GO TO 60
50 J1=J-KX+NBAND
60 SZ=SZ+A(KX,J1)*F(J)
70 CONTINUE
  IF (KX-NBAND) 80,80,90
80 J1=KX
  GO TO 100
90 J1=NBAND
100 F(KX)=(F(KX)-SZ)/A(KX,J1)
110 CONTINUE
  SOL(NEQ)=F(NEQ)
  KX=NEQ
120 L=KX-1
  IF (KX-KY) 140,130,130
130 KA=NEQ
  GO TO 150
140 KA=KX+NA-1
150 SZ=0.
  DO 200 J=KX,KA
  IF (L-NBAND) 160,160,170
160 J1=J
  GO TO 180
170 J1=J-L+NBAND
180 IF (J1-NTT) 190,190,200
190 SZ=SZ+A(L,J1)*SOL(J)
200 CONTINUE
  SOL(L)=F(L)-SZ
  KX=KX-1
  IF (L-1) 210,210,120
210 CONTINUE
  RETURN
  END
```

```

SUBROUTINE PLTCLT(T,CL,KT,AL,RC,NC)
DIMENSION T(250),CL(250)
CALL PLOTS(30,24.,10.75,2)
CALL PLTCOM(26HPLEASE USE .4 MM BLACK INC,26)
CALL PLOT(1.0,1.25,-3)
CALL SCALE4(T,8.0,KT,1,0,TMIN,TDA)
CALL SCALE4(CL,9.0,KT,1,0,CLMIN,CLDA)
CALL CRAXES(8.,9.,TMIN,CLMIN,TDA,CLDA,4)
CALL PLOT((T(1)-TMIN)/TDA,(CL(1)-CLMIN)/CLDA,3)
CALL LINE4(T,CL,KT,1,TMIN,TDA,CLMIN,CLDA,0,0,0)
CALL SYMBOL(2.5,8.5,.125,
X38HRANDOM VORTICES APPROACHING FLAT PLATE,0.0,38)
CALL SYMBOL(5.,8.,.125,5HRC = ,0,0,5)
CALL NUMBER(5.6,8.,.125,RC,0.0,2)
CALL SYMBOL(5.,7.5,.125,5HC = ,0.0,5)
CALL NUMBER(5.6,7.5,.125,AL,0.0,2)
IF(NC.GT.1)GO TO 8
CALL SYMBOL(-.5,3.5,.125,18HLIFT COEFFICIENT C,90.,18)
CALL WHERE(XPT,YPT,FCTR)
XPT=XPT+.125*.6
YPT=YPT+.035
CALL SYMBOL(-.425,5.4,.125,1HL,90.0,1)
GO TO 10
8 CALL SYMBOL(-.5,2.9,.125,29HPITCHING MOMENT COEFFICIENT C,
$90.,29)
CALL WHERE(XPT,YPT,FCTR)
XPT=XPT+.125*.6
YPT=YPT+.035
CALL LOWER(-.425,6.,.125,1HM,90.0,1)
10 CONTINUE
CALL PLTERR(1)
C PAUSE
CALL ENDPLT
RETURN
END

```



```

SUBROUTINE PLTALL(XDUM,YDUM,N,NN,NC)
DIMENSION X1(250),X2(250),X3(250),X4(250),Y1(250),Y2(250)
1,Y3(250),Y4(250),XDUM(1000),YDUM(1000)
CALL PLOTS(30,10.0,10.75,2)
CALL PLTCOM(26HPLEASE USE .4 MM BLACK INC,26)
CALL PLOT(1.0,1.25,-3)
DO 5 I=1,NN
X1(I)=XDUM(I)
Y1(I)=YDUM(I)
X2(I)=XDUM(NN+I)
Y2(I)=YDUM(NN+I)
X3(I)=XDUM(2*NN+I)
Y3(I)=YDUM(2*NN+I)
X4(I)=XDUM(3*NN+I)
Y4(I)=YDUM(3*NN+I)
5 CONTINUE
CALL SCALE4(XDUM,8.0,N,1,0,XMIN,XDA)
CALL SCALE4(YDUM,9.0,N,1,0,YMIN,YDA)
CALL CRAXES(8.,9.,XMIN,YMIN,XDA,YDA,2)
C
CALL SYMBOL(2.5,8.5,.125,
X38HRANDOM VORTICES APPROACHING FLAT PLATE,0.0,38)
IF(NC.GT.1)GO TO 8
CALL SYMBOL(-.5,3.5,.125,18HLIFT COEFFICIENT C,90.,18)
CALL WHERE(XPT,YPT,FCTR)
XPT=XPT+.125*.6
YPT=YPT+.035
CALL SYMBOL(-.425,5.4,.125,1HL,90.0,1)
GO TO 10
8 CALL SYMBOL(-.5,2.9,.125,29HPITCHING MOMENT COEFFICIENT C,
$90.,29)
CALL WHERE(XPT,YPT,FCTR)
XPT=XPT+.125*.6
YPT=YPT+.035
CALL LOWER(-.425,6.,.125,1HM,90.0,1)
10 CONTINUE
CALL PLOT((X1(1)-XMIN)/XDA,(Y1(1)-YMIN)/YDA,3)
CALL LINE4(X1,Y1,NN,1,XMIN,XDA,YMIN,YDA,0,0,0)
CALL PLOT((X2(1)-XMIN)/XDA,(Y2(1)-YMIN)/YDA,3)
CALL LINE4(X2,Y2,NN,1,XMIN,XDA,YMIN,YDA,0,0,0)
CALL PLOT((X3(1)-XMIN)/XDA,(Y3(1)-YMIN)/YDA,3)
CALL LINE4(X3,Y3,NN,1,XMIN,XDA,YMIN,YDA,0,0,0)
CALL PLOT((X4(1)-XMIN)/XDA,(Y4(1)-YMIN)/YDA,3)
CALL LINE4(X4,Y4,NN,1,XMIN,XDA,YMIN,YDA,0,0,0)
CALL SYMBOL(5.,8.,.125,8HC = 2.45.0.0,8)
CALL SYMBOL(4.,7.5,3./32.,9H = 0.50,0.0,9)
CALL LOWER(4.,7.5,3./32.,1HR,0.0,1)
CALL LOWER(4.,7.44,3./32.,2H C,0.0,2)

```

```
CALL SYMBOL(4.,7.,3./32.,9H = 0.60,0.0,9)
CALL LOWER(4.,7.,3./32.,1HR,0.0,1)
CALL LOWER(4.,6.94,3./32.,2H C,0.0,2)
CALL SYMBOL(4.,6.5,3./32.,9H = 0.70,0.0,9)
CALL LOWER(4.,6.5,3./32.,1HR,0.0,1)
CALL LOWER(4.,6.44,3./32.,2H C,0.0,2)
CALL SYMBOL(4.,6.,3./32.,9H = 0.80,0.0,9)
CALL LOWER(4.,6.,3./32.,1HR,0.0,1)
CALL LOWER(4.,5.94,3./32.,2H C,0.0,2)
CALL PLTERR(1)
CALL ENDPLT
RETURN
END
```

```

SUBROUTINE TURBFLO(AMW,STGLN,CIRC,CR,X,Y,VCR,GAMMA,XERO)
C CCCCCCCCCCCCCCCCCCCCCCCCCCCCCCCCCCCCCCCCCCCCCCCCCCCCCCCCCCCCC
C SUBROUTINE TURBFLO TO GENERATE THE PSEUDO-TURBULENT FLOW C
C USING RANDOMLY POSITIONED EQUIVALENT RANKINE VORTICES C
C CCCCCCCCCCCCCCCCCCCCCCCCCCCCCCCCCCCCCCCCCCCCCCCCCCCCCCCCCCCCC
DIMENSION X(100),Y(100),RN(200),WZ(200),GAMMA(100)
DIMENSION U(25,25),V(25,25),XPT(25),YPT(25),VCR(100)
XERO=0.34676264158
ND=20
N=4*ND
CRMS=0.0
CALL RANDNR(X,N,XERO)
CALL ASORT(X,N)
CALL RANDNR(Y,N,XERO)
CALL RANDNG(VCR,N,XERO)
NR=1
DO 28 I=1,N
VCR(I) = 2.*VCR(I)*CR
8 IF(VCR(I)-CRMS)7,9,9
7 CONTINUE
CALL RANDNG(WZ,NR,XERO)
VCR(I)=2.*WZ(1)*CR
GO TO 8
9 GAMMA(I)=CIRC*(VCR(I)/CR)**2
Y(I) = AMW*Y(I)
28 X(I) = STGLN*(2.-4.*X(I))
NK = 2
CALL SIGNSR(X,Y,GAMMA,VCR,N,NK)
RETURN
END

```

```
SUBROUTINE WKSHT(TT, TINCR, X, Y, VCR, GAMMA, XPT, YPT,  
&UREF, OMEG, EPS, U, V, NP, AMW, STGLN, CIRC, CR, XERO)  
  DIMENSION X(100), Y(100), RN(200), WZ(200), GAMMA(100)  
  DIMENSION U(25,25), V(25,25), XPT(25), YPT(25), VCR(100)  
  DIMENSION EPS(25,25), OMEG(25,25)  
  ND=20  
  N=4*ND  
  X1=TT*UREF  
  IF(X1.GE.STGLN)10,6  
10  CONTINUE  
    TT=0.0  
    CALL CRDSHT(X, Y, GAMMA, VCR, RN, WZ, AMW, CIRC, CR, STGLN, XERO, ND)  
6    CONTINUE  
    CALL UVPTS(X, Y, VCR, GAMMA, UREF, N, XPT, YPT, U, V, EPS, OMEG, NP)  
    DO 51 KK=1, N  
51  X(KK) = X(KK)+TINCR*UREF  
    RETURN  
  END
```

```
SUBROUTINE RANDNR(Z,N,XERO)
DIMENSION Z(100)
DO 3 I=1,N
Z(I) = 23.*XERO+.21132486579
Z(I) = Z(I)-FLOAT(INT(Z(I)))
3 XERO = Z(I)
RETURN
END
```

```
SUBROUTINE RANDNG(Z,N,XERO)
DIMENSION Z(100)
DO 3 I=1,N
Z(I)=23.*XERO+.21132486579
Z(I)=Z(I)-FLOAT(INT(Z(I)))
XERO=Z(I)
SUM=0.
DO 2 J=1,10
Z(I)=10.*Z(I)
TEMP=FLOAT(INT(Z(I)))
Z(I)=Z(I)-TEMP
2 SUM=SUM+TEMP
3 Z(I)=SUM/90.
RETURN
END
```

```
SUBROUTINE SIGNSR(X,Y,GAMMA,VCR,N,NK)
DIMENSION X(100),Y(100),GAMMA(100),VCR(100)
DO 1 I=NK,N
TEMP = 0.
K = I - 1
DO 2 J=1,K
R = (X(J)-X(I))**2+(Y(J)-Y(I))**2
2 TEMP = TEMP-GAMMA(J)*SQRT(R)/(VCR(J)**2+R)
IF (TEMP) 4,3,4
3 GAMMA(I) = -GAMMA(I-1)
GO TO 1
4 GAMMA(I) = GAMMA(I)*TEMP/ABS(TEMP)
1 CONTINUE
RETURN
END
```

```

SUBROUTINE UVPTS(X,Y,VCR,GAMMA,UREF,N,XPT,YPT,U,V,EPS,OMEG,NP)
CCCCCCCCCCCCCCCCCCCCCCCCCCCCCCCCCCCCCCCCCCCCCCCCCCCCCCCCCCCC
C   SUBROUTINE UVPTS TO CALCULATE THE BOUNDARY VELOCITIESC   C
C   DUE TO THE RANDOM VORTICESC   C
CCCCCCCCCCCCCCCCCCCCCCCCCCCCCCCCCCCCCCCCCCCCCCCCCCCCCCCCCCCC
      DIMENSION X(100),Y(100),VCR(100),GAMMA(100)
      DIMENSION EPS(25,25),OMEG(25,25),V(25,25),U(25,25),XPT(25)
      &,YPT(25),DX(25),DY(25)
      I=2
      NZ=NP+1,
      DO 2 J=1,NZ
      UPT=0.0
      VPT=0.0
      EPT=0.0
      OMT=0.0
      DO 1 K=1,N
      GAMAS=GAMMA(K)
      RC=VCR(K)
      XO=X(K)
      YO=Y(K)
      CALL UPSTF(EPS,XPT,YPT,XO,YO,UREF,GAMAS,RC,NP,0.0,I,J)
      CALL VORT(OMEG,XPT,YPT,XO,YO,UREF,GAMAS,RC
      &,NP,0.0,U,V,I,J)
      UPT=UPT+U(I,J)
      VPT=VPT+V(I,J)
      EPT=EPT+EPS(I,J)
      OMT=OMT+OMEG(I,J)
1     CONTINUE
      EPS(I,J)=EPT+UREF*(YPT(J)-YPT(2))
      OMEG(I,J)=OMT
      U(I,J)=UPT+UREF
      V(I,J)=VPT
C     PRINT 15,I,J
15    FORMAT(2I10)
C     PRINT 20, EPS(I,J),OMEG(I,J),U(I,J),V(I,J)
20   /  FORMAT(1X,'EPS=',F10.4,1X,'OMEG=',F10.4,1X,'U=',F10.4,
      &'V=',F10.4)
2     CONTINUE
      RETURN
      END

```



```

SUBROUTINE CRDSHT(X,Y,GAMMA,VCR,RN,WZ,AMW,CIRC,CR,STGLN,XERO,ND)
DIMENSION X(100),Y(100),RN(200),WZ(200),VCR(100),GAMMA(100)
CRMS=0.0
NR=1
L = 3*ND
DO 4 I=1,L
  NDI=I+ND
  Y(I)=Y(NDI)
  VCR(I)=VCR(NDI)
  GAMMA(I)=GAMMA(NDI)
4 X(I)=X(NDI)
M = 2*ND
CALL RANDNR(RN,M,XERO)
DO 5 I=1,ND
  LI=I+L
  NDI=I+ND
  X(LI)=-STGLN*(1.+RN(I))
5 Y(LI)=AMW*RN(NDI)
  CALL RANDNG(RN,ND,XERO)
DO 10 I=1,ND
  LI=L+I
  VCR(LI)=2.*CR*RN(I)
8 IF(VCR(LI)-CRMS)7,10,10
7 CONTINUE
  CALL RANDNG(WZ,NR,XERO)
  VCR(LI)=2.*WZ(1)*CR
  GO TO 8
10 GAMMA(LI)=CIRC*(VCR(LI)/CR)**2
  NK = L + 1
  CALL SIGNSR(X,Y,GAMMA,VCR,N,NK)
RETURN
END

```

```
SUBROUTINE ASORT(X,N)
DIMENSION X(N)
IT=2
IF(N-IT)19,18,18
19 CONTINUE
DO 18 I=1,N
K=2**I/2-1
GO TO 1
18 IT=2*IT
1 IF(K)7,7,6
6 I=1
2 J=I
Y=X(I+K)
3 IF(Y-X(J))4,5,5
5 X(J+K)=Y
I=I+1
IF(I+K-N)2,2,9
9 K=(K-1)/2
GO TO 1
4 X(J+K)=X(J)
J=J-K
IF(J)5,5,3
7 CONTINUE
RETURN
END
```

```

SUBROUTINE UPSTF(EPS,X,Y,XO,YO,UI,GAMA,RC,N,T,I,J)
C CCCCCCCCCCCCCCCCCCCCCCCCCCCCCCCCCCCCCCCCCCCCCCCCCCCCCCCCCCCCC
C SUBROUTINE UPSTF TO EVALUATE THE EQUIVALENT RANKINE VORTEX C
C EQUATION C
C CCCCCCCCCCCCCCCCCCCCCCCCCCCCCCCCCCCCCCCCCCCCCCCCCCCCCCCCCCCCC
DIMENSION X(25),Y(25),EPS(25,25),DX(25),DY(25)
YY=Y(2)
PI=ABS(ACOS(-1.))
C=PI/(2.*(Y(N)-YY))
X(I)=X(I)-XO-UI*T
Y(J)=Y(J)-YY
IF(J-N)5,6,5
5 CONTINUE
AK=1./(TAN(C*YO))
AA=(1-AK**2*(TAN(C*Y(J)))**2-AK**2*(TANH(C*X(I)))**2+
*(TAN(C*Y(J)))**2*(TANH(C*X(I)))**2)**2
AB=(2.*AK*TANH(C*X(I))+2.*AK*(TAN(C*Y(J)))**2*TANH(C*X(I)))**2
AC=((1.-AK*TAN(C*Y(J)))**2+(AK*TANH(C*X(I))+TAN(C*Y(J))
**TANH(C*X(I)))**2)**2
REQS=ABS(AC/(AA+AB))
GO TO 7
6 CONTINUE
REQS=1.0
7 CONTINUE
EPS(I,J)=(-GAMA/(2.*PI))*(ALOG(REQS+RC**2)-ALOG(1.,+RC**2))
X(I)=X(I)+XO+UI*T
Y(J)=Y(J)+YY
RETURN
END

```

```

SUBROUTINE VORT(F, OMEG, X, Y, XO, YO, UI, GAMA, RC, N, T, U, V, I, J)
CCCCCCCCCCCCCCCCCCCCCCCCCCCCCCCCCCCCCCCCCCCCCCCCCCCCCCCCCCCC
C SUBROUTINE VORT TO EVALUATE THE VORTICITY AND VELOCITY C
C COMPONENTS AT THE POINT X, Y DUE TO A VORTEX AT A POINT C
C XO, YO. C
C CCCCCCCCCCCCCCCCCCCCCCCCCCCCCCCCCCCCCCCCCCCCCCCCCCCCCCCCCCCC
DIMENSION F(25,25), OMEG(25,25), DX(25), DY(25), X(25), Y(25)
DIMENSION U(25,25), V(25,25)
H=0.0001
FC=F(I, J)
X(I)=X(I)+H
CALL UPSTF(F, X, Y, XO, YO, UI, GAMA, RC, N, T, I, J)
X(I)=X(I)-H
FE=F(I, J)
X(I)=X(I)-H
CALL UPSTF(F, X, Y, XO, YO, UI, GAMA, RC, N, T, I, J)
X(I)=X(I)+H
FW=F(I, J)
Y(J)=Y(J)+H
CALL UPSTF(F, X, Y, XO, YO, UI, GAMA, RC, N, T, I, J)
Y(J)=Y(J)-H
FN=F(I, J)
Y(J)=Y(J)-H
CALL UPSTF(F, X, Y, XO, YO, UI, GAMA, RC, N, T, I, J)
Y(J)=Y(J)+H
FS=F(I, J)
OMEG(I, J)=- (FW+FE+FN+FS-4.*FC)/H**2
V(I, J)=- (FE-FW)/(2.*H)
U(I, J)=(FN-FS)/(2.*H)
F(I, J)=FC
RETURN
END

```

```

SUBROUTINE LIFTC(CL,CM,KT)
CCCCCCCCCCCCCCCCCCCCCCCCCCCCCCCCCCCCCCCCCCCCCCCCCCCCCCCCCCCC
C                                                                    C
C          SUBROUTINE LIFTC TO CALCULATE THE                          C
C                                                                    C
C          LIFT AND PITCHING MOMENT COEFFICIENTS                      C
C                                                                    C
C CCCCCCCCCCCCCCCCCCCCCCCCCCCCCCCCCCCCCCCCCCCCCCCCCCCCCCCCCCCCC
COMMON F(25,25), OMEG(25,25), BOMEG(25,25)
COMMON X(25), Y(25), DX(25), DY(25), U(25,25), V(25,25), CP(25,25)
COMMON FI(25), IPV(250), M, N, M1, M2, N1, MM2, NM2, UI, ITN, IC, DT, T
COMMON FP(25,25)
DIMENSION CL(250), CM(250), G1(25), G2(25), G3(25), DU(25), DP(25)
AL=X(M2)-X(M1)+0.25
SUM1=0.0
SUM2=0.0
DO 35 I=M1, M2
UB=(F(I, N1)-F(I, N1-1))/DY(N1-1)
UT=(F(I, N1+1)-F(I, N1))/DY(N1)
DU(I)=UB-UT
G3(I)=(UB**2-UT**2)/2.0
G2(I)=0.0
DO 30 J=M1, I
IF(J.EQ.M1)GO TO 30
G2(I)=G2(I)+(DU(J-1)+DU(J))*DX(J-1)/2.0
30 CONTINUE
G2(I)=G2(I)+0.5*DU(M1)*0.25
IF(KT.EQ.1)G1(I)=G2(I)
DP(I)=-((G2(I)-G1(I))/DT+G3(I))
G1(I)=G2(I)
IF(I.EQ.M1)GO TO 35
SUM1=SUM1+DX(I-1)*(DP(I-1)+DP(I))/2.0
SUM2=SUM2+DX(I-1)*(DP(I-1)*(X(I-1)-X(M1))+DP(I)*(X(I)-X(M1)))/2.
35 CONTINUE
CL(KT)=SUM1/(0.5*UI**2*AL)
CM(KT)=SUM2/(0.5*UI**2*AL**2)
RETURN
END

```

```

PROGRAM STAT(INPUT,OUTPUT,TAPE7,TAPE10)
CCCCCCCCCCCCCCCCCCCCCCCCCCCCCCCCCCCCCCCCCCCCCCCCCCCCCCCCCCCC
C
C PROGRAM STAT TO DO STATISTICAL ANALYSIS TO THE PSEUDO-TURBULENT C
C
C RESULTS OBTAINED FROM PROGRAM MOD1 C
C
CCCCCCCCCCCCCCCCCCCCCCCCCCCCCCCCCCCCCCCCCCCCCCCCCCCCCCCCCCCC
DIMENSION F(25,25),U(25,25),V(25,25),X(25),Y(25),US(1001),
$VS(1001)
DIMENSION OMEG(25,25),TI(1001),CL(1001),CP(25,25),CLQC(1001)
READ(7,106)M,M1,M2,M3,MM2,N,N1,NM2,N3,STGLN,AMW,RC,CIRC
READ(7,103)(X(I),I=1,M3)
READ(7,103)(Y(I),I=1,N3)
DO 3 KK=1,1001
READ(7,103)((F(I,J),I=2,M),J=2,N)
READ(7,103)((OMEG(I,J),I=2,M),J=2,N)
READ(7,103)((U(I,J),I=2,M),J=2,N)
READ(7,103)((V(I,J),I=2,M),J=2,N)
READ(7,103)((CP(I,J),I=2,M),J=2,N)
READ(7,104)US(KK),VS(KK),CL(KK),TI(KK),CLQC(KK),KT
3 CONTINUE
TINCR=TI(KT)-TI(KT-1)
PRINT 103,(US(I),I=1,KT)
PRINT 103,(VS(I),I=1,KT)
CALL STPK1(US,KT,TINCR)
CALL STPK1(VS,KT,TINCR)
CALL PLTCLT(TI,CL,KT)
CALL PLTCLT(TI,US,KT)
CALL PLTCLT(TI,VS,KT)
108 FORMAT(3F10.4)
103 FORMAT(15F8.3)
104 FORMAT(5F8.3,I10)
106 FORMAT(9I5,4F8.3)
STOP
END

```

```

PROGRAM STAT(INPUT,OUTPUT,TAPE7,TAPE10)
CCCCCCCCCCCCCCCCCCCCCCCCCCCCCCCCCCCCCCCCCCCCCCCCCCCCCCCCCCCC
C
C PROGRAM STAT TO DO STATISTICAL ANALYSIS TO THE PSEUDO-TURBULENT C
C
C RESULTS OBTAINED FROM PROGRAM MOD1 C
C
CCCCCCCCCCCCCCCCCCCCCCCCCCCCCCCCCCCCCCCCCCCCCCCCCCCCCCCCCCCC
DIMENSION F(25,25),U(25,25),V(25,25),X(25),Y(25),US(1001),
$VS(1001)
DIMENSION OMEG(25,25),TI(1001),CL(1001),CP(25,25),CLQC(1001)
READ(7,106)M,M1,M2,M3,MM2,N,N1,NM2,N3,STGLN,AMW,RC,CIRC
READ(7,103)(X(I),I=1,M3)
READ(7,103)(Y(I),I=1,N3)
DO 3 KK=1,1001
READ(7,103)((F(I,J),I=2,M),J=2,N)
READ(7,103)((OMEG(I,J),I=2,M),J=2,N)
READ(7,103)((U(I,J),I=2,M),J=2,N)
READ(7,103)((V(I,J),I=2,M),J=2,N)
READ(7,103)((CP(I,J),I=2,M),J=2,N)
READ(7,104)US(KK),VS(KK),CL(KK),TI(KK),CLQC(KK),KT
3 CONTINUE
TINCR=TI(KT)-TI(KT-1)
PRINT 103,(US(I),I=1,KT)
PRINT 103,(VS(I),I=1,KT)
CALL STPK1(US,KT,TINCR)
CALL STPK1(VS,KT,TINCR)
CALL PLTCLT(TI,CL,KT)
CALL PLTCLT(TI,US,KT)
CALL PLTCLT(TI,VS,KT)
108 FORMAT(3F10.4)
103 FORMAT(15F8.3)
104 FORMAT(5F8.3,I10)
106 FORMAT(9I5,4F8.3)
STOP
END

```

```
SUBROUTINE STPK1(UE,NVS,TINCR)
DIMENSION UE(NVS)
DIMENSION CC(300),G(300),GS(300)
PRINT 150
150 FORMAT (27H ANALYSIS AT A SINGLE POINT)
TIME = TINCR*FLOAT(NVS-1)
LGM = IFIX(SQRT(FLOAT(NVS)))
IGM=LGM
NI = IFIX(SQRT(FLOAT(NVS)))
NCV=LGM+1
CALL AMNSQR(UE,NVS,UMN,USGMA)
PRINT 103,UMN,USGMA
103 FORMAT (12H MEAN VALUE=,F10.5,24H ROOT MEAN SQUARE VALUE=,F10.5)
DO 1 I=1,NVS
1 UE(I) = (UE(I)-UMN)/USGMA
PRINT 2,(UE(I),I=1,IGM)
2 FORMAT (10F12.3)
CALL AUTOCR(UE,NVS,IGM,SGMA,CC)
TINCR = 1000.*TINCR
CALL PSDFU(CC,NCV,TINCR,G,GS)
TINCR = .001*TINCR
RETURN
END
```



```
SUBROUTINE AMNSQR(A, NN, AMU, SGMA)
DIMENSION A(NN)
AMU = 0
SGMA = 0
DO 21 I=1, NN
AMU = AMU + A(I)
21 SGMA = SGMA+A(I)**2
AMU = AMU/FLOAT(NN)
SGMA = SQRT(SGMA/FLOAT(NN)-AMU*AMU)
PRINT 100, AMU, SGMA
100 FORMAT (12H MEAN VALUE=, 1PE15.5, 24H ROOT MEAN SQUARE VALUE=,
$1PE15.5)
RETURN
END
```

```
      SUBROUTINE AUTOCR(X, NN, LGM, SGMB, CC)
      DIMENSION X(NN), CC(LGM), F(50)
      PRINT 100
100  FORMAT (30H AUTO CORRELATION COEFFICIENTS)
      NCV = LGM + 1
      DO 1 K=1, NCV
      L = K - 1
      F(K) = L
      J = NN - L
      SGMA = 0
      SGMB = 0
      CC(K) = 0
      DO 2 I=1, J
      SGMA = SGMA + X(I)**2
      SGMB = SGMB + X(I+L)**2
      2  CC(K) = CC(K) + X(I)*X(I+L)
      1  CC(K) = CC(K) / SQRT(SGMA*SGMB)
      E = SQRT(FLOAT(LGM) / FLOAT(NN))
      CALL PLTCLT(F, CC, K-1)
      PRINT 101, NN, LGM, E
101  FORMAT (20H NUMBER OF NUMBERS =, I10, 14H MAXIMUM LAG =, I10, 24H M
      1 AX. EQUIVALENT ERROR =, F10.5)
      SGMB = SQRT(SGMB)
      PRINT 103, SGMB
103  FORMAT (42H STANDARD DEVIATION OF CORRELATING SIGNAL =, 1PE15.5)
      PRINT 102, (CC(I), I=1, NCV)
102  FORMAT (10F10.5)
      RETURN
      END
```

```

SUBROUTINE PSDFU(R,NCV,H,G,GS)
DIMENSION R(NCV),G(NCV),GS(NCV),FR(100)
PRINT 30
30 FORMAT (/32H1POWER SPECTRAL DENSITY FUNCTION//)
PRINT 31
31 FORMAT (/32H ECHO CHECK OF AUTO CORRELATIONS)
PRINT 100,(R(I),I=1,NCV)
100 FORMAT (10F10.5)
LGM = NCV-1
ASIGN = -1.
AM = FLOAT(LGM)
SUM = 0.
DO 20 I=2,LGM
20 SUM = SUM + R(I)
G(1) = 2.*H*(R(1)+2.*SUM+R(NCV))
DO 1 K=2,NCV
SUM = 0.
AMI = 3.141593*FLOAT(K-1)/AM
DO 2 I=2,LGM
2 SUM = SUM+R(I)*COS(AMI*FLOAT(I-1))
G(K) = 2.*H*(R(1)+2.*SUM+ASIGN*R(NCV))
1 ASIGN = -1.*ASIGN
GS(1) = .5*(G(1)+G(2))
GS(NCV) = .5*(G(LGM)+G(NCV))
DO 23 I=2,LGM
23 GS(I) = .25*(G(I-1)+G(I+1))+.5*G(I)
FC = 500./H
BE = 2.*FC/AM
PRINT 3
3 FORMAT (86H TIME INCR.(H)M.SEC. MAX LAG CUT OFF FREQ.(C.P.S) EQ
1UIV. RESOLUTION BANDWITH(C.P.S)//)
PRINT 4,H,LGM,FC,BE
4 FORMAT (F10.4,I20,F20.0,F30.0)
NLO = NCV+1-3*((NCV+1)*3)
PRINT 5
5 FORMAT(108HHARM. FREQ. P.S.D.FU. P.S.D.FU. HARM. FREQ. P.S
1.D.FU. P.S.D.FU. HARM. FREQ. P.S.D.FU. P.S.D.FU.)
PRINT 50
50 FORMAT (/113H NO(K) (C. (RAW) (SMOOTH) NO(K) (C.P.S)
$P.S)
1 (RAW) (SMOOTH) NO(K) (C.P.S) (RAW) (SMOOTH))
FM = FC/AM
DO 6 I=1,NCV,3
F1 = FLOAT(I-1)*FM
IJ = I-1
IK = I+1
FP = F1+FM
FB = F1+2.*FM

```

```
FR(I)=F1
FR(I+1)=FP
FR(I+2)=FB
PRINT 10,IJ,F1,G(I),GS(I),I,FP,G(I+1),GS(I+1),IK,FB,G(I+2),
$GS(I+2)
10 FORMAT (I4,F9.3,F12.6,F11.6,2(I8,F9.3,F12.6,F11.6))
6 CONTINUE
CALL PLTCLT(FR,G,8)
CALL PLTCLT(FR,GS,8)
IF (NLO-1) 8,11,7
7 F1 = FLOAT(LGM)*FM
FP = F1+FM
PRINT 19,LGM,F1,G(LGM),GS(LGM),NCV,FP,G(NCV),GS(NCV)
19 FORMAT (I4,F9.3,F12.6,F11.6,I8,F9.3,F12.6,F11.6)
GO TO 8
11 F1 = FLOAT(NCV)*FM
PRINT 9,NCV,F1,G(NCV),GS(NCV)
9 FORMAT (I4,F9.3,F12.6,F11.6)
8 CONTINUE
RETURN
END
```

```
SUBROUTINE PLTCLT(T,CL,KT)
DIMENSION T(KT),CL(KT)
CALL PLOTS(30,24.,10.75,2)
CALL PLTCOM(26HPLEASE USE .4 MM BLACK INC,26)
CALL PLOT(1.0,1.25,-3)
CALL SCALE4(T,5.0,KT,1,0,TMIN,TDA)
CALL SCALE4(CL,6.0,KT,1,0,CLMIN,CLDA)
CALL CRAXES(5.,6.,TMIN,CLMIN,TDA,CLDA,2)
CALL AXIS4(0.0,0.0,4HTIME,4,-.15,-.1,5.,0.0,TMIN,TDA,2,.5,1)
CALL- AXIS4(0.0,0.0,31HLONGITUDINAL VELOCITY COMPONENT,31,.15,.1
$,6.,90.0,CLMIN,CLDA,2,.5,1)
CALL PLOT((T(1)-TMIN)/TDA,(CL(1)-CLMIN)/CLDA,3)
CALL LINE4(T,CL,KT,1,TMIN,TDA,CLMIN,CLDA,0,0,0)
CALL SYMBOL(.5,7.,.21,14HCL VERSUS TIME,0.0,14)
CALL SYMBOL(.5,8.,.21,27RANDOM VORTICES APPROACHING,0.0,27)
CALL SYMBOL(.5,7.5,.21,24HSEMI-INFINITE FLAT PLATE,0.0,24)
CALL PLTERR(1)
PAUSE
CALL ENDPLT
RETURN
END
```

## REFERENCES

- Ahmadi, G. and Goldschmidt, V.W., (1971), "Creation of a Pseudo-Turbulent Velocity Field", *Developments in Mechanics*, Vol. 6, Proc. of the 12th Midwestern Conf., pp. 291-304.
- Allen, D.N. and Southwell, R.V., (1955), "Relaxation Methods Applied to Determine the Motion in Two Dimensions, of a Viscous Fluid Past a Fixed Cylinder", *Quarterly J. of Mech. and Appl. Math.*, Vol. 8, pp. 129-145.
- Atkinson, B., Brocklebank, M., Card, C. and Smith, J., (1969) "Low Reynolds Number Developing Flows", *A.I.Ch.E. Journal*, Vol. 15, No. 4, pp. 548-553.
- Atkinson, B., Card, C. and Irons, B., (1970), "Application of the Finite Element Method to Creeping Flow Problems", *Trans. Ins. Chem. Engrs.*, Vol. 48, pp. T276-T284.
- Badr, H.M., (1977), "Response of the Laminar Layer on a Flat Plate to Free Stream Disturbances", Ph.D. Thesis, The University of Western Ontario, London, Ontario, Canada.
- Badr, H.M. and Base, T.E., (1978/1979), "A Variational Finite Element Method for Solving Unsteady Viscous Flow Problems", *J. Can. Soc. Mech. Eng.*, Vol. 5, No. 1, pp. 39-45.
- Baker, A.J., (1973), "Finite Element Solution Algorithm for Viscous Incompressible Fluid Dynamics", *Int. J. for Numerical Methods in Engg.*, Vol. 6, pp. 89-101.
- Baker, A.J., (1974), "Finite Element Solution Algorithm for Incompressible Fluid Dynamics", *Finite Element Methods in Flow Problems*, edited by Oden et al., UAH Press, Huntsville, Alabama, pp. 51-56.
- Base, T.E., (1970), "Mathematical Studies of Vortex Model to Represent Unsteady Fluid Flow", Ph.D. Thesis, I.S.V.R., The University of Southampton, England.
- Base, T.E. and Davies, P.O.A.L., (1974), "A Vortex Model to Relate Eulerian and Lagrangian 'Turbulent' Velocity Fields", *The Canadian Journal of Chemical Engineering*, Vol. 52, pp. 11-16.
- Bendat, J.S. and Piersol, A.G., (1971), "Random Data Analysis and Measurement Procedures", Wiley & Sons, New York.
- Blottner, F.C., (1970), "Finite Difference Methods of Solution of the Boundary Layer Equations", *A.I.A.A. Journal*, Vol. 8, No. 2, pp. 193-205.

- Blottner, F.G., (1974), "Variable Grid Scheme Applied to Turbulent Boundary Layers", Computer Methods in Applied Mechanics and Engineering, Vol. 4, pp. 179-194.
- Bratanow, T., Ecer, A. and Kobiske, M., (1974), "Numerical Calculations of Velocity and Pressure Distribution Around Oscillating Aerofoils", NASA CR-2368, February.
- Bratanow, T., Ecer, A. and Kobiske, M., (1973), "Finite Element Analysis of Unsteady Incompressible Flow Around Oscillating Obstacle of Arbitrary Shape", A.I.A.A. Journal, Vol. 11, No. 11, pp. 1471-1477.
- Camiletti, S.E., and Zamir, M., (1980-1981), "Perturbation Analysis of Poiseuille Flow in a Divided Channel", Trans. of C.S.M.E., Vol. 6, No. 4.
- Camiletti, S.E., (1980), "Incompressible Flow in a Divided Channel", Ph.D. Thesis, Dept. of Appl. Math., The University of Western Ontario.
- Cebeci, T. and Smith, A.M.O., (1970), "A Finite Difference Method for Calculating Compressible Laminar and Turbulent Boundary Layers", Trans. A.S.M.E. Journal of Basic Engineering, Vol. 92, pp. 523-535.
- Cebeci, T., Smith, A.M.O. and Mosinskis, G., (1970), "Calculation of Adiabatic Turbulent Boundary Layers", A.I.A.A. Journal, Vol. 8, No. 11, pp. 1974-1982.
- Cebeci, T., (1975), "Calculation of Three-dimensional Boundary Layers II. Three-dimensional Flow in Cartesian Coordinates", A.I.A.A. Journal, Vol. 13, No. 8, pp. 1056-1064.
- Cheng, R.T., (1972), "Numerical Solution of the Navier-Stokes Equations by the Finite Element Method", The Physics of Fluids, Vol. 15, No. 12, pp. 2098-2105.
- Cooke, C.H., (1981), "On Artificial Vorticity in Numerical Simulation of Incompressible Flow", Mathematics and Computers in Simulation XXIII, North-Holland Publishing Company, Amsterdam, The Netherlands, pp. 51-55.
- Cooper, P. and Reshotko, E., (1975), "Turbulent Flow Between a Rotating Disk and a Parallel Wall", A.I.A.A. Journal, Vol. 13, No. 5, pp. 573-578.
- Crocco, L., (1965), "A suggestion for the Numerical Solution of the Steady Navier-Stokes Equations", A.I.A.A. Journal, Vol. 3, No. 10, pp. 1824-1832.

- Crow, S.C., (1967), "A Physical Explanation of the Tendency of Potential Vortices to Cluster", Lawrence Radiation Laboratory, University of California, Livermore, U.C.R.L.-70481, Reprint, May.
- Dasai, C.S. and Abel, J.F., (1972), Introduction to the Finite Element Method, Van Nostrand Reinhold Comp., New York.
- Dennis, S.C.R. and Staniforth, A.N., (1970), "A Numerical Method for Calculating the Initial Flow Past a ~~Cylinder~~ in a Viscous Fluid", Proceedings of the Second International Conference of Numerical Methods in Fluid Dynamics, University of California, Berkeley, September 15-19, pp. 343-349.
- deRivas, E.K., (1972), "On the Use of Non-uniform Grids in Finite Difference Equations", Journal of Computational Physics, Vol. 10, pp. 202-210.
- deVries, G. and Norrie, D.H., (1971), "The Application of the Finite Element Technique to Potential Flow Problems", Trans. A.S.M.E., Series E, Journal of Applied Mechanics, Vol. 38, pp. 798-802.
- Dhanak, M.R., (1981), "Interaction Between a Vortex Filament and an Approaching Rigid Sphere", J. Fluid Mech., Vol. 110, pp. 129-147.
- Doctors, L.J., (1970), "An Application of the Finite Element Technique to Boundary Value Problems of Potential Flow", International Journal for Numerical Methods in Engineering, Vol. 2, pp. 243-252.
- Dwyer, H.A. and McCroskey, W.J., (1972), "Computational Problems in Three- and Four-dimensional Boundary Layer Theory", Proceedings of the 3rd International Conference on Numerical Methods in Fluid Dynamics, July, pp. 138-145.
- Erens, P.J. and Chasteau, V.A.L., (1974), "Laminar Boundary Layer Response to Freestream Disturbances", A.I.A.A. Journal, Vol. 12, No. 1, January, pp. 93-94.
- Filotas, L.T., (1969), "Theory of Airfoil Response in a Gusty Atmosphere: Part I, Aerodynamic Transfer Function", UTIAS Report 139, October.
- Fromm, J.E. and Harlow, F.H., (1963), "Numerical Solution of the Problem of Vortex Street Development", The Physics of Fluids, Vol. 6, No. 7, pp. 975-982.



- Gadald, M.S., (1982), Personal Communication, Ontario Hydro, Mississauga, Ontario, Canada.
- Glauert, M.B., (1956), "The Laminar Boundary Layer on Oscillating Plates and Cylinders", *Journal of Fluid Mechanics* Vol. 1, pp. 97-110.
- Glauert, M.B., (1962), "The Pressure Gradient Induced by Shear Flow Past a Flat Plate", *Journal of the Aerospace Sciences*, Vol. 29, pp. 540-542.
- Glauert, H., (1959), "The Elements of Aerofoil and Air Screw Theory", Second Edition, Cambridge at the University Press.
- Guymon, G.L., (1972), "Finite Element Solution for General Fluid Motion", *J. Hydn. Div., A.S.C.E.*, Vol. 99, pp. 913-919.
- Hirsh, R.S., (1975), "Higher Order Accurate Difference Solutions of Fluid Mechanics Problems by a Compact Differencing Technique", *Journal of Computational Physics*, Vol. 19, pp. 90-109.
- Hornbeck, R.W., (1975), "Numerical Methods", Quantum Publishers, Inc., New York, New York 10010.
- Huebner, K.H. (1975), The Finite Element Method for Engineers, John Wiley & Sons, New York.
- Jain, P.C. and Rao, K.S., (1969), "Numerical Solution of Unsteady Viscous Incompressible Fluid Flow Past a Circular Cylinder", *High Speed Computing in Fluid Dynamics, The Physics of Fluids Supplement II*, pp. 57-64.
- Katsanis, T., (1967), "A Computer Program for Calculating Velocities and Streamlines for Two-dimensional Incompressible Flow in Axial Blade Rows", NASA TN D-3762, January.
- Kawaguti, M., (1965), "Numerical Solutions of the Navier-Stokes Equations for the Flow in a Channel with a Step", MRC TSR 574, Mathematics Research Center, Madison, Wisconsin.
- Kestin, J., (1966), "The Effect of Freestream Turbulence on Heat Rates", Advances in Heat Transfer, Vol. 3, Academic Press, New York. pp. 1-32.
- Lamb, H., (1932), "Hydrodynamics", Sixth Edition, Dover Publications, New York.
- Lieber, P., Wen, K. and Attia, A., (1974), Finite Element Methods in Flow Problems, edited by Oden et al., UAH Press, Huntsville, Alabama, pp. 85-96.

- Liepmann, H.W., (1952), "On the Application of Statistical Concepts to the Buffeting Problem", J. Aero. Sci., Vol. 19, No. 12, December, pp. 793-800.
- Liepmann, H.W., (1955), "Extension of the Statistical Approach to Buffeting and Gust Response of Wings of Finite Span", J. Aero. Sci. Vol. 22, No. 3, March, pp. 197-200.
- Lighthill, M.J., (1954), "The Response of Laminar Skin Friction and Heat Transfer to Fluctuations in the Stream Velocity", Royal Society of London Proceedings, Series A, Vol. 224, pp. 1-23.
- Lilly, D.K., (1969), "Numerical Simulation of Two-dimensional Turbulence", High Speed Computing in Fluid Dynamics, The Physics of Fluids Supplement II, Vol. 12, pp. 240-249.
- Mahmoud, A.A., (1981), Personal Communication, Math. Department, Cairo University, Egypt.
- Mark, R.M., (1962), "On Shear Flow Past Flat Plates", Journal of Fluid Mechanics, Vol. 14, pp. 452-462.
- Michael, P., (1966), "Steady Motion of a Disk in a Viscous Fluid", The Physics of Fluids, Vol. 9, No. 3, pp. 466-471.
- Morse, P.M., and Feshbach, H., (1953), Methods of Theoretical Physics, Part II, McGraw-Hill.
- Moretti, G., (1966), "Importance of Boundary Conditions in the Numerical Treatment of Hyperbolic Equations", Physics of Fluids, Vol. 12, No. 12, December, pp. II 13-20.
- Olsen, J.H., Goldberg, A. and Rogers, M., (1970), "Aircraft Wake Turbulence and its Detection", Proceedings of a Symposium on Aircraft Wake Turbulence held in Seattle, Washington, September 1-3.
- Olson, M.D., (1974), "Variational-Finite Element Methods for Two-dimensional and Axisymmetric Navier-Stokes Equations", Finite Element Methods in Flow Problems, edited by Oden et al., UAH Press, Huntsville, Alabama, pp. 103-106.
- Onsager, L., (1949), "Statistical Hydrodynamics", Nuovo Cimento, Supplement 6, 274.
- Pao, Y.H. and Daugherty, R.J., (1969), "Time-Dependent Viscous Incompressible Flow Past a Finite Flat Plate", Boeing Scientific Research Laboratories, DL-82-0822, January.

- Paris, J. and Whitaker, S., (1965), "Confined Wakes: A Numerical Solution of the Navier-Stokes Equations", A.I.Ch.E. Journal, Vol. 11, No. 6, pp. 1033-1041.
- Perry, A.E., Lim, T.T. and Teh, E.W., (1981), "A Visual Study of Turbulent Spots", J. Fluid Mech., Vol. 104, pp. 387-405.
- Phillips, J.H. and Ackerberg, R.C., (1973), "A Numerical Method for Integrating the Unsteady Boundary Layer Equations When There Are Regions of Back Flow", Journal of Fluid Mechanics, Vol. 58, Part III, pp. 561-579.
- Plotkin, A. and Flugge-Lotz, I., (1968), "A Numerical Solution for the Laminar Wake Behind a Finite Flat Plate" Journal of Applied Mechanics, Trans. A.S.M.E., Vol. 90, pp. 625-630.
- Prandtl, L. and Tietjens, O.G., (1957), "Fundamentals of Hydro- and Aeromechanics", Dover Publications, Inc., New York, New York.
- Rasmussen, H., (1980), Personal Communication, Appl. Math. Department, The University of Western Ontario, London, Ontario, Canada.
- Roache, P.J., (1976), Computational Fluid Dynamics, Hermosa Publishers, New Mexico.
- Sarpkaya, T., (1963), "Unsteady Flow Over Bluff Bodies", Developments in Mechanics, Vol. 2, Part I, Fluid Mechanics, Pergamon Press, Proc. of the Eighth Midwestern Mechanics Conference, pp. 45-68.
- Schlichting, H., (1979), Boundary Layer Theory, McGraw-Hill, New York, Seventh Edition.
- Sears, W., (1956), "Some Recent Developments in Airfoil Theory", J. Aero. Sci. Vol. 23, No. 5, May, pp. 490-498.
- Singleton, R.E. and Nash, J.F., (1974), "Methods for Calculating Unsteady Turbulent Boundary Layers in Two- and Three-dimensional Flows", A.I.A.A. Journal, Vol. 12, No. 5, pp. 590-595.
- Smith, S.L. and Brebbia, C.A., (1975), "Finite Element Solution of Navier-Stokes Equations for Transient Two-dimensional Incompressible Flow", Journal of Computational Physics, Vol. 17, pp. 235-245.
- Son, J.S. and Hanratty, T.J., (1969), "Numerical Solution for the Flow Around a Cylinder at Reynolds Numbers of 40, 200 and 500", J. of Fluid Mechanics, Vol. 35, Part 2, pp. 369-386.

- Taylor, C. and Hood, P., (1973), "A Numerical Solution of the Navier-Stokes Equations Using the Finite Element Technique", Computers and Fluids, Vol. 1, pp. 73-100.
- Thoman, D.C. and Szewczyk, A.A., (1969), "Time-Dependent Viscous Flow Over a Circular Cylinder", High Speed Computing in Fluid Dynamics, The Physics of Fluids Supplement II, pp. 76-86.
- Thompson, E.G. and Hauque, M.I., (1973), "A High Order Finite Element for Completely Incompressible Creeping Flow", Int. Journal for Numerical Methods in Engg., Vol. 6, pp. 315-321.
- Thomson, L.M. Milne, (1958), "Theoretical Aerodynamics", London, Macmillan & Co. Ltd.
- Ting, L., (1960), "Boundary Layer Over a Flat Plate in Presence of Shear Flow", The Physics of Fluids, Vol. 3, No. 1, pp. 78-81.
- Vooren, J.V. and Labrujere, T.E., (1973), "Finite Element Solution of the Incompressible Flow Over an Airfoil in a Non-uniform Stream", Proc. of the Int. Conf. for Numerical Methods in Fluid Dynamics held at the University of Southampton, England, September 26-28.
- Wu, J.C., (1976), "Numerical Boundary Conditions for Viscous Flow Problems", A.I.A.A. Journal, Vol. 14, August, pp. 1042-1049.
- Yoshizawa, A., (1970), "Laminar Viscous Flow Past a Semi-Infinite Flat Plate", J. of the Physical Society of Japan, Vol. 28, No. 3, pp. 776-779.
- Zienkiewicz, O.C., (1971), "The Finite Element Method in Engineering Science", McGraw-Hill, London.

**END**

2	1	0	9	8	3
---	---	---	---	---	---

**FIN**